# A review of flexible fluid-structure interactions in the ocean

## Progress, challenges, and future directions

Tavakoli, Sasan; Singh, Mansi; Hosseinzadeh, Saeed; Hu, Zhengyu; Shao, Yaniln; Wang, Shan; Huang, Luofeng; Grammatikopoulos, Apostolos; Li, Yuzhu Pearl; More Authors

**DOI**
10.1016/j.oceaneng.2025.122545

**Publication date**
2025

**Document Version**
Final published version

**Published in**
Ocean Engineering

**Citation (APA)**
Tavakoli, S., Singh, M., Hosseinzadeh, S., Hu, Z., Shao, Y., Wang, S., Huang, L., Grammatikopoulos, A., Li, Y. P., & More Authors (2025). A review of flexible fluid-structure interactions in the ocean: Progress, challenges, and future directions. *Ocean Engineering*, *342*, Article 122545. https://doi.org/10.1016/j.oceaneng.2025.122545

Ocean Engineering 342 (2025) 122545

Contents lists available at ScienceDirect

Ocean Engineering

journal homepage: www.elsevier.com/locate/oceaneng

Research paper

# A review of flexible fluid-structure interactions in the ocean: Progress, challenges, and future directions

Sasan Tavakoli [a,b,*,1], Mansi Singh [c], Saeed Hosseinzadeh [d], Zhengyu Hu [e], Yaniln Shao [f], Shan Wang [g,1], Luofeng Huang [h], Apostolos Grammatikopoulos [i,1], Yuzhu Pearl Li [e], Danial Khojasteh [j], Jin Liu [k], Azam Dolatshah [l], Hui Cheng [m], Spyros Hirdaris [n,1]

[a] Australian Maritime College, University of Tasmania, Newnham, 7250, TAS, Australia
[b] Department of Infrastructure Engineering, The University of Melbourne, Parkville, 3052, VIC, Australia
[c] MIDS, Katholische Universität Eichstätt-Ingolstadt, Ingolstadt, 85049, Germany
[d] Maritime Engineering, School of Engineering, University of Southampton, SO16 7QF UK
[e] Department of Civil and Environmental Engineering, National University of Singapore, Singapore
[f] Department of Mechanical Engineering, Technical University of Denmark, 2800, Kgs. Lyngby, Denmark
[g] Centre for Marine Technology and Ocean Engineering (CENTEC), Instituto Superior Técnico, Universidade de Lisboa, 1049-001, Lisboa, Portugal
[h] Faculty of Engineering and Applied Sciences, Cranfield University, Cranfield MK43 0AL, UK
[i] Department of Maritime & Transport Technology, Delft University of Technology, the Netherlands
[j] School of Civil and Environmental Engineering, UNSW, NSW, Australia
[k] School of BioSciences, The University of Melbourne, Parkville, 3052, VIC Australia
[l] Faculty of Science, Engineering and Technology, Swinburne University of Technology, Hawthorn VIC 3122 Australia
[m] AKVA Group ASA, Inger Bang Lunds vei 14, N-5059 Bergen, Norway
[n] Global Ship Systems Centre, American Bureau of Shipping, Athens, Greece

ARTICLE INFO

*Keywords:*
Flexible fluid-structure interactions
Marine hydroelasticity
Computational fluid dynamics
Ship dynamics
Wave-structure interactions
Slamming
Marine propellers
Marine vegetation
Sea ice
Soft Mud

ABSTRACT

Flexible Fluid-Structure Interaction (FFSI) has emerged as an important, but challenging research direction in modern ocean engineering. This line of research gradually evolved in response to the pressing need to model the dynamic responses of ships and marine structures to sea loads; to predict the performance of flexible marine propellers, energy converters, and coastal protection systems; and to understand the mutual interactions between sea ice, marine vegetation, and mud with oceanic and coastal processes occurring near the surface and seabed. This review presents the state of knowledge and art of modelling of FFSI in the maritime environment, tracing research progress from early physical tests to high-fidelity computational ones emerged recently. Flexible wave–structure interaction, global ship hydroelasticity, hydroelastic slamming, flexible marine propellers, vegetation dynamics, and wave–mud interactions are covered. Limitations and strengths of existing models, and the challenges that remain are discussed in-depth, and it is concluded that FFSI-based research in ocean engineering has very well grown, though some gaps are still open. In specific, hydroelastic effects are still overlooked in the design practices and classification rules do not fully incorporate them, and there are still concerns regarding uncertainties related to FFSI modelling of flexible slamming, dynamic of flexible marine vegetation, and wave-mud interactions. Hence, future research must bridge computational modelling with real-world applications, expand benchmarking coverage for marine engineering problem, and incorporate AI-based methods for modelling FFSI problems, predicting related dynamic responses, or accelerating simulations.

* Corresponding author.Australian Maritime College, University of Tasmania, Newnham, 7250, TAS, Australia.
*E-mail address:* sasan.tavakoli@utas.edu.au (S. Tavakoli).
[1] These authors are ISSC2025 committee members.

https://doi.org/10.1016/j.oceaneng.2025.122545
Received 5 May 2025; Received in revised form 19 August 2025; Accepted 19 August 2025
Available online 22 September 2025

## 1. Introduction

Oceans are very precious to us and to all living creatures for different reasons. It is well accepted that they regulate the climate, support biodiversity, enable maritime transportation, and offer clean energy resources (Tavakoli et al., 2023a). Apart from the vast mass of water in the oceans, there are many solid objects in the oceans, such as ships, engineering installations, and ice covers that are found in polar zones. All these objects, whether welcomed by the ocean or not, are exposed to environmental forces, caused by oceanic (e.g. waves, Hirdaris et al., 2010, 2014) or atmospheric processes (e.g. winds, Haddara and Guedes Soares, 1999). This leads to shear and normal stresses in the solid body which can sometimes cause flexible responses (static or dynamic responses). For example, water waves may elastically vibrate a 344-m-long ship (Senjanović et al., 2009a) or excite vibrations in ice shelves (Kalyanaraman et al., 2020). These phenomena are commonly categorised as Flexible Fluid-Structure Interaction (FFSI) processes, occurring in oceans, seas, and lakes, or in general in marine environment.

Within the field of ocean engineering, the term "hydroelasticity"[2] is frequently used to describe the flexible-fluid structure interactions. This term was first introduced to the naval architecture community in the late 1950s by Heller and Abramson (1959), who are widely regarded as pioneers in using this term and addressing this topic (Hirdaris and Temarel, 2009; Wu and Cui, 2009; Fu et al., 2022). However, research into FFSI began decades earlier, when scholars sought new formulations to describe gravity wave propagation in elastically covered lakes (Greenhill, 1886). While the term “hydroelasticity” is often sufficient to refer to FFSI problems, it does not fully capture the viscoelastic behaviour exhibited by some flexible bodies in response to fluid forces. For this reason, the phrase "flexible fluid-structure interactions" is favoured in the present review article.

The concept of FFSI in the marine environment was introduced gradually to the ocean engineering community, particularly through early observations by oceanographers who noted the flexible motion of sea ice in response to water waves (Robin, 1963; Dean, 1966; Wadhams, 1972, 1975, 1978, 1979; Wadhams et al., 1988). This was followed by a line of thought of the International Ship and Offshore Structures Congress (ISSC) committee in 1970s (Bishop and Taylor, 1973), which emphasised the need to unify ship structural analysis with seakeeping performance (ISSC, 1973; Bishop et al., 1986). The idea that hydroelasticity significantly influences slamming loads, especially for lightweight structures, also began to take shape during the 1980s and 1990s (Kvalsvold and Faltinsen, 1993). Concurrently, the development of flexible marine systems, such as composite marine propellers (inspired by Calclough and Russell, 1972) and wave energy converters (French, 1979), highlighted the growing relevance of FFSI in the design and performance assessment of next-generation ocean engineering systems.

Our early understanding of FFSI problems was shaped through real-world observations and replicated in laboratory settings (e.g., tanks, basins, and cavitation tunnels). Theoretical and mathematical models based on advanced mathematics subsequently emerged (e.g., Bishop and Price, 1979). Subsequently, computational models began to appear in the 2010s. Modern computational models (e.g., Khayyer et al., 2018) are first validated against well-known academic test cases, and then applied to complex FFSI problems (examples are shown in Fig. 1).

With the development of increasingly either advanced or fundamental models for solving FFSI problems in the ocean, alongside the growing applications of these interactions in engineering and other scientific fields, the need for a comprehensive review of state-of-the-art models has become more apparent. While there have been notable and engaging review papers focusing on specific FFSI problems, such as those by Prof. Vernon Squire on wave-ice interactions (Squire et al., 1995; Squire, 2007) or others addressing flapping of foils (Wu et al., 2020), a comprehensive review covering the majority of models addressing FFSI problems is currently lacking in the literature.

Such a review benefits researchers, scientists and modelers by providing technical and modelling visions applicable across various fields related to ocean and maritime environment. It also supports potential interdisciplinary research emerging from FFSI. To address this gap, the present paper presents a state-of-the-art review of FFSI modelling in the ocean, covering physical experiments, inviscid-based models, and CFD approaches. Unlike earlier review papers, this work brings together six major FFSI problems, ranging from wave–structure interaction to flexible marine propellers under a unified and comparative framework, aimed at providing cross-cutting insights into FFSI modelling in maritime environment. As such, this review paper introduces a structured modelling pathway that generalises how FFSI models are formulated, including fluid and solid idealisation, coupling strategies, and solver integration, which, to the best of the authors' knowledge, has not been systematically presented in previous reviews. This approach enables readers to clearly understand the similarities and differences in modelling techniques across problems and may inspire the transfer of modelling concepts from one application to another. Following this, the paper synthesises developments in FFSI modelling in marine environment and highlights important lessons from recent advances. It addresses the main strengths and limitations of current models, discusses future research opportunities, and outlines remaining challenges. The framework is deliberately designed to help engineers and researchers identify, compare, and select appropriate FFSI modelling strategies, or develop new ones, based on their specific needs. Although knowledge-driven, the review includes a focused literature analysis, introducing the historical development of FFSI models and classifying them by problem where practical.

This review paper is structured as follows. Section 2 introduces the FFSI problems considered and explains why flexibility needs to be accounted for in each of the problems. Section 3 provides a general overview of how models can be developed through the simplification and idealisation of fluid and solid as two continuum models. Section 4 reviews experimental-based models developed for FFSI in the ocean. Section 5 presents a state-of-the-art review of models based on inviscid flow assumptions. Section 6 reviews CFD-based models. Sections 4 to 6 contain tables that present studies either introducing FFSI models (from experimental ones to CFD ones) or applying them to specific engineering or application-related problems. Section 7 provides a general outlook for future research, and Section 8 presents the concluding remarks.

## 2. Flexible fluid-solid interaction problems

Our definition of FFSI helps determine the scope of studies and research progress to be covered in this review paper. We define the problem as the flexible motions that arise in a continuous solid body under the influence of hydrodynamic forces. These flexible motions “may” or “may not” significantly influence the velocity and pressure fields in the surrounding fluid domain, depending on the extent of the motions arising in the solid body. For example, the elastic motions of a ship may not substantially affect the wave field, unlike its rigid body motions (e.g. Lakshmynarayanana and Hirdaris, 2020). However, the elastic motions of a body entering the water can significantly influence the velocity and pressure fields within the fluid domain (e.g. Tavakoli et al., 2023b).

This review paper excludes multi-physical problems involving internal mechanics, such as hard grounding or vibrations of the main deck of a ship, or solid-solid interactions, such as ice-structure interactions, although these may be influenced by hydrodynamic effects (e.g. Kim et al., 2021; Keijdener et al., 2018; Jiang et al., 2024). Additionally, only non-hyperflexible deformations are addressed in this review paper.;

[2] This term is derived from two Greek elements, "hydro" (ὕδωρ), meaning water, and "elasto" (ἐλαστός), meaning flexibility. These two elements are combined with the Latin-derived suffix "-ity".

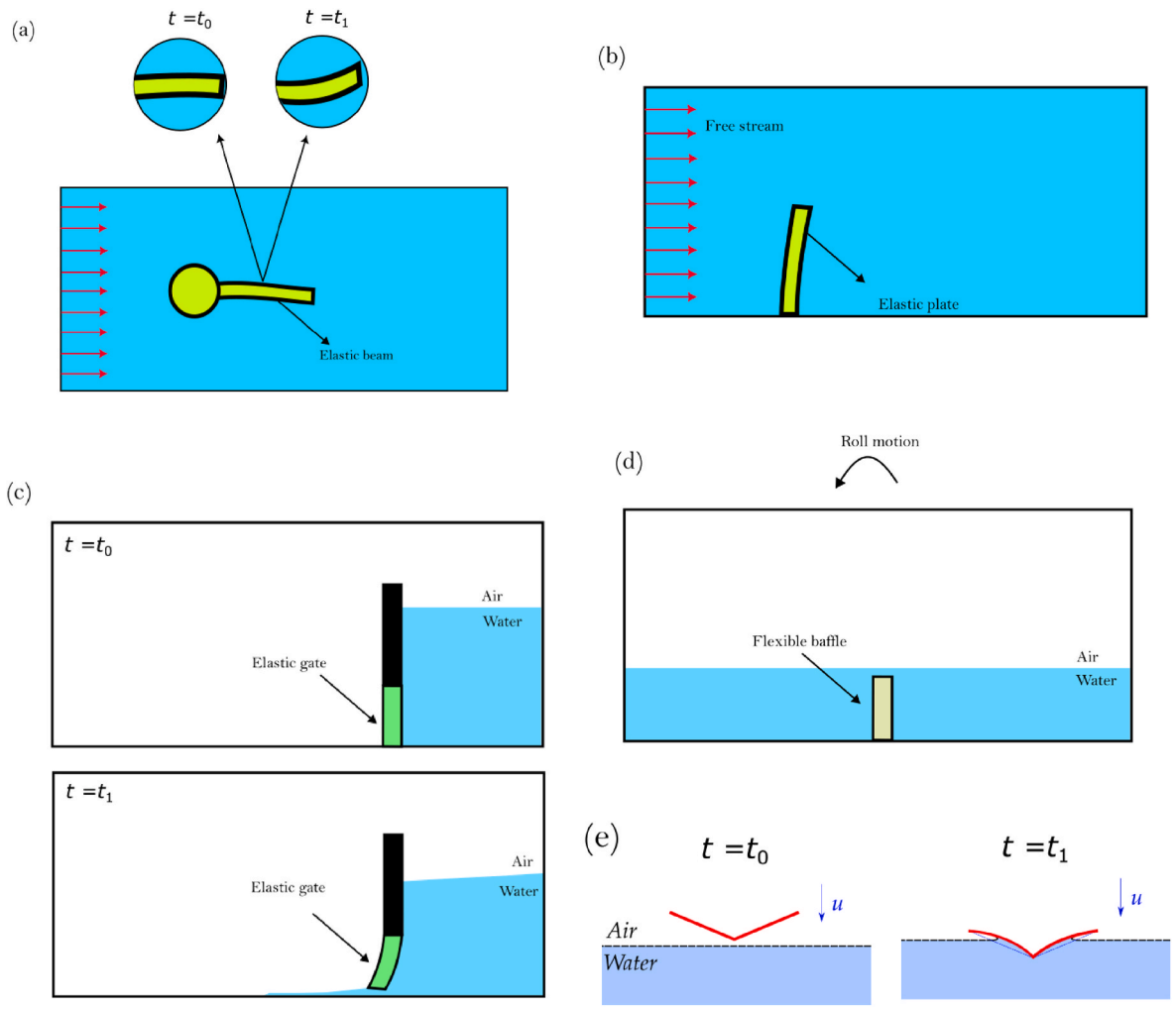


**Fig. 1.** Examples of basic problems used for validating CFD-based codes developed to solve flexible fluid-structure interaction problems. These include the dynamic responses of a flexible beam placed behind a fixed cylinder, (a) an elastic plate exposed to a free stream, (b) a dam break on a flexible gate, (c) the dynamic responses of a flexible baffle in a rolling tank, and (d) the flexible water entry of a V-shaped body at a constant speed (e).

Phenomena such as plastic deformations (e.g. Yu, 2025), hydroelasto-plasticity (e.g. Lu et al., 2024; Liu et al., 2017, 2022d), crushing (e.g. ice crushing, Ranta et al., 2018), crack propagation (Zhao et al., 2021), and breaking (e.g. Voermans et al., 2020) fall outside the scope of this review paper.

As such, this review paper covers flexible wave-structure interaction problems (introduced in sub-section 2.1), global ship hydroelasticity (introduced in sub-section 2.2), flexible slamming (introduced in sub-section 2.3), flexible marine propellers (introduced in sub-section 2.4), flexible motions of marine vegetation (introduced in sub-section 2.5), and wave-mud interactions (introduced in sub-section 2.6). These problems along with their associated engineering domains (Ocean Engineering, Coastal Engineering, and Naval Engineering), examples of flexible bodies, key outputs, and potential engineering and scientific applications are detailed in Table 1. All of these problems are relevant to the field of ocean engineering.

### 2.1. *Wave-structure interaction*

Flexible wave-structure interactions refer to the mutual influence between water waves and flexible structures (floating, submerged, vertical, horizontal, or inclined). When a flexible structure is subjected to water waves, it transmits part of the wave energy and reflect another portion (Bennetts et al., 2015; Kostikov et al., 2021, 2022; Polly et al., 2025) and may also dissipate energy via linear and nonlinear mechanisms (e.g. Bi et al., 2022). Specifically, dissipation may be caused by visco-elastic responses (e.g. Mosig et al., 2015). In addition, a flexible structure may influence wave dispersion (Collins et al., 2017). If a flexible floating structure is unmoored, it may drift. For a structure of finite length, the response is a combination of various elastic modes (Meylan and Squire, 1995). However, for very long flexible structures, progressive flexible waves emerge (Zhao et al., 2015a). Fig. 2 demos examples of flexible wave-structure interactions.

Flexible wave-structure interactions are fundamental to various engineering and natural systems, such as offshore structures (Niedzwecki and Huston, 1992), coastal protection (e.g. Zhang et al., 2023a), wave energy conversion (Collins et al., 2021; Teixeira-Duarte et al., 2022; Wang et al., 2024b), and marine ecosystems (e.g. wave-ice interactions, Williams et al., 2013). On a smaller scale, models developed for flexible-wave structure interactions are applied in the design of marine structures (e.g. Very Large Floating Structures, VLFS, Lamas-Pardo et al., 2015), wave energy systems (wave energy converters, WEC), and coastal protection. When scaled up to a geophysical level, they are used in global/regional wave models (e.g. Liu et al., 2020).

Mathematical modelling of waves first started in the 17th century, with early models being largely theoretical and focused primarily on wave dynamics. However, from the 20th century onwards, the advent of computers transformed the study of flexible wave-structure interactions by enabling numerical simulations and the development of more sophisticated mathematical models.

**Table 1**
FFSI problems reviewed in the present paper, with key outputs and engineering applications outlined.

| FFSI problem | Engineering Domain(s) | Example of the flexible body | Key outputs | Engineering/science applications |
|---|---|---|---|---|
| Wave-structure interactions | Coastal, Ocean | VLFS, flexible seawall, sea ice, flexible breakwaters | • Wave transmission and/or reflection coefficients<br>• Energy dissipation<br>• Drift force/mooring tension force<br>• Mode shapes and deformation<br>• Wave dispersion | • Coastal protection<br>• Energy harvesting<br>• Minimising structural fatigue and improving resilience<br>• Global/regional wave modelling |
| Global ship hydroelasticity | Naval, Ocean | Containerships, trimarans | • Vertical, and horizontal bending moment, along with torsional moment<br>• Springing and whipping responses<br>• Fatigue damage index<br>• Natural frequencies | • Design/fatigue load<br>• Ship structural design<br>• Ultimate strength estimation<br>• Fatigue life estimation<br>• Reducing slamming-induced loads<br>• Ensuring classification compliance |
| Flexible slamming | Naval, Ocean, Coastal | Bow section, amidship section | • Design pressure<br>• Local deformation (dynamic/static response)<br>• Whipping excitation force | • Hull protection<br>• Design load<br>• Predicting transient load inputs<br>• Material damage assessment |
| Flexible marine propellers | Naval, Ocean | Composite propellers (off-design operations), SPPs, Marine Turbines | • Blade bending/twisting angles<br>• Unsteady pressure on blades<br>• Propeller performance<br>• Cavitation signatures | • Performance optimisation<br>• Noise reduction<br>• Preventing blade failure<br>• Improving adaptability to inflow changes |
| Marine vegetation | Coastal, Ocean | Seagrass, marshes | • Wave attenuation coefficients<br>• Turbulent kinetic energy (TKE)<br>• Shear stress near seabed<br>• Vegetation drag and reconfiguration | • Nature-based coastal protection<br>• Ecosystem service quantification<br>• Designing nature-based solutions<br>• Global/regional wave modelling |
| Wave-mud interactions | Coastal, Ocean | Navigational channels, soft seabed zones | • Wave decay rate<br>• Bed shear stress<br>• Mud deformation depth | • Dredging frequency prediction<br>• Ship sinkage/squat assessment<br>• Global/regional wave modelling<br>• Sediment transport |

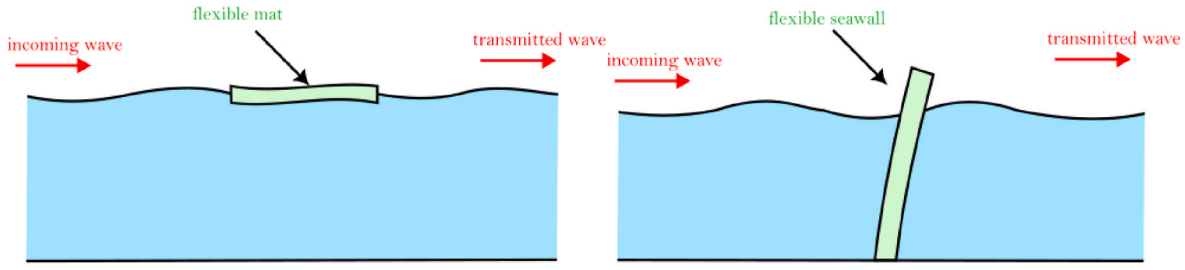


**Fig. 2.** Examples of flexible wave-structure interactions, including wave interactions with a flexible mat (left) and wave interactions with a flexible seawall (right).

### 2.2. Global ship hydroelasticity

Global ship hydroelasticity refers to the elastic, dynamic responses of a hull girder caused by fluid actions (Fig. 3). Unlike engine and propeller-induced vibrations, which typically occur in the order of millimetres, ship hydroelastic responses can be in the order of metres (Senjanović et al., 2008). Recognised since the 1970s, this issue led to a new research direction to unify seakeeping and structural analysis, as raised by Committee 10 of the Fourth International Ship Structures Congress, ISSC (Bishop and Taylor, 1973; Bishop and Price, 1974).

Ships exhibit flexible responses to waves when their length is very long and when travelling at high speeds (Wu and Moan, 2005). Composite high-speed ships and river-going vessels may also display flexible responses to wave loading. The flexibility of a ship is believed to increase vertical and torsional bending moments (Wu and Moan, 2005; Vijith and Rajendran, 2023).

The flexible responses of a ship to waves can be classified into two categories: steady-state responses (springing), and transient responses (whipping). Springing occurs when the exciting frequency aligns with one of the eigenfrequencies (natural frequencies) of the ship.

These elastic responses of a ship can be classified as symmetric (vertical bending), asymmetric (bending and torsion), or anti-symmetric (vertical bending, torsion, and horizontal bending). For ships with open decks and for trimarans, the lowest natural frequency is typically associated with torsional modes (e.g., Chen et al., 2019a), whereas for vessels with closed sections it corresponds to vertical bending (Senjanović et al., 2008). Springing is categorised as either linear or nonlinear (Riesner and El Moctar, 2021a). Linear springing occurs when the encounter frequency of the hull girder closely matches its natural frequency, while nonlinear springing arises when the natural frequency aligns with the second, third, or higher harmonics of the water waves, or is influenced by body nonlinearities. Springing is reported to contribute roughly 40–45 % of fatigue damage in ships (Storhaug et al., 2003; Drummen et al., 2008). An example of the effects of ship flexibility and the resulting springing on Vertical Bending Moments (VBM), Horizontal Bending Moments (HBM), and Torsional Moments (TM) is illustrated in Fig. 4.

Whipping occurs when a sudden imposed load, such as slamming, acts on the ship, and due to the structural damping of the ship, this response tends to decay slowly (Zhu and Moan, 2014). Whipping is therefore more likely to occur in harsh wave environments, such as the Southern Ocean and the North Atlantic, or also in extreme sea conditions (Wang and Guedes Soares, 2016a, 2025). It has been noted that slamming, while contributing to whipping, may increase the loads acting on the ship by as much as 30 % (Hirdaris et al., 2023). An example of the whipping response of a flexible ship due to slamming force, including

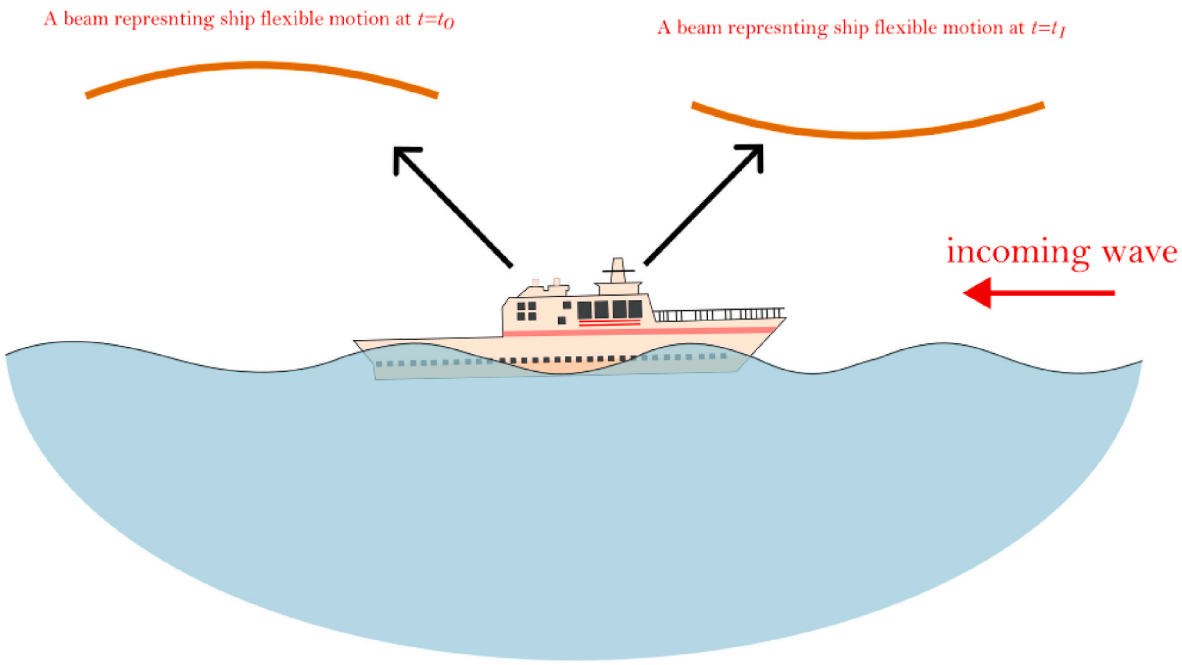


**Fig. 3.** A simple representation of global ship hydroelasticity.

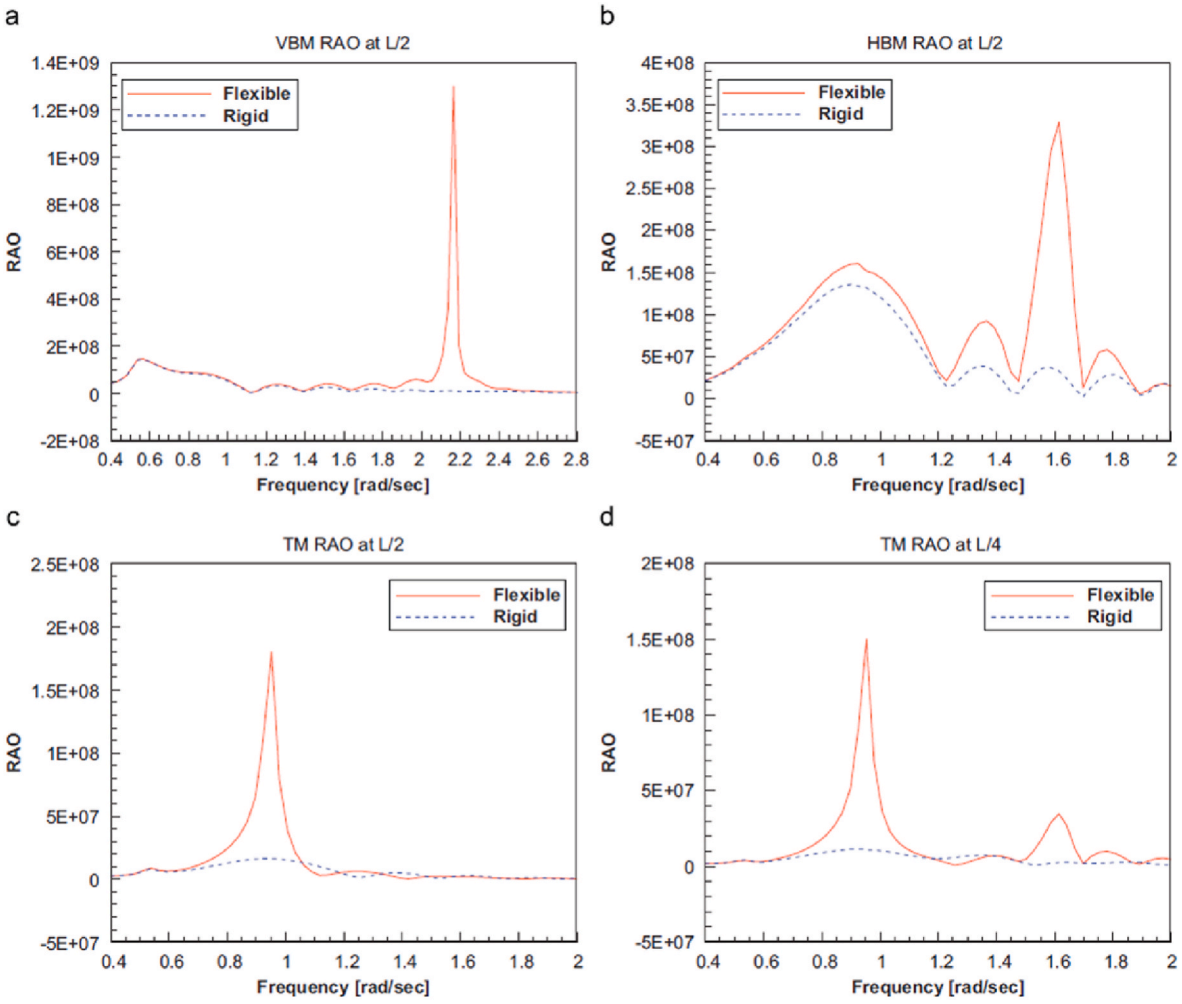


**Fig. 4.** Response Amplitude Operators (RAOs) of the VMB at amidships (panel a), HBM at amidships (panel b), and TM at two different stations (panels c and d), comparing a flexible ship (solid red lines) with a rigid ship (dashed blue lines). Figure adapted from Kim et al. (2009a). © Elsevier.

HBM and TM, is shown in Fig. 5.

### 2.3. Flexible slamming

Slamming refers to the sudden impact of a body with a mass of liquid, occurring under various scenarios (Abrate, 2011; Faltinsen, 2000; Jung, 2025). The most common slamming event occurs when part of a vessel or a ship re-enters the water, frequently observed in ships and high-speed boats (e.g., planing hulls; see Tavakoli et al., 2020, 2024a). These events are also referred to as water entry. Slamming predominantly occurs at the bow of ships and boats (e.g. Wang and Guedes Soares, 2016a; Judge and Ibrahim, 2025), although it can also take place amidships (flat bottom slamming) or at the stern (stern slamming, Wang and Guedes Soares, 2016b). Oblique and angular velocities may also be considered when studying slamming phenomena (e.g., Judge et al., 2004; Xu et al., 2008; Javanmardi et al., 2018; Li et al., 2022a). The solution of the water entry problem, while applicable for determining design pressures and whipping forces, can also be used to simulate the motion of planing hulls in calm water and waves (e.g., in Zarnick, 1978, Sun and Faltinsen, 2011; Haase et al., 2015; Morabito, 2015; Tavakoli and Dashtimanesh, 2019; Niazmand Bilandi et al., 2020, 2021; Ciampolini et al., 2022; Hosseini et al., 2024), which is beyond the scope of the present paper.

Other types of slamming, including ditching and side slamming, may also occur. Slamming that takes place during the landing of seaplanes and helicopters is referred to as ditching (e.g., Iafrati, 2016). Side slamming occurs when a breaking wave impacts the side of a marine structure or a ship, typically in vessels with a large bow flare (e.g., Zou et al., 2024; Hu and Li, 2025). Fig. 6 illustrates different slamming scenarios. Slamming can be considered from a flexible structural perspective. For amphibious craft landing on water, the effects of slamming can be particularly severe, potentially causing plastic deflections (Iafrati et al., 2015; Iafrati, 2016). The water entry/slamming problem has also been studied recently under aerated conditions (e.g. Zhao et al., 2025) and in non-Newtonian fluids (Ebrahimi and Azimi, 2025a, b).

The dynamic response of a slammed structure may be studied through quasi-steady or dynamic response analyses, depending on the natural frequency and the loading period (Faltinsen, 1999; Stenius et al., 2007). It has been noted that, for flexible structures, slamming loads may reduce the overall impact pressures (e.g., Tavakoli et al., 2023b, 2023c). This behaviour presents a compelling FFSI problem. The output of the slamming analysis (forces and moments) can serve as the input for the whipping analysis of the ship. The slamming problem has been studied since the late 1920s (Kapsenberg, 2011). Early research focused on the water entry of rigid bodies, but over time, attention has shifted towards flexible water entry problems.

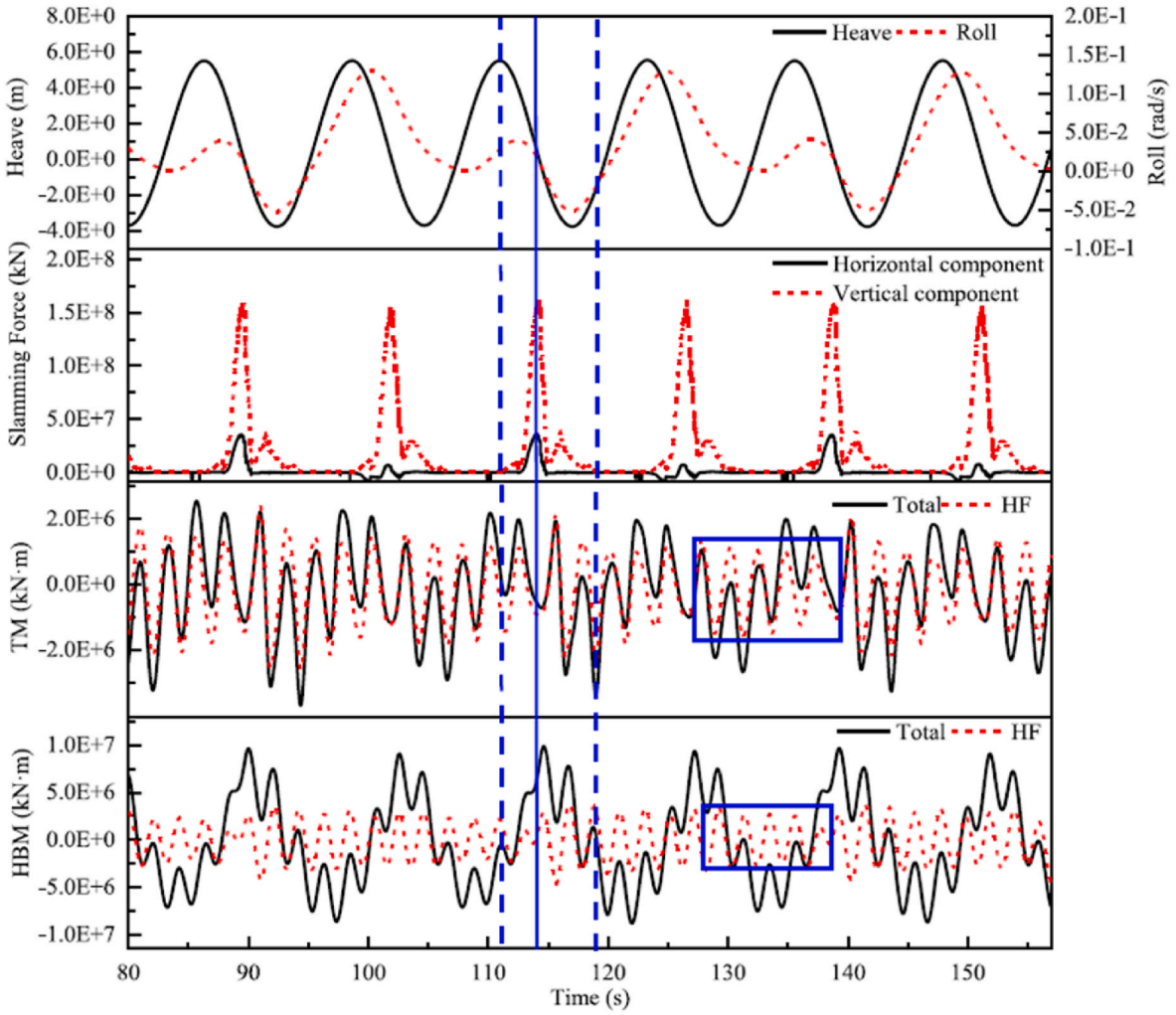


**Fig. 5.** Time histories of heave and pitch motions (top panel) of a flexible ship subjected to slamming loads under asymmetric conditions. The second panel shows the corresponding slamming forces. The third and fourth panels present the TM and HBM, respectively. The decay observed in the high-frequency components of TM and HBM (the rectangles) shows the transient nature of the whipping response of a flexible ship. Figure adapted from Lu et al. (2023). © Elsevier.

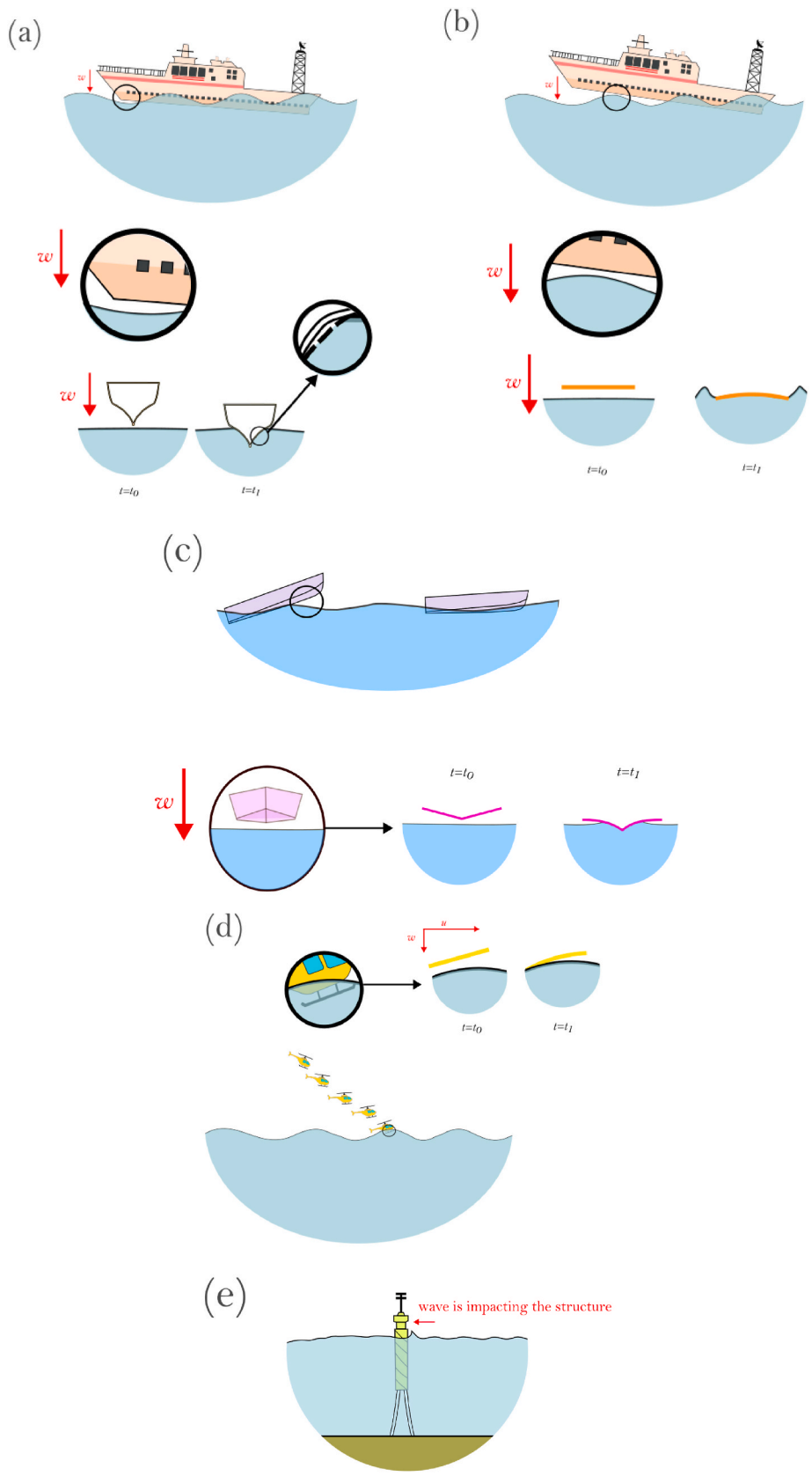


**Fig. 6.** Examples of slamming phenomena, including occurrences in ship's bow (a), bottom slamming (c), planing boats (c), helicopters (d), and structures exposed to water waves (e). Breaking waves impacting the ship bow flare are not shown, but the sketch would be similar to that of (e).

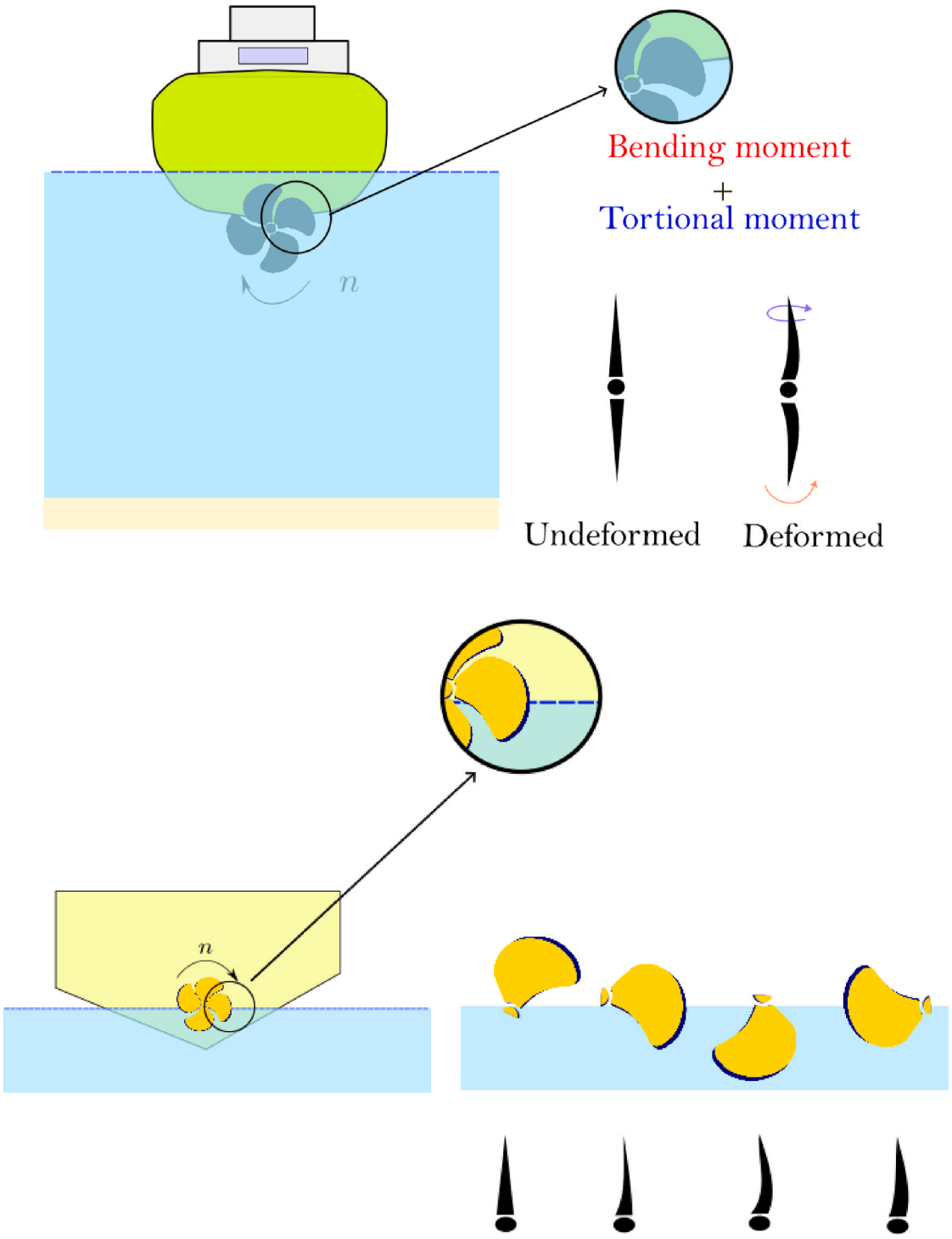


**Fig. 7.** Distortion of a composited marine propeller (up) and dynamic response of a semi-submersible propeller during one single rotation.

### 2.4. Flexible marine propellers

Similar to ships, marine propellers can exhibit flexible responses. These motions are particularly relevant to modern composite propellers, which are designed to deform (bending and twisting) under fluid actions, when operating in off-design conditions (Zhang et al., 2020). Other types of propellers (non-composite ones) may vibrate due to non-uniform forces caused by the fluid flow, which can also induce vibrations in the hull girder and decks, albeit typically on the order of millimetres. Fig. 7 shows examples of flexible motions occurring in

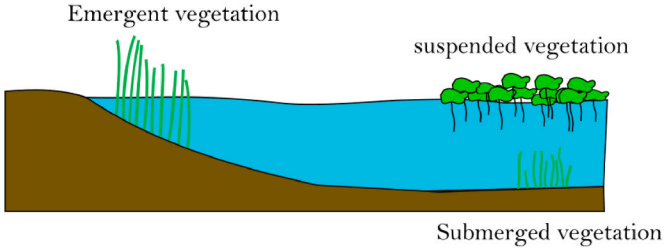


**Fig. 8.** Marine vegetation that may be found in a coastal zone.

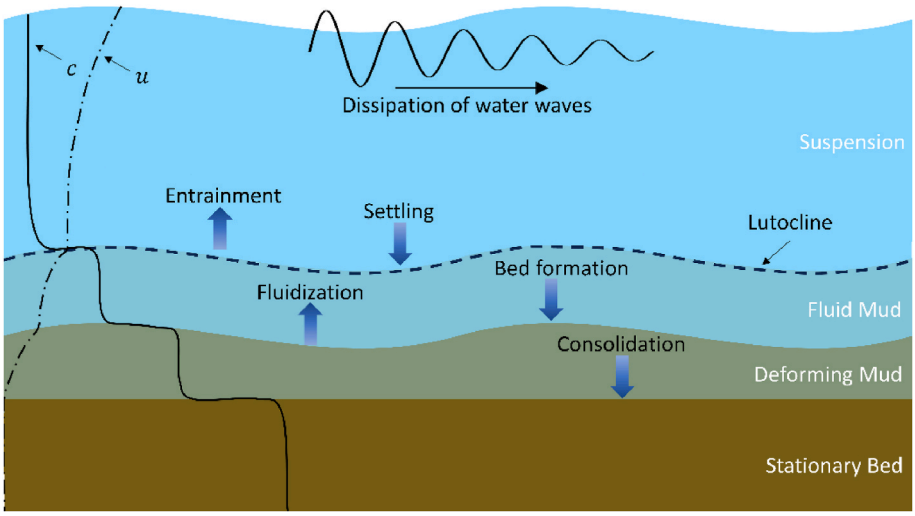


**Fig. 9.** Schematic of mud response to water waves.

marine propellers.

The elastic distortion of a composite propeller can be classified as either steady or dynamic. The steady response occurs under a uniform flow pattern. In contrast, the dynamic response describes how a marine propeller reacts to non-uniform flow, which may be triggered by ship appendages or the formation of cavitation. Self-adaptive deformation, involving bending and twisting, is specifically optimised for such conditions, commonly referred to as off-design conditions (Mulcahy et al., 2010).

In non-composite propellers, particularly semi-submersible propellers, dynamic responses may occur. These are most commonly recognised as propeller vibrations, which can induce significant stresses in the propeller blades that vary over each rotation. The study of flexible motions and dynamic responses of marine propellers can be traced back to the 1960s (Young et al., 2016), but significant research in this field gained momentum in the mid-2000s (e.g. Young, 2007a,b).

### 2.5. Flexible motions of aquatic vegetation

Marine vegetation, such as seagrass and marshes, particularly in coastal zones, is often exposed to waves and wave-driven currents that move towards the shoreline (Fig. 8). This vegetation is highly flexible and interacts dynamically with the surrounding water flow. The resulting interaction forms a reciprocal relationship between the flexible plant structures and the fluid environment. Marine vegetation can significantly attenuate wave energy, reduce the current energy and wave runup (Kobayashi et al., 1993; Quartel et al., 2007), thereby offering natural coastal protection by mitigating the risks and hazards (Koch et al., 2009; Borsje et al., 2011).

In addition to the energy attenuation of water waves caused by marine vegetation, turbulent flow may develop between plants due to their large, flexible movements when in close proximity (Brunet, 2020). This turbulence can generate significant shear stresses near the seabed, potentially affecting sediment transport and bed morphology.

In the real maritime environment, marine vegetation rooted in the seabed or floating on the water surface often exhibits variation in topology (e.g., height and diameter) and mechanical properties (rigidity). However, in both numerical and physical tank studies, an idealised setup is typically used (e.g. Markov et al., 2023), where the vegetation is represented with uniform geometry and material properties to best capture the dominant physics (e.g., Henry and Myrhaug, 2013; Yin et al., 2021a,b). Based on these idealised models, regression equations are then formulated, which can be applied in wave modelling over wetland regions (e.g., Wang and Hu, 2023).

### 2.6. Flexible mud

Soft mud is commonly found in estuaries, wetlands, and coastal areas, where it provides habitats for marine life, supports nutrient cycling, naturally protects coastal ecosystems, and helps stabilise shorelines. These mud layers typically originate from the weathering and erosion of rocks, with sediments transported via tidal currents, water waves, and river plumes with high turbidity (Geyer et al., 2004; Traykovski et al., 2015).

Fig. 9 presents a schematic of wave-mud interactions based on the qualitative framework proposed by Mehta (1989) for the vertical structure of sediment concentration ($c$) and horizontal velocity ($u$) in a water-mud mixture. The vertical profile is divided into four distinct layers, separated by sharp gradients in mud concentration. The lutocline demarcates the interface between the upper, relatively clear water and the lower, more turbid fluid mud (Parker and Kirby, 1982). Beneath the fluid mud lies a deforming mud layer that transitions into a stationary cohesive bed. This intermediate layer exhibits both fluid-like and solid-like behaviour, modulated by wave orbital motion.

Wave–mud interactions become particularly important under low-frequency, long-period wave conditions (e.g. swell waves or infragravity waves), where the wave orbital motion is capable of penetrating deeper into the water column and interacting with the mud bed (Elgar and Raubenheimer, 2008). In shallow, low-energy environments, even moderate wave conditions can induce significant deformation in soft mud beds, leading to erosion, fluidization, and suspension of cohesive sediments (Jaramillo et al., 2009). Conversely, in high-energy conditions, intense turbulence and shear can resuspend settled mud, inhibiting consolidation (Sheremet et al., 2011). Erosion (entrainment and fluidization), deposition (settling and bed formation), and consolidation occur cyclically and are sensitive to both wave characteristics and sediment properties (Ge et al., 2020; Jaramillo et al., 2009; Sheremet et al., 2011).

Understanding the threshold wave conditions for these transitions is very important for accurate modelling of wave propagation. For instance, viscoelastic or viscoplastic rheological models are often employed to capture the complex response of cohesive sediments under oscillatory wave loading. Moreover, the inclusion of wave-induced pore pressure dynamics and stratified fluid–mud layering in numerical models can significantly improve predictive capabilities of models. This This understanding is critical not only for environmental and sediment transport studies but also for practical considerations in navigation and port operations, where soft mud layers may affect vessel sinkage and underkeel clearance (e.g. Delefortrie et al., 2010)

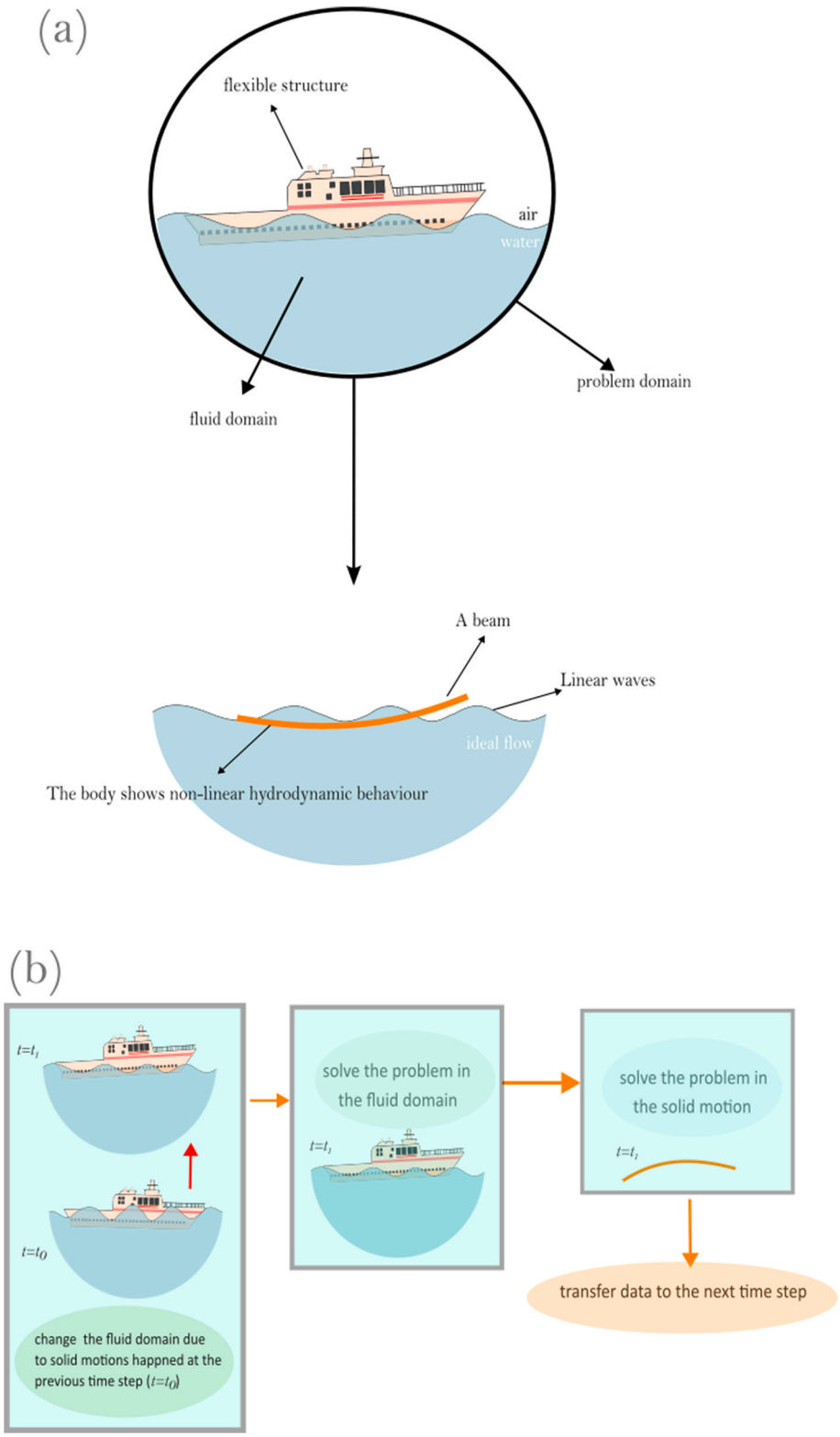


**Fig. 10.** Example of the idealisation of a fluid-structure interaction problem (a) and (b) example of the way the fluid-structure interaction problem is numerically solved by a one-way algorithm (flexible motions are not fed back to the fluid-domain).

## 3. General assumptions and modelling approaches

The general assumptions made about any FFSI problem serve as the foundation for its formulation or conceptualisation. If a non-physical approach is adopted (as opposed to tank, tunnel, flume tests, or field measurements), various mathematical, numerical, or hybrid models can be developed to simulate FFSI problems.

This section outlines the assumptions that are typically made when formulating FFSI problems and seeking their solutions using numerical or mathematical approaches. These assumptions may relate to fluid idealisation, structural idealisation, or the manner in which the numerical approach is constructed. Fig. 10 provides an example of how

**Table 2**
Sources of body hydrodynamic and free surface nonlinearities in different FFSI problems covered in this review paper.

| Problem | Source of nonlinearity | |
|---|---|---|
| | Body hydrodynamics | Free surface |
| Flexible wave-structure interactions | • Temporal changes of wetted area<br>• Nonlinear deflection of the structure | • Nonlinear water waves<br>• Overwash<br>• Wave breaking<br>• Wave-wave interactions |
| Global ship hydroelasticity | • Temporal changes of wetted area<br>• Nonlinear ship responses<br>• Transient response to slamming loads<br>• Turbulence around the ship | • Nonlinear water waves<br>• Wave breaking<br>• Green water<br>• Wave-wave interactions |
| Flexible slamming | • Temporal changes of wetted area<br>• Large deflections | • Nonlinear jet formation<br>• Nonlinear splash<br>• Air entrapment (aerated slamming, of flow separation in asymmetric/oblique slamming)<br>• Cavity generation |
| Flexible marine propellers | • Temporal change of the blade shape<br>• Cavitation formation<br>• Non-uniform flow | • Free surface effects around the propeller (SPPs) |
| Marine vegetation | • Relatively large deformation<br>• Turbulence generation around the body<br>• Nonlinear drag force<br>• Stem-stem interaction | • Nonlinear water waves<br>• Wave-wave interactions |
| Wave-mud interactions | • Turbulence generation above the mud<br>• Nonlinear mud deformation | • Depth induced shoaling<br>• Wave-wave interactions<br>• Nonlinear waves |

**Table 3**
Importance of turbulence consideration in different FFSI problems covered in this review paper.

| Problem | Turbulence Importance | Reason |
|---|---|---|
| Wave–Structure Interactions | High | Turbulence may be present in case of wave breaking or emergence of overwash. |
| Ship Hydroelasticity | Moderate-High | Turbulence is important when ship is exposed to large waves, green water emerges, and ship advances in high speeds. |
| Flexible slamming | Low | Turbulence may be important in case of bottom slamming. |
| Flexible marine propellers | High | Tip vortices, cavitation and free surface effects (in case of surface piercing propellers). |
| Marine vegetation | Moderate-High | When the turbulent flow generation emerges between stems of marine vegetation. |
| Wave–mud | Low | Surface turbulence is less critical, yet turbulence can cause sediment suspension or pore pressure. It may be relevant near the seabed boundary layer under wave action. |

problem idealisation for global ship hydroelasticity, and the setup of an appropriate numerical approach, can support effective simulation.

### 3.1. Idealising the fluid

#### 3.1.1. Ideal or viscous

The fluid can be assumed to be either non-viscous, commonly referred to as inviscid, or viscous. Under the assumption of an inviscid fluid, fluid motions around any solid body are typically governed by Euler momentum equations (e.g. Kim et al., 2022a). In specific, the velocity potential concept may be used, and thus the fluid motion is governed by the Laplace equation, with the solution of the potential field being sought (Birk, 2019). When the FFSI problem is studied near the upper oceanic boundary layer, free surface boundary conditions must be applied. Free surface boundary condition can be either linear or nonlinear.

When the fluid is assumed to be viscous, energy dissipation is included in the governing equations. Hence, the Navier–Stokes (NS) equations hold the fluid motion (Graebel, 2007). Energy equations may also be considered when cavitation or thermal effects are significant (Wang et al., 2020a). These cases are particularly relevant for marine propellers or scenarios involving water entry under cavitation effects, such as flat bottom slamming (e.g. Chen et al., 2019b; Wu et al., 2023; Yang et al., 2024). Meshed or meshless methods can be used to solve the problem numerically, although only meshed methods are covered in the present research (for a general overview of meshless methods, see Gotoh and Khayyer, 2018). For FFSI problems, a viscous-based formulation is preferred over an ideal-flow assumption when shear stresses are expected to become significant or when ideal flow fails to effectively capture all nonlinear effects (e.g., wave breaking around a ship).

#### 3.1.2. Linear or nonlinear nature for fluid model

Nonlinearities in the fluid flow may arise due to fluid motion on the free surface (not relevant to a fully submerged body) or the hydrodynamics of the flexible body, which are listed in Table 2. Nonlinearities associated with the free surface are due to deformations in the water surface due to dynamic motions of a flexible/rigid body (e.g. Wei et al., 2025a), propagation of nonlinear water waves (steep waves), wave–wave interactions (e.g. Abroug et al., 2020), green water or overwash (e.g. wave-ice interactions, Tavakoli and Babanin, 2021), and splashing (water entry, Vincent et al., 2018). The topic of nonlinear water waves, including the formation of rogue waves (e.g. Chabchoub et al., 2011; Kirezci et al., 2021; He et al., 2025; Zhai et al., 2025) and the emergence of wave sequences below a certain limit (e.g. Al-Ani and Belmont, 2021; Tavakoli et al., 2024b, 2025), the former providing insight into sea hazards for marine structures and the latter assisting in the planning of maritime operations, is a major area of research and has been extensively studied in the literature (refer to Onorato et al., 2013; Dudley et al., 2019; Xue et al., 2023).

Nonlinearities associated with body hydrodynamics are related to the temporal change of the wetted area of the floating body or ship, or temporal changes in the shape of a flexible body (such as a blade), drag force generation, turbulent flow, cavitation, and non-uniform flow patterns. These effects need to be addressed through time-domain simulations, where the temporal change in the area exposed to fluid forces must be considered.

When using inviscid-based flow modelling, nonlinearities associated with the free surface (e.g. Da Silva and Peregrine, 1990; Green et al., 1974; Green and Naghdi, 1976) must be defined within the boundary conditions of the free surface, or the waves themselves must be assumed to be nonlinear (e.g. Părău and Dias, 2002; Hartmann et al., 2022), as linearised free surface conditions are not applicable (refer to Lamb, 1932; Dean and Dalrymple, 1991; Mandal and Chakrabarti, 2000; Linton and McIver, 2001 for fundamental concepts). Additionally, nonlinearities in body hydrodynamics must be temporally accounted for. For example, in modelling the hydrodynamic nonlinearities of a flexible ship, the instantaneous position of the body must be considered (Watanabe and Guedes Soares, 1999), as it determines the temporal wetted area and displaced volume. When using a viscous fluid model,

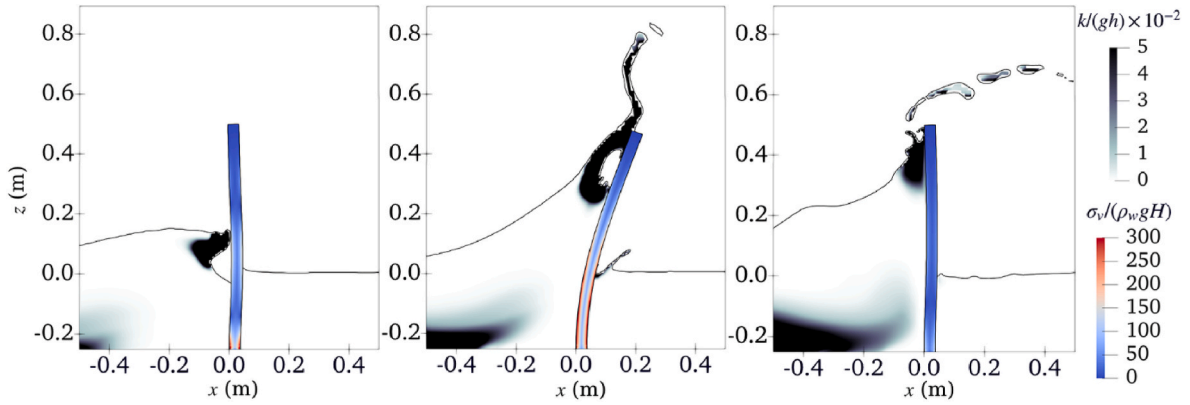


**Fig. 11.** Wave profiles, turbulence levels, and structural responses of a flexible wall under the high-aeration impact (Hu and Li, 2023). © Elsevier.

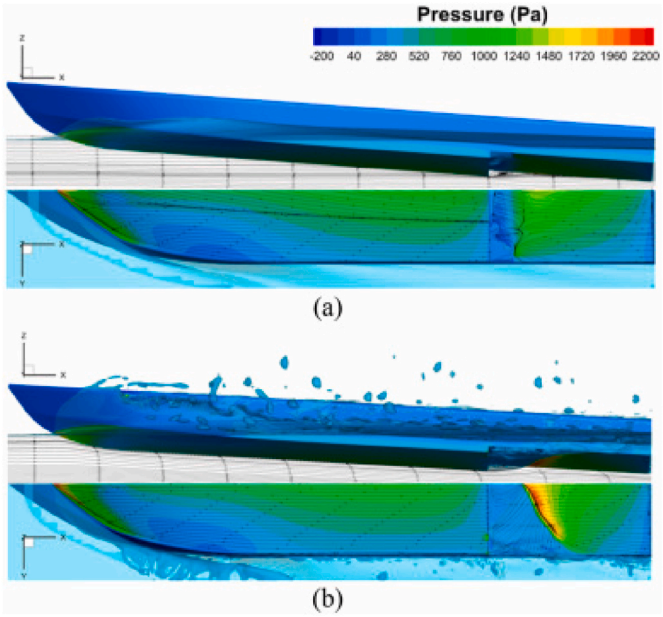


**Fig. 12.** Cavity flow and free surface around a single stepped planing hull advancing at a beam Froude number of 1.46, captured using (a) a LSM and (b) a VOF model. Adapted from Park et al. (2022). © Elsevier.

nonlinearities are fully considered in the model.

### 3.1.3. Turbulent idealisation

Turbulence in the fluid domain can arise from a variety of factors, including boundary layer instabilities (Posa et al., 2022), vortex shedding (Zhang et al., 2021a), and wave-related processes such as non-breaking (Babanin, 2006, Babanin and Haus, 2009) and breaking waves (Liu et al., 2019).

Incorporating turbulence into FFSI problems can be achieved via advanced modelling techniques. The modelling of turbulent flows in marine hydrodynamics is commonly achieved using the Reynolds-Averaged Navier-Stokes (RANS) equations, coupled with turbulence models such as eddy viscosity models, or those use Reynolds Stress Models (RSM). These models solve for the mean velocity and pressure fields while accounting for the effects of turbulence through additional terms like Reynolds stresses. Alternative approaches, including Large-Eddy Simulations (LES), Very Large Eddy Simulations (VLES) hybrid ones, Detached Eddy Simulations (DES), and Direct Numerical Simulations (DNS). A detailed review on these models and their applications in ship hydrodynamics is presented in Pena and Huang (2021).

Turbulence may be present in different FFSI problems. The importance of turbulent flow in the various FFSI problems discussed in this paper is summarised in Table 3. For instance, the interaction of breaking waves with flexible structures generates highly energetic, turbulent flows (e.g. Hu and Li, 2023), necessitating accurate representation of dissipation mechanisms and pressure fluctuations. An example of the turbulence flow generation around a flexible wall impacted by a breaking wave is shown in Fig. 11.

### 3.1.4. Free surface modelling in CFD studies

When a meshed method is used, the free surface can generally be tracked using either the level-set method (LSM) (Osher and Sethian, 1988) or the Volume of Fluid (VOF) model (Hirt and Nichols, 1981), with the latter utilising a volume fraction parameter to represent fluid phases within each computational cell.

The main physical difference between the methods is that the VOF model represents the interface as the transport of a mass fraction, whereas the LSM applies the free-surface boundary condition via a signed distance function. The inclusion of surface tension is more straightforward in the LSM than in the VOF (see Lee, 2015). Wang et al. (2009) noted that the LSM can be more readily implemented in three-dimensional problems, unlike the VOF method, which requires a more complex geometric procedure.

One reported drawback of the VOF method is the possible occurrence of artificial numerical ventilation near solid walls when the fluid flow is relatively fast. This issue has been addressed through various numerical approaches and has been reported in studies on the hydrodynamics of planing hulls (Cui et al., 2021a, 2021b).

The VOF approach represents the interface using a discontinuous step function, which has been identified as a key weakness, as it may generate weak but artificial currents near the air–water interface when modelling sharp interfaces (Lafaurie et al., 1994; Chatzimarkou et al., 2022). In contrast, the main limitation of the LSM, despite its ability to capture a smoother free surface, lies in its non-conservative treatment of mass for both liquid and gas phases, as well as the requirement for re-initialisation. As a result, phenomena such as wave breaking, spray formation, and air entrapment may not be accurately captured (Wang et al., 2009).

To address these issues, a coupled LSM and VOF methods (CLSVOF) has been introduced (Sussman and Puckett, 2000). This hybrid approach has been applied in the modelling of breaking waves by Wang et al. (2009) and Chatzimarkou et al. (2022), as well as in simulations of wave breaking near the stern of a ship entering the water (Chen et al., 2022b).

Both the VOF and LSM have undergone significant development over the past two decades, with examples found in Muzaferija (1998), Ubbink and Issa (1999), Olsson and Kreiss (2005), Weymouth, G. D. and Yue (2010), Leroyer et al. (2011), Bureš et al. (2021), Ferro et al. (2025). In particular, detailed explanations of various improvements made to the VOF solvers in OpenFOAM are provided by Huang et al. (2022b).

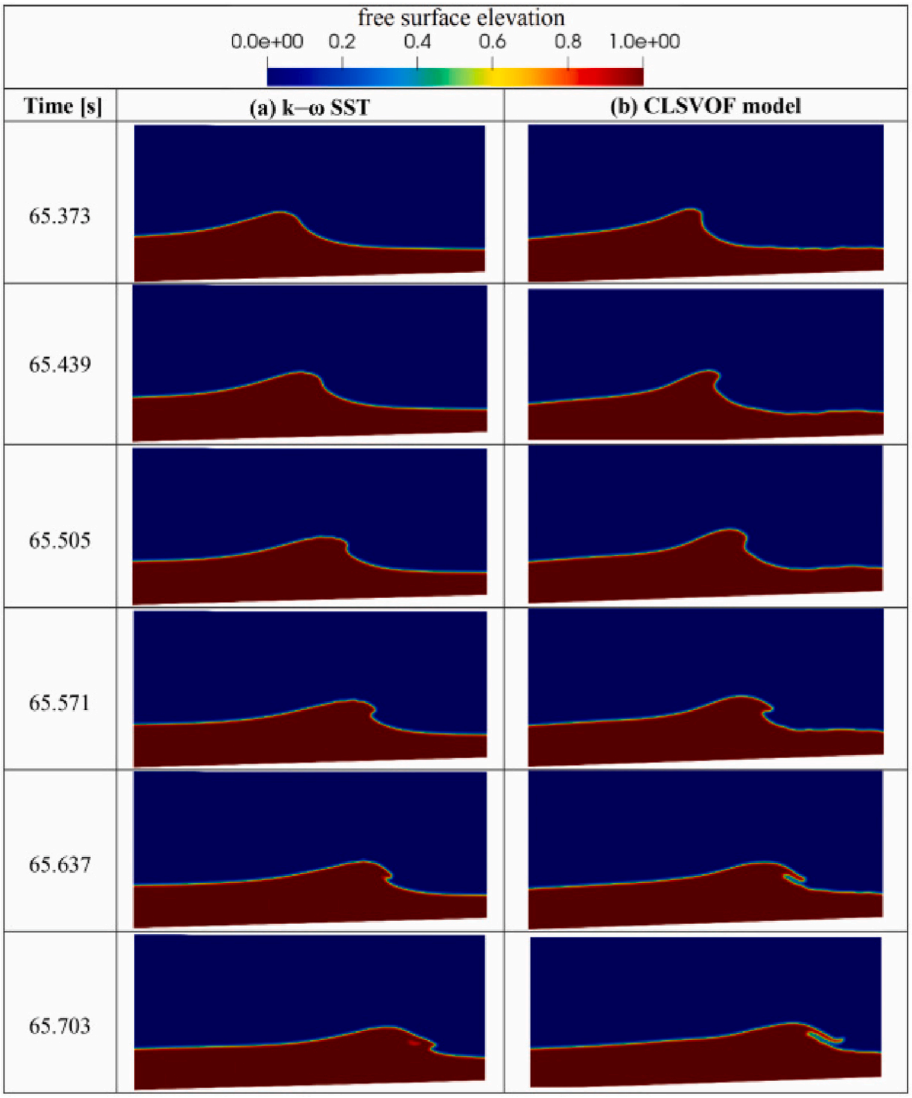


**Fig. 13.** Snapshots of a breaking wave simulated using the VOF and CLSVOF models, as presented by Chatzimarkou et al. (2022). © Elsevier.

**Table 4**
Different approaches used to idealise the mechanical behaviour of the solid body in the FFSI problems covered in this review paper.

| Mechanical behaviour | Wave-structure interaction | Ship hydroelasticity | Flexible slamming | Marine propellers | Marine vegetation | Wave-mud interactions |
|---|---|---|---|---|---|---|
| Elastic | ✓ (e.g. VLFS) | ✓ | ✓ | ✓ | ✓ | ✓ (very soft seabed) |
| Viscoelastic | ✓ (e.g. sea ice) | – | – | – | ✓ | ✓ |
| Porous Elastic/ Viscoelastic | ✓ (e.g. perforated breakwaters and sea ice) | – | – | – | ✓ | ✓ |
| Viscous | ✓ (e.g. sea ice) | – | – | – | – | ✓ |

An illustrative comparison of free-surface flow around a planing hull, captured using LSM and VOF models, is shown in Fig. 12. Additionally, an example of a breaking wave modelled using CLSVOF and VOF is presented in Fig. 13. Finally, it should be noted that other models have also been developed to capture the free surface, some of which are unique to OpenFOAM solvers; further details can be found in Huang et al. (2022b).

### 3.2. Assumption for the solid body

#### 3.2.1. Mechanical behaviour idealisation

In the absence of plastic and hyperelastic behaviour, a flexible solid body responding to hydrodynamic forces can be idealised as an elastic, viscoelastic, viscous, or porous medium (e.g., poroelastic or porous viscoelastic). The choice of idealisation depends on the rheological properties of the solid body and the nature of the fluid–structure interaction.

Under an elastic behaviour assumption, the solid body undergoes reversible deformation in response to hydrodynamic loads. Elastic models are commonly employed to study both static and dynamic responses: for instance, uniform flows acting on flexible marine propellers can be considered as inducing static responses, while unsteady or non-uniform flows may cause dynamic effects such as ship springing or flexural vibrations in floating ice shelves. This idealisation has been applied in diverse contexts, including ship hydroelasticity, VLFS, flexible coastal mats, and the motion of marine vegetation under wave

**Table 5**
Different elemental idealisation used for modelling FFSI problems covered in this paper (C: common, NC: Not common, OC: occasionally common).

| Problem | 1D beam idealisation | 1D Thin-walled beam idealisation | Plate idealisation | N-Pendula idealisation | Multi-Rigid-Body idealisation | Discrete element idealisation | Truss idealisation | Full 3-D Geometry (solved via FEM, FVM, meshless methods, etc.) |
|---|---|---|---|---|---|---|---|---|
| Wave–structure interactions | C | NC | C | NC | C | OC | OC | C |
| Ship hydroelasticity | C | C | NC | NC | C | NC | NC | NC |
| Flexible slamming | C | NC | C | NC | NC | NC | NC | C |
| Flexible marine propellers | OC | NC | OC | NC | NC | NC | NC | C |
| Marine vegetation | OC | NC | OC | C | NC | NC | NC | OC |
| Wave-mud interactions | C | NC | C | NC | NC | NC | NC | OC |

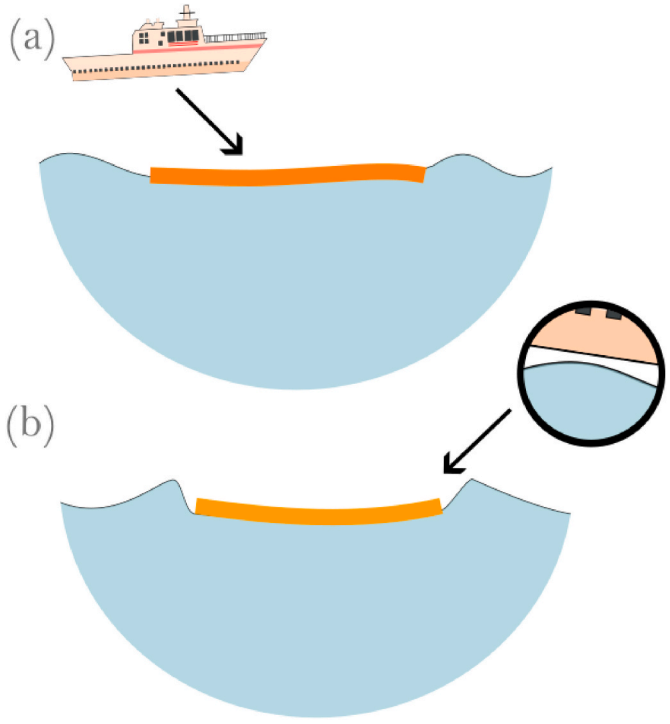


**Fig. 14.** Two examples of beam idealisation for a structure. (a) shows a beam idealisation of ship structure, and (b) shows beam idealisation of flat bottom slamming of ships.

loading.

Viscoelastic behaviour, in contrast, captures both elasticity (recoverable) and viscosity (dissipative) responses. The behaviour is particularly appropriate for sea ice, soft seabeds and muddy bottoms that dissipate wave energy through internal friction and molecular rearrangement.

Viscoelastic behaviour of solid bodies, such as ice covers and muddy seabeds (e.g. Huang et al., 1992), is primarily identified through physical observations, upon which idealised viscoelastic models are then developed. For instance, Shakeel et al. (2020) conducted rheological tests on natural cohesive sediments from the Port of Hamburg, revealing distinct viscoelastic behaviour characterised by two yield stresses (see also Yang and Yu, 2018). Ice cover has similarly been characterised as a viscoelastic material in the work of Marchenko et al. (2021), who reported the viscosity and elasticity of ice formed in an ice tank, based on wave–ice interaction experiments.

To build FFSI models for wave-mud or wave-ice interactions, a simple idealised model that represents viscoelastic behavior of the material is required. These simple idealised models typically use spring–dashpot systems (e.g., KV and Maxwell models; see Flügge, 1975 for more technical information) to simulate the combined elastic and

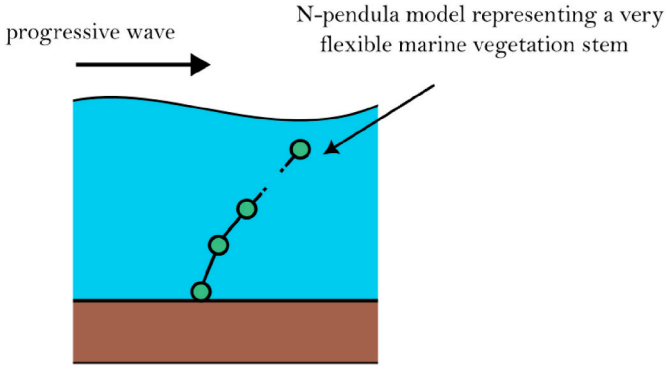


**Fig. 16.** Idealisation of a very flexible vegetation stem using the N-pendula model.

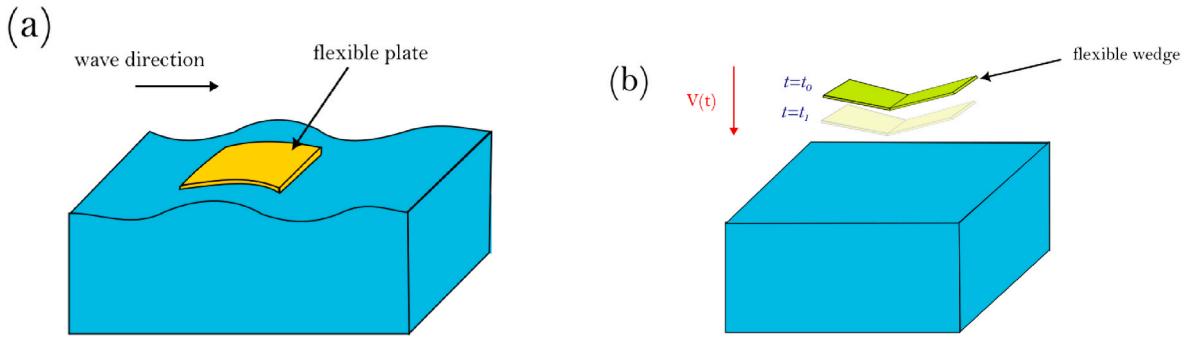


**Fig. 15.** Two examples of plate idealisation for a structure. (a) shows a plate idealisation for a thin structure interacting with water waves, and (b) shows plate idealisation for a panel of a flexible wedge entering water.

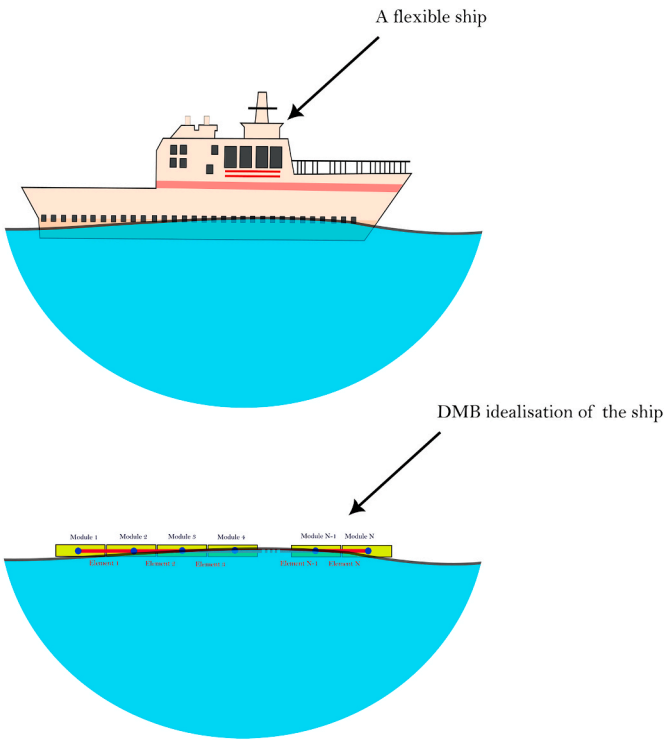


**Fig. 17.** Idealisation of ship by using DMB model.

viscous behaviour of seabed materials. Some examples include the wave–ice interaction models developed by Tavakoli and Babanin (2023), which are based on both KV and Maxwell formulations, as well as the wave–mud interaction model by Liu and Chan (2007), which uses the KV approach.

The flexible body may also be idealised as a porous medium, assuming the structure allows internal fluid flow through interconnected pores. This results in additional dissipation due to fluid–solid interactions. In porous media, fluid within the pores is often governed by Darcy's law (Darcy, 1856) for low-Reynolds number flows (e.g. Chwang and Chan, 1998; Kim et al., 2000), or the Forchheimer extension for inertial flows. The solid skeleton can be further idealised as poroelastic (e.g. Nandi et al., 2024) or viscoelastic porous (e.g. Xu and Guyenne, 2022), enabling more accurate representations of marine sediments or reef substrates. This idealisation is particularly relevant in modelling wave attenuation over porous structures such as coral reefs (e.g. Huang et al., 2024; Han et al., 2025), brine-channelled sea ice, and deformable seabeds (e.g. Jeng and Lin, 2000; Williams and Jeng, 2007).

Finally, a purely viscous assumption may be used to represent the solid as a dense fluid, especially in modelling Newtonian or non-Newtonian fluid responses of mud or ice. This assumption is commonly used in studies of wave–mud (e.g. Dalrymple and Liu, 1978; Ng, 2000) and wave–ice interactions (e.g. Keller, 1998) where the material exhibits flow-like behaviour under wave-induced shear. Other constitutive models, such as elastoplastic or hyperelastic formulations, may also be applied depending on the material and loading conditions, but such topics are beyond the scope of this review. They are referenced briefly where relevant (e.g. wave-mud interactions). A summary of the different mechanical behaviours that can be assigned to the solid body is presented in Table 4.

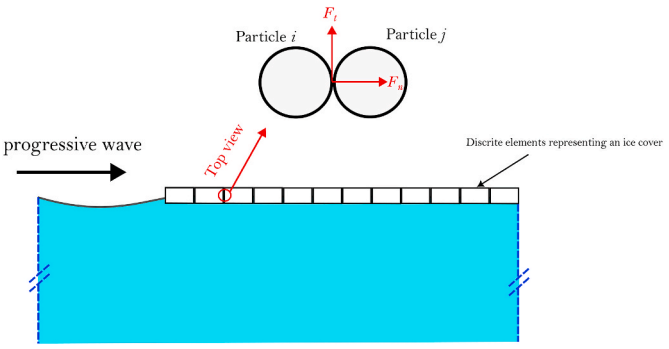


**Fig. 18.** Idealisation of an ice cover by using a discrete element model.

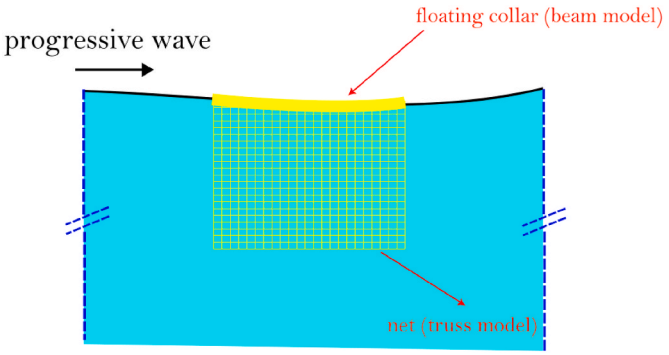


**Fig. 19.** Net of a fish cage idealised using a truss model.

### 3.2.2. *Elemental idealisation of a flexible solid body*

Another important step in the idealisation of the flexible body is related to how it is represented as a structural element, which is listed in Table 5. Elemental idealisation permits formulating the equations of motion for the solid body. Various elemental idealisations can be applied, and the most relevant ones are introduced here.

*3.2.2.1. Beam idealisation.* A 2D/3D structure is simplified into a beam. This idealisation works for slender structures. The main assumption that holds for this simplification is that the distortion along the beam is relatively small compared to the length of the structure, and shear deformations are assumed to be very small. This is a very common practice in modelling flexible wave-structure interactions, global ship hydroelasticity, and 2D water entry problems. An example of beam idealisation for modelling a flexible ship hydroelasticity problem is shown in Fig. 14. Different beam models such as Euler–Bernoulli Beam Theory, Timoshenko Beam Theory, and Tapered Beam Theory are commonly used in the literature (see Timoshenko, 1953; Elishakoff, 2020).

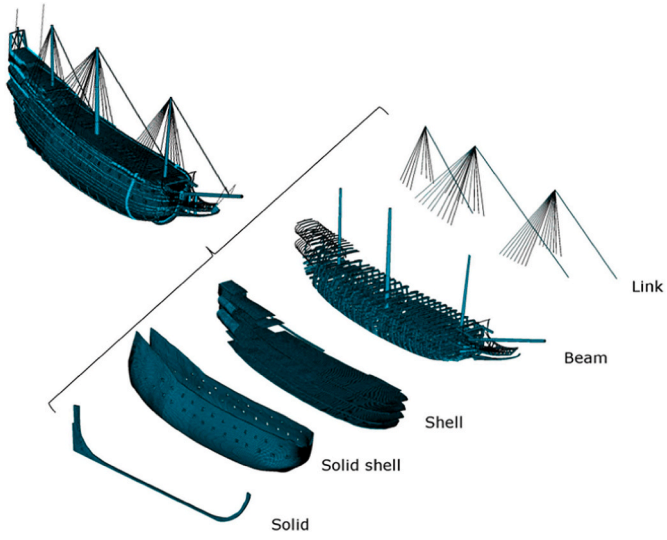


**Fig. 20.** 3D idealisation of 17th-century warship Vasa by Afshar et al. (2021) by using FEM. © Elsevier.

*3.2.2.2. 1D thin-walled beam idealisation.* 1D thin-walled beams have three distinct dimensions, each differing in magnitude. The wall thickness of these beams is assumed to be significantly smaller than the other dimensions. The cross-sectional dimension is considerably smaller than the beam length, and they are also termed "long prismatic shells" (Vlasov, 1961). A distinctive feature of 1D thin-walled beams is their tendency to undergo longitudinal extension when subjected to torsional moments (e.g. antisymmetric responses of ships). See Senjanović and Grubišić, 1991, as an example of a thin-walled beam model for idealising the global dynamic response of a ship.

*3.2.2.3. Plate idealisation.* Plate theories assume that one dimension of the structure is much smaller than the other dimensions, i.e., a thin structure. Hence, the body is idealised as a plate. In most of the theories, the structure is assumed to have small deflections compared to its width. Two examples of plate idealisation for a thin body exposed to water waves, and a 3D wedge entering water are shown in Fig. 15. Kirchhoff-Love Plate Theory (Reddy, 2007) and First-order Shear Deformation Theory (Reissner, 1945; Mindlin, 1951) are the most common ones that used in the literature. This approach of idealisation is also referred to as shell idealisation, which can be geometrically extended to circular, cylindrical, spherical, or conical shells when curvilinear coordinate systems are used to formulate the FFSI problem (e.g. Khabakhpasheva et al., 2024).

*3.2.2.4. N-pendula idealisation.* A flexible body is assumed to be composed of a finite number of pendulum segments, and motions of each segment are solved using a local force balance, hence the model would be called a local force-balance model (Fig. 16). Fluid forces are calculated at the nodes. N-pendula idealisation can be very common in modelling very flexible structures, such as marine vegetation (e.g. Marjoribanks and Hardy, 2014), though it has also been used in modelling wave energy converters (e.g. Yurchenko and Alevras, 2013).

*3.2.2.5. Multi-rigid-body idealisation.* A flexible structure is idealised as a multi-rigid-body system connected via elastic beams, as shown in Fig. 17. Each rigid body represents a segment of the overall structure, moving as a rigid body but treated individually, with freedom in six degrees of freedom. The elastic beams connecting rigid bodies enable relative motion between them, representing the flexibility of solid bodies. This approach maintains displacement and rotational continuity between adjacent modules. Two distinct types of multi-rigid-body models have been used to date: Discrete Module Beam (DMB) models (e.g., Zhang and Lu, 2018) and Macro-Submodule Division, MBD, (e.g., Chen et al., 2023a). The former uses a single transverse division. The latter, however, considers a second direction, which allows multiple transverse discretisation across the structure.

*3.2.2.6. Discrete element idealisation.* The solid object may also be idealised as discrete elements (e.g. Fig. 18), with their motions governed by particle dynamics. These elements can fully or partially occupy a portion of the fluid domain and may collide with each other. Using such idealisation necessities the introduction of friction and damping terms in the modelling. This approach is commonly used in modelling the performance of ships in pack ice or ice loads on marine structures. More recently, this method has been applied to idealise the structural motions of an ice sheet covering water (e.g. He et al., 2022).

*3.2.2.7. Truss idealisation.* A truss is made up of elements that are connected to each other by joints. Each element of a truss is only subjected to axial loads that give rise to tension or compress stresses. Trusses can be either defined in a plane, or in space. The junction node of

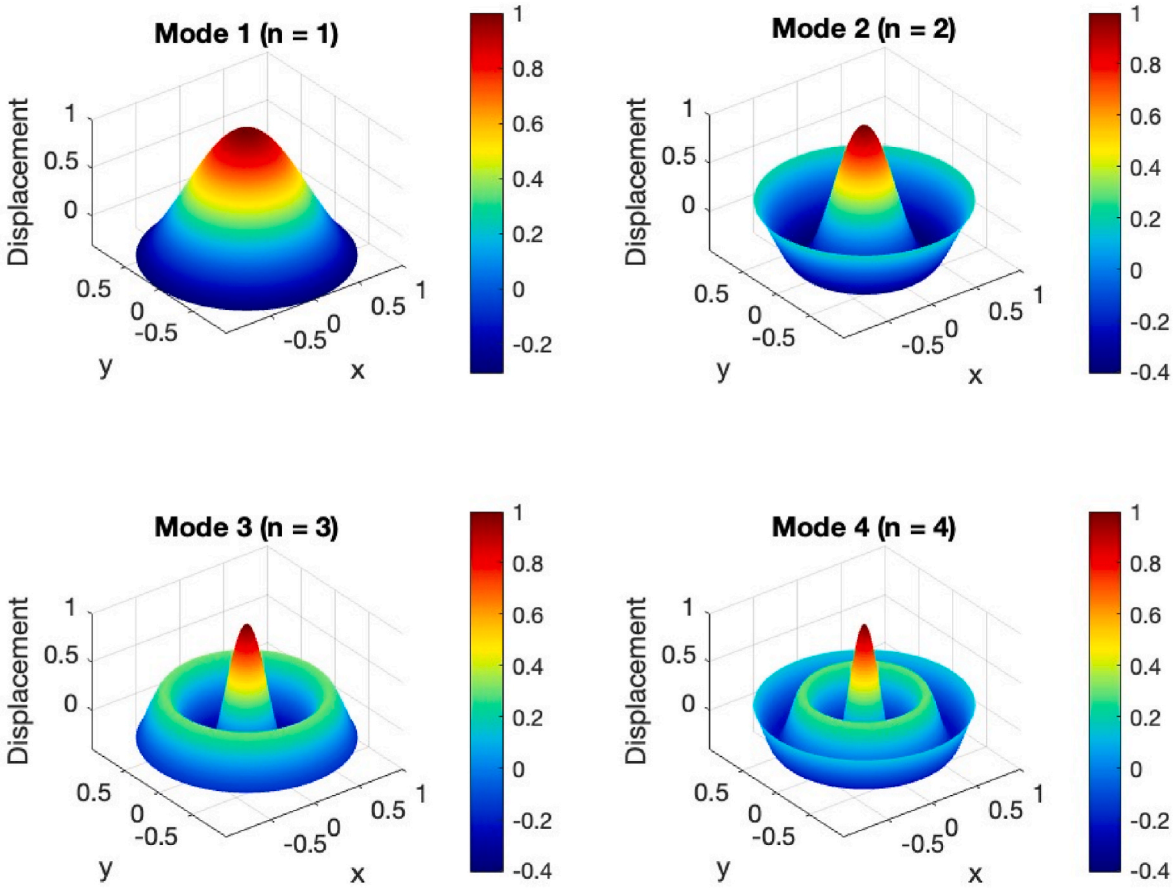


**Fig. 21.** First four dry mode shapes of a thin circular flexible plate.

**Table 6**
Possible pathways for solving the fluid and structural dynamics in the various FFSI problems discussed in this paper, along with the levels of nonlinearity they can accommodate.

| Fluid region | | Solid dynamic problem | | FSI-coupling in time domain? | Fluid-solid interface tracking? | Wave-structure interactions | Global ship hydroelasticity | Flexible slamming | Flexible marine propeller | Marine vegetation | Wave-mud interactions | Possible level of nonlinearity | | |
|---|---|---|---|---|---|---|---|---|---|---|---|---|---|---|
| Fluid dynamic solution? | Physically applied to the fluid domain? | Solid dynamic solution? | Physically applied to the solid domain? | | | | | | | | | Linear | Weakly nonlinear | Fully nonlinear |
| Frequency domain | Frequency domain | Frequency domain | Frequency domain | No | No | ✓ | ✓ | | | ✓ | ✓ | ✓ | | |
| Frequency domain | Time (HROM) | Frequency domain | Time (HROM) | Yes | No | ✓ | ✓ | | | ✓ | ✓ | | ✓ | |
| Time | Time (FOM) | Frequency domain | Time (HROM) | Yes | Yes | ✓ | ✓ | ✓ | ✓ | ✓ | ✓ | ✓ | ✓ | ✓ |
| Time | Time (FOM) | Time | Time (FOM) | Yes | Yes | ✓ | ✓ | ✓ | ✓ | ✓ | ✓ | ✓ | ✓ | ✓ |

a truss defined in a plane would have two transitional degrees of freedom, and that of a truss defined in space would have three transitional motions. In some FFSI models such as those idealising dynamic motions of flexible fish cage, truss elements are favoured (e.g. Moe et al., 2010; Li et al., 2013). Fig. 19 shows an example of the use of a truss model for idealisation of a net of a fish cage, the floating structure of which is idealised using a beam model.

*3.2.2.8. 3D geometry idealisation.* The last option to model a flexible structure is to use the full 3D geometry of the body. The full 3D model would represent the actual shape of the structure. However, the structure can either be modelled as a 3D solid volume (e.g. Huang et al., 2019) or, alternatively, the 3D geometry can be idealised, with different elements of the structure represented by some of the topologies described earlier (mixed topology), possibly combined with localised 3D solid volumes, though the connections between the elements need to be mathematically defined (e.g. Afshar et al., 2021). For example, when a ship hull girder is modelled as a 3D geometry using a mixed topology approach, the outer and inner shells are set to be shells, and the frames can be treated as beams.

In the case where a 3D solid volume is modelled, the governing equations are the balance of linear momentum in the continuum and needs to be solved over the full 3D solid domain without further idealisation, and in the mixed topology case, the governing equations for each element type are integrated into a single system of equations. When solving the problem for the full 3D geometry, either by considering the 3D solid volume or by an elemental idealisation of different parts of it, the equations governing the motions of the structure need to be solved numerically, which is most often done using FEM, though FVM-based approaches also exist (Cardiff and Demirdžić, I., 2021).

Fig. 20 shows the FE model of a 3D ship structure, developed by Afshar et al. (2021) on the basis of elemental idealisation. It is worth noting that in mixed topology idealisation, solid elements can still be used for localised components; however, the entire body is not represented solely by a 3D solid discretisation (see Fig. 20). Meshless methods can also be used for solving equations governing solid dynamics, though this is outside the scope of the present review paper (e.g. Lin et al., 2014; Leroch et al., 2016).

### *3.2.3. Nonlinearities*

Nonlinearity in solid mechanics arises from a distinct set of assumptions that may need to be considered when formulating FFSI problems in marine environments, depending on the mechanical behaviour of the solid body. Nonlinearity can originate either from the material properties (e.g., Liu et al., 2022a) or from geometric properties (Benjamin et al., 1999; Yoo et al., 2017). Materials exhibiting nonlinearity may display hyperelastic, plastic, elastoplastic, or other non-elastic behaviours. These phenomena are not covered in this review.

Geometric nonlinearity, on the other hand, must be introduced into the model when deformations are large. This is very common in the case the body is relatively very flexible (e.g. Su and Cesnik, 2011; Hasan et al., 2023; Gao et al., 2025), and due to the presence of external hydrodynamic loads that may result in nonlinear strain-displacement relations which dynamically vary over time. Nonlinear geometry can lead to changes in stiffness and may also result in buckling or instability. The importance of nonlinearity in marine structures has been emphasised since the 1980s by the ISSC (Pedersen, 1985), and the use of nonlinear FEM for strength analysis of marine structures is now documented in the recommendations of various classification societies (e.g., Det Norske Veritas, 2013; American Bureau of Shipping, 2021).

## *3.3. FSI modelling approach*

### *3.3.1. Frequency domain, time domain and reduced-order modelling*

Fluid and solid dynamics problems can be solved in either the

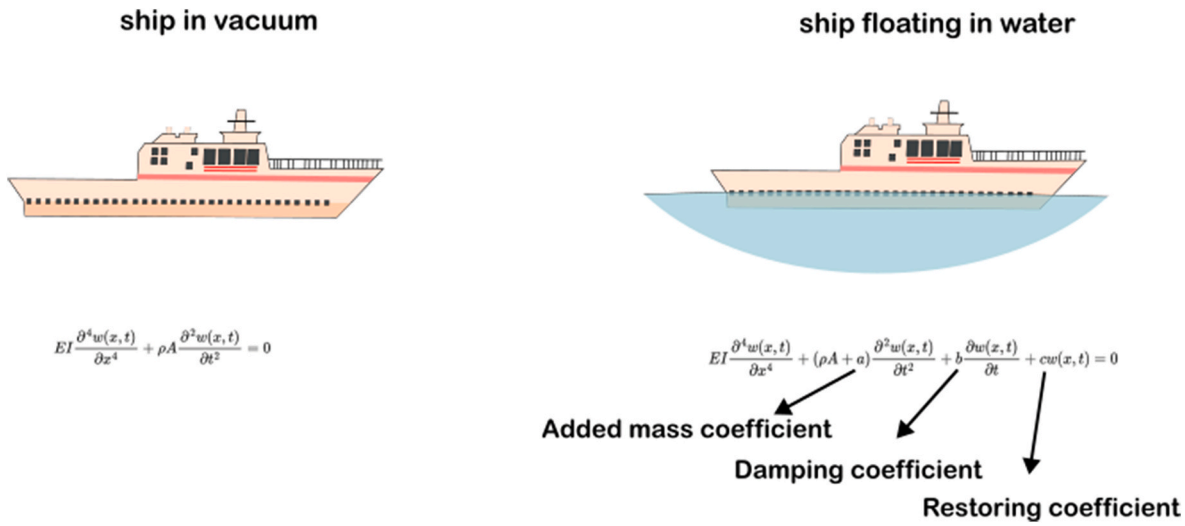


**Fig. 22.** An illustration of the difference between the concept of dry and wet modes of a flexible ship. The left side represents the ship in vacuum, where only structural stiffness and inertia determine the vibration characteristics, yielding free modes. The right side depicts the ship floating in water, where hydrodynamic effects modify the structural response. Added mass (shown by $a$) alters the effective inertia, damping (shown by $b$) accounts for energy dissipation due to wave radiation, and restoring forces (shown by $c$) influence the oscillatory behaviour, resulting in wet modes. This distinction is crucial for understanding fluid-structure interaction in hydroelasticity and ship motion analysis. Here $w$ is the vertical displacement along the ship, $EI$ is the ship rigidity, and $\rho A$ gives sectional displaced area.

**Table 7**
Importance of considering wet modes in the identification of elastic modes for different problems, with examples of both dry and wet mode analyses reported in the literature.

| Problem | Importance of wet mode analysis | Examples of wet mode analysis | Example of dry mode analysis |
|---|---|---|---|
| Flexible wave-structure interactions | Wet modes are better to be considered. | Humamoto and Fujita (2002) | Newman (1994) |
| Global ship hydroelasticity | Dry modes were mostly used in past, but most recent studies favour use of wet modes. | Hirdaris et al. (2003) | Hirdaris et al. (2003), Senjanović et al. (2008) |
| Flexible slamming | In the early stage of the slamming (inertia phase), dry modes are dominant, but in the whipping stage, the solid body responses in the wet modes. | Faltinsen (1997) | Kvalsvold and Faltinsen (1993, 1994) |
| Flexible marine propellers | If the propeller is fully submerged, wet are preferred to be used. | Young (2008) | Ghassemi et al. (2012), no added mass is considered |
| Marine vegetation | Wet modes are dominantly used. | Wei et al. (2024d) | N/A |
| Wave-mud interactions | While the fluid-solid interface of mud is fully wet, there is not much wet analysis available. | Nothing special is found | Mohapatra and Sahoo (2011) |

frequency or time domain. To solve a problem in the frequency domain, harmonic components must be identified (Newman, 1977; Mei et al., 2005). In fluid dynamics, excitation frequencies (e.g., wave frequencies) are the modes, whereas in the solid dynamic problems, the dominant modes of vibration must be identified either numerically (mostly often using FEM) or analytically (e.g. Kashiwagi, 1998; Meylan and Squire, 1996; Riyansyah et al., 2010). Fig. 21 shows the first four modes of a dry circular elastic plate.

In contrast, solving a problem in the time domain is achieved via a step-by-step evaluation of the dynamic response over time, and is referred to as a full order model (FOM) (Shi and Mei, 1996; Liu and Sakai, 2002). Some approaches bridge the frequency and time domain solutions by using frequency-domain solutions to reconstruct the time-domain response (e.g. Reinhard et al., 2013; Ilyas et al., 2018; Singh et al., 2023; Ucar et al., 2025). Such approaches are classed as highly reduced-order methods (HROM). In fluid dynamics, HROM are commonly achieved using weakly nonlinear inviscid approaches, such as nonlinear strip theory. For solid dynamics, modal analysis is widely adopted by HROM (modal superposition), which ultimately yields the time-dependent response of the solid body (e.g. Khabakhpasheva and Korobkin, 2013).

If both the fluid and solid problems are solved in the frequency domain, nonlinear effects cannot be captured, and there is no need to track the evolution of the fluid–solid interface over time, as all quantities are assumed to vary harmonically. Table 6 summarises the main differences between frequency-domain and time-domain approaches, along with the four possible modelling pathways based on the chosen simulation domain.

### 3.3.2. *Wet mode versus dry mode analysis of FFSI problem*

If vibration modes of the solid body are required, two different types of modes, “dry modes” (e.g. Newman, 1994; Senjanović et al., 2008) and “wet modes” (e.g. Humamoto and Fujita, 2002; Loukogeorgaki et al., 2012), can be used for the analysis of an FFSI problem. Dry modes are calculated for a solid body fully surrounded by air (also termed in vacuo), whereas wet modes are calculated by assuming that the solid body is surrounded by water, thereby incorporating added mass effects. Fig. 22 illustrates the difference between wet and dry mode calculations for a flexible ship, idealised as an elastic beam.

The choice between dry and wet mode analysis depends on the specific problem, the key outputs expected from the model, and the topology of the structure. However, wet mode analysis is generally more comprehensive. The concept of wet and dry modes has been introduced in ship hydroelasticity since its early development, but a comprehensive study distinguishing between dry and wet modes for ships is presented by Hirdaris et al. (2003). Table 7 summarises the importance of wet and dry modes for various problems. A comparison of wet and dry modes of flexible marine propellers is also presented by Li et al. (2020c).

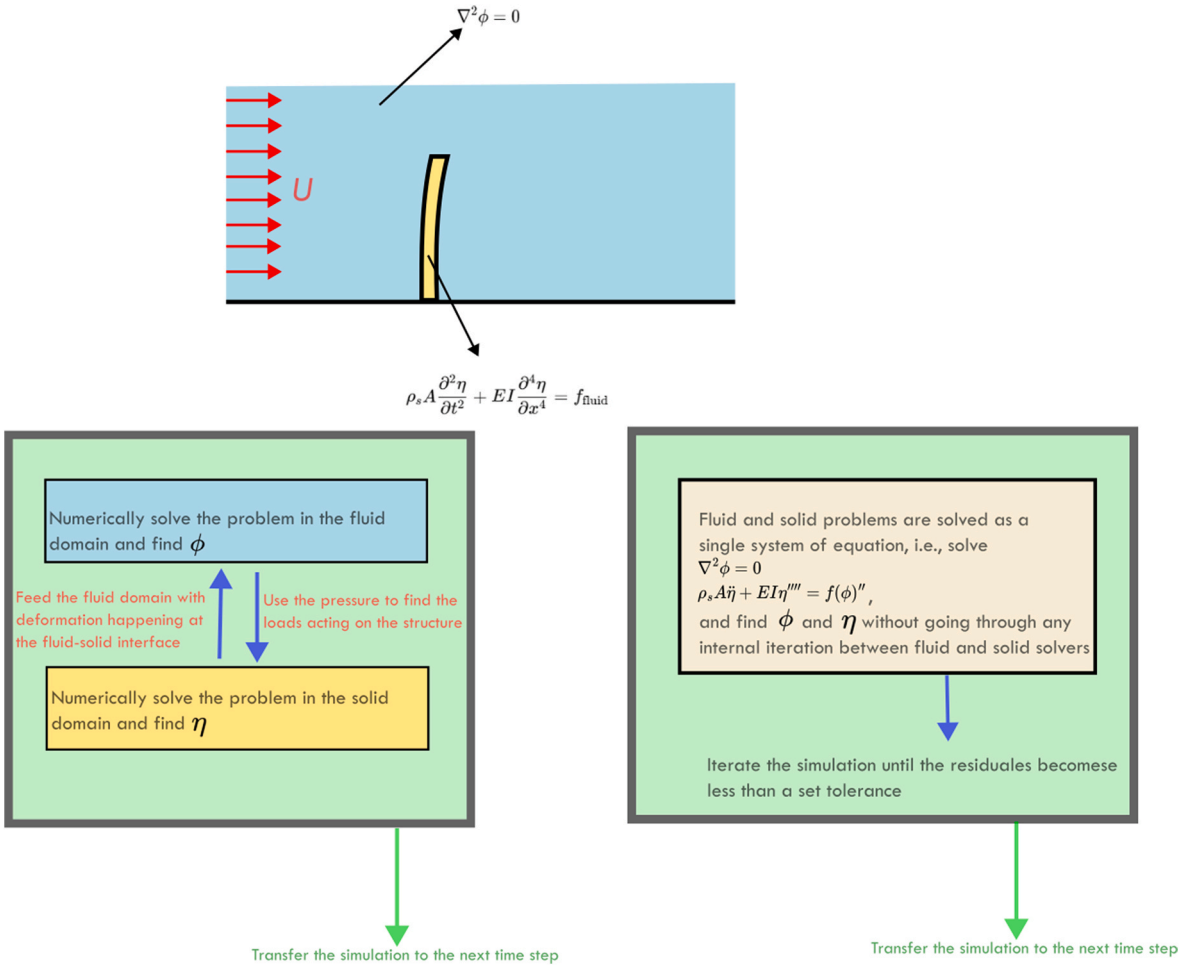


**Fig. 23.** A simplistic comparison between partitioned and monolithic approaches for FFSI modelling of an ideal fluid flowing around an elastic Euler–Bernoulli beam. When using the partitioned approach (left), fluid and solid domains are solved separately, with information exchanged at the fluid–structure interface through displacement and pressure coupling. When using monolithic method (right), the fluid and structural equations are simultaneously solved as a single nonlinear system, with an internal solver iteration to establish consistent interface conditions at each time step.

### 3.3.3. *Integration of fluid and solid dynamics solvers*

Fluid and solid dynamic solvers can be integrated or disintegrated. If they are integrated as a single system, where fluid and solid dynamic equations are solved together, the approach is called monolithic. The main advantage of monolithic approaches is reduced concern about the instability of computational algorithms. Linear ship hydroelasticity and flexible wave–structure interaction models are mostly built using monolithic approaches (examples of monolithic solvers are Colomés et al. (2022) and Agarwal et al. (2024)).

The alternative approach is known as the partitioned method, fluid and solid motion equations are solved separately. The solution of fluid and solid motion problems is transferred to each other through the fluid-solid interface. This dynamic evolution of governing equations may introduce computational problems, and establishing a stable framework for fluid-solid coupling becomes challenging. Fig. 23 shows the general difference between both methods.

### 3.3.4. *Fluid-solid interface tracking*

An approach to modelling an FFSI problem, from a mesh perspective, is to track the fluid–solid interface, which is mostly required when the fluid problem is solved over time. One class of methods is the body-fitted approach, in which the fluid domain is explicitly influenced by the dynamic or static responses of the solid body. The fluid mesh conforms to the structure and deforms as the solid body moves (El Aouad et al., 2022). The fluid–solid interface is typically tracked using the Arbitrary Lagrangian–Eulerian (ALE) approach (e.g. Sarrate et al., 2001; Donea et al., 2004; Kalliontzis, 2022). Using this approach, the mesh must be updated at each time step, which may require frequent remeshing. This can become computationally expensive and may lead to numerical instabilities when interface deformations are large.

In contrast, non-body-fitted approaches treat the solid body as being embedded within the fluid domain, without requiring the fluid mesh to conform to it (Mittal and Iaccarino, 2005). Instead, the influence of the solid is introduced via source terms added to the fluid equations (e.g. Peskin, 2002; Taira and Colonius, 2007). This class of methods is commonly referred to as Immersed Boundary Methods (IBM), as seen in various works in the literature (e.g. Jenkins and Maute, 2016; Tseng and Ferziger, 2003). In IBM, no remeshing is required, which makes the method well-suited to problems involving large deformations (Tian et al., 2014; Tschisgale et al., 2020. As noted by Zhang et al. (2004), IBM methods offer mesh simplicity, automatic interface tracking, and are highly compatible with modular partitioned coupling strategies. They are particularly popular in applications such as modelling flexible marine vegetation and flexible stems exposed to wave and current-induced flows (e.g. Prüter et al., 2025; Chen and Li, 2025), but they have also recently used for modelling the water entry problem by Di et al. (2024) and wave-structure interactions (fixed structure) by Luo et al. (2024).

### 3.3.5. *Coupling options*

When employing a partitioned method to formulate a flexible fluid-structure interaction problem, an important consideration is whether to establish mutual coupling between the fluid and solid solvers. This

decision primarily hinges upon the extent of the motion of the solid body.

A decoupled approach in designing an FFSI model or algorithm for solving problem neglects the influence of the solid motion on the fluid and assumes no momentum exchange across the fluid-solid interface over time. This method is particularly suitable when the motions of the solid are small. Conversely, a coupled approach accounts for the effects of the solid on the fluid domain, which favoured when the motions of the solid are relatively significant. This is a common practice in viscous modelling of ship hydroelasticity (flexible motions are not fed back to the fluid domain, e.g., Wilson et al., 2008).

Coupled fluid-solid methods can be classified into loosely coupled fluid-solid interaction modelling and tightly (fully) coupled FFSI modelling (e.g. Huang et al. (2019). This former a very common practice in modelling flexible slamming using LS-Dyna solver (e.g. Wang et al., 2021), and the latter provide superior accuracy.

There is also a third method which is referred to as semi-implicit method. A part of the fluid mesh is frozen and is considered in iteration until the convergence on both sides of the fluid and solid is established (e.g. Sy and Murea, 2008).

## 4. Physical tests and observations

This section reviews advancements in physical testing and observations of the flexible motions of solid bodies in the ocean. Experiments, for sure, provide an early understanding of physical phenomena and may yield valuable data for the validation of mathematical and computational models developed to solve such problems. Additionally, empirical or parameterised equations can be derived from experimental data, which may be directly implemented in climate models. While this review emphasises small-scale physical experiments conducted in laboratories (e.g., tanks, basins, cavitation tunnels), physical observations can also be made in real-world environments. This is more common for oceanic and coastal processes (e.g., Robin, 1963; Wadhams, 1972, 1978; Meirelles and Vinzon, 2016), although ship strain measurements may also be collected in the field (Andersen and Jensen, 2014).

A review of studies addressing each individual problem is presented in this subsection. However, for the problem of wave–structure interaction, we focus solely on wave interactions with ice, as this represents the interaction of a highly flexible body with waves. Readers interested in a review of experiments on wave–structure interactions are referred to Zhang and Schreier (2022).

When conducting experiments, both point measurements, either contact or non-contact, and field mapping techniques (such as Particle Image Velocimetry, PIV) may be employed. The choice between point-based or field-based measurements depends on the specific objectives of the study.

### 4.1. Wave-ice interactions

The early physical observations of wave-ice interactions were made through field measurements. The dispersion of waves in ice-covered water was initially observed by Ewing et al. (1934) and subsequently measured by Crary et al. (1952). Later, comprehensive field measurements of wave attenuation in the marginal ice zone (MIZ) commenced in the 1960s (Robin, 1963; Wadhams, 1972, 1975, 1979; Wadhams et al., 1988). The wave energy decay in ice fields was later observed to result from various mechanisms, including wave reflection by the ice, ice-ice collisions (Li et al., 2020b), the viscoelastic behaviour of the ice (Squire and Allan, 1977), and shear stresses arising from the nonlinear nature of the fluid (Kohout et al., 2011; Skene et al., 2015; Tavakoli and Babanin, 2021).

Wave-ice interaction tests can generally be categorised into two main types. The first focuses on investigating the dispersion and attenuation of waves as they travel through an extended ice cover, which may represent consolidated ice (i.e. long ice sheet), segmented ice covers,

**Table 8**
A summary of wave-ice interaction tests.

| Reference | Reported parameters | Facility | Finite length | Relatively long length | Tested cover/ floe |
|---|---|---|---|---|---|
| Martin and Kauffman (1981) | Wave attenuation and dispersion | Flume | | ✓ | Grease ice |
| Squire (1984) | Wave attenuation | Flume | | ✓ | Grease ice |
| Meylan (1993) | Wave reflection and/or transmission coefficients | Flume | ✓ | | Elastic floe |
| Newyear and Martin (1997) | Wave attenuation | Flume | | ✓ | Grease ice |
| Sakai and Hanai (2002) | Wave dispersion | Flume | | ✓ | Segmented elastic cover |
| Wang and Shen (2010) | Wave attenuation and dispersion | Basin | | ✓ | Grease ice |
| Montiel et al. (2013a, 2013b) | Modal analyses | Basin | ✓ | | Elastic discs |
| Toffoli et al. (2015) | Wave reflection and/or transmission coefficients | Flume | ✓ | | Elastic 1D floe |
| Meylan et al. (2015a) | Modal analyses | Basin | ✓ | | Elastic 2D floe |
| Bennetts et al. (2015) | Wave reflection and/or transmission coefficients | Basin | ✓ | | Elastic 2D floe |
| Sutherland et al. (2017) | Wave attenuation | Flume | | ✓ | Elastic covers |
| Nelli et al. (2017) | Wave reflection and/or transmission coefficients | Flume | ✓ | | Elastic 1D floe |
| Sree et al. (2017, 2018) | Wave attenuation and dispersion | Flume | ✓ | ✓ | Viscoelastic covers |
| Dolatshah et al. (2019) | Wave attenuation and ice breakup | Flume | | ✓ | Freshwater ice |
| Bennetts and Williams (2015) | Wave attenuation | Basin | | ✓ | Array of elastic discs |
| Rabault et al. (2019) | Wave attenuation | Flume | | ✓ | Grease/ pancake ice |
| Yiew et al. (2019) | Wave attenuation and dispersion | Flume | | ✓ | Grease ice/ consolidated ice cover/ grease-pancakes/ segmented cover |
| Cheng et al. (2019) | Wave attenuation | Ice Basin | | ✓ | Segmented scaled ice cover |

(continued on next page)

**Table 8** (*continued*)

| Reference | Reported parameters | Facility | Finite length | Relatively long length | Tested cover/ floe |
|---|---|---|---|---|---|
| | and dispersion | | | | |
| Parra et al. (2020) | Wave attenuation | Flume | | ✓ | Grease ice/ consolidated ice cover |
| Sree et al. (2020) | Wave attenuation and dispersion | Flume | | ✓ | Segmented viscoelastic covers |
| Passerotti et al. (2022) | Wave attenuation | Ice basin | | ✓ | Freshwater scaled ice |
| Toffoli et al. (2022) | Wave attenuation | Basin | ✓ | ✓ | Array of elastic discs and Elastic 2D floe |
| Brown et al. (2022) | Elastic motions | Flume | ✓ | | Elastic 1D floe |
| Huang et al. (2022a) | Wave reflection and/or transmission coefficients | Basin | ✓ | | Elastic 2D floe |
| Behnen et al. (2025) | Wave reflection and/or transmission coefficients | Flume | ✓ | | Elastic 1D floe |

grease ice, grease ice-pancake ice, frazil ice, or pancake ice (e.g. Martin and Kauffman, 1981; Sree et al., 2018).

Several methods exist for creating this ice cover. Ice can be formed directly in the tank (e.g. Dolatshah et al., 2019; Yiew et al., 2019), purchased as ice cubes from a supermarket (e.g. Dolatshah et al., 2019a, b), or represented using a polymer sheet placed on the water (e.g. Sree et al., 2018). When forming ice in the tank, one approach involves spraying ice onto the surface to create an ice layer, as practised in the Aalto Ice Tank (e.g. Passerotti et al., 2022). Alternatively, the tank environment can be cooled to sub-zero temperatures, allowing ice to form naturally, a method previously employed at the University of Washington and the University of Melbourne (e.g. Dolatshah et al., 2019).

The mechanical properties of ice generated through these two methods can vary significantly. Ice formed by spraying typically exhibits a lower Young's modulus. Yet ice formed under sustained sub-zero conditions may reach a Young's modulus of approximately 3 GPa (e.g. Dolatshah et al., 2019). However, given the scaled nature of laboratory experiments, achieving a Young's modulus equivalent to natural sea ice may be relatively high for a scaled-down test. In tanks maintained at sub-zero temperatures, the combined influence of waves and wind can lead to the formation of grease ice or grease ice-pancake mixtures (Martin and Kauffman, 1981; Rabault et al., 2019).

Long polymer plates have also been used to represent ice covers in laboratory tests (artificial ice). Owing to their lower elastic modulus, these materials can be well-suited for scaled-down experiments (e.g. Sree et al., 2017, 2018). Similarly, elastic discs can be placed on the water surface over a defined area to mimic pancake ice (e.g. Bennetts and Williams, 2015).

In the second group of experiments, the focus is on studying the interaction between a flexible ice floe and water waves, where the length of the floe is comparable to the wavelength. In these experiments, wave reflection and transmission coefficients are measured alongside the elastic motions of the flexible body (e.g. Nelli et al., 2017).

In both types of experiments, water surface elevation is measured using probes or wave gauges, and the flexible motion of the ice floe/ cover can be measured via strain gauges or accelerometers. The overwash on the upper surface of the ice floe can also be measured by a wave gauge (e.g. Bennetts et al., 2015). Field measurements of the fluid flow around the ice are very limited and have only been reported in one of the studies conducted by Rabault et al. (2019).

While the focus of most studies is on wave decay along the ice and the flexible motion of the ice, along with wave reflection/transmission by the ice, other experimental studies in the field of wave–ice interaction may also be conducted. These can relate to ice drift (e.g. Meylan et al., 2015b), ice rafting (Dolatshah et al., 2019a,b), and ice–ice collision (Yiew et al., 2017). However, although these studies are affected by flexible motion of ice cover/floe, they do not directly investigate FFSI, and for this reason, they are not covered in the present review paper.

The main parameters that need to be considered when scaling flexible ice depend on the specific focus of the experiment. Assuming that a flexible cover, whether an elastic sheet, a viscoelastic polymer, or artificial ice, is generated on the water surface, the scaling of elasticity can be achieved using dimensionless numbers that govern fluid-structure interactions. An elasticity number is introduced as per

$$\widetilde{G} = \sqrt{\frac{G}{\rho_s}} \Big/ \sqrt{g h_s}, \tag{4-1}$$

where $G$ is the shear modulus of the solid cover, $\rho_s$ is the density of solid cover, $g$ is gravitational acceleration and $h_s$ is the thickness of the solid cover. This parameter has been utilised by Yu et al. (2019a) to present dimensionless dispersion relationships for ice-covered oceans. Another important non-dimensional number is the Reynolds number for waves propagating through a viscoelastic cover, which characterises the ratio of inertial forces to viscous forces within the cover (Yu et al., 2019a). It is given by

$$\widetilde{R} = h_s \sqrt{g h_s} \Big/ \nu_s, \tag{4-2}$$

where $\nu_s$ is kinematic viscosity of ice. The wavenumber and wave attenuation rate are normalised to facilitate comparison across different scales as

$$\widetilde{k} = k h_s, \quad \text{and} \quad \widetilde{\alpha} = \alpha h_s. \tag{4-3}$$

Wave frequency is normalised as

$$\widetilde{\omega} = \omega \sqrt{h/g}\,. \tag{4-4}$$

Other non-dimensional numbers, such as wave steepness, are also of significant importance. In problems where the focus is on wave reflection and transmission by a single ice floe, wave reflection and transmission coefficients need to be introduced. Additionally, RAOs of elastic modes, caused by vertical bending moments, should be presented as a function of the ratio of wavelength to the length of the ice cover (e.g. Meylan et al., 2015a). Tests will be introduced in the rest of this sub-section, a detailed summary of which is outlined in Table 8.

#### 4.1.1. *Long ice cover tests*

Long ice cover tests have been conducted since the 1980s and are often considered more traditional compared to wave interaction experiments with single floes. However, performing such tests is considerably more challenging due to the requirement to generate ice within the tank. The earliest related experiments were designed and carried out in a wave flume at the University of Washington by Martin and Kauffman (1981). Grease ice covers were produced by maintaining sub-zero temperatures under the combined influence of waves and wind. The authors reported the corresponding attenuation rates across different frequencies. Subsequently, Squire (1984) along with Newyear and Martin (1997) conducted another series of tests in the same tank. A simple schematic of the wave interaction test with grease ice is sketched in Fig. 24a. A series of other tests with grease ice and grease ice-pancake formations were performed by Wang and Shen (2010), Rabault et al.

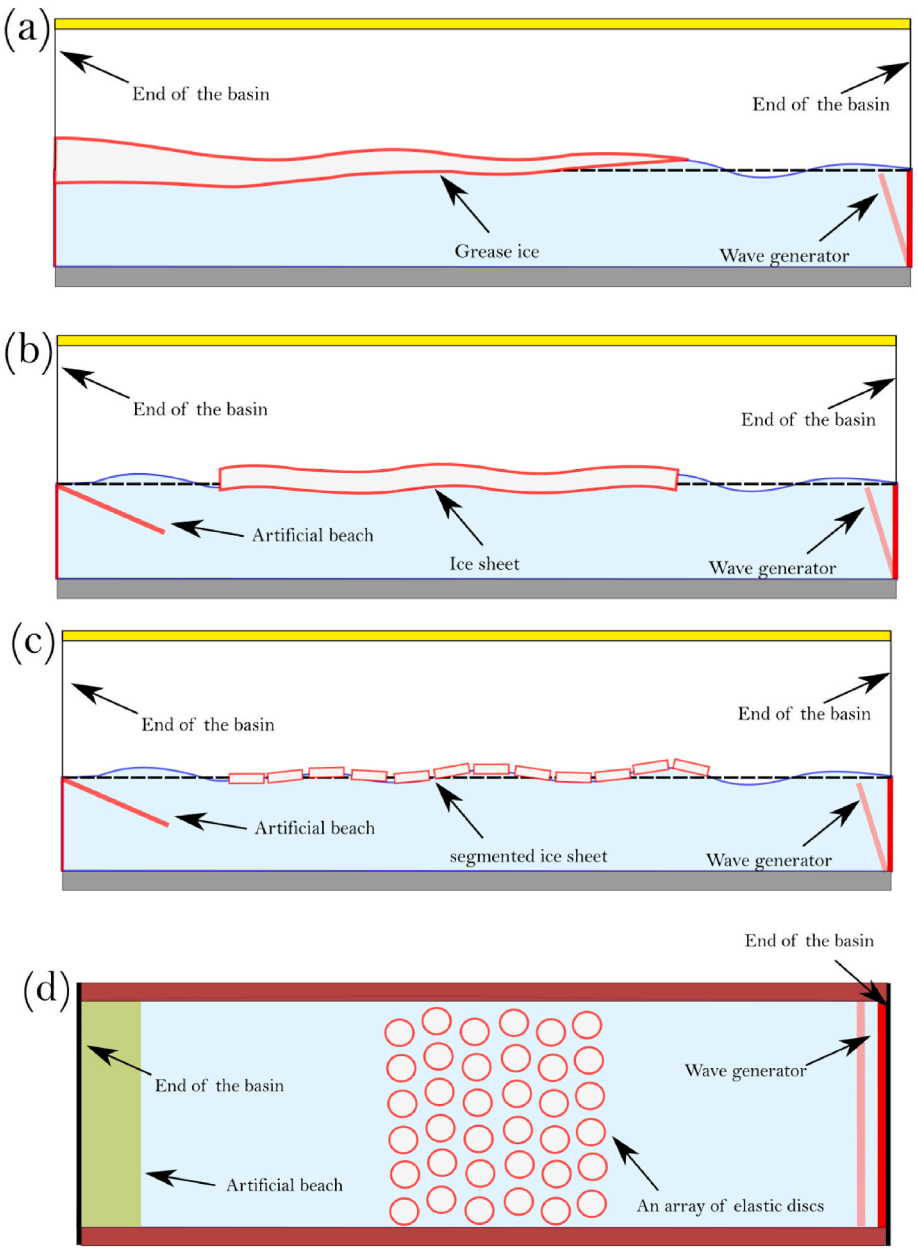


**Fig. 24.** Schematic of common wave-ice interaction tests: (a) grease ice, (b) ice sheet, (c) segmented ice cover, (d) elastic ice discs.

(2019), Yiew et al. (2019) and Parra et al. (2020).

Consolidated ice cover tests have been conducted more recently. An illustrative schematic of such a type of test is shown in Fig. 24b. As mentioned earlier, using flexible covers to represent ice has become a common practice for such experiments. The earliest study was performed by Sutherland et al. (2017). Sutherland et al. (2017) placed three different elastic covers on the surface of a flume and tested the wave attenuation rates for each cover. The authors did not report wave dispersion, as the effects of elasticity on wave dispersion within such a low-frequency range was hypothetically believed to be negligible. Similar tests on viscoelastic covers were later conducted by Sree et al. (2017, 2018). Both wave attenuation rates and wave dispersion were measured and reported. The authors noted that overwash might also influence dispersion, although they did not report the overwash depth. Similar tests were conducted on naturally formed ice by Dolatshah et al. (2019) and Yiew et al. (2019).

Later, Passerotti et al. (2022) undertook an experimental study to examine the interaction between irregular waves and ice covers in the 40m by 40m Aalto Ice Tank. The study focused on the temporal evolution of the ice edge, the progression of the breaking front, floe size distribution, and the evolution of the wave spectrum in terms of wave energy, mean wave period, and spectral bandwidth as waves propagated into the ice cover. A wave energy attenuation coefficient was derived, following a power-law dependency on frequency.

Tests on segmented ice (Fig. 24c) date back to the early 2000s. Credit goes to Sakai and Hanai (2002), who hypothesised that segmenting an elastic ice cover into smaller floes would influence wave dispersion. Initial experiments measured the dispersion of waves propagating into an unsegmented elastic cover with a length of 8m. Subsequent tests involved segmenting the cover into smaller elastic pieces, with the smallest segments measuring 0.25min length. Similar tests were later conducted by Sree et al. (2020). And a series of test on segmented ice cover formed in an ice basin was conducted by Cheng et al. (2019).

The first test on an array of elastic discs exposed to water waves, representing pancake ice, was conducted by Bennetts and Williams (2015). Two different disc concentrations were tested. The wave

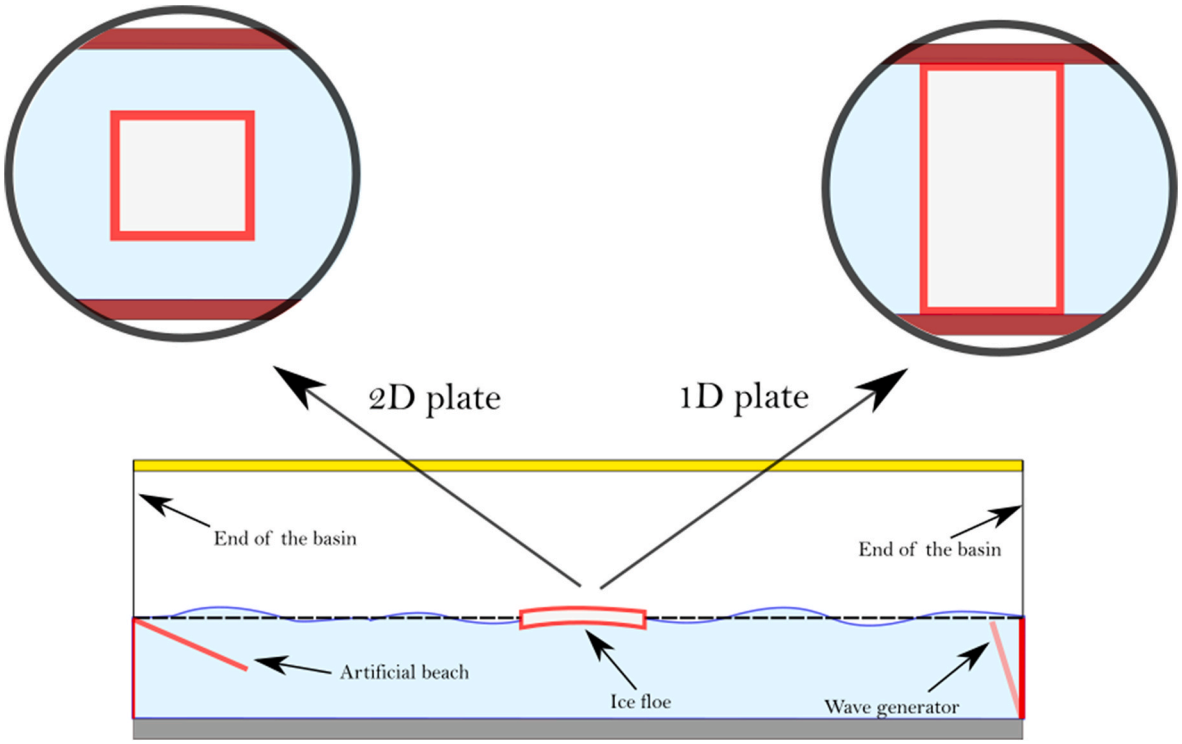


**Fig. 25.** Schematic of wave-ice interaction tests for ice floes.

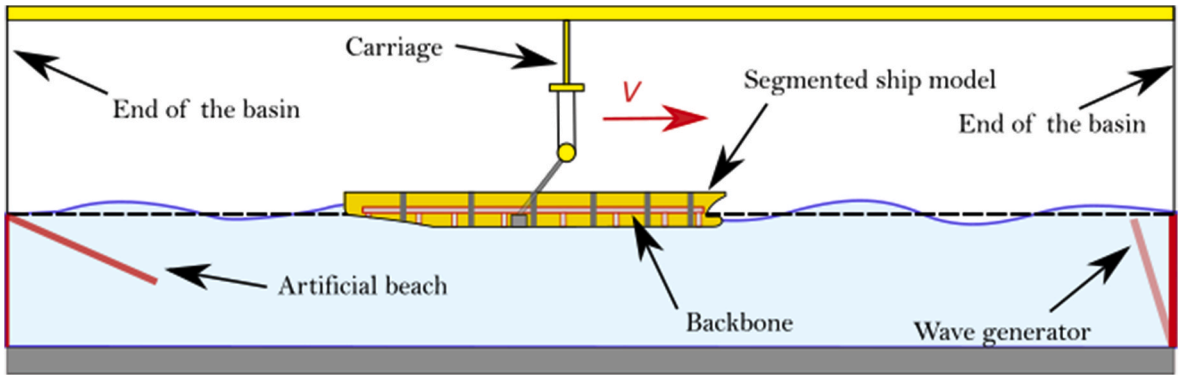


**Fig. 26.** Schematic of a flexible ship test in a towing tank.

transmission coefficients for both configurations were reported as functions of wave periods and wave amplitudes. Toffoli et al. (2022) later presented and analysed results from irregular wave tests conducted with both disc concentrations. A top-view schematic of the wave interaction with elastic discs is shown in Fig. 24d.

The results of the tests mentioned above have significant applications in global wave modelling and in advancing the understanding of wave physics within marginal ice zones. However, they did not include directional waves across the various ice covers studied in the experiments discussed in this subsection.

#### 4.1.2. *Ice floes*

Model tests on the interaction of ice floes with water waves are more recent than to those focusing on wave interactions with long ice sheets or grease ice. These experiments first emerged in the 1990s, but there was a hiatus until they resumed in the early 2010s. This set of experiments targeted both 1D and 2D floes.

The 1D floe experiments were conducted by placing a finite-length plate on the water, covering the entire width of the flume (Fig. 25). In contrast, the 2D experiments are conducted by placing a flexible thin plate or elastic disc in a wide basin. While these tests share similarities with ship hydroelasticity experiments, or flexible wave-structure interactions, such as those carried out by Yago and Endo (1996), the key characteristic that makes them unique and particularly relevant to wave-ice interactions is the very shallow draught of the ice floe. This shallow draught allows for the potential emergence of overwash.

The first set of experiments mimicking wave interaction with a single elastic ice floe was conducted by Meylan (1993), representing a 1D elastic floe. After two decades, another series of 1D experiments on wave interaction with a single 1-m-long ice floe was conducted by Toffoli et al. (2015). The authors demonstrated that overwash-induced energy dissipation occurred at higher steepness values, suggesting that linear potential flow models may not be suitable for accurately modelling such wave-ice interaction under such forcing conditions. Later, Nelli et al. (2017) conducted a similar set of tests, this time comparing effects of an ice floe on wave motions under free-to-drift and restricted-drift conditions. Other recent 1D floe experiments in wave flumes were carried out by Brown et al. (2022) and Behnen et al. (2025).

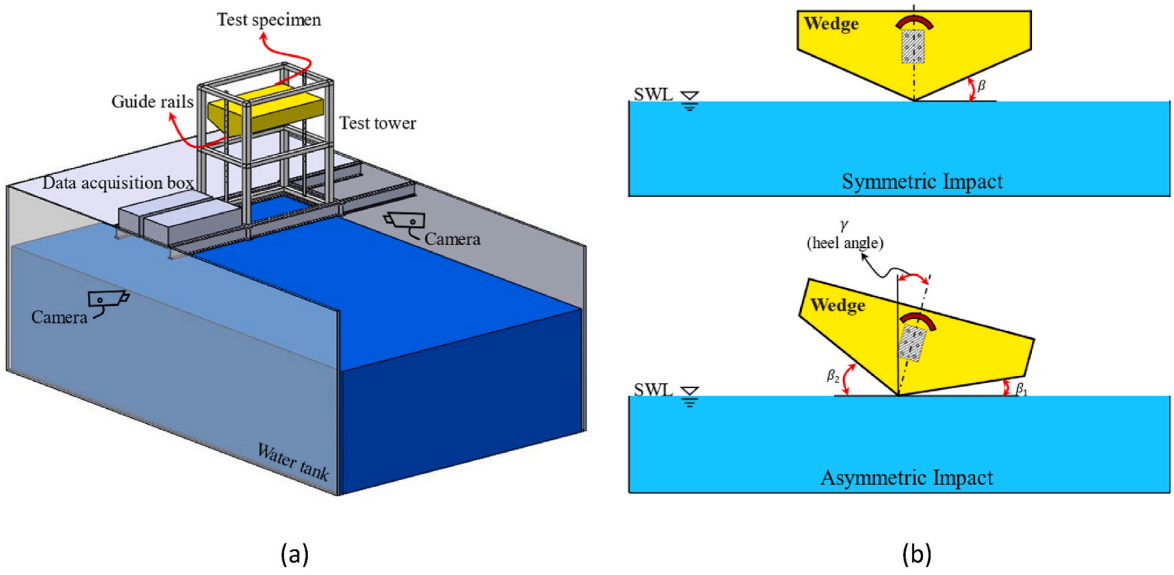


**Fig. 27.** A schematic view of tank experiments; a) slamming test setup of a 3D section b) a 2D view of symmetric and asymmetric impact.

A series of tank tests examining the elastic responses of a floating disc exposed to regular waves was performed and analysed by Montiel et al. (2013a, b). In Montiel et al. (2013a), only the vertical motions at various points on the disc were presented and analysed. The modelling and analysis of the elastic motions of discs were further detailed in Montiel et al. (2013b).

The first experiments on 2D plates were conducted by Bennetts et al. (2015), who investigated wave transmission and reflection using two different 1 m × 1 m flexible plates in a wave basin. The study demonstrated that flexural motion significantly contributes to wave reflection, thereby reducing the wave transmission coefficient. The RAOs of the first four elastic modes of the plates were also reported by Meylan et al. (2015a). The results of tests with irregular waves were later presented by Toffoli et al. (2022). A very recent 2D ice floe experiment was carried out by Huang et al. (2022a).

### 4.2. Flexible ship tests

A major challenge when testing flexible ship models is the concurrent scaling of structural and fluid aspects. In an ideal maritime world, we would be able to perform perfect Froude scaling of all aspects, and since viscous effects are less important in ship hydroelasticity, this would be perfectly sufficient. Indeed, the external geometry of the ship must be Froude scaled, so that its interaction with the gravity waves is correct. However, if all the structure was Froude scaled as well, it would mean that:

a) All structural elements, however small, are reproduced at model scale.
b) The thickness of all elements scales linearly, as do all other dimensions.
c) The elastic modulus of the material scales linearly as well.

The first point is already quite problematic: traditional manufacturing methods do not allow to produce such level of detail, even if the cost of the model was not an issue. The advance of additive manufacturing allowed the introduction of significantly more structural detail than before (see Grammatikopoulos et al. (2020); Grammatikopoulos et al. (2021); Keser et al. (2023)). Nevertheless, the second point is still a limitation, as there is a minimum thickness which can be produced. Additionally, models with small wall thickness are increasingly fragile, which can rapidly become an issue during handling and testing. The third point is perhaps the most crucial limitation, as the limited range of materials which can be used for such applications would result in very few (and specific) scaling factors being available, which can also come in contradiction with the capabilities of testing facilities, in terms of maximum model size and scaling of forward speed and waves.

It is evident that this process is quite restricting, leading virtually all researchers to the use of the so-called "distorted" models (Harris and Sabnis, 1999). The term refers to scaled models where unimportant aspects are not scaled (which is already the case with the lack of Reynolds scaling), and less important aspects can be less accurately scaled, assuming that the impact of these deviations can be quantified. An example of that is the common use of segmented models for ship hydroelasticity (Fig. 26): the external shell of the ship is manufactured as rigid segments, which are linked together by a somewhat artificial stiffness source, usually either a backbone/beam (e.g. Dessi and Mariani (2008)) or a series of flexible joints (e.g. Lavroff et al., 2013). In both of these cases, the stiffness distribution along the length of the ship can be uniform or non-uniform, with the former generating a more distorted model. In pursuit of a more detailed response, some researchers use continuous models, often manufactured from polyurethane (or similar) foam, which tend to include the external shell, the main deck, and the transverse bulkheads of the vessel (e.g. Houtani et al., 2018). The aforementioned additively manufactured models, which include significantly more structural detail, have been a recent development and they still appear sparsely in the literature. Further discussion regarding the different types of models used in hydroelastic experiments of ships were recently published by Grammatikopoulos (2023).

### 4.3. Flexible slamming tests

Flexible slamming tests are conducted to measure dynamic response or hydrodynamic loads during the water entry process, or they may also report velocity and pressure field around the section entering the water (e.g. Panciroli and Porfiri, 2015). Conducting these tests is challenging due to large structural deformations and the extremely short duration of impact events. Capturing localised variables, such as impact pressure, requires high sampling rates (e.g. Van Nuffel, 2014). This necessitates advanced instrumentation and precise experimental setups to ensure accurate and reliable data. Fig. 27a illustrates a schematic view of a traditional drop test system. Depending on the experimental objectives, various instruments can be employed to accurately measure the required data. A comprehensive list of flexible slamming tests is presented in

**Table 9**
An overview of experimental studies measuring impact induced loads and structural responses (NR: Not Reported, NA: Not Applicable, PVC: Polyvinylchloride, GFRP: Glass fibre reinforced plastics, PE: Polyethylene, PP: Polypropylene). This table is an updated and extended version of that presented in Hosseinzadeh et al. (2023a).

| Authors | Tank dimension (m) | Structure dimension (m) | Deadrise (deg.) | Mass (kg) | Material | Plate thickness (mm) | Impact velocity, Drop height (m/s, m) | Test Condition | Structure |
|---|---|---|---|---|---|---|---|---|---|
| Peseux et al. (2005) | 1.2 × 1 | R = 0.32 (Cone) | 42461 | NR | Aluminium, Steel | 0.5,1,1.5, 25 | 2–8 m/s | Symmetric | Rigid and Flexible |
| Yettou et al. (2006) | 30.0 × 2.0 × 1.0 | 1.2 × 1.2 | 25 | 94, 112, 130, 148 | Plywood | 19 | 1.0 and 1.3 m | Symmetric | Rigid |
| Tveitnes et al. (2008) | NR | 0.3 × 0.6 | 0–45 | 2.8–5.2 | PVC sheet with aluminium | 10 | 0.24–1.19 m/s (Constant Velocity) | Symmetric | Rigid |
| Lewis et al. (2010) | 5.8 × 0.75 × 0.59 | 0.944 × 0.735 × 0.22 | 25 | 23.4 and 33.4 | Plywood | 18 | 0.5 and 0.75 m | Symmetric | Rigid |
| Huera-Huarte et al. (2011) | Slingshot Impact Testing System | 0.3 × 0.3 (Flat plate) | 0.3–25 | 38 | Sandwich panel | | Up to 5 m/s | Symmetric | Rigid |
| Luo et al. (2012) | 24 × 8 × 8 | 2.88 × 3.36 × 1.3 | 22 | 3250 | Steel | 3, 4 | 0.3–2.5 m | Symmetric | Flexible |
| Panciroli et al. (2012) | 1.6 × 1 × 0.6 | 0.3 × 0.25 | 15–35 | NR | Aluminium (6068-T6), GFRP | 2, 4 | 0.5–3 m | Symmetric | Flexible |
| Stenius et al. (2013) | 3.5 × 1.3-1.4 | 1 × 0.5 | 10 and 20 | 18.3, 10.1, 31.9 | GFRP | 9.5, 2.5,3 | 0.5–7.0 m/s | Symmetric | Flexible |
| Panciroli and Porfiri (2014) | NR | 0.2 × 0.15 | 30 | 0.48 | Aluminium (6061-T6) | 1 | 0.25–1.0 m | Symmetric | Flexible |
| Van Nuffel (2014) | 1 × 1 × 0.6 | Cylindrical and Flat plate | NA | various | Steel, Aluminium, Ertalon, PVC, GERP, PE, PP | various | 0.1–1.2 m | Symmetric | Flexible |
| Allen and Battley (2015) | 3.5 m diameter cylindrical water tank | 1.03 × 0.58 | 10 | NR | Fibre, Composite Panel | varios thickness | 1.0–6.0 m/s | Symmetric | Flexible |
| Swidan et al. (2016) | Servo-hydraulic Slam Testing System (SSTS) | 0.5 × 0.638 × 0.327 (Catamaran hull form) | NA | 14.8 | Glass reinforced plastic | 10 | 2.5–5 m/s | Symmetric | Rigid |
| Barjasteh et al. (2016) | 1.122 × 0.572 × 0.681 | 0.53 × 0.41 | Various | 44 | Steel | 8 | 0.2–0.75 m | Symmetric and Asymmetric | Rigid |
| Eastridge and Taravella (2017) | 30.8 × 4.6 × 2.4 | 1.45 × 1.19 × 0.53 | 20 | 186.9 | Aluminium (5086-H116) | 6.35 | 0.15–0.61 m | Symmetric | Flexible |
| Korkmaz and Güzel (2017) | 1.7 × 1.0 × 1.2 | Cylinder and Sphere | NA | 11, 12, 16 | Aluminium, Acrylic, UPVC | 2, 4, 10 | 0.05–4 m | Symmetric | Flexible |
| Shams et al. (2017) | 0.8 × 0.32 × 0.1 | 0.203 × 0.193 | 25 | NR | Aluminium | 0.6 | 1.25 m/s | Symmetric | Flexible |
| Hassoon et al. (2017) | 3 × 2 × 1.1 | 0.5 × 0.25 | 10 | 3.7, 6, 8 | Composite Panels | 8, 13 | 4.0–10.0 m/s | Symmetric | Flexible |
| Sun and Wang (2018) | 4 × 4 × 2 | 1.6 × 1.2 (Flat Plate) | 0 | 112 | Steel | 2.5 | 0.5–2.0 m | Symmetric | Flexible |
| Russo et al. (2018) | 0.8 × 0.32 × 0.35 | 0.19 × 0.2 | 37 | 0.89 | Balsa wood panel | NA | 0.5 m | Asymmetric | Rigid |
| Wang et al. (2019) | 13.7 × 2.4 × 1.35 | 1.22 × 0.38 (Flat plate) | 0 | NR | Polycarbonate and Aluminium (6061-T6) | 12.7 and 7.94 | 3.1, 4.1, 5.1 m/s | Oblique | Rigid and Flexible |
| Dong et al. (2019) | 108 × 7 × 3.5 | 1.5 × 0.9 × 0.75 | 45 | 553 | Aluminium, Steel | 4, 5 | 0.25–1.0 m | Symmetric | Flexible |
| Tödter et al. (2020) | 6 × 1.5 × 0.75 | 0.3 × 0.3 × 0.2 (Flat Plate) | 0 | 18.5, 20.3 | Aluminium (5083), POM | 4.7,12 | 0.52–1.04 m/s | Symmetric | Flexible |
| Duan et al. (2020) | 30 × 4 × 1 | 0.3 × 0.7 | 0–40 | 282 | Aluminium, Steel | 1, 2, 4,10 | 0.1–1.0 m | Symmetric | Flexible |
| Seo and Shin (2020) | 3.5 × 4 × 5 | 2 × 1.2 × 0.28 | 10 | 340 | Steel | 3, 5, 8 | 1.0 and 1.7 | Symmetric | Flexible |
| Mai et al. (2020) | 35 × 15.5 × 3 | 0.25 × 0.25 (Flat Plate) and 0.56 × 0.6 (truncated vertical wall) | NA | 52 | Aluminium | 12 | 1–7 m/s | Symmetric | Flexible |
| Ren et al. (2021) | 4.4 × 2.4 × 1.2 | 0.635 × 0.57 × 0.409 | 20 | 40.65 | Aluminium (6061-T6), Composite | 3.17,12.7 | 0.079–0.508 m | Symmetric | Flexible |
| Iafrati et al. (2021) | 470 × 13.5 × 6.5 | 1.25 × 0.650 (Flat plate) | NA | 850, 950 | Aluminium (2024-T3), Composite | 0.8, 1.65, 3 | 30–47 m/s | Oblique | Flexible |
| Hosseinzadeh and Tabri (2021a) | 60 × 5 × 3 | 1.5 × 0.94 × 0.45 | 20–30 | 55 | Aluminium (5083-H111) | 4 | 0.25 m | Symmetric | Flexible |
| Spinosa and Iafrati (2021) | 470 × 13.5 × 6.5 | 1 × 0.5 (Flat Plate) | 0 | NR | Aluminium (2024-T3) | 0.8,3,15 | Horizontal Impact | Symmetric | Flexible |

(continued on next page)

**Table 9** (*continued*)

| Authors | Tank dimension (m) | Structure dimension (m) | Deadrise (deg.) | Mass (kg) | Material | Plate thickness (mm) | Impact velocity, Drop height (m/s, m) | Test Condition | Structure |
|---|---|---|---|---|---|---|---|---|---|
| Meziane et al. (2022) | hydraulic shock test-rig | 0.56 × 1.1 × 0.34 | 30 | 47.26 | Aluminium (6061-T651) | 5 | Up to 10 m/s (Constant Velocity) | Symmetric | Flexible |
| Liu et al. (2022b) | NR | 1.1 × 0.9 × 0.542 (Truncated stern) | NA | 256 | Fiberglass | 8 | 0.25–0.9 m | Symmetric | Rigid |
| Chen et al. (2023b) | 108 × 7 × 3.5 | 1.5 × 0.9 × 0.75 | 45 | 553 | Steel | 5 | 0.1–1.0 m | Symmetric | Flexible |
| Hosseinzadeh et al. (2023a) | 60 × 5 × 3 | 1.5 × 0.94 × 0.45 | Non-prismatic | 55, 82.5 | Aluminium (5083-H111) | 4 | 0.25–2.0 m | Symmetric | Flexible |
| Pan et al. (2024) | 15 × 5 × 3 | Trimaran section | 35, 70 | NR | Steel | 1.0, 2.0 | 1.5–5.26 m/s | Symmetric | Flexible |
| Xie et al. (2024a) | NR | 1.2 × 0.8 × 0.316 (Flat plate) | NA | 784 | Steel | 2 and 4 | 0.25–0.7 m | Asymmetric | Flexible |
| Hosseinzadeh and Tabri (2024) | 60 × 5 × 3 | 1.5 × 0.94 × 0.45 | Non-prismatic | 55 | Aluminium (5083-H111) | 4 | 0.25 and 0.5 m | Asymmetric | Flexible |

Table 9, detailing the geometry of the impacting body, the nature of the slamming event, mechanical properties, and the dimensions of the test tank used. Note that this table is an extension of the one presented in Hosseinzadeh et al. (2023a).

#### 4.3.1. *Symmetric flexible slamming tests*

One of the earliest experiments on the slamming of deformable bodies was conducted by Chuang (1970). Free-fall drop tests of rigid and elastic flat plates with wedge sections were carried out to investigate the effects of air entrapment and structural elasticity on hydrodynamic pressure during impact. In subsequent experiments, Chuang (1973)

**Table 10**
A summary of flexible marine propeller tests.

| Reference | Propeller Diameter (meters) | Number of Blades | Material | Test section | Measuring tool | Test type |
|---|---|---|---|---|---|---|
| Maljaars et al. (2017) | 0.34 | 2 | Glass-epoxy laminate | Turning lathe | DIC | Static loading |
| Kumar et al. (2019) | 0.45 | 3 | CFRP and Aluminium | Towing tank | Load cell and Height gauge | Static loading |
| Rokvam et al. (2021) | 0.6 (height) | Single blade | CFRP (carbon fibre-reinforced polymer) | Cavitation tank | DIC and Strain gauges | Static loading |
| Seaver et al. (2006) | 0.6096 | 1 | CFRP | Water tunnel | FBG sensors and Dynamometer | Steady elastic |
| Lin et al. (2009) | 0.305 | 5 | Composite | Cavitation tank | Photography | Steady elastic |
| Hara et al. (2011) | 0.68 and 0.25 | 3 | Polyvinyl chloride (CFRP and PVC) | Cavitation tank | Tracing laser beam and Dynamometer | Steady elastic |
| Paik et al. (2013) | 0.25 | 5 | Carbon/epoxy and Glass/epoxy | Cavitation tank | Dynamometer, PIV, Hydrophone | Steady elastic |
| Taketani et al. (2013) | 0.25 | 5 | Aluminium, Dry-Carbon, Nylon Powder | Cavitation tank | Propeller dynamometer and Acrylic window (wire-meshed screen) | Steady elastic |
| Savio (2015) | 0.25 | 4 | Aluminium and Plastic | Towing tank | Digital stereo imaging system | Steady elastic |
| Maljaars et al. (2018) | 0.34 | 2 | Bronze and epoxy | Cavitation tank | DIC | Steady elastic |
| Kawakita (2019) | 0.25 | 5 | Aluminium and Resin | Cavitation tunnel | Wire mesh system and Propeller dynamometer | Steady elastic |
| Savio et al. (2020) | 0.25 | 4 | Aluminium and Casting resin epoxy | Towing tank | Dynamometer | Steady elastic |
| Ding et al. (2022) | 0.22 | 4 | Composite | Towing tank | FBG sensors | Steady elastic |
| Shiraishi et al. (2023) | 0.22 and 0.25 | 5 | Aluminium and Carbon-filled nylon | Cavitation tunnel | Charge-coupled device (CCD) camera | Steady elastic |
| Savio et al. (2024) | 0.25 | 4 | Aluminium and Casting resin epoxy | Cavitation tunnel | S-PIV, S-DIC, Propeller dynamometer | Steady elastic |
| Young et al. (2016) | 0.61 and 0.3048 | 6 and 5 | Composite and Aluminium | Cavitation tunnel | LDV and High-speed camera | Dynamic response |
| Javdani et al. (2016) | 1.9 | 5 | NR | Water tank | FBG sensors | Dynamic response |
| Zondervan et al. (2017) | NR | 5 | Composite | Wave Basin | DIC | Dynamic response |
| Tian et al. (2017) | 0.25 | 7 | Bronze and Plastic | Water tunnel | LDV, Wake screen, Accelerometer | Dynamic response |
| Grasso et al. (2019) | 1 | 2 | Composite | Cavitation tunnel | DIC | Dynamic response |
| Maljaars et al. (2020) | 1 | 4 | Nickel–aluminium bronze (NAB) and Composite | Sea trials | Stereo camera system | Dynamic response |
| Zou et al. (2017) | 0.317 | 5 | Aluminium alloy | Water tank | Strain gauges and Accelerometer | Dynamic response |
| Ducoin et al. (2023) | 1.2 | 1 | Carbon fibre fabric | Towing tank | LDV and FBG sensors | Dynamic response |

observed a reduction in impact pressure for flexible bodies, attributing this to the effect of elasticity. Later, Aarsnes (1994) conducted full-scale measurements of slamming-induced strains, which were subsequently reviewed by Faltinsen (2000).

Experiments continued in the following decades, with two particularly notable studies conducted in the 2000s and 2010s. The first was carried out by Peseux et al. (2005), who were the first research team to conduct free-fall tests on cone-shaped flexible bodies. They investigated the effects of structural flexibility on hydrodynamic pressure during impact. Later, Stenius et al. (2013) employed a Servo-hydraulic Slam Testing System (SSTS) to study the hydroelastic slamming of three different composite panels with a deadrise angle of 10-degrees. They analysed hydroelastic effects by comparing deflections and strains from constant-velocity experiments on both rigid and elastic bodies with corresponding rigid reference solutions obtained via a numerical model.

#### 4.3.2. Asymmetric and oblique flexible slamming tests

Apart from the symmetric cases, which are the dominant ones listed in Table 9, asymmetric (heeled) and oblique slamming tests have also emerged over time. The setup for the former can be seen in Fig. 27b. Oblique condition tests are typically conducted at high horizontal speeds to replicate the ditching of seaplanes (e.g. Iafrati et al., 2021). Performing such tests is more challenging compared to symmetric water entry, as a non-symmetric flow pattern must be accurately reproduced in the experimental setup.

A notable experimental study on the water entry of flexible asymmetric wedges was conducted by Shams et al. (2017), who investigated the impact behaviour of a highly flexible body at various heel angles. Another significant contribution to flexible ditching tests was made by Iafrati et al. (2021), who carried out two extensive experimental campaigns. The test setup was specifically designed at the National Research Council (NRC) of Italy and was defined by Dr. Alessandro Iafrati. Recently, a series of drop experiments under oblique impact conditions was conducted by Xie et al. (2024a) to investigate the effects of slamming loads on flexible thin-walled structures. The experiments covered a range of drop heights and inclination angles. The results showed that, despite lower loads on the leeward side, the stress responses remained comparable to those on the windward side.

#### 4.3.3. From point sensors to full-field imaging in flexible slamming tests

Full-field imaging of the fluid flow around a flexible body entering water, as well as the solid displacement of the structure itself, have also been incorporated into flexible water entry/slamming tests. A pioneering study in this area was conducted by Panciroli et al. (2015), who used PIV to measure the fluid field around curved wedges during water entry. Subsequently, Panciroli and Porfiri (2015) applied this technique to measure the velocity field around a flexible aluminium structure.

More recently, Ren et al. (2021) investigated hydroelastic slamming effects on flexible wedges. They employed a comprehensive set of instruments, including accelerometers, pressure sensors, strain gauges, and a stereoscopic digital image correlation (S-DIC) system, to measure the kinematic motions of flexible body, spray root propagation, hydrodynamic pressure, and strain responses.

#### 4.3.4. Repeatability and uncertainty of flexible slamming tests

Studies have also been conducted to improve understanding of the repeatability and uncertainty associated with flexible water entry experiments. The first study addressing this aspect was conducted by Lewis et al. (2010). The authors performed an uncertainty analysis on the recorded data during water entry tests to ensure the accuracy and reliability of the measurements. Other notable studies were conducted by Van Nuffel et al. (2013, 2014). In the former, the authors found that, due to the short duration of impact events, pressure should be measured at rates above 300 kHz to accurately capture peak values. They recommended a sampling rate above 8 kHz for slamming force measurements and stressed the need for precise dynamic sensor calibration.

#### 4.3.5. Future research direction

Several aspects of flexible slamming remain not fully understood and can be further explored through experimental testing. These include the detailed mechanisms of fluid-structure interaction, the influence of material properties on impact dynamics, and the effects of varying heel angles on slamming loads. Additionally, the use of new technologies in experimental setups, such as advanced imaging techniques and high-speed data acquisition systems, enables more accurate sampling of impact pressures and structural deflections.

### 4.4. Flexible marine propeller tests

In the physical model testing of flexible marine propellers, thrust force, torque, deformations, and the natural frequencies of the blades are key parameters that are measured. Tests are conducted under uniform or non-uniform flow conditions. They may be designed to measure either performance or steady and dynamic responses, while also allowing for the measurement of other properties such as fluid flow patterns, pressure, and sound pressure levels of rotating propellers (e.g. Paik et al., 2013).

Scaling is of great importance when conducting tests in towing tanks or cavitation tunnels. (Motley and Young, 2012). The performance of the propeller can be identified by the thrust coefficient, torque coefficient, and advance coefficient, which are respectively presented as follows:

$$K_T = \frac{T}{\rho_w D^2 n^2 D^4}, \tag{4–5}$$

$$K_Q = \frac{Q}{\rho_w D^2 n^2 D^5}, \tag{4–6}$$

$$J_A = \frac{V_A}{nD}. \tag{4–7}$$

In the above equations, $T$, $Q$ and $V_A$ represent thrust, torque, and advance speed, respectively, and $D$ denotes the propeller diameter. Here, $n$ is the rotational speed of the propeller (rotation per second). The structural related coefficients (Young, 2010) are also expresses as

$$\alpha_E = \frac{E}{\rho n^2 D^2}, \tag{4–8}$$

$$\alpha_{BT} = \frac{GJ}{EI}, \tag{4–9}$$

$$\alpha_C = \frac{K}{EI}, \tag{4–10}$$

$$\alpha_\rho = \frac{\rho_w}{\rho_s}. \tag{4–11}$$

Here, $E$ is the elastic modulus of the propeller, $G$ is the shear modulus of the propeller, and $K$ is the effective bending–twisting coupling rigidity. More details on scaling laws for flexible propellers are presented in Young (2010).

In the context of hydroelastic analysis of marine propellers through physical tests, three major clusters of tests can be identified in the literature. The first type of tests is performed to understand the elastic behaviour of a propeller subjected to a static point load (e.g. Rokvam et al., 2021). The second set of tests focuses on the elastic motions, deflection, and changes in the pitch of a flexible propeller under steady loads (uniform flow pattern). These tests can be conducted either in cavitation tunnels or towing tanks (e.g. Lin et al., 2009). The third cluster of tests is dynamic in nature. In these tests, scholars focus on the dynamic response of propellers subjected to non-uniform flow conditions (e.g. Maljaars et al., 2020). Free vibration tests, conducted to measure the natural frequency of the propeller, are also reported in the literature (Javdani et al., 2016). A detailed list of experimental tests on flexible marine propellers is provided in Table 10.

#### 4.4.1. Static tests

In static experiments, a propeller is placed in a cavitation tank and subjected to a static fluid load, with deflections measured using strain gauges or cameras. The work of Rokvam et al. (2021) is an example of such experiments. The load was applied to the propeller blade by suspending metal weights from two specific loading points. The authors employed DIC to measure the deflection of the blade. Additionally, strain gauges were attached to the blade to measure the strain developing in the propeller blade. Two other sets of experiments applying static loads to composite propellers were conducted by Maljaars et al. (2017) and Kumar et al. (2019). In the study conducted by Maljaars et al. (2017), deflections were measured using the DIC method.

#### 4.4.2. Uniform flow and steady elastic deformation

In these tests loads are generated under a uniform flow regime, and as stated the main driver of these tests is the need to understand the self-adaptation behaviour of composite propellers. In the literature, one of earliest experimental studies on the hydroelasticity of flexible composite propellers under dynamic load is the work of Chen et al. (2006a). The deflection of the flexible composite propellers was monitored using high-speed cameras.

Another experimental study on composite propellers was conducted by a team of researchers from the Naval Research Laboratory (Seaver et al., 2006). In these tests, fibre Bragg grating (FBG) sensors were used to measure the strains developing in a composite propeller, with experiments carried out in a water tunnel under uniform flow conditions. The research by Seaver et al. (2006) appears to be the first (at least publicly available) instance where the FBG method was used to measure the structural response of flexible marine propellers.

Another experimental study was later conducted by Lin et al. (2009), who tested three different composite propellers. These tests were performed in a cavitation tank. Propeller performance was measured for all cases at moderate rotational speeds, while blade tip deflection was assessed by comparing images taken during the tests, superimposing the deflected and undeflected blade shapes. Other similar tests were conducted by Hara et al. (2011), Paik et al. (2013), and Taketani et al. (2013).

Some other tests were conducted by Maljaars and Dekker (2014) and Maljaars et al. (2018) between 2014 and 2018. Firstly, Maljaars and Dekker (2014) conducted experimental tests on the performance and blade deflections of composite propellers subjected to steady flow. A notable innovation in their experiments was the use of a correlation technique to measure tip displacements and axial deformations at the mid-chord points of the propeller. Later, Maljaars et al. (2018) extended their experiments to validate a potential-based flow model they developed for simulating fluid flow around flexible propellers. They noted that experiments on larger scales or with highly flexible composite blades would be preferable, as these could potentially reduce the uncertainties associated with the measurements.

A set of experimental tests on the performance and deflection patterns of flexible propellers in uniform flow was conducted by Savio (2015) at the MARINTEK towing tank. Savio (2015) used a DSI system to measure the deflection pattern across the flexible propeller blades. Later, Savio et al. (2020) conducted a more comprehensive study on the performance of three different propeller designs under uniform flow conditions. In a follow-up study, Savio et al. (2024) extended their previous work by measuring the wake flow of one of the propellers using PIV. Savio et al. (2024) concluded that no specific fluid flow pattern could be directly correlated to the elasticity of the blades. Another set of experiments was carried out by Savio and Koushan (2019).

Other recent experiments on flexible propellers in a uniform flow pattern can be found in the research conducted by Kawakita (2019), Ding et al. (2022), and Shiraishi et al. (2023). Interestingly, Kawakita (2019) tested reverse rotation conditions and observed unstable vibrations in the propeller, representing a unique set of physical tests conducted to date.

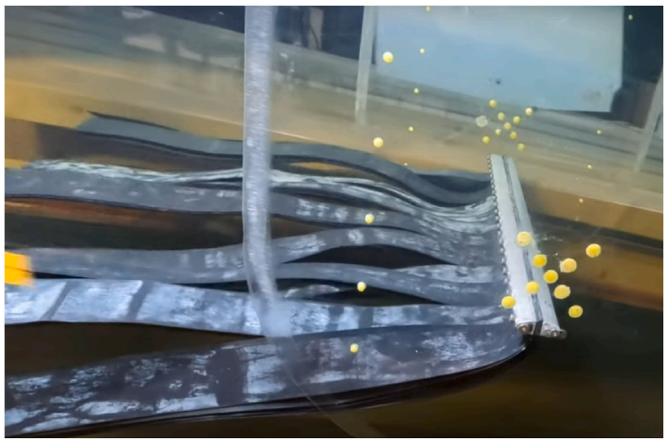

**Fig. 28.** Model test of artificial kelp blades under forced oscillations in a wave flume at NTNU Trondheim to understand the flow around the blades and the dynamic responses of the blades.

#### 4.4.3. Non-uniform flow and dynamic responses

Non-uniform flow tests first require the generation of a specific flow pattern. This is typically achieved by positioning the propeller behind the ship and conducting tests in towing tanks. The appendages attached to the ship can induce vortices, resulting in unsteady flow that may expose the propeller to non-uniform conditions. It can also be caused by placing a wake screen on the path of the flow.

One of the earliest non-uniform flow tests was carried out by Chen et al. (2006a). The authors reported that, under the effects of non-uniform flow, the performance of a no-twisting propeller was decreased, while that of a self-twisting propeller was increased. In parallel, Seaver et al. (2006) conducted non-uniform flow tests and measured the strains in a propeller blade using a fibre Bragg grating-based sensor network. It was observed that the strains measured over a very short period exhibited nearly sinusoidal patterns near the hub, whereas farther out, the temporal pattern of strain became more complex, resembling square waves.

Zondervan et al. (2017) and Maljaars et al. (2020) applied the DIC technique to measure the hydro-structural performance of a propeller positioned behind a model ship. Specifically, Maljaars et al. (2020) addressed the uncertainties associated with the experiments before validating a numerical potential-based flow model developed to simulate the hydroelastic behaviour of flexible propellers. Other non-uniform flow tests were conducted by Grasso et al. (2019) and Tian et al. (2017), with the former employing PIV to measure the fluid motion around the flexible propeller.

More recently, a distinct investigation into the dynamic response of a composite propeller was carried out by Ducoin et al. (2023). The authors examined the dynamic response of a propeller blade in a towing tank, testing various carriage speeds without any rotational motion while considering different angles of attack. They reported the strains (measured via fibre Bragg gratings) experienced by the blade, as well as the fluid forces acting on the propeller. The time histories of the strains were also analysed through spectral analysis.

### 4.5. Marine vegetation tests

Due to the challenges in numerically modelling the dynamic responses of flexible vegetation canopies in waves and currents, model tests are commonly used to understand the hydrodynamic loads and structural responses of the vegetation, as well as wave attenuation resulting from the interaction between vegetation motion and fluid flow.

#### 4.5.1. Key parameters

Three key dimensionless parameters have been defined by Luhar and

**Table 11**
A summary of the field observations of wave-mud interaction.

| Study | Location | Wave Type | Observed Dissipation | Wave decay Mechanism/ Physical observation |
|---|---|---|---|---|
| Gade (1958) | Louisiana coast | Long waves | Up to full attenuation | Viscous dissipation |
| Wells and Coleman (1981) | Suriname coast | Solitary-like waves | ~90 % energy loss over 20 km | Mud interaction |
| Mathew et al. (1995) | SW India | NR | Complete attenuation with mudflats, <25 % without | Mudflats effects are observed |
| Forristall and Reece (1985) | Mississippi Delta | Wind waves (nonlinear, wave height-dependent) | Increased with wave height | Nonlinear attenuations are observed |
| Sheremet and Stone (2003) | Louisiana inner shelf | Short and high-frequency waves | Significant damping | Challenges long-wave-only assumption |
| Elgar and Raubenheimer (2008) | Louisiana shelf | Sea (4s), swell (7s), infragravity (14s) | >70 % energy flux reduction | Energy transfer across spectrum is observed |
| Meirelles and Vinzon (2016) | Cassino Beach, Brazil | Wave periods of 3.75–18.7 s | Significant damping | Fluid mud interaction |
| Traykovski et al. (2015) | Louisiana shelf | Peak wave period of 7–10 s | Greatest dissipation during high energy | Transition from turbulent to laminar flow in fluid-mud layer |
| Sheremet et al. (2011) | Atchafalaya inner shelf | Seas between 0.5 and 1 m significant height and swells that peaked 1.5 m significant height | Strong dissipation | Wave-bed coupling |
| Safak et al. (2017) | Atchafalaya Shelf | Broad-spectrum waves during storm with the spectral peak of 0.13 Hz | Maximal during hindered-setting fluid mud phase (post-storm), secondary peak during bed-reworking | Mud-induced dissipation reverses nonlinear energy cascade |
| Rogers and Holland (2009) | Cassino Beach, Brazil | Wind waves (typical periods 8–12 s) | Significant nearshore damping; overprediction without mud physics | Viscous dissipation in fluid mud layer |
| Winterwerp et al. (2012) | Wadden Sea | Peak wave period of 4 s | Wave damping | Viscous dissipation in fluid mud |
| Liu et al. (2022c) | Yellow River delta | Significant wave periods of 4.21–8.60 s | Increased fluid mud thickness | Wave-induced liquefaction |

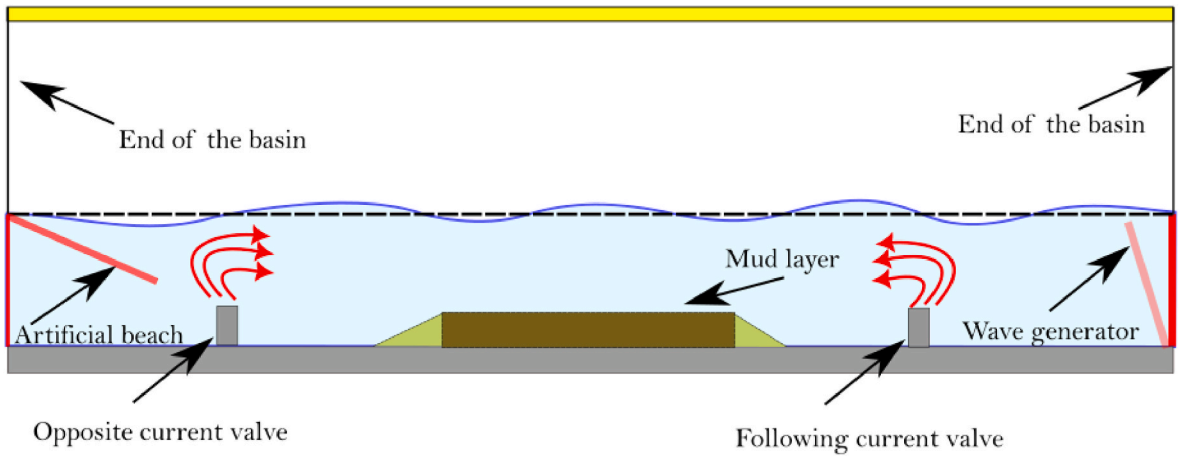


**Fig. 29.** A schematic of wave-mud interaction tests.

Nepf (2011, 2016), namely the buoyancy number $B$ defining the ratio of plat buoyancy force to the restoring force due to plant rigidity, the Cauchy number $C_a$ defining the ratio of hydrodynamic force to the restoring force due to plant rigidity, and the length ratio L defining the ratio of vegetation length ($l$) to wave orbital excursion $A_w = \frac{U_w}{\omega} = U_w T_w/(2\pi)$, with $T_w$ as wave period, $U_w$ as fluid-particle velocity and $\omega$ as the wave angular frequency. Those three parameters are defined as following:

$$\mathrm{B} = |\Delta\rho| g V_p, \mathrm{C_a} = \frac{\rho A U_{max}^2 l^2}{EI}, \mathrm{L} = \frac{l}{A_w}, \tag{4–12}$$

Here, $\Delta\rho$ is the difference between the water density ($\rho$) and that of the plant ($\rho_p$). $g$ is the gravitational acceleration. $V_p$ is the volume of the vegetation element. $E$ is the elastic modulus, and $I$ is the second moment of area. $A$ is the plant frontal area without reconfiguration.

In case of combined wave and current, the Cauchy number can be redefined using the maximum horizontal velocity $U_{max} = U_m + U_w$ (Luhar and Nepf, 2016). For vegetation that has higher density than that of the fluid, the buoyancy number may also be named as equivalent weight number. The length ratio L is equivalent to the Keulegen-Carpenter (KC) number.

#### 4.5.2. Morphology and mechanical property

Physical or numerical models that aim to replicate flow-vegetation interactions require the morphological and mechanical characteristics of vegetation found in coastal waters. However, this information remains insufficient. The three dimensionless parameters mentioned earlier define the scaling laws that should be followed when performing model tests to extrapolate the behaviour of full-scale vegetation. Unlike manmade structures, where mechanical properties are known before construction, vegetation properties vary. To design laboratory experiments that are geometrically and dynamically similar to marine vegetation, appropriate materials must be selected to ensure that the Cauchy

**Table 12**
An overview of experimental studies measuring wave-mud interactions (NR: Not Reported).

| Study | Mud type | Mud rheology | Bulk density | Mud viscosity (Pa · s) | Mud thickness (m) | Water depth (m) | Wave type | Wave period (s) | Damping coefficient ($m^{-1}$) |
|---|---|---|---|---|---|---|---|---|---|
| Gade (1958) | Natural mud | Newtonian | 1.75 | 2667 | <0.82 | 1.22 | Monochromatic wave | 8 | 0.005–0.023 |
| Sakakiyama and Byker (1989) | Commercial kaolinite | Viscoelastic | 1.23 | 0.4–19.87 | 0.09–0.095 | 0.3 | Monochromatic wave | 0.6–2.0 | 0.005–0.2 |
| Maa and Mehta (1990) | Commercial kaolinite/ natural mud | Viscoelastic | 1.12–1.16 | 26–1150 | 0.11–0.15 | 0.182–0.287 | Monochromatic wave | 1.0–1.9 | 0.02–0.18 |
| De Wit and Kranenburg (1996) | Commercial kaolinite/ kaolinite and muscovite | Non-Newtonian | 1.31/1.57 | 3.55/0.33-0.7 | 0.2 | 0.3 | Monochromatic wave +current | 1.5 | 0.03/0.02 |
| Zhao et al. (2006) | Natural mud | Viscoelastic | 1.19–1.4 | 1–23 | 0.06–0.12 | 0.2–0.38 | Monochromatic wave +current | 0.82–1.61 | 0.019–0.139 |
| Soltanpour and Samsami (2011) | Commercial kaolinite/ natural mud | Viscoelastic and viscoplastic | 1.77/1.75 | 4-4300/50-8000 | 0.08 | 0.181–0.24 | Monochromatic wave | 0.7–1.4 | 0.033-0.251/ 0.036-0.180 |
| Hsu et al. (2013) | Commercial kaolinite | Non-Newtonian | 1.42 | 1.64–10.59 | 0.06 | 0.3 | Monochromatic | 0.6–2.1 | 0.022–0.071 |
| Soltanpour et al. (2014) | Commercial kaolinite | Viscoelastic | NR | 29–9000 | 0.1 | NR | Irregular wave +current | 0.781–0.850 | 0.015–0.211 |
| Almashan and Dalrymple (2015) | Commercial kaolinite | Viscoelastic | 1.25–1.35 | 7.6–8.4 | 0.1 | 0.44 | Wave groups | 0.60–0.66 | 0.009–0.031 |
| Soltanpour et al. (2018) | Commercial kaolinite | Viscoelastic | NR | NR | 0.11 | 0.3 | Monochromatic wave +current | 0.7–1.7 | 0.02–0.27 |
| Aleebrahim and Jamali (2023) | Commercial kaolinite | Newtonian | 1.12 | 0.0014–0.002 | 0.06 | 0.2 | Monochromatic wave | 1.05–1.14 | NR |
| Robillard et al. (2023) | Natural mud | Elastoviscoplastic and thixotropy | 1.19 | 0.06–115 | 0.08 | 0.19 | Monochromatic wave | 1.25–1.6 | 0.099–0.163 |

and buoyancy numbers remain within the same range as those of the full scale.

One possibility is to take vegetation samples from the ocean. Examples of this approach can be found in Vettori and Nikora (2017) and Lei et al. (2021). However, a challenge with this approach is that marine vegetation, such as seaweed, may degrade quickly if not stored or transported properly, leading to significantly different mechanical properties.

Another approach is what most of the work reported in the literature has followed. Different materials have been used in different research groups. For instance, Polyethylene was used by Vettori and Nikora (2017), while HDPE and silicone foam were used by Luhar and Nepf (2011).

#### 4.5.3. Deformation of vegetation (reconfiguration)

Fluid loads, such as drag forces, cause deformation (also referred to as reconfiguration in the literature) of the vegetation blade. Reconfiguration reduces drag through two mechanisms: first, it decreases the frontal area of the vegetation, and second, the reconfigured shape tends to be more streamlined (De Langre, 2008). To quantify the reduction of drag loads due to reconfiguration, Luhar and Nepf (2011) proposed the concept of effective blade length (lel_ele). For uniform currents, the authors have developed a simplified model to predict lel_ele and the horizontal drag force.

Experimental tests have been conducted with different types of ambient flows, including:

- Current only (e.g. Luhar and Nepf, 2011; Lei et al., 2021; Vettori and Nikora, 2021)
- Waves (e.g. Zhu et al., 2020a; Zhu et al., 2022)
- Uniform oscillatory flows (e.g. Leclercq and de Langre, 2018)
- Combined wave and current (e.g. Zhang and Nepf, 2022, 2024)

An example of model tests in oscillatory flow is shown in Fig. 28.

### 4.6. Wave-mud interactions

#### 4.6.1. Field observations

Muddy substrates have long been recognised for damping ocean waves through viscous dissipation. As such, various researchers have attempted to measure wave damping over muddy bottoms in the field since the 1950s. The earliest study was conducted by Gade (1958), who measured wave decay along the Louisiana coast. Similarly, Wells and Coleman (1981) carried out field observations along Suriname's muddy coast and reported that approximately 90 % of wave energy was lost over a 20-km stretch of muddy seabed.

Subsequent field observations were conducted in the following years, including those by Mathew et al. (1995), Forristall and Reece (1985), Sheremet and Stone (2003), and Elgar and Raubenheimer (2008). In the former, the authors measured the decay of short-period sea waves (4 s) and observed the transfer of energy from swell waves to long-period (14 s) infragravity waves, which exhibited the highest dissipation rates. Other notable field observations can be found in the studies by Sheremet et al. (2011), Meirelles and Vinzon (2016), Traykovski et al. (2015), Safak et al. (2017), Rogers and Holland (2009), Winterwerp et al. (2012), and Liu et al. (2022c). A detailed list of notable field observations is presented in Table 11.

#### 4.6.2. Laboratory experiments

Laboratory experiments on wave-mud interactions are conducted in tanks, where waves are physically generated by a wave maker, propagated over a muddy bottom, and then absorbed at the opposite end of the tank. In different tests, either real mud (e.g. Gade, 1958) or artificial mud (e.g. Sakakiyama and Byker, 1989) is placed on the tank bottom. If the objective is to determine wave energy decay, waves are measured at

**Table 13**
A summary of the common approaches used for solving flexible wave–structure interaction, with their advantages and limitations listed.

| Method | The main feature | Advantages | Limitations | Example of Applications | Its capability in modelling nonlinearity | Its capability in modelling complex geomerties | Domain tyoe |
|---|---|---|---|---|---|---|---|
| Wiener–Hopf | Semi-infinite domain solution via Fourier analysis | Semi-analytical; precise in linear cases | Limited to semi-infinite geometries | Ice–wave interaction | Poor | Low | Semi-infinite |
| Perturbation | Expands solution in small parameters | Good for weakly nonlinear problems | Fails in strong nonlinearities | WEC analysis | Moderate | Moderate | General |
| Fourier transform | Wave decomposition into frequencies | Effective for periodic problems | Not suitable for irregular waves | Flexible risers, wave tanks | Poor | Moderate | Infinite |
| Eigenfunction matching | Orthogonal mode expansion with interface continuity | Accurate for piecewise problems | Slow convergence for complex shapes | Floating plates, ice floes | Poor | Moderate | Layered |
| Green's Function + Integral equations | Integral equations using Green's theorem | Good for complex boundaries | Difficult to compute kernels | Submerged barriers | Poor | High | Infinite |
| Variational method | Energy minimisation principles | Powerful general framework | Computationally expensive | Sea ice dynamics | Moderate | High | General |
| Modal analysis | Decomposition into vibration modes | Efficient for linear analysis | Limited to finite linear domains | Ice sheets, floating platforms | Poor | Low | Finite |
| BEM | Boundary-only discretisation using Green's functions | Efficient for unbounded domains | Limited internal resolution | Porous plates, offshore structures | Moderate | High | Unbounded |
| FEM | Full domain discretisation with variational methods | Handles complex geometry, materials | Requires full meshing; sensitive to mesh quality | Flexible structures, pipelines | High | Very High | General |
| Linear GN theory | Extends potential theory for shallow water | Captures mild nonlinearity in shallow regimes | Limited beyond mild nonlinearity | Subsurface structures, bathymetric effects | Moderate | Moderate | Shallow water |

various locations along the bottom, and their decay rate is calculated (e.g. Maa and Mehta, 1990). However, if the focus is also on mud transport induced by waves, both direct and indirect methods must be employed to quantify mud erosion and deposition. Tests may also be conducted under the influence of currents, introducing wave-current-mud interactions. Consequently, a specialised method may be required to generate a current in the tank, which can be circulated and returned. Currents are typically generated using valves installed on the tank bed. A schematic of a typical wave-mud interaction is shown in Fig. 29.

In wave-mud interaction tests, the key parameters influencing these experiments are the thickness of the muddy layer and its viscosity. It is important to note that the viscosity of mud is determined based on its rheological behaviour, which characterises its flow properties.

The earliest experiments on wave-mud interactions date back to the 1950s were conducted by Gade (1958). This study focused on wave attenuation and marked the beginning of experimental research on wave-mud interaction tests. In these tests, natural mud was placed on the bottom of a tank, and wave attenuation caused by the mud was measured. Not many tests on wave attenuation were conducted during the 1960s and 1970s, with significant experimental work resuming in late 1980s and early 1990s. A notable study was carried out by Sakakiyama and Byker (1989). They tested wave propagation over an artificial muddy cover, and measured wave damping and mud transportation. The other significant experimental work of that era was conducted by Maa and Mehta (1990), who investigated wave decay rates over both commercial kaolinite and natural mud for various wave periods. The authors found that the degree of bed consolidation and sediment composition influenced wave attenuation coefficients.

Currents were absent from experiments conducted before the mid-1990s. However, their coexistence with waves can influence sediment transport dynamics, as fluid flow above the mud layer may create distinct shear flow patterns. This gap in tank testing was first addressed by De Wit and Kranenburg (1996). They designed a set of experiments to test wave-current-mud interactions. Commercial kaolinite and a kaolinite-muscovite mixture were used to simulate mud behaviour, whilst both waves and currents were generated in the tank. The authors reported findings on wave damping, turbulence intensity, and mud transport. Following this, Zhao et al. (2006) conducted another set of experiments to simulate wave-mud-current interactions in a tank.

In another set of experiments conducted in 2011, Soltanpour and Samsami (2011) experimentally investigated the rheological behaviour and wave attenuation of Hendijan mud (Hendijan is a city close to Persian Gulf) and commercial kaolinite, finding that both exhibited similar viscoelastic and viscoplastic behaviours. Later, other tests were

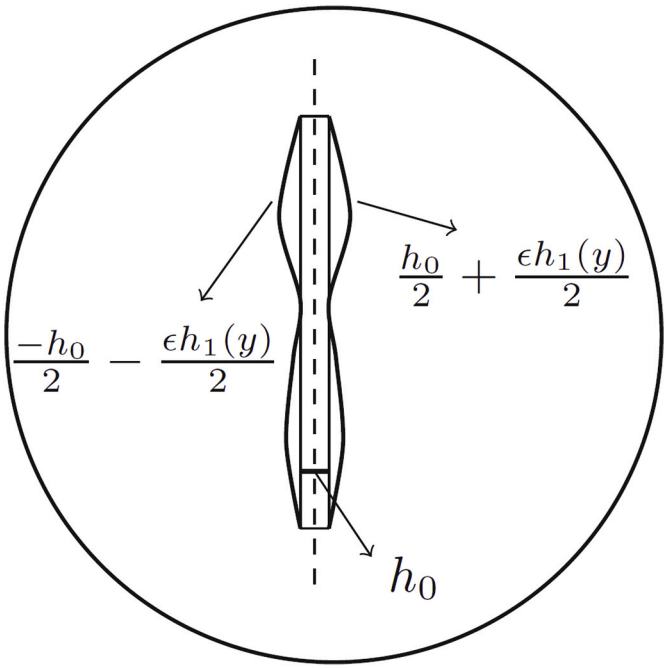


**Fig. 30.** Perturbed flexible thin plate with thickness $d(y) = h_0 + h_1(y)$; Singh and Gayen (2023a). © Elsevier.

carried out Hsu et al. (2013) and Almashan and Dalrymple (2015). A summary of the experiments of wave-mud interactions is outlined in Table 12.

The progress in wave-mud interaction tests has been gradual but very promising. Our knowledge of wave attenuation by mud, and mud transportation is mature enough that we can implement the results in regional wave modelling. Future research should focus on developing nonlinear wave models and incorporating non-Newtonian rheology to better predict wave-mud interactions. Aleebrahim and Jamali (2023) experimentally investigated the resonant interaction between surface and interfacial waves. The formation and amplitude of quasi-standing interfacial waves can influence the density profile and sediment mixing within a fluid mud layer. Robillard et al. (2023) underscored the importance of considering both short-term and long-term rheological responses in wave attenuation predictions. Short-term responses can be modelled using simple frameworks with rheometric data, but long-term predictions require accounting for thixotropic behaviour and time-dependent changes in mud properties. Developing comprehensive models incorporating these factors is crucial for accurate and reliable predictions of wave attenuation over mud-laden shores.

## 5. Non-viscous models

This section reviews the FFSI models developed for the problems introduced in Section 2, under the assumption of inviscid flow. Most of these models are built using the potential flow approach. However, some studies solve the problem for Euler equations. In the final sub-section of the present section, a number of viscous fluid models for wave–mud interactions are also introduced. This is an exception, included because these models are analytically developed and therefore align more closely with the content of this section, rather than the next section, which focuses on CFD-based studies.

### 5.1. Flexible wave-structure interactions

The study of flexible wave-structure based on the inviscid flow assumption interactions has undergone significant evolution over the years mostly using mathematical modelling. Various mathematical modelling, ranging from analytical methods to advanced numerical simulations, have been developed so far.

Historically, Dean (1945) and Ursell (1947) were among the earliest researchers to develop exact solutions for the problem of water-wave diffraction by two-dimensional flat rigid plates. However, despite their contributions, the literature presenting exact solutions has been very limited, with significant emphasis placed on semi-analytical or numerical approaches. But the initial works focusing on hydroelasticity concepts are contributions from Bishop and Price (1979) and Mei and Tuck (1980) (2-dimensional problems) and Wu (1984) (3-dimensional models). A series of work led by Bishop et al. was focusing on the global ship hydroelasticity problem, which will be introduced in more detail in sub-section 5.2, as they are more closely related to ship hydroelasticity. In the rest of this sub-section, various widely employed mathematical techniques used for modelling flexible wave-structure interaction problems within the framework of potential flow theory are introduced. Details of each approach with their strength and limits are outlined in Table 13.

#### 5.1.1. Wiener–Hopf method

The Wiener–Hopf method (Noble, 1959; Lawrie and Abrahams, 2007) is a powerful analytical technique utilised in various fields of applied mathematics and engineering to solve a wide range of boundary value problems (BVPs). At its core, the method aims to solve linear integral equations by employing complex variable theory and Fourier analysis. In practical terms, the Wiener–Hopf method is often applied to problems involving semi-infinite domains, where the domain can be divided into two regions with distinct boundary conditions. By transforming the original problem into the Fourier domain, the equations are simplified. The key step involves solving the kernel equation, which enables the separation of the transformed equations into solvable components. Subsequently, inverse Fourier transforms are applied to obtain the solutions in the original spatial domain, providing valuable insights into the physical phenomena under study. The method offers a straightforward semi-analytical approach to addressing problems that are conventionally resolved using numerical techniques.

The Wiener–Hopf method was initially employed to tackle the challenge of linear wave scattering by a floating thin elastic semi-infinite plate in the work of Evans and Davies (1968). However, this attempt did not yield a complete solution. Eventually later, the problem was solved by other researchers using the same technique (Balmforth and Craster, 1999; Tkacheva, 2001; Chung and Fox, 2002). Subsequently, the solution for a semi-infinite submerged elastic plate, utilising the Wiener–Hopf method, was achieved by Williams and Meylan (2012). Other studies on flexible wave-structure interactions that consider the use of Wiener–Hopf method include Kanoria et al. (1999), Abrahams (2002), Tkacheva (2003), Cunbao et al. (2007), Zhao et al. (2008, 2015b).

The Wiener–Hopf method has some limitations. Its efficacy is contingent upon the factorisation of the kernel function, which can be complex and non-trivial for certain geometries and boundary conditions. Moreover, the applicability of the method is primarily restricted to semi-infinite domains. Nonlinear dynamics, pervasive in realistic wave-structure interactions, often lie beyond its analytical scope, necessitating resorting to numerical methods. Furthermore, the mathematical rigor required for its application, involving advanced concepts in complex variable theory, may make it inaccessible to non-specialists. Additionally, the dependence on Fourier transforms implies that irregular or non-periodic boundary conditions may not be adequately addressed using this method.

For future research on this method, its application can be extended to finite or irregular geometries by developing advanced kernel factorisation techniques. Further, its use can be investigated for solving nonlinear wave-structure interaction problems, potentially by combining it with numerical methods to handle higher complexity.

#### 5.1.2. Perturbation method

Perturbation methods involve solving equations by systematically expanding the solution in terms of a small parameter, typically denoted as $\varepsilon$ (Fig. 30). The small parameter represents a deviation from a known or simple solution. Perturbation methods are used when the problem can be divided into a dominant part (usually a known solution) and a smaller perturbation part. The primary objective is to analyse the behaviour of waves and structures by introducing small perturbations to an idealised system, allowing for the systematic study of their effects. In the context of water wave-structure interactions, perturbation methods involve breaking down the problem into a simpler, known solution (usually an unperturbed system) and a series of corrections introduced gradually.

The works by Shaw (1985), and Liu and Yue (1998) are examples of early studies that employed perturbation expansions to analyse the behaviour of waves in the vicinity of various types of structures. The method has also been applied to various water wave problems while considering the effects from variable bottom topographies in the absence of any structure (Alam et al., 2009; Couston et al., 2017). The method also sees applications to study potential flow past flexible structures with non-uniform structural properties, where the boundary condition on the flexible structure is a differential equation with variable coefficients (Singh and Gayen, 2023a). With applications to harness ocean wave energy using wave energy converters, the method has been employed by many researchers (Michele et al., 2018, 2020; Michele and Renzi, 2019).

The application of perturbation methods, while advantageous in many scenarios, encounters limitations that must be acknowledged. Firstly, their utility diminishes when confronted with strongly nonlinear problems or situations characterised by substantial perturbations.

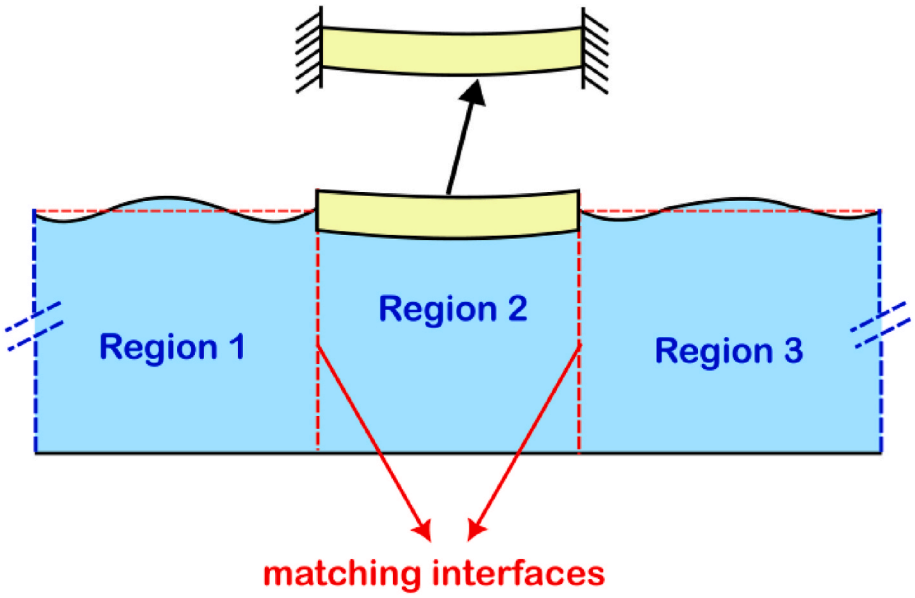


**Fig. 31.** A general sketch of the matching method used for solving the flexible wave-structure interaction.

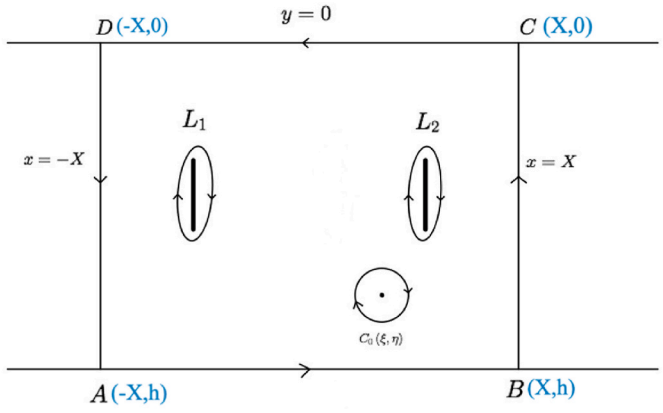


**Fig. 32.** Contour region for application of Green's integral theorem for a two-plate system.

Additionally, achieving convergence of the perturbation series poses a notable challenge, particularly for higher-order terms. This convergence issue jeopardises the accuracy of the solution obtained through perturbation methods, thereby warranting careful consideration of their feasibility in addressing flexible wave-structure interaction problems.

In future the method can be refined by developing more robust perturbation expansions to improve convergence for higher-order terms, especially in strongly nonlinear flexible wave-structure interactions. The method can be explored for use in multiscale problems related to wave energy converters or systems with highly irregular wave environments.

### 5.1.3. Fourier transform method

The Fourier transform method is a mathematical approach used to analyse flexible wave-structure interaction problems by expressing waves as a sum of sinusoidal components. It enables the representation of wave behaviour and structural responses in the frequency domain. By representing these quantities in the frequency domain, the method facilitates the analysis of wave-structure interactions across different frequencies, allowing engineers to assess dynamic characteristics, resonances and springing. The method allows for the examination of resonance phenomena, frequency-dependent behaviour, and energy transfer mechanisms between waves and structures. The Fourier Transform method is often applied to linearised equations governing the problem.

Rienecker and Fenton (1981) were the first to apply the Fourier method to study the steady water waves problem. Later, Soltanahmadi (1992) obtained the natural frequency of a flexible riser system using this method. Since then, many other significant studies based on the Fourier method can be found in literature (Balmforth and Craster, 1999; Kuznetsov et al., 2002; Mei et al., 2005; Porter and Evans, 2007; Halliday et al., 2011; Montiel, 2012; Chen et al., 2022a; Paprota, 2023).

The method is constrained by two primary factors. The method assumes linear behaviour of both the waves and the structures, which may not hold true for certain extreme conditions or materials. It works best for analysing regular waves with known frequencies and wave heights. Also, the efficiency of the Fourier transform method remains hindered by the time-consuming computation of the added mass at infinite frequency, the memory-effect function, and the convolution integral.

The Fourier transform method can be further improved for irregular and non-periodic waveforms, expanding its applicability to real ocean conditions. Also, incorporating nonlinearities and broader material properties into the Fourier analysis can enhance its use in practical engineering applications like flexible marine structures.

### 5.1.4. Eigenfunction expansion and matching method

Eigenfunction expansion method (Linton and McIver, 2002) capitalises on the properties of eigenfunctions, which are solutions to linear potential flow problems and form an orthogonal set. The method allows the expansion of arbitrary functions such as the velocity potential or structural displacements in terms of these orthogonal eigenfunctions. Then, a matching method is employed to ensure continuity of solutions across different regions of the problem domain, such as the fluid domain and the structure. It involves matching the solutions obtained from the eigenfunction expansion within each region and at their interfaces. The eigenfunction expansion is employed to represent the solution within each region, while the matching method ensures the compatibility of solutions across regions and interfaces. A general sketch of the matching method is shown in Fig. 31.

The problem related to wave scattering by a semi-infinite floating elastic plate using the eigenfunction matching method was first solved by Fox and Squire (1994), while that for a submerged semi-infinite elastic plate using this method by Hassan et al. (2009). Later, Kohout and Meylan (2009) utilised this approach to tackle multiple floating

elastic plates with arbitrary boundary conditions. The matched eigenfunction technique can be readily adapted to incorporate the influence of waves arriving at an oblique angle (Fox and Squire, 1994). Consequently, the majority of matched eigenfunction approaches account for the presence of angled incident waves. Likewise, there are other significant studies for investigating potential flow past elastic structures based on the matched eigenfunction expansion method (Teng et al., 2001; Khabakhpasheva and Korobkin, 2002; Lin and Lu, 2013; Cho, 2021; Pu and Lu, 2023).

This method has its own limitations. The convergence of the expansion series may be slow, especially if a large number of eigenfunctions are required, impacting the accuracy of the solution. Further, representing complex geometries may require a large number of eigenfunctions, leading to computational challenges.

In future, faster convergence techniques can be developed for eigenfunction expansions to reduce the computational burden for complex geometries. The idea of investigating the integration of eigenfunction expansion methods with numerical simulations can be explored for more generalised geometries and boundary conditions.

#### 5.1.5. Green's function and integral equations technique

Named after the mathematician George Green, this method involved solving the Laplace equation with appropriate boundary conditions to determine the velocity potential in the fluid domain. Green's function represented the response of the fluid to localised sources or forcing functions, such as the presence of a structure. By convolving the Green's function with the boundary conditions, the velocity potential (and hence the flow field) around the structure could be obtained. This method is particularly useful for determining the flow field in the vicinity of complex geometries and for calculating wave-induced loads on structures. An example of the application of Green's integration for solving a two-plate system is shown in Fig. 32.

The integrated method of integral equations and Green's function (Heins, 1948; Thorne, 1953; Jaswon and Symm, 1977) involves formulating integral equations using Green's integral theorem and appropriate Green's function associated with the problem. Integral equations arise from the application of Green's functions to boundary value problems. These integral equations relate the unknown quantities, such as the fluid velocity or structural displacement, to known boundary conditions and external forcing functions.

Meylan (1995) was the first to solve the problem of wave scattering by an elastic plate by employing the integrated method of integral equations and Green's function. Prior to that the method was utilised to tackle rigid structures. Later, the mathematical technique of Meylan (1995) was modified to use a free surface Green's function rather than the free space Green's function, which not only satisfied by the Laplace's equation but also the fluid domain boundary conditions, for elastic plates problems (Thorne, 1953; Mandal and Chakrabarti, 2000; Sahoo, 2012; Koley et al., 2015; Kaligatla et al., 2015; Chakraborty et al., 2016; Kundu et al., 2018; Singh et al., 2022). This method offers a distinct advantage over existing techniques like the least square approximation method and eigenfunction expansion method found in literature. It offers easy applicability in handling wave interactions with partially flexible plates or membrane barriers, regardless of whether the water depths are finite or infinite.

Calculating Green's function can be computationally demanding, especially for complex geometries or situations where closed-form solutions are challenging to obtain. Green's function methods are inherently limited to linear wave-structure interactions and may not capture highly non-linear effects. Implementing integral equations can be numerically challenging, and convergence issues may arise, particularly in situations with discontinuities or complex boundary conditions. The accuracy is sensitive to the quality of discretisation, and meshing irregular geometries can be challenging.

For enhanced research, the method can be extended to study nonlinear wave-structure interactions by incorporating advanced Green's functions that capture nonlinearity. Likewise, more efficient numerical techniques for Green's function computations can be developed, particularly for irregular geometries and complex boundary conditions.

#### 5.1.6. Variational methods

Variational methods are based on the principle of minimising or maximising certain functionals to obtain solutions to differential equations. In the context of wave-structure interaction, variational methods seek solutions that minimise the total potential energy of the system, subject to appropriate boundary conditions. In linear potential wave theory, the governing equations for the fluid flow are derived from variational principles, such as the principle of minimum potential energy. These principles state that the actual fluid motion is such that the total potential energy of the system is minimised, given the constraints imposed by the geometry of the domain and the boundary conditions.

The method typically involves expressing the velocity potential in terms of a trial function and then minimising the corresponding energy functional. The derivation of the free surface gravity water wave equations can be achieved efficiently through Luke's variational principle (Luke, 1967; Whitham, 1967) or its dynamical equivalent proposed by Miles (1977). These methodologies offer concise and insightful approaches to understanding the dynamics of surface waves in fluid systems. Luke's variational principle encapsulates the entire problem within a single functional, providing a comprehensive framework for analysing the behaviour of water waves. By minimising this functional, one can derive the governing equations that describe the evolution of surface waves under the influence of gravity and other pertinent factors. Other prominent studies carried out using variational method for studying hydrodynamic response of sea-ice can be seen in the works of Fox and Squire (1994), Porter and Porter (2004), Bennetts et al. (2007, 2024).

Variational methods may become computationally demanding for complex problems, requiring careful consideration of variational formulations and solution techniques. The accuracy heavily depends on the appropriateness of the chosen variational model, and deviations from model assumptions can lead to inaccuracies.

For future exploration, investigating more efficient solution strategies for large-scale variational formulations can help reduce computational costs. Also, one can think of extending the application of variational methods to study more complex, nonlinear wave-structure interactions, including those in turbulent flow regimes.

#### 5.1.7. Modal analysis method

The modal analysis method provides a systematic approach for understanding water wave-structure interactions by simplifying complex systems into fundamental modes of vibration (refer to sub-section 3.3.1). It is particularly useful in linear potential wave theory. Early works on the application of modal analysis method to hydroelasticity problems can be found in the work of Bishop and Price (1979) and Wu (1984), related to ship hydroelasticity that shares similarity with flexible wave-structure interactions. The method of modal analysis is widely employed to solve such problems (Michele et al., 2020, 2022, 2024; Zhang et al., 2018; Singh and Gayen, 2023b). When using a model analysis approach, stresses emerging in the solid body are achieved by combining the stress contributions from each of the modes (Malenica et al., 2008; Yang and Gu, 2015; Lee et al., 2021; Meylan, 2021).

Modal analysis is strictly applicable in the linear regime, limiting its use for strongly nonlinear problems or situations where the linear potential wave theory breaks down. Interactions between modes can be complex, and neglecting certain interactions may lead to inaccuracies in the analysis. While much of the research on analysing floating ice sheets relies on the modal expansion method, it is worth noting that this approach is applicable only to structures of finite dimensions (Sahoo et al., 2001).

Combining analytical techniques with numerical simulations seems

to be a promising direction for future research in wave-structure interactions. Thus, the modal analysis method can be extended to fully nonlinear systems to improve its applicability in real-world marine engineering problems. Further, the influence of irregular waves and multidimensional wave interactions on the modal behaviour of complex structures, such as floating ice sheets and wave energy converters can also be investigated.

#### 5.1.8. BEM

BEM gained prominence in the latter half of the 20th century. BEMs discretise the boundary of the structure, leading to efficient and accurate solutions for wave-structure interactions. The governing Laplace equation was solved on the boundary of the structure using Green's function or fundamental solutions. BEM offers advantages in terms of computational efficiency, as it avoids the need for discretising the entire fluid domain and only requires meshing the boundary of the structure.

Considering various fluid assumptions, the three-dimensional hydrodynamics can be efficiently addressed using BEMs (Kim et al., 2013; Lee et al., 2020). Also, analytical solutions for the hydroelastic problem of an offshore submerged porous-elastic plate have been derived utilising BEM by Cho and Kim (2000).

BEM has limitations when applied to potential water wave theory and elastic structures. The method often requires high computational resources to model large domains with intricate wave behaviours, making it less efficient for real-time simulations or large-scale studies. Although BEM relies on surface discretisation, which is advantageous for problems with complex geometries, it may encounter difficulties in accurately representing volumetric effects or interior stresses.

Hybrid applications that combine the BEM and FEM may also be used. Such modelling approaches efficiently handles the unbounded fluid domain by discretising only the boundaries, whereas FEM excels in capturing the structural response of complex, nonlinear, or heterogeneous materials. Such hybrid modelling approach enables accurate and computationally efficient simulation of the FFSI problems. For instance, Cho and Kim (2000) applied BEM for fluid interaction with a submerged porous-elastic plate, while FEM was used to model the structural flexibility. Such hybrid frameworks are particularly beneficial in multi-physics problems where fluid and structural complexities must be addressed simultaneously without the prohibitive cost of full-domain discretisation.

Future research could focus on coupling BEM with other computational methods, such as FEM or CFD, to better simulate complex phenomena like fluid-structure interaction, thermal effects, and nonlinear material behaviour. Expanding BEM's applicability to time-domain simulations could improve its usefulness for dynamic wave-structure interaction problems, particularly in real-time simulations of ocean energy devices or offshore structures.

#### 5.1.9. FEM

FEM have been adapted to model wave-structure interaction problems, where the motion of flexible structures is coupled with potential flow calculations. This approach allows for the analysis of complex interactions between waves and flexible structures, including the dynamic response of offshore platforms, mooring systems, and underwater pipelines. In this approach, the fluid domain is discretised into finite elements, and the governing Laplace equation is solved numerically using variational methods. FEM can handle complex geometries and unstructured meshes, making it suitable for simulating wave-structure interactions in realistic environments (Wang and Wu, 2011). Initially, Kim and Bai (1999) and Kim et al. (2003) provided finite element formulations for modelling free surface waves using potential flow theory.

While using the FEM, accurately modelling open boundaries or unbounded domains, such as those encountered in ocean wave propagation, can be computationally demanding and prone to errors. Further, FEM typically requires discretisation of the entire domain into finite elements, which can be computationally intensive and may lead to inaccuracies, especially in regions with high stress gradients or material nonlinearities.

Accuracy in FEM simulations heavily depends on mesh quality. Fine meshing near high-gradient regions (e.g., near structural edges or singularities) improves solution fidelity but increases computational cost. Poorly resolved meshes may cause numerical instability and misrepresentation of stress fields. Recent studies explore adaptive mesh refinement (AMR) and unstructured meshing to strike a balance between efficiency and accuracy. FEM-BEM hybrid models also help reduce the need for high-resolution meshing in the entire fluid domain. FEM could be further explored in multi-phase flow simulations, especially for wave-structure interactions where air and water interact (e.g. wave breaking or foam formation).

#### 5.1.10. Linear Green–Naghdi theory

Linear Green–Naghdi (NG) theory enhances the linear potential wave theory by incorporating corrections that account for moderately non-linear effects. It is applied to wave-structure interactions where the linear theory may not provide sufficient accuracy. It is suitable for describing the interaction of waves with coastal structures in shallow water. The theory provides a more accurate representation of wave-structure interactions in shallow water conditions, capturing the effects of finite depth and wave nonlinearity.

Green et al. (1974), and Green and Naghdi (1976) introduced a novel approach for investigating nonlinear wave transformation in shallow water, drawing inspiration from continuum models commonly utilised in structural mechanics. It is a significant non-linear wave theory. This theory is constructed upon the concept of the directed or Cosserat surface, which represents a deformable surface embedded within a Euclidean three-dimensional space. At each point of this surface, a deformable vector, referred to as a director, is assigned. Although the Cosserat surface possesses three-dimensional characteristics, it solely relies on two spatial dimensions and time.

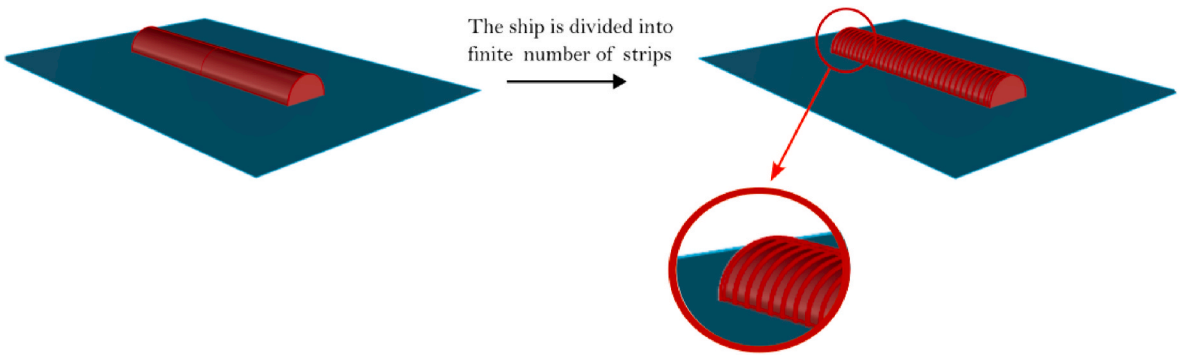


**Fig. 33.** Application of the strip theory in solving dynamic motions of a floating cylinder.

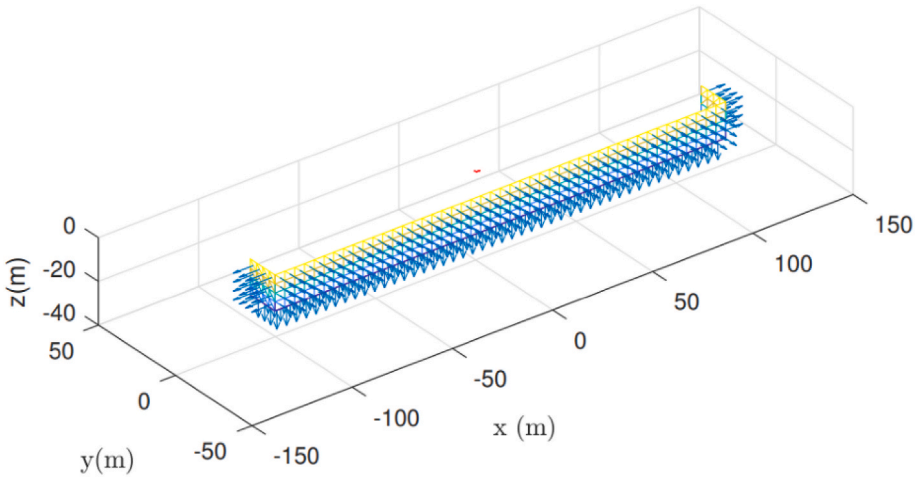


**Fig. 34.** Panels generated on the wet part of a floating box.

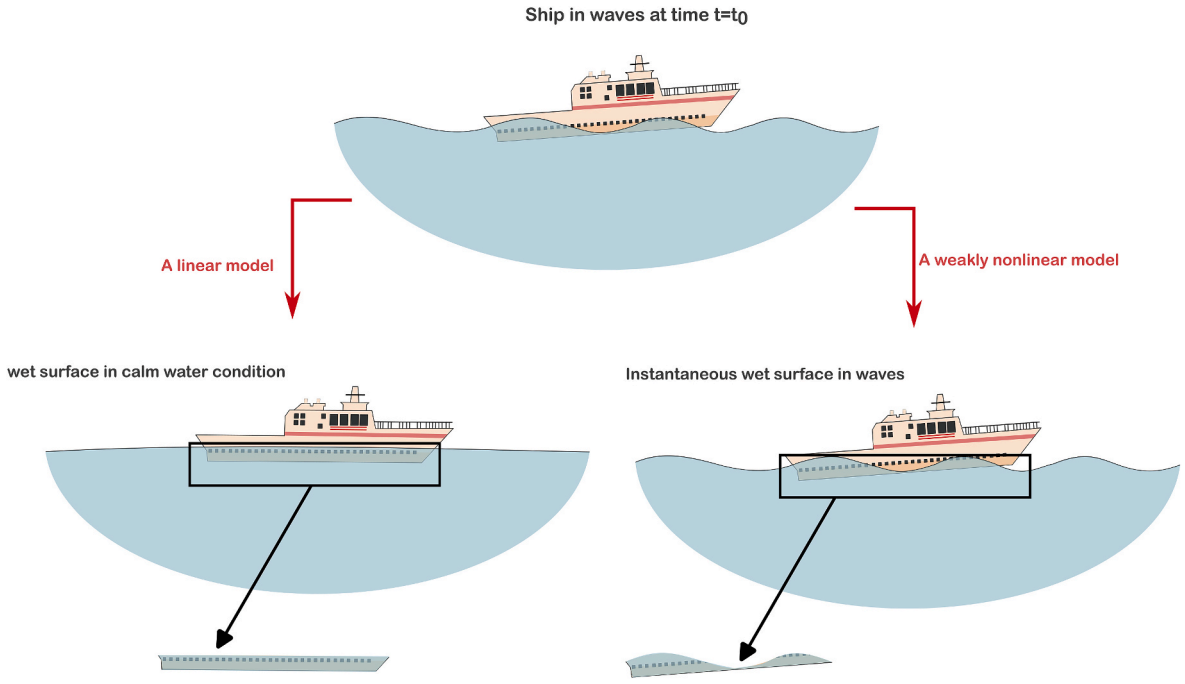


**Fig. 35.** A diagram illustrating linear and weakly nonlinear ship motion models that can be built under inviscid-based fluid assumption. The down-left illustration represents the basis of a linear model, where the wetted surface is approximated using the calm waterline, neglecting instantaneous variations due to waves. The down-right illustration depicts the weakly nonlinear model, which accounts for the dynamic changes in wetted surface as the ship interacts with waves.

**Table 14**
Early 2D models developed to solve global ship hydroelasticity.

| References | Hydrodynamic model | Solid dynamic model | Notes |
|---|---|---|---|
| Bishop et al. (1977, 1980), Bishop and Price (1976a), 1976b) | Strip theory | 1D beam | The first set of hydroelastic models developed by Bishop et al. |
| Wu et al. (1993) | 2.5D theory | 1D beam | Start of using 2.5D model. |
| Hermundstad et al. (1999) | 2.5D theory | 3D FEM | Use of 2.5D model for a multi-hullform |
| Skjørdal and Faltinsen (1980) | Slender body theory | 1D beam | One of the only slender body based models. |

Refining GN theory for shallow water environments could improve predictions of wave-structure interactions in regions with significant bathymetric effects or in systems involving interactions between surface waves and subsurface structures. Integrating GN theory with FSI models could enhance the prediction of the dynamic response of flexible or deformable structures interacting with nonlinear waves, which is crucial for wave energy devices or offshore structures exposed to harsh environments.

### 5.2. *Global ship hydroelasticity*

The models developed for global ship hydroelasticity may be viewed as any simple or advanced model that couples/combines any 2D, 2.5D or 3D potential flow model with any 1D (beam theories) or 3D structural model to solve the problem either in frequency or time domain (Shin et al., 2015). The 2D potential flow models are typically based on strip

theory (e.g. Salvesen et al., 1970 or Gerritsma and Beukelman, 1967) or slender body theories. When the 2D strip is used, the ship is typically divided into a finite number of strips (Fig. 33), often 20 sections (e.g. Aksu, 1993).

The 2.5D theory models sits somewhere between 2D strip theories and 3D models and are built upon the foundations of strip theory. Sectional forces are calculated by setting a three-dimensional boundary condition for the free surface, permitting the inclusion of forward speed effects in the modelling of sectional forces. This approach was initially proposed by Faltinsen and Zhao (1991a, 1991b) and classified as a modified strip theory, and is usually termed 2.5D strip theory (Hermundstad, 1995).

Slender-body models, often classified as two-dimensional, offer a more physically grounded modelling framework and can be employed to overcome the limitations of traditional strip theory. These models offer the advantage of capturing longitudinal disturbance effects and addressing forward-speed influences, which are not fuly represented in 2D strip theory models (Newman, 1964). The 3D potential flow models, on the other hand, solve the problem in a fully three-dimensional fluid domain. These models may require panelisation either on the wetted surface of the ship alone (Fig. 34), or on both the wetted surface and the free surface. Non-viscous models can be configured to exhibit varying degrees of nonlinearity, ranging from weakly nonlinear (sometimes referred to as partly nonlinear) to weakly scattered nonlinear models.

Nonlinearities associated with the ship hydroelasticity model can be introduced through the free surface boundary conditions often activated using perturbation methods or by directly incorporating them into the body motion equations. Nonlinearities can also be incorporated into the model by accounting for the temporal change of the wetted surface (Fig. 35). If its effects on hydrostatic, Froude–Krylov, added mass, or damping forces are considered, the model is referred to as weakly nonlinear. Including body motion effects in diffraction and radiation makes the model body-exact nonlinear, leading to smoothly scattered nonlinearity.

The structural analysis of the ship, however, can be modelled using 1D analysis or 3D analysis (FEM modelling of the ship structures). It is of note that flexible ships are not modelled typically as 2D plates. 1D modelling of a ship as a beam is a widely accepted approach and has been predominantly used for ships since the 1920s (Inglis, 1929). 3D dimensional modelling of the ship structure is typically applied to non-conventional vessels, such as catamarans.

### 5.2.1. 2D potential flow models

*5.2.1.1. linear 2D models.* It should not be a surprise that the very early model that was developed for ship hydroelasticity was built based on a 2D potential flow model, and 1D beam model (the lower dimension for fluid and solid domains can have) for a pure linear condition. This model was developed by Bishop et al. (1977) for stationary conditions. The two-dimensional fluid flow model was developed using the strip theory concept. The one-dimensional beam was idealised using non-uniform Timoshenko beam theory under a free-free boundary condition. This early study specifically considered rigid modes and symmetric elastic modes (e.g. two-node vertical bending mode) of the beam identified in vacuo (i.e. dry modes), and the response of the elastic ship to the wave was achieved via a model superposition.

The model developed by Bishop et al. (1977) initiated a new research stream in naval architecture and ocean engineering, prompting many researchers to develop models that either advance previous approaches or offer greater practicality and ease of use. Later, similar models were developed for flexible ships exhibiting responses in antisymmetric modes (coupled horizontal and torsional bending; Bishop and Price, 1976a; Bishop et al., 1980) and in asymmetric modes (coupled vertical, horizontal, and torsional bending; Bishop and Price, 1976b). The credit for taking the first steps towards modelling transient responses also goes to Bishop et al. (1978), who used convolution methods to model the transient responses of a flexible ship. A similar study was conducted by Belik et al. (1980).

The linear 2.5D theory was firstly adopted for modelling hydroelastic motions of high-speed ships by Wu et al. (1993) and Hermundstad et al. (1994). They further extended the early 2.5D model developed by Faltinsen and Zhao (1991a, 1991b) to consider symmetric modes of elastic ships. Later, Hermundstad et al. (1999) applied 2.5D theory to model the hydroelastic responses of a catamaran. Slender body theory has also been used in modelling hydroelastic responses of the ships. An early example is the work of Skjørdal and Faltinsen (1980), and another one conducted in the 1990s is work of Wu et al. (1991). A summary of early linear 2D models is listed in Table 14.

**Table 15**
High-order strip theories (quadratic terms) developed to solve global ship hydroelasticity.

| Study | Ship model | Solid model | Notes |
|---|---|---|---|
| Jensen and Pedersen (1979, 1981) | Strip theory | 1D beam | One of the first nonlinear strip theory model. |
| Vidic-Perunovic and Juncher Jensen (2005) | Strip theory | 1D beam | Extension of Jensen and Pedersen (1979, 1981) model for bidirectional waves. |
| Jang et al. (2007) | Strip theory | 1D beam | Springing analysis to symmetric and asymmetric responses. |

**Table 16**
A list of weakly nonlinear 2D models developed for solving global ship hydroelasticity.

| Studies | Ship model | Solid model | Memory effects Included? | Notes |
|---|---|---|---|---|
| Yamamoto et al. (1978). | Strip theory | 1D beam | No | One of the first weakly nonlinear models. |
| Toki et al. (1983) | Strip theory | 1D beam | No | Improvements to Yamamoto et al. (1978). |
| Tao and Incecik (2000) | Strip theory | 1D beam | No | Water entry models of by Stavovy and Chuang (1976) alongside Ochi and Motter (1973) were used for slamming load prediction. |
| Xia et al. (1987) | Strip theory | 1D beam | Yes | Momentum variation was used for prediction of slamming load. |
| Gu et al. (1989) | Strip theory | 1D beam | Yes | |
| Park and Temarel (2007) | Strip theory | 1D beam | Yes | A quasi-static approach is used for prediction of green water loads (see Baarholm and Jensen, 2004). |
| Söding (1982) | Strip theory | 1D beam | Yes | high-order differential equations are used. |
| Schlachter (1989) | Strip theory | 1D beam | Yes | high-order differential equations are used. |
| Wang and Xia (1992) and Xia et al. (1998) | Strip theory | 1D beam | Yes | high-order differential equations are used. |
| Rajendran et al. (2016) and Vijith and Rajendran (2023) | Strip theory | 1D beam | Yes | Nonlinear radiation and diffraction are considered. |
| Wang et al. (2020b) | Strip theory | 1D beam | Yes | Partial nonlinearity on radiation and diffraction. |
| Peddamallu et al. (2024). | Strip theory | 1D beam | Yes | A CFD model is used to predict slamming loads. |

*5.2.1.2. Non-linear 2D models.* The early version of any 2D model such as those developed using pure 2D strip theories in the 1970s were linear in nature. The linear 2D models are believed to accurately predict heave and pitch motions, as well as the resulting loads, under low to moderate wave climates (Rajendran et al., 2016), but they have significant limitations in large waves and at higher forward speeds.

In rough sea conditions, where one of the key assumptions of the 2D method, that the relative motions of the ship with respect to the water surface are small, breaks down, particularly at the fore part of the ship (Wu and Moan, 2005). Hence, the significant hydrodynamic forces in these regions are not expected to be captured by a linear model, a phenomenon observed to emerge in various model-scale and full-scale experiments (e.g. Smith, 1966, noted that the sagging moments of a ship were much higher than the hogging moments in extreme wave climate, suggesting the presence of nonlinearities). To address these limitations, efforts were made to develop nonlinear 2D hydroelastic models, which require solving the problem in the time domain.

The first approach to develop a nonlinear model is to upgrade the 2D strip theory to a nonlinear framework by incorporating contributions from nonlinearities associated with the sectional forces. Hence, this approach permits the direct incorporation of nonlinear contributions from steep waves (i.e., nonlinear waves). Such modelling is useful in the statistical analysis of the dynamic responses of flexible ships in non-Gaussian seas (e.g., Jensen, 1991).

Notably, the first steps towards modelling nonlinear hydroelastic motions of ships using strip theory, observed in the late 1970s, were based on this approach. Jensen and Pedersen (1979) developed a nonlinear 2D strip theory considering symmetric modes of a flexible ship. Their work employed a perturbation approach, incorporating quadratic terms to account for the nonlinearities associated with wave forces, non-vertical sides of the ship, and the variations in hydrodynamic forces during the vertical motions of the ship. Thus, this model represented a second-order nonlinear strip theory. Vidic-Perunovic and Juncher Jensen (2005) further developed this method to model springing of elastic ships in bidirectional wave fields.

Another high-order strip theory model, which considered both symmetric and asymmetric hydroelastic responses of a flexible ship, was developed by Jang et al. (2007). While such models would enable us to consider nonlinearities, their application would still be limited to moderate waves if they are developed up to the second-order nonlinearity (Tao, 1996). In summary, this pathway has not been extensively explored by the naval architecture community, and researchers were

**Tale 18**
List of available codes that solve global ship hydroelasticity using a 3D modelling approach.

| Available codes | Developer/Reference | Other comment |
|---|---|---|
| HydroE-FD | Lloyd's Register Group Ltd | Waveload-FD is the rigid body code |
| WAMIT | Lee and Newman (2006) | |
| WISHFLEX-beam and WISHFLEX-3DM | Kim et al. (2009a), Kim and Kim (2016) | WISH is the rigid body code |
| Hydroflex | Das and Cheung (2012b) | |
| THAFTS and NTHAFTS | Hu et al. (2012) | |
| ITU-wave | Kara (2015, 2022) | |
| Oceanwave3D-seakeeping | Zhou et al. (2024, 2024b) | |

**Tale 17**
A summary of the 3D models of ship hydroelasticity.

| Study | Method | Fluid problem | Linear or nonlienar? | Solid model | Case study |
|---|---|---|---|---|---|
| Hirdaris et al. (2003) | Frequency domain | BEM | Linear | 3D FEM and 1D beam | Container ship |
| Bingham et al. (2001) | Frequency domain | BEM | Linear | 3D FEM | Trimaran |
| Iijima et al. (2008) | Time domain | BEM | Weakly nonlinear | 3D FEM | S175 and 5250 TEU Container Ship |
| Senjanović et al. (2009b) | Frequency domain | BEM | Linear | 1D thin-walled beam | Barge |
| Hu et al. (2012) | Time domain | BEM | Weakly nonlinear | 1D beam | Ore Carrier |
| Das and Cheung (2012a) | Frequency domain | BEM with Double-body flow | Linear | 3D FEM | Wigley hull |
| Kim et al. (2013) | Time domain | BEM | Weakly nonlinear | 3D FEM | Barge, 6500 and 1000 TEU Container Ship |
| Yang et al. (2018) | Time domain | BEM (TDGF) and BEM (IORM) | Weakly nonlinear | 3D FEM | Bulk Carrier |
| Ren et al. (2018) | Time domain (HROM) | BEM | Weakly nonlinear | 3D FEM | 8500 and 10000 TEU Container Ship |
| Datta and Guedes Soares (2020) | Time domain | BEM (TDGF) | Weakly nonlinear | 1D beam | S175 Container Ship |
| Park et al. (2019) | Time domain | BEM | Weakly nonlinear | 3D FEM | Wigley hull and 18000 TEU Container Ship |
| Chen et al. (2019a) | Time domain (HROM) | BEM | Weakly nonlinear | 3D FEM | 13000 TEU Container Ship |
| Heo and Kashiwagi (2019) | Time domain | High-order BEM | Weakly nonlinear | 1D beam | Wigley hull |
| Jiao et al. (2021a) | Time domain (HROM) | BEM | Weakly nonlinear | 3D FEM, Timoshenko Beam | Naval ship |
| Lee et al. (2020) | Time domain | Higher-order BEM | Weakly nonlinear | Higher-order shell FEM | Wigley hull |
| Zhang et al. (2021d) | Time domain (HROM) | 3D hydrodynamic model (time domain) | Weakly nonlinear | 1D beam | 21000 TEU Container Ship |
| Riesner and el Moctar (2021a,b) | Time domain (HROM) | BEM with nonlinear effects of forward speed | Weakly nonlinear | 1D beam | Container Ship |
| Yang et al. (2021) | Time domain | BEM (IORM) | Weakly nonlinear | 3D FEM | 20000 TEU Container Ship |
| Hong et al. (2021) | Frequency domain | BEM | Linear (forward speed inclusion) | 1D beam | Barge and Modified Wigley hull |
| Bakti et al. (2021) | Frequency domain | BEM | Linear (forward speed inclusion) | DMB | Modified Wigley hull |
| Duan et al. (2022) | Time domain | (Taylor Expansion) BEM | Weakly nonlinear | 1D beam | 6750 TEU Container Ship |
| Wang et al. (2022a) | Time domain | (Taylor Expansion) BEM | Weakly nonlinear | Transfer Matrix Method | S175 and 6750 TEU Container Ship |
| Tang et al. (2023) | Time domain | BEM | Weakly nonlinear | 1D beam | Ultra-large Container Ship |
| Lu et al. (2023) | Time domain | BEM | Weakly nonlinear | 3D FEM | 21000 TEU Container Ship |
| Zhou et al. (2024, 2024b), | Frequency domain | FDM | Linear | 1D beam | Barge and Wigley hull |

mostly keen to follow the other approach. The high-order strip theory models are listed in Table 15.

The second path ahead of us is to incorporate nonlinearity into the motions. This can be achieved by deciding whether to include memory effects in the model, to account for the instantaneous wetted area/immersion in the calculation of: (I) restoring forces and Froude–Krylov forces, and/or (II) sectional added mass and damping forces, or to include body-exact nonlinear radiation and diffraction forces. The advantages of a body-exact model over a weakly nonlinear one are discussed by Rajendran et al. (2011, 2012, 2015), who pointed out that weakly nonlinear models may overestimate the peak hogging moments in extreme sea conditions.

The first generation of weakly nonlinear 2D models was developed in the absence of memory effects. The earliest model in this category was created by Yamamoto et al. (1978). This model incorporated nonlinear restoring forces and Froude–Krylov forces, while also calculating the instantaneous added-mass and damping coefficients. Additionally, slamming and wet-deck loads were accounted for. The validity of the model was demonstrated through modelling the hydroelastic responses of a model-scale containership with a length of 3 m by Fukasawa et al. (1981). This model was later partially improved by Toki et al. (1983) and subsequently tested by Mizokami et al. (2001), who showed that the Toki et al. (1983) model could effectively capture the vertical bending moment of a 4900-TEU container ship, compared with a unified enhanced slender-based model developed by Kashiwagi et al. (2000). Tao and Incecik (2000) developed another similar weakly nonlinear model.

The second generation of weakly nonlinear models was developed by incorporating memory effects. The linear fluid forces are mostly derived from convolution integrals based on the impulse response function (Cummins, 1962). The time-domain modelling is directly related to how the dynamic response of a flexible ship evolves over time based on past inputs and permits consideration of linear memory effects. In such an approach, linear fluid forces are represented as a convolution of past wave elevations and the impulse response function, permitting a direct calculation of forces based on historical data. When such an approach is used, nonlinear effects are typically treated separately or incorporated within the time-domain simulation, and they are not fully integrated into the fundamental equations of motions (heave and pitch modes). Following this approach, Xia et al. (1987) used the convolution approach to model the hydroelastic responses of the symmetric modes of a ship. Nonlinear contributions from the hydrostatic restoring force and Froude-Krylov forces were included. Similar nonlinear two-dimensional model based on strip theory were developed by Gu et al. (1989) and Park and Temarel (2007).

Another generation of weakly nonlinear models are developed using high-order differential equations. In these models, instead of tracking the entire history of the motion, high-order differential equations are used to capture the essential past interactions through higher-order terms, simplifying the problem, reducing computational effort. This approach was pioneered by Söding (1982), followed by Schlachter (1989) and Wang and Xia (1992) along with Xia et al. (1998).

The latest generation of nonlinear strip theories, incorporating memory effects, was developed by Rajendran et al. (2016). This model is classified as a body-exact type and was initially designed for modelling rigid body motions of ships by considering nonlinear radiation and

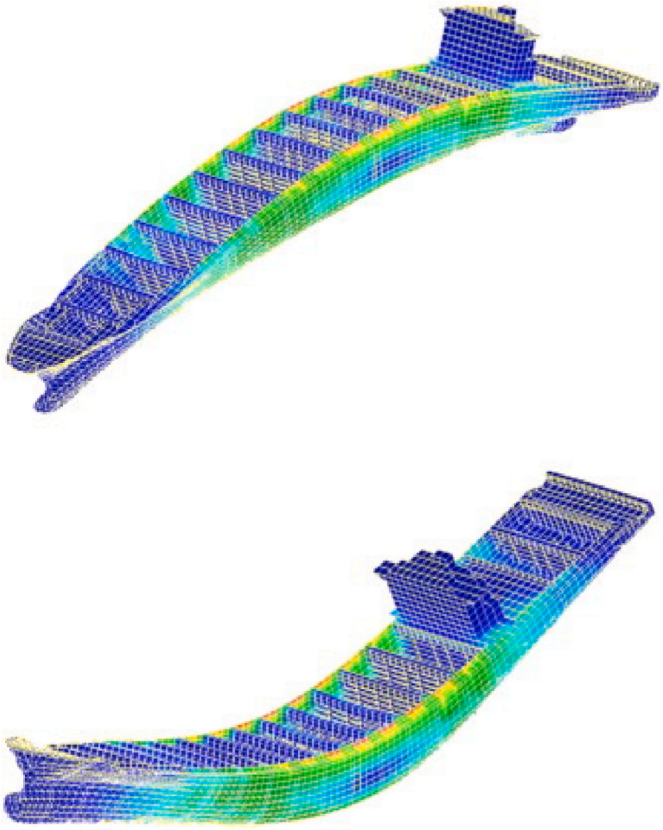

**Fig. 37.** Stress and deformations along a 6500 TEU container ship found through running BEM-FEM code by Kim et al. (2013). The longitudinal Froude Number is 0.04 and encounter frequency is nearly equal to the first mode of the ship. © Elsevier.

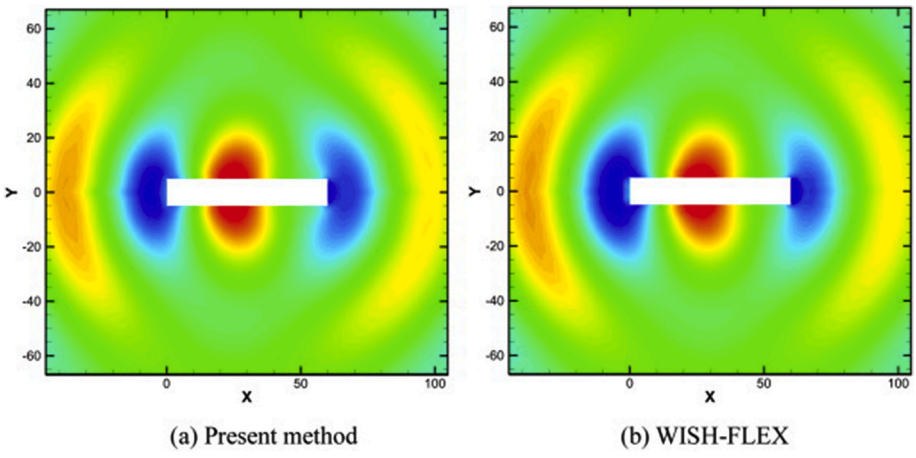


**Fig. 36.** Wave field around a flexible barge exposed to head sea with a wavelength equal to its length. This figure is presented in Kim et al. (2013). Panel (a) shows the results of BEM-FEM model, and panel (b) shows the results of WISH-FLEX code. © Elsevier.

diffraction (Rajendran et al., 2015). It was later extended to account for the elastic, symmetric response of ships in head sea (Rajendran et al., 2016), and symmetric responses of elastic ships in oblique waves (Vijith and Rajendran, 2023). A hybrid version of this model was later developed by Peddamallu et al. (2024). A summary of the nonlinear 2D models is listed in Table 16.

#### 5.2.2. 3D potential flow models

The need to use a 3D model for global ship hydroelasticity under a potential flow arises from the need to model 1) more complicated hullforms, and 2) to consider three-dimensional evaluation of fluid motion and advanced speed, both of which can be hardly captured via a 2D/2.5D modelling approach.

Modelling can be done in frequency domain (e.g., Das and Cheung, 2012b), or time domain (e.g., Kim et al., 2014). Similar to 2D problems, nonlinearities associated with the upper layer of water, and the body hydrodynamics can be taken into account. The choice of the solution method would affect the panel generation. Under a choice of Rankine Source Method (e.g. Kim et al., 2014), panels are required to be generated on the water surface, and the wet part of the flexible ship, and a damping zone is required to dampen the waves. A list of studies based on 3D modelling of ship hydroelasticity is presented in Table 17, and the corresponding numerical codes are outlined in Table 18.

*5.2.2.1. Early models.* The first 3D foundation for hydroelastic modelling of elastic ships was introduced by Bishop et al. (1986). The fluid problem was solved through Green's integrals, and the structural problem was solved using a 3D FEM. The model would provide a model analysis for the dynamic responses of the ship. Hence, following this research, different frequency domain models, based on Green's integration, were developed (e.g. Riggs et al., 2007).

The most famous modal analyses in the 2000s were performed by Hirdaris et al. (2003), Senjanović et al. (2008, 2009a). Hirdaris et al. (2003) coupled a BEM code (Green's function based pulsating source distribution) with 1D and 3D FEM models for idealisation of ship structure and then analysed hydroelastic motions of the ship with large open hatch and closed decks. The code used for modal analysis of the flexible ship was called HydroE-FD. Dry and wet modes were both calculated. This study provided a very deep understanding of the way the 1D or 3D approaches would be used for structural modelling, and whether wet or dry mode concepts need to be considered. Senjanović et al. (2008, 2009a, 2009b) performed a series of global hydroelastic studies on ships, and applied a hydroelastic restoring coefficient formulated by Malenica et al. (2003) to develop 3D frequency-based linear hydroelastic models.

In another work, Ijima et al. (2008) developed a one-way FSI methodology for structure analysis of elastic ships by considering hydroelasticity by utilising a time-domain three-dimensional panel method. Nonlinear components of pressure that could potentially influence hydrodynamic forces, particularly in cases where discrepancies arise between sagging and hogging moments due to the forward speed and fluctuations of the wetted surface were considered.

*5.2.2.2. Emergence of fully coupled 3D FFSI models.* A new generation of 3D two-way FSI models for simulating dynamic responses of ships exposed to water waves began development in the late 2000s in Seoul National University (SNU). These models were built on the foundation of the Rankine Source Method and aimed to solve the hydroelastic responses of flexible ships in the time domain under linearised boundary conditions. Initially, Kim et al. (2009a) developed a time-domain method for simulating a flexible, beam-like ship in waves at zero speed for linearised boundary conditions. The code was subsequently expanded to include forward speed effects under a double-body flow consideration (Kim et al. 2009b, 2010, 2013) for head sea and oblique wave conditions, and a very similar weakly nonlinear model was also developed by Kim et al. (2014). For examples of the simulations run by the BEM–FEM code developed by Kim et al. (2013), see Figs. 36 and 37, which respectively show the wave field around a barge, and the stresses and deformations along a flexible 6500 TEU containership exposed to head waves. The versions of the codes developed at SNU that idealise ship structure using a 1D Vlasov-beam idealisation are referred to as WISHFLEX-beam, while those that employ a 3D FEM idealisation are termed WISHFLEX-3DM (Kim and Kim, 2014, 2016). Recent updates on the code can be found in Park et al. (2017, 2019), and similar studies are conducted by Shin et al. (2015), Lu et al. (2023).

Das and Cheung (2012b) introduced another 3D fully coupled FSI model for flexible ships exposed to water waves, that would use a double-body approach for consideration of steady fluid flow by introducing a wave-scattered method in frequency domain (developed in Das and Cheung, 2012a). The model would solve the problem in a frequency domain, and developed software was named Hydroflex. The method however does not take into account the body nonlinear effects and does not take into account slamming and green water effects, though it can be further developed to consider these effects. This remains as a future research opportunity.

*5.2.2.3. Convolution-based time-domain hydroelastic models.* Since late 2010, a series of 3D time-domain hydroelastic models have been developed that utilise convolution integrals to apply 3D frequency domain. Notable examples of these models are presented in Chen (2017), Chen et al. (2017, 2019a), Im et al. (2017), Ren et al. (2018), Zhang et al. (2021d), and Sengupta et al. (2016, 2023). However, these models do not account for the steady fluid flow generated by the forward movement of the flexible ship.

*5.2.2.4. Incorporating nonlinear forward-speed effects in 3D hydroelastic models.* Other types of hydroelastic solvers have been developed by considering the non-linear forward movement of the ship, rather than using the double-body approach initially employed by Kim et al. (2009a), and Das and Cheung (2012b).

This shift toward development of such models was motivated by the desire to account for the potential effects of forward speed on the trim and sinkage of the vessel, which would be overlooked under a linearisation of forward-speed movement. Söding (2009) developed a hydroelastic model that solves the potential flow around a ship exposed to regular waves by considering the non-linear forward movement of the vessel using a hybrid method. Later by including the damping due to radiated waves, Riesner and el Moctar (2018) developed an improved model that solves the problem for two different wave sets: short and long waves.

In the next step, Riesner and el Moctar (2021a, b) advanced the model by developing a weakly non-linear hybrid model that couples the non-linear steady forward movement of the ship with the linearised fluid flow around a flexible ship exposed to waves. Riesner and el Moctar (2021a,b) simulated hydroelastic responses of a 333 m long post-Panamax containership, which was previously tested by Maron and Kapsenberg (2014). Another 3D hydroelastic model, termed the Forward Speed Correction Method (FSCM), with consideration of forward speed, was developed by Yang et al. (2020, 2021).

*5.2.2.5. Additional time-domain rankine-based models for springing.* Several other time-domain Rankine-based models have been developed to analyse ship dynamic responses or springing. For instance, Shao and Faltinsen (2012) created a weakly nonlinear model that utilised a three-dimensional high-order BEM to calculate second-order ship springing effects. Other examples include the studies of Duan et al. (2022), based on an earlier model developed by Wenyang (2012), and Wang et al. (2022a).

**Table 19**
A summary of inviscid-based flexible water entry models developed over time.

| Reference | Modelled body | 2D or 3D | Vertical | Oblique | Fluid model | Solid Model |
|---|---|---|---|---|---|---|
| Meyerhoff (1965a, b) | Wedge | 2D | ✓ | | Wagner-type solution | 1D beam model (modal superposition) |
| Kvalsvold and Faltinsen (1993, 1994) | Horizontal Plate (Wet-deck slamming) | 2D | ✓ | | Wagner-type solution | 1D beam model (modal superposition) |
| Kvalsvold and Faltinsen (1995) | Horizontal Plate (Wet-deck slamming) | 2D | ✓ | | Wagner-type solution | 1D beam model (modal superposition) |
| Faltinsen (1997) | Horizontal Plate (Wet-deck slamming) | 2D | ✓ | | Wagner-type solution | 1D beam model (modal superposition) |
| Faltinsen (2000) | Horizontal Plate (Wet-deck slamming) | 2D | ✓ | | Wagner-type solution | 1D beam model (modal superposition) |
| Lu et al. (2000) | Wedge | 2D | ✓ | | BEM | FEM |
| Bereznitski (2001) | Wedge | 2D | ✓ | | Euler Equations (FVM) | FEM |
| Korobkin et al. (2006) | Wedge | 2D | ✓ | | Wagner-type solution | FEM |
| Sun (2007) | Cylindrical shell | 2D | ✓ | | BEM | 1D beam model |
| Stenius et al. (2007, 2011) | Wedge | 2D | ✓ | | Euler Equations (FEM) | FEM |
| Wang and Guedes Soares (2011, 2018) | Wedge and horizontal plate | 2D | ✓ | | Euler Equations (FEM) | FEM |
| Reinhard et al. (2013) | Inclined Plate | 2D | | ✓ | Wagner-type solution | 1D beam model (modal superposition) |
| Khabakhpasheva and Korobkin (2013) | Wedge | 2D | ✓ | | Wagner-type solution | 1D beam model (modal superposition) |
| Lv and Grenestedt (2013, 2015) | Wedge | 2D | ✓ | | Point Pressure Load | 1D beam model (Fourier sine integral transformation in space and a Laplace–Carson) |
| Datta and Siddiqui (2013, 2016) | Wedge | 2D | ✓ | | Wagner-type solution (with radiation) | 1D beam model (modal superposition) |
| Shams and Porfiri (2015) | Wedge | 2D | ✓ | | Wagner-type solution | FEM |
| Wang et al. (2016) | Horizontal Plate (Wet-deck slamming) | 2D | | ✓ | Wagner-type solution | 1D beam model (modal superposition) |
| Shams et al. (2017) | Wedge | 2D | ✓ | | Wagner-type solution | FEM |
| Jalalisendi and Porfiri (2018) | Wedge | 3D | ✓ | | Wagner-type solution | 1D beam model (modal superposition) |
| Kafshgarkolaei et al. (2019) | Wedge | 2D | ✓ | | Wagner-type solution | Euler-Bernoulli beam (orthonormal polynomial series expansion method) |
| Yu et al. (2019b) | Stiffened wedge | 2D and 3D | ✓ | | Wagner-type solution (MLM) | 1D beam model (modal superposition) |
| Zhu et al. (2020b) | Rectangular plate | 3D | ✓ | | Spatially uniform distributed pulse loads | modal superposition method and Lagrange's equation |
| Sun et al. (2021) | Wedge | 2D | ✓ | | Wagner-type solution (MLM) | 1D beam model (modal superposition) |
| Feng et al. (2021a) | Wedge | 2D | ✓ | | Wagner-type (MLM) | 1D beam model (modal superposition) |
| Feng et al. (2021b) | Wedge | 2D | ✓ | | BEM | 1D beam model (modal superposition) |
| Zhang et al. (2021b) | Wedge | 2D | ✓ | | BEM | 1D beam model (modal superposition) |
| Wang et al. (2021) | Horizontal plate | 2D | ✓ | | Euler Equations (FEM) | FEM |
| Wang et al. (2022c) | Plate | 3D | ✓ | | Load simplification | 2D plate (modal superposition) |
| Wang et al. (2022b) | Horizontal plate | 2D | ✓ | | Euler Equations (FEM) | FEM |
| Ren et al. (2023) | Wedge | 2D | ✓ | | Wagner-type solution | FEM |
| Korobkin et al. (2023) | Elastic plate | 2D | ✓ | | Wagner-type solution | 1D beam model (modal superposition) |
| Abrahamsen et al. (2023) | Concrete shell | 3D | ✓ | | Wagner-type solution | concrete shell (modal superposition) |
| Hosseinzadeh et al. (2023b) | Wedge | 3D | ✓ | | Euler Equations (FEM) | FEM |
| Feng et al. (2024) | Wedge | 2D | ✓ | | Wagner-type solution (MLM) | 1D beam model (modal superposition) |
| Khabakhpasheva et al. (2024) | Conical shell | 3D | ✓ | | Wagner-type solution | conical shell (modal superposition) |

*5.2.2.6. Recent advancements in computational efficiency and domain reduction.* More recently, Yang et al. (2019, 2020) introduced an Inner and Outer Regions Matching (IORM) Method for 3D modelling of hydroelastic motions in ships using the Rankine Source Method. This approach aimed to reduce the computational domain by minimising the surfaces where panels need to be generated. A virtual matching surface was established, and the radiation conditions were designed to be satisfied in the outer region.

*5.2.2.7. More advanced nonlinear models.* Wu et al. (1997) developed a 3D nonlinear hydroelasticity model that incorporates both the first-order wave potentials and their corresponding responses to evaluate the second-order hydrodynamic actions on flexible floating structures. Similar studies were carried out by Tian and Wu (2006), Hu et al. (2012), and Ni et al. (2020). The related linear and nonlinear codes developed at the China Ship Scientific Research Center are called THAFTS and NTHAFTS, respectively (Hu et al., 2012). A very recent nonlinear model is presented in Tang et al. (2023).

*5.2.2.8. Models developed on the basis of transient green functions.* In contrast to time-domain solutions that utilise a direct or indirect FSI coupling method, such as the Rankine Source method employed by Kim et al. (2013), or those that transfer frequency domain solutions to the time domain via convolution integrals (e.g. Riesner and el Moctar, 2021a), some time-domain solutions are based on transient Green's functions. These approaches are widely applied in seakeeping analyses of ships, as demonstrated by studies from Kara (2011), Datta et al. (2011, 2013), and Sengupta et al. (2016).

These models typically require only the panelisation of the wet hull of the flexible floating body. A notable early example in this field is the work of Wang and Wu (1998), who modelled the dynamic responses of an elastic ship using both a transient Green function and a frequency domain panel method. Their findings indicated that the transient Green function approach provided more accurate predictions of micro strains.

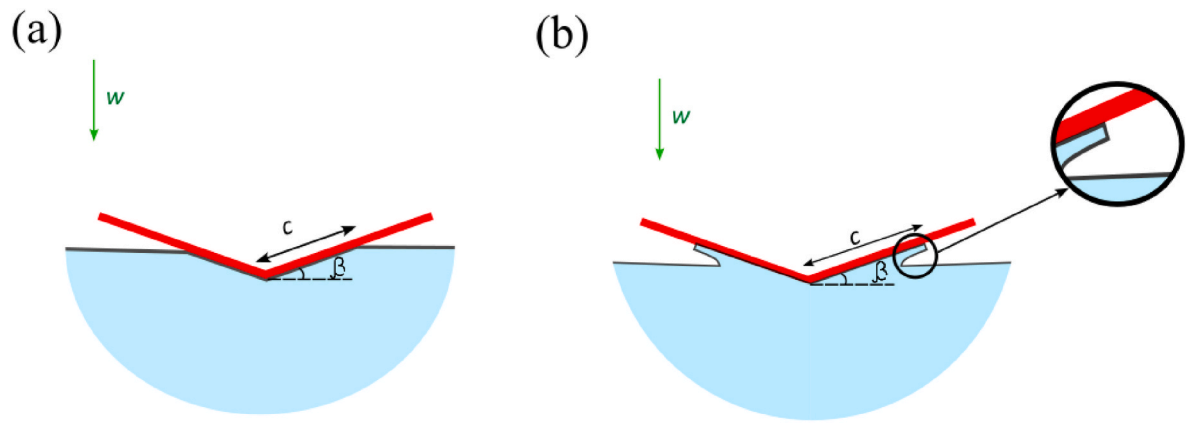


**Fig. 38.** Water entry models from (a) von Kármán (1929) and (b) Wagner (1932). The wetted contact length is denoted with and deadrise angle is denoted with $\beta$. $w$ is the water entry speed. Spray root formation in the contact region is shown in the magnified section.

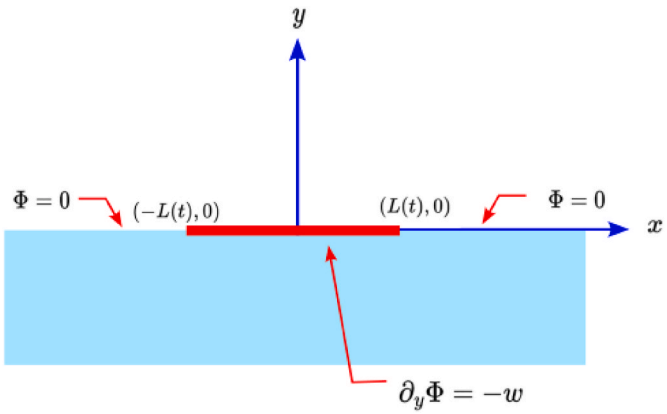


**Fig. 39.** Flat-disc approximation for solving water entry problem. Here $\Phi$ represents velocity potential, $-L$ and $L$ denote the longitudinal positions of the wetted region of the disc The parameter $w$ represents the water entry speed. The no-flux boundary condition is applied on the wall of the disc, i.e., $\partial_y\Phi = -w$.

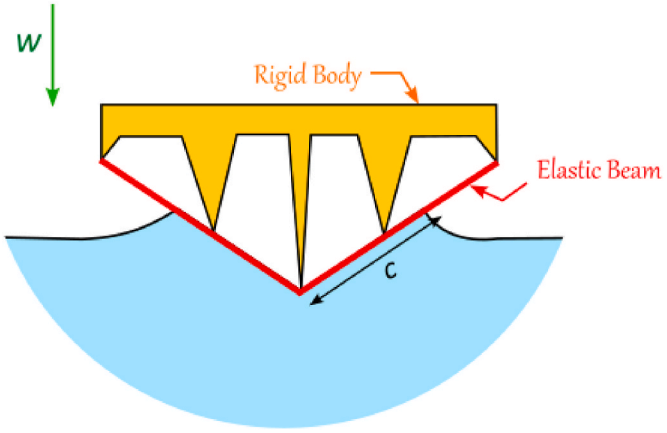


**Fig. 40.** A schematic of a hydroelastic water entry model developed by Meyerhoff (1965a). The body entering water consists of a rigid mass (yellow) with two elastic beams (red) that deforms upon water pressure. The downward velocity $w$ represents the entry speed, and $c$ denotes the wetted contact length, that increases as the immersion increases and can be found using Wagner model.

Very recent examples are the studies carried out by Kara (2015), Sengupta et al. (2017), Pal et al. (2018), Datta and Guedes Soares (2020),

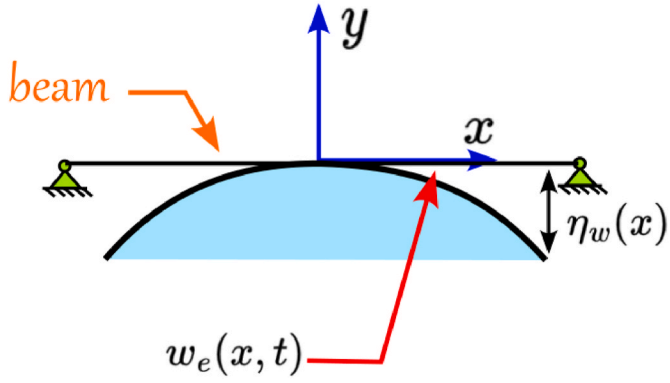


**Fig. 41.** The general idea of the flexible slamming model developed by Kvalsvold and Faltinsen (1993, 1994). Here, $w_e$ represents the displacement of the beam, and $\eta_w$ shows the water surface distance from the beam.

Show et al. (2022), Yang et al. (2018, 2019, 2021), and Kara (2022).

*5.2.2.9. FDM-based modelling.* In contrast to all BEM-based 3D models developed for global ship hydroelasticity, FDM has also been employed more recently by Zhou et al. (2024, 2024b), who further developed the OceanWave3D-Seakeeping model to simulate the flexible motion of ships in waves. The model is limited to linear conditions, with both the fluid and structural problems solved in the frequency domain. This presents opportunities for further improvement of the code.

### 5.3. Flexible water entry

The water entry problem is inherently complex and occurs over a very short timescale, as discussed in Sub-section 4.3. Modelling the problem under the assumption of an inviscid fluid presents significant challenges. One of the primary difficulties lies in accurately capturing the spray root formation along the surface of non-flat objects during the water entry process. This sub-section systematically reviews the models developed to solve flexible water entry problem. A detailed list of the studies is presented in Table 19.

#### 5.3.1. A very brief review of rigid water entry models

Before reviewing the gradual development and evolution of inviscid-based models for flexible water entry problems, a brief introduction to the earliest models developed for idealising rigid body water entry is presented. There is broad agreement among researchers in the field of sea loads that the two classical studies by von Kármán (1929) and Wagner (1932), as illustrated in Fig. 38, mark the beginning of the

theoretical models developed for solving water entry problems in the next decades. The formulations presented in these two studies were developed for the simplest case, a 2D water entry problem.

The model developed by von Kármán (1929), known as the von Kármán momentum theory, is an asymptotic model that idealises the water entry of flat and nearly flat bodies (i.e., wedges with very small deadrise angles) under perfectly linearised free surface and body boundary conditions. This model assumes no water rise emerges along the walls of solid body entering water. In contrast, Wagner (1932) developed a model based on a flat-disc approximation (see Fig. 39), which accounts for the piled-up water (water rise or spray root) on the wall of the solid body.

Since its introduction, the Wagner model has undergone significant developments, often involving modifications to the body boundary conditions (e.g. Dobrovol'skaya, 1969) or the free surface boundary conditions (e.g. Howison et al., 1991; Logvinovich, 1973; Zhao et al., 1996; Zhao and Faltinsen, 1993; Korobkin, 2004). Korobkin (2004) presented the Original Logvinovich Model (OLM), the Modified Logvinovich Model (MLM), and the Generalised Wagner Model (GWM). All these models were developed for the initial water entry process (no wet chine condition). However, Tassin et al. (2014) mathematically showed how a wet chine condition can be incorporated in MLM.

#### 5.3.2. *Introduction of flexible slamming for wedges*

Historically, the introduction of flexibility, slamming, and hydroelasticity in water entry research dates back to the early 1960s, with Meyerhoff (1965a, b) pioneering the field (Fig. 40). Meyerhoff (1965a, b) modelled the water entry of a wedge with elastic walls and solved the fluid problem using the Wagner model. However, the approach was limited to the early stage of water entry which is very reasonable for the first work in this field. The elastic wall of the wedge was idealised as a Euler–Bernoulli beam model and dry modes considered in formulation of problem. A similar model was later developed by Vasin (1993).

#### 5.3.3. *Second generation of slamming models emerged in the 1990s: flat plates*

The second generation of flexible slamming models emerged in the 1990s, nearly three decades after Meyerhoff's (1965a, b) pioneering work. This new approach, developed by Kvalsvold and Faltinsen (1993, 1994), focused on slamming on wet decks, a hydroelastic problem highly relevant to catamaran wet deck impacts, but also applicable to bottom slamming. This is because the authors modelled the flexible slamming of a flat plate, which is different from what was modelled by Meyerhoff's (1965a, b).

The core idea in Kvalsvold and Faltinsen (1993, 1994) was that the dynamic response of a thin body impacting water could be modelled using a beam representation, shown in Fig. 41, with hydrodynamic forces determined by solving the fluid flow around the impacting object (a modelling approach similar to that of Meyerhoff (1965a, b)). For flat plate slamming, this required calculating the instantaneous wetted area, which was achieved using the Wagner model. The models were first developed by considering dry modes. Later, Faltinsen (1997) introduced a two-phase framework to the problem, distinguishing between the structural inertia phase and the free vibration phase. For the former, dry modes were used, and for the latter, wet modes were used. Similar models were later developed by Wang et al. (2016) and Reinhard et al. (2013).

#### 5.3.4. *Mathematical models for flexible water entry models of 2D wedges: wagner-type solutions and other simplifications*

Following the introduction of flexible slamming of flat plates in the 1990s, 2D mathematical modelling of flexible water entry gradually emerged as a research direction and continues to evolve. Most models adopt an Euler–Bernoulli beam idealisation for the wedge wall, employing the Wagner-type water entry models to represent fluid motion around the object (e.g. Khabakhpasheva and Korobkin, 2013; Shams and Porfiri, 2015; Shams et al., 2017; Yu et al., 2019b; Feng et al., 2024). The solid motion was solved by using model super positioning or FEM.

A significant contribution in this research direction is that of

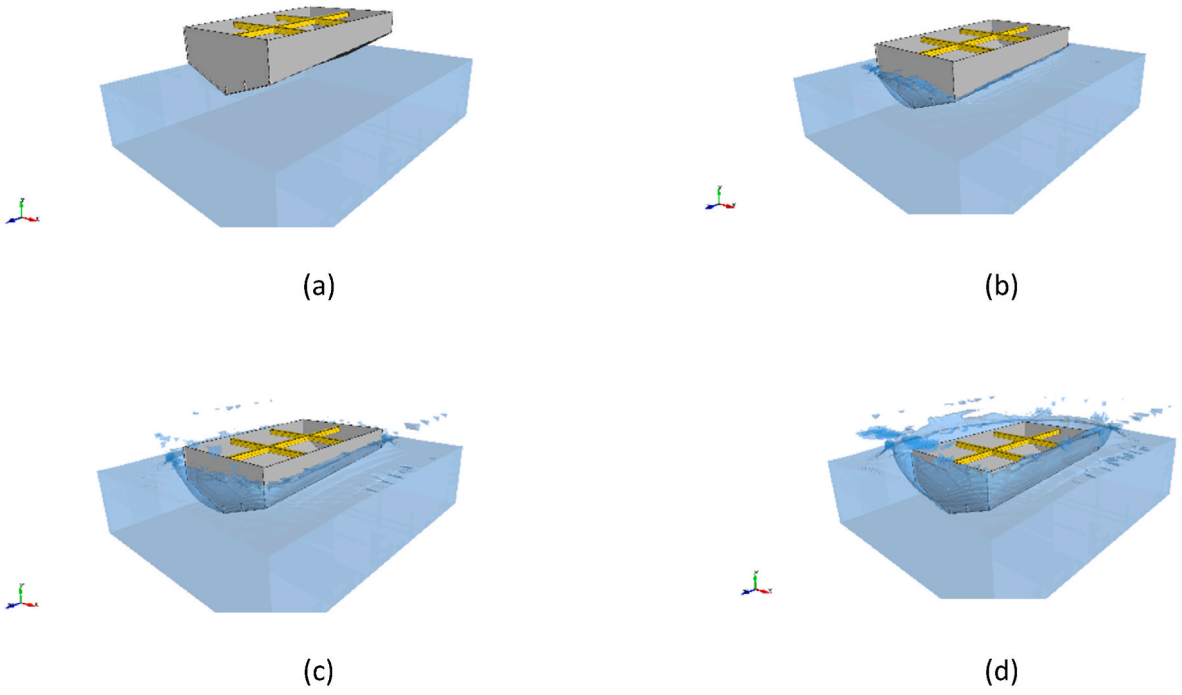


**Fig. 42.** Multi-material ALE simulation of the FFSI water entry of a 3D wedge, performed by Hosseinzadeh (2023). Snapshots (a)–(d) illustrate different stages of the water entry process. Snapshot (a) shows the pre-entry stage, and snapshot (d) captures the initial penetration of the wedge into the water. The full simulation results and analysis are presented in Hosseinzadeh et al. (2023b).

Khabakhpasheva and Korobkin (2013). Developing a flexible water entry model, they derived an analytical formulation for the added mass matrix of elastic modes of a uniform beam representing the elastic wall of the wedge under various boundary conditions. The model is constrained by the dry chine condition and does not account for flow detachment from the chine, limiting its application to the early stages of the water entry problem of a wedge section. Yu et al. (2019b) developed a model (based on the water entry model of Tassin et al. (2014)) to also consider the wet chine condition. Other similar models are presented in Feng et al. (2024) and Sun et al. (2021a,b).

Shams and Porfiri (2015) later developed a flexible water entry model by deriving an "exact" solution to the boundary value problem of hydroelastic impact for flexible wedges. The water entry depth, speed, and acceleration are prescribed functions measured in experiments, which limits the application. Shams et al. (2017) subsequently extended this model to account for both water entry and exit of a wedge dropped into water.

Other flexible water entry models based on Wagner-type solution can be found in Korobkin et al. (2006), Datta and Siddiqui (2013, 2016), Kafshgarkolaei et al. (2019), Ren et al. (2023), Feng et al. (2021a, 2021b) to model flexible water entry of wedge sections. Use of load simplification models can also be seen in the studies of Lv and Grenestedt (2013, 2015), Zhu et al. (2020b) and Wang et al. (2022c).

#### 5.3.5. BEM-based models

BEM has been widely applied in simulating the water entry of rigid bodies and has also been used in FFSI modelling of two-dimensional water entry problems. The early concept of employing BEM for flexible structures dates back to 2000, coinciding with advancements in the numerical modelling of rigid water entry using BEM. Drawing from this research direction, Lu et al. (2000) introduced the first BEM-based model for flexible wedges entering water, developing a BEM–FEM approach capable of modelling the hydroelastic response of a wedge during the early stage of impact. Later, Sun (2007) introduced a BEM–modal superposition model for the dynamic response of a two-dimensional cylindrical shell entering water. More advanced BEM-based models for flexible water entry have been introduced in recent years by Zhang et al. (2021b) and Feng et al. (2021b). Zhang et al. (2021b) developed two coupling solutions for the hydroelastic modelling of flexible wedges at constant vertical velocities, incorporating the hydroelastic response during the flow detachment phase.

**Table 20**
A summary of numerical BEM–FEM and FEM–FEM studies conducted to model flexible marine propellers.

| Study | Problem | Fluid flow modelling | Structural modelling | Notes |
|---|---|---|---|---|
| Young (2007) | Propeller | BEM | FEM | Cavitation modelling, unsteady flow |
| Young (2008) | Propeller | BEM | FEM | Steady/unsteady hydroelasticity |
| Motley et al. (2009); Young et al. (2010a,b) | Propeller | BEM | FEM | Composite propeller design, marine renewables |
| Ghassemi et al. (2012) | Propeller | BEM | FEM | Steady, uniform flow only |
| Blasques et al. (2010) | Propeller | BEM | FEM | No validation, composite optimisation |
| Lee et al. (2014) | Propeller | BEM | FEM | Damping, added mass, 2-way FSI |
| Lee et al. (2017) | Propeller | BEM | FEM | Tapered blade geometry, simplified ply |
| Li et al. (2018) | Propeller | BEM | FEM | Time/freq panel methods, non-uniform, 2-way |
| Li et al. (2020b) | Propeller | BEM | FEM | Parametric hydroelastic analysis |
| Li et al. (2021, 2022b) | Propeller and shaft | BEM | FEM + 1D Beam | 6DOF + elastic shaft-propeller system |
| Li et al. (2023) | Propeller | BEM | FEM | Non-penetration boundary condition is considered |
| Zou et al. (2017, 2021) | Propeller and shaft | BEM | FEM + 1D Beam | Rotodynamic, bearing model, nonlinear Bernoulli |
| Joe et al. (2021) | Propeller | FEM | FEM | Euler Force is considered |

#### 5.3.6. Beyond 2D modelling

Whilst most research has focused on 2D flexible water entry problems, 3D modelling is also present in the literature, though significantly more limited. Interestingly, there has been a recent surge in 3D modelling of flexible water entry under inviscid fluid assumptions.

Jalalisendi and Porfiri (2018) presented one of the first models for 3D hydroelastic water entry, focusing on the water entry of a flexible 3D slender body. Their model coupled a 1D beam model with a fluid dynamics model that treats the fluid as two-dimensional at each cross-section, with integration across 2D sections yielding the overall 3D fluid motion around the slender body. Additionally, recent research has advanced our understanding of hydroelastic slamming across various geometric structures impacting water.

Khabakhpasheva et al. (2024) presented a model capable of predicting deflections and strains of a conical shell with a small deadrise angle entering water. It was found that hydrodynamic pressures acting on an elastic cone entering water initially lag behind but eventually surpass those on a rigid cone as the impact progresses. Other 3D model are presented by Korobkin and Khabakhpasheva (2022) along with Abrahamsen et al. (2023). In the latter, the authors employed a simplified potential flow strip theory combined with a modal method, demonstrating significant hydroelastic effects even in large, thick concrete shells.

#### 5.3.7. ALE-FEM coupling

Another set of flexible water entry models are based on ALE-FEM coupling, which has been introduced to the engineering community since the early 2000s. The fluid problem is solved for an inviscid air–water mixture, often incorporating weak compressibility through an equation of state. Unlike the previous models introduced in this section, the potential flow concept is not used for solving the fluid problem. The solid problem, which can represent either a rigid body or a flexible structure, is modelled using a structural FE solver.

This modelling framework has been implemented primarily within LS-DYNA, using its built-in ALE formulation and penalty-based FSI algorithms. However, in the early 2000s, a two-code strategy was also employed, in which MSC.Dytran (for the fluid) and LS-DYNA (for the structure) were coupled to solve the hydroelastic water impact problem. This approach was demonstrated by Bereznitski (2001).

A significant milestone in unified ALE–FEM modelling came with the work of Stenius et al. (2007, 2011), who used LS-DYNA to simulate the hydroelastic water entry of wedge-shaped sections. The authors have also tried to show when and where dynamic response of flexible water entry can be considered.

The application of LS-DYNA for simulating the water entry of rigid sections was well demonstrated by Wang and Guedes Soares (2011, 2013a, 2014a, 2014b) in a series of studies. In a separate series of works, Wang and Guedes Soares (2013b, 2017, 2018) along with Wang et al. (2021, 2022) modelled the dynamic response of 2D flexible wedges and plates during water entry using the LS-DYNA solver. More recently, Hosseinzadeh et al. (2023b) used LS-DYNA to simulate the hydroelastic water entry of 3D wedges and compared the results with those from CFD simulations, as will be discussed in Sub-section 6.2. Snapshots of the

simulations by Hosseinzadeh et al. (2023b) are shown in Fig. 42.

#### 5.3.8. Limitation and opportunity for future research

All the discussed semi-analytical models and coupled FFSI solvers have been validated through experiments or compared with other numerical models, demonstrating their efficiency and accuracy in predicting slamming pressures, strains, and deflections in simpler structures. However, as these models are based on the potential flow theory, they fail addressing more complex scenarios, such as those that involve cavitation, air cushions, air compressibility, and turbulence effects. Air cavitation and air compressibility, however can be partially covered by an ALE-FEM mode, but a fully nonlinear simulation that considers energy dissipation required CFD modelling which will be covered in sub-section 6-2.

### 5.4. Flexible marine propellers

To model flexible marine propellers, the fluid forces acting on the blades can be determined through various methods, each giving the fluid forces exerted on the surface of the blades. Several approaches can be used for solving the ideal flow around the propeller blade and are classified by Young et al. (2016). A list of numerical models that are used for doing so is presented in Table 20.

#### 5.4.1. BEMT, LL and LS models

The first group of models used for solving flexible marine propellers are based on Blade Element Momentum Theory (BEMT), Lifting Line (LL) and Lifting Surface (LS) methods. Any of these methods can be coupled with FEM to solve the FFSI of marine propellers. However, they may not fully capture the complex fluid dynamics surrounding the propeller and may prove inadequate for addressing transient problems. A notable early study by Lin and Lin (1996) exemplifies one of the pioneering efforts where LS and FEM were integrated in a two-way coupling to solve the fluid-structure interaction of flexible propellers. Another recent LS-FEM based models was recently developed by Kim et al. (2019). Such approaches to solving fluid flow around the propeller may also be applicable in the numerical modelling of the rigid responses of propellers. Such studies are beyond the scope of the present research (for an example of applying the LL model to the numerical modelling of a propeller free in six degrees of freedom, see Mao and Young, 2016).

#### 5.4.2. BEM-FEM based models

The second group of models used for solving fluid flow around the propeller blade and coupling it with solid motion, is the BEM. In the literature, BEM has been widely applied to solve the FFSI of marine propellers by various researchers since the late 2000s, although its initial use for solving fluid flow around marine propellers dates back to the 1970s (Kerwin and Lee, 1978). The application of BEM in solving fluid-structure interactions of marine propellers is notably demonstrated in the work of Young (2007a,b), where a BEM solver was coupled with a FEM solver (ABAQUS). This research sparked up a series of subsequent studies, which employed similar approaches to solve the fluid-structure interactions of flexible marine propellers.

The first follow-up study by Young (2008) developed steady and unsteady hydroelastic simulations of marine propellers using the BEM/FEM approach. This paper remains one of the most prominent in the field. This numerical approach has since demonstrated its practicality and applicability for engineering purposes (Motley et al., 2009; Young et al., 2010a). Additionally, the method is relevant in the marine renewable energy sector, where it can be employed to analyse the hydrostructural behaviour of marine turbines (Young et al., 2010b).

A similar numerical model was subsequently developed by Ghassemi et al. (2012), who also coupled BEM and FEM to address fluid-structure interactions of flexible propellers, subjected to uniform flow patterns. Other studies were later performed by Blasques et al. (2010) and Lee et al. (2014, 2017). Notably, the temporal pitch angle predicted by Lee et al. (2014) for non-uniform tests aligned more closely with the experimental data when hydrodynamic damping was incorporated.

Li et al. (2018) developed a new BEM-FEM coupled method to solve the fluid flow around elastic marine propellers operating under non-uniform conditions, demonstrating that a two-way fluid-structure interaction approach is more accurate and superior to a one-way approach. The two-way method requires consideration of added mass and damping coefficients, which are neglected in the one-way method. The key advantage of this model lies in its ability to account for fluid flow nonlinearity. The method was later used for parametric analysis of hydroelastic behaviours of marine propellers (Li et al., 2020b). More advanced models, building upon the foundation of Li et al. (2018), were developed by Li et al. (2021, 2022b, 2023) to solve the dynamic responses of the elastic propeller-shaft system. Additionally, a separate group of researchers conducted studies aimed at addressing the same problem (Zou et al., 2017, 2019a, 2019b, 2020, 2021).

#### 5.4.3. FEM-FEM based models

The third group of models for flexible marine propellers solve the fluid flow around the blades using FEM. Pioneering research in this area was conducted by Joe et al. (2021), who developed a FEM–FEM-based model to simulate the hydrostructural response of a flexible propeller. They developed a FFSI solver for marine propellers by utilising the Euler force. Interestingly, the fluid and solid domains were discretised using tetrahedral elements, and a perfect linear fluid dynamic problem was addressed within the time domain.

#### 5.4.4. Other models

The last model in the literature addressing the hydroelastic behaviour of flexible propellers with a theoretical foundation was developed by Chen et al. (2022b). This model posited that the rotating blades of a flexible propeller can be treated as cantilever plates subjected to fluid flow, thereby extending the hydrodynamic computation formula originally proposed by Blake and Maga (1975). The equations of motion were formulated using velocity as the variable and include parameters such as mechanical damping, density, and flexural stiffness. This framework embodies a two-way coupling characteristic and effectively addresses the fluid-structure interactions of flexible propellers.

### 5.5. Marine vegetation

The modelling of flexible marine vegetation needs understanding of hydrodynamic models used for modelling of the fluid flow around them, and structure models used for idealising their motions. Unlike other problems described in this section, we first introduce the hydrodynamic models, then the structural models, and in the end, we introduce the coupled hydrodynamic-structural models.

#### 5.5.1. Hydrodynamic models

To model flexible marine vegetation, each blade or stem of marine vegetation can be considered a slender structure. The most comprehensive hydrodynamic model for a single blade can be found in Leclercq and de Langre (2018). This model was inspired by the large-amplitude elongated-body theory proposed by Lighthill (1971) to study fish locomotion. Compared to models based on Morison's equation, which have also been commonly applied in the literature (Luhar and Nepf, 2016; Zhu et al., 2019), it is mathematically more consistent, particularly for the distributed reactive force along the length of the structure. The added mass force, included in Morison's equation, is only one of three contributions to the reactive force. The other two reaction force terms, which are ignored in Morison's equation, may not be negligible when the blade is far from perpendicular to the flow direction.

There is limited discussion in the literature on the applicability of the standard Morison model. Wei et al. (2024a) used the same comprehensive model as Leclercq and de Langre (2018) to study the deformation of a single blade under oscillatory flows and reported that the

**Table 21**
A summary of models developed for flexible marine vegetation exposed to water waves.

| Studies | Deformation Regime | Structural Model | Coupling Approach | Strengths | Limitations |
|---|---|---|---|---|---|
| Dalrymple et al. (1984) | Small to moderate | Rigid vegetation | One-way | Pioneering study on wave attenuation | No flexibility is considered |
| Kobayashi et al. (1993) | Large deformation | Rigid or simplified flexible blades | One-way | Simple and widely used in engineering | No dynamic response is considered |
| Zhu et al. (2020a, 2022) | Small deformation | Euler-Bernoulli beam | One-way | Ideal for small response regimes | Limited to small deflections |
| Wei et al. (2024c, d, 2025a) | Large deformation | Truss-spring model | Two-way | High efficiency and can capture large deflection. It is also open-source | Linearised flow model |

complete model seems to predict deformation better than the results of Zhu et al. (2019), where a standard Morison model was applied.

In rational models, the required cross-sectional hydrodynamic coefficients, namely the added mass and viscous drag coefficients, need to be calibrated from model tests or sophisticated CFD modelling. However, there is a lack of experimental data or reliable CFD results that can facilitate the practical application of these rational models. This represents one of the biggest challenges in applying rational models effectively.

### 5.5.2. *Modelling of structural dynamics*

Despite the challenges associated with large structural deformation, modelling the structural dynamics of marine vegetation alone is less daunting. In the literature, numerous numerical structural models have been developed for highly compliant structures with large deformations in waves and currents. To address the significant nonlinearity arising from large deflections, there are primarily two strategies.

One method involves discretising the governing equations of the flexible structure model to derive a nonlinear system of equations, which is then solved using the Newton-Raphson method (Mattis et al., 2015; Luhar and Nepf, 2016; Chen and Zou, 2019; Zhu et al., 2020a). Another technique transforms the nonlinear finite difference scheme into a linear one through a time delay approach (Yin et al., 2021a,b, 2022). This results in a linear system of equations involving unknowns, such as internal tensions and bending angles of the segments, albeit requiring matrix updates and solving at each time step.

Additionally, an approach similar to the N-pendulum model (Marjoribanks and Hardy, 2014) or that proposed by Cheng et al. (2019) divides the structure into multiple segments. The governing equations are derived from the local force balance for each segment, which leads to a system of equations solvable explicitly according to Newton's second law. To maintain stability in time-domain solutions, the added-mass force in the governing equation is approximated using relative acceleration rather than its normal component (Chang et al., 2020). However,

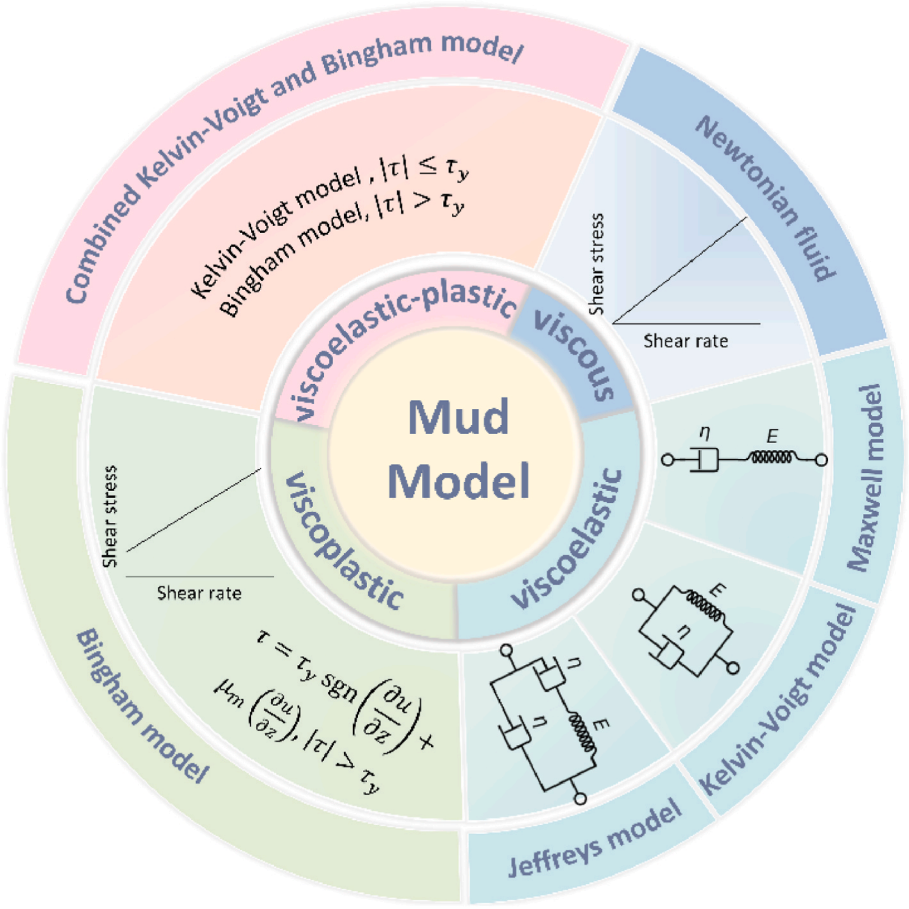


**Fig. 43.** Rheological modelling of mud. $z$ denotes the vertical coordinate and $\mu_m$ represents the Bingham-plastic viscosity.

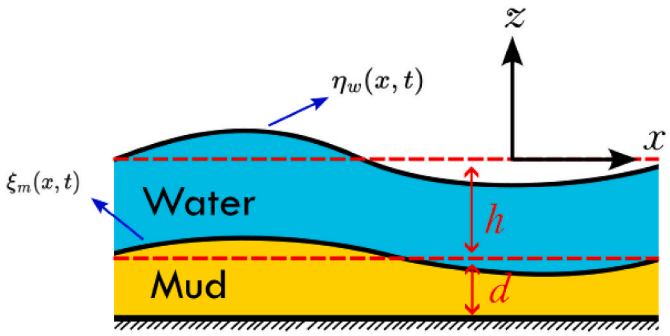


**Fig. 44.** A pictograph of the wave–mud interaction concept used in the formulation of dispersion relations for wave propagation over a muddy layer. The displacement of the free water surface is denoted with $\eta_w(x,t)$ and displacement of the water–mud interface is denoted by $\xi_m(x,t)$. This schematic serves as conceptual basis for understanding how the dispersion relation can be formulated. This figure is inspired by the original one presented in Liu and Chan (2007a).

these models, based on local force balance, do not provide a continuous governing equation to fully describe the physical problem.

Recently, Wei et al. (2024b) extended the truss model, successfully applied by Kristiansen and Faltinsen (2012, 2015) to study aquaculture net cages, to highly compliant seaweed blades. The original truss model does not account for the bending moment in the compliant structure. The extension by Wei et al. (2024a, b) involves an easy-to-implement strategy that adds rotational springs between adjacent trusses.

When applying a time-domain approach to solve the structural dynamics of submerged flexible structures in water, special care must be taken to ensure the stability of the numerical solver. This concern is associated with the added-mass term as part of the hydrodynamic loads. If an explicit time-marching scheme, such as the Runge-Kutta method, is employed, the solution may become unstable. Effective remedies have been developed, including using an implicit solver involving iterations within each time step (Leclercq and de Langre, 2018) or moving the added mass terms to the left-hand side of the time-domain equations to stabilise standard explicit approaches (Wei et al., 2024a, 2024b, 2025b).

Due to the nonlinearity caused by large deflections, an implicit method typically necessitates solving a nonlinear system of equations, often through the Newton-Raphson method (Leclercq and de Langre, 2018). Alternatively, a semi-implicit approach may yield a linear system of equations, albeit with a matrix that must be frequently updated and solved based on the blade posture. Models based on local force balance and lumped-mass approaches allow fully explicit methods. However, the stability condition can be stringent due to the significant difference between the body mass of the thin and slender vegetation blade and the added mass. To enable time integration with larger time steps and optimise computational efficiency, it becomes essential to segregate the added mass term from the inertial force, separating the body acceleration from the normal component of the relative acceleration between the vegetation blade and the flow (Wei et al., 2024a, 2024b, 2025b).

### 5.5.3. *Coupled hydrodynamics and structural dynamics*

In existing literature, studies on large deformation of vegetation blades predominantly focus on structural dynamics while overlooking flow solutions. These models typically use estimated or calibrated added mass and viscous drag coefficients to approximate hydrodynamic loads from the fluid to the structure. However, the loads exerted by the structure onto the fluid alter flow and wave fields. Consequently, hydrodynamic coupling between neighbouring blades occurs, and upstream vegetation influences inflow to downstream vegetation. A summary of developed models is presented in Table 21.

For small deformations of flexible vegetation, Zhu et al. (2020a, 2022) derived analytical solutions in the frequency domain to study

**Table 22**
Dispersion relationships developed for wave-mud interaction.

| Reference | Fluid idealisation | Mud idealisation | Water-mud interface modelling | Outputs of the model |
|---|---|---|---|---|
| Gade (1958) | Inviscid | Newtonian Fluid | Shear stress continuity | Wave dispersion |
| Dalrymple and Liu (1978) | Viscous | Newtonian Fluid | Velocity and shear stress continuity | Wave dispersion, interfacial amplitude, and velocity/ pressure profile |
| Macpherson (1980) | Inviscid | KV model | Vertical displacement and normal stress | Wave dispersion and interfacial amplitude |
| Mei and Liu (1987) | Viscous | Bingham plastic | Yield-based stress tracking | Plug/shear structure |
| Maa and Mehta (1990) | Viscous | KV model | Velocity, normal stress, and shear stress continuity | Shear stress, velocity/ pressure profile, wave damping |
| Piedra Cueva (1993) | Viscous | KV model | Layered model with matching | Shear stress, velocity profile, wave damping |
| Ng (2000) | Viscous | Newtonian Fluid | Two-layer Stokes model | Wave damping and mass transport |
| Liu and Chan (2007) | Viscous | KV model | Normal stress and vertical velocity continuity | Wave damping, shear stress, and velocity/ pressure profile |
| Jain and Mehta (2009) | Viscous | Different viscoelastic models | Stress balance | Wave damping and mass transport |
| Mei et al. (2010) | inviscid | KV model | Full shear and displacement coupling | Wave damping and interface displacement |
| Mohapatra and Sahoo (2011) | inviscid | Elastic | Elastic plate coupling | Wave dispersion |
| Rashidi-Juybari et al. (2020) | inviscid | Elastic beam sitting on a viscous damper | Elastic plate coupling | Wave dispersion and damping |

wave attenuation due to structural responses of the vegetation, modelling structures with a simple Euler-Bernoulli beam equation. However, this model's validity diminishes when considering large waves, which induce significant deformations or response patterns beyond what beam theory can accurately model.

Inspired by earlier work on wave attenuation by vegetation (Dalrymple et al., 1984; Kobayashi et al., 1993), Wei et al. (2024c, d, 2025b) developed a fully coupled wave-vegetation interaction model capable of efficiently solving coupled wave dynamics and flexible vegetation motion with large deflections. The flow model uses the continuity equation and linearised momentum equations of an incompressible fluid, with additional terms within the canopy region accounting for vegetation presence. This linearised flow solver is unconditionally stable and second-order accurate.

In their approach, the truss-spring model captures vegetation motion with substantial deflections, allowing explicit time integration with large time steps suitable for highly compliant vegetation. This coupled model, integrating the linearised flow solver and truss-spring model, has been applied to investigate wave propagation over a heterogeneous,

**Table 23**
A summary of phase resolving models developed for wave-mud interactions.

| Model Type | Fluid Model | Mud Model | Key Features | Studies | Strengths | Limitations |
|---|---|---|---|---|---|---|
| TRIADS-based models | Nonlinear mild-slope wave model (spectral) | Simplified damping layer ( Ng, 2000) | Triad interactions (sum/difference), 1D and 2D wave evolution with energy dissipation | Ng (2000), Kaihatu et al. (2007), Safak et al. (2017), Tahvildari and Sharifineyestani (2019) | Captures nonlinear wave-wave interactions; efficient for large-scale problems | Mud motion is not modelled |
| Shallow water models | Time-domain nonlinear shallow water equations | Bingham plastic | Fully nonlinear fluid model, time-stepping via FDM | Jiang and LeBlond (1993) | Captures full nonlinearity and viscoplasticity | High computational cost |
| Boussinesq-type models | Weakly nonlinear wave equations (frequency/time domain) | KV or Maxwell viscoelastic models | Harmonic energy tracking ( Garnier et al., 2013), explicit FFSI (Xia, 2014) with multi-layer mud | Garnier et al. (2013), Xia (2014) | Tracks energy dissipation across harmonics; transient simulation capability | Limited to weakly nonlinear waves |
| GN Models | Fully nonlinear GN equations | KV viscoelastic model | Nonlinear advection and mud feedback; solved in time domain | Kostikov et al. (2024) | Captures finite-amplitude wave effects with reasonable efficiency | Ignores horizontal shear in mud |

suspended, and flexible canopy, demonstrating high efficiency and good agreement with experimental data on wave attenuation and hydrodynamic loads on vegetation. The source code for this model has been publicly released (Wei et al., 2024c), emphasising its accessibility and transparency.

Wei et al. (2024c) reported high computational efficiency of their solver, noting that for a scenario involving over 400 flexible blades, the CPU time required on a single Intel(R) CPU E5-2660 v3@2.60 GHz to run full-scale simulations was only 88 s, demonstrating the practical applicability of the model.

### 5.6. Wave-mud interactions

Wave-mud interaction modelling can be approached from two distinct pathways, both of which have seen significant progress over time. The first pathway can be classed as an analytical research direction, where the primary objective is to develop a dispersion relationship for the wave-mud system, which can be used for prediction of wave attenuation coefficient. The second pathway pertains to the modelling of wave propagation, which can be conducted for both linear and nonlinear waves. In wave modelling terminology, this approach is referred to as phase-resolving models (not to be confused with phase-averaged modelling).

In modelling wave-mud interactions, one of the most important assumptions concerns how mud is mechanically idealised, which depends on its rheology and the frequency of oscillations (wave frequency). In the literature, various behaviours have been proposed for the muddy seabed, ranging from a perfectly elastic medium (Dawson, 1978; Dean and Dalrymple, 1991; Mallard and Dalrymple, 1977) to an elastic solid (Hu et al., 2023; Hu and Li, 2023; Li et al., 2020a), as well as viscous (Jiang et al., 1990; Li et al., 2020a; Ng and Mei, 1994), viscoelastic, viscoplastic, and viscoelastic-plastic rheological models, as illustrated in Fig. 43. The viscous representation can be modelled using both Newtonian and non-Newtonian power-law fluids. In this regard, Hayter and Mehta (1982) suggested that 18 parameters are necessary to characterise the rheological behaviour of mud.

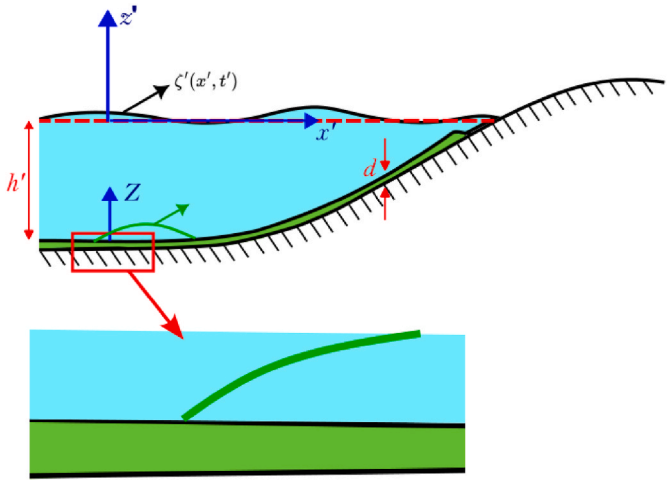


**Fig. 45.** Representation of the phase-resolving long-wave model developed by Garnier et al. (2013) for wave-mud interaction. The fluid domain is divided into two layers: an upper inviscid liquid layer, motions of which is governed by a Laplace Equation and a lower mud layer, motions of which is governed by continuity and momentum equations.

#### 5.6.1. Dispersion relationships

The art of the wave-mud interaction modelling began with the formulation of the dispersion relationship for the wave-mud system in the work of Gade (1958). The author idealised the water-mud medium as a two-layer system, where gravity waves propagating on the upper layer of an inviscid irrotational liquid were hypothesised to flow over a laminar, viscous muddy layer (See Fig. 44 as an example). The model developed by Gade (1958) sparked a new research direction, leading to the development of several wave-mud interaction models. Two decades later, Dalrymple and Liu (1978) extended Gade's model by incorporating the viscosity of the water above the mud. Their model demonstrated that the most significant mud-induced wave damping occurs when the mud thickness closely matches the boundary layer thickness. Ng (2000) further advanced these models by deriving explicit analytical expressions that allowed for a more detailed characterisation of wave attenuation. This model has been seen to be the core of some of phase-resolving models developed in 2000s and 2010s as will be discussed in 5.6.2.

In the models cited above, flexibility was still absent, as mud was treated purely as a viscous layer. However, mud can also exhibit elastic responses due to its viscoelastic nature as discussed in Section 3. Macpherson (1980) laid the groundwork for incorporating viscoelasticity by using the KV model to derive dispersion relations for water waves propagating over a viscoelastic seabed. Building on this, Maa and Mehta (1990) introduced viscoelastic models where elasticity acted as a restoring force and viscosity served as the dissipative mechanism. Later, Piedra-Cueva (1993) relaxed the assumption that water was viscous, instead modelling it as inviscid.

Following this, Liu and Chan (2007) introduced a thin viscoelastic mud layer into inviscid wave models, identifying resonance effects at particular frequencies, meaning that the elasticity of the muddy layer could either amplify or suppress wave attenuation. The model presented in Liu and Chan (2007) is mostly for a viscoelastic thin mud layer, though the authors have also introduced pure viscous and pure elastic models alongside the main presented model. A similar viscoelastic model was later developed by Mei et al. (2010).

The Bingham model, known for representing yield-stress fluids, was

**Table 24**
A summary of CFD models used for solving global ship hydroelasticity (in all cases CFD problem is solved using FVM, and hence CFD term is used for all).

| Authors | Method | CFD Solver | CSD Solver | Coupling | | Turbulence model | Case study |
|---|---|---|---|---|---|---|---|
| | | | | One way | Two-way | | |
| el Moctar et al. (2006) | CFD-FEM | COMET | ANSYS | ✓ | | RNG-k- turbulence model | Containerships |
| Lee et al. (2009) | CFD-FEM | Tenasi | ABAQUS | ✓ | | Menter SAS (Scale-Adaptive Simulation) | S175 |
| Wilson et al. (2008) | CFD-FEM | Tenasi | ABAQUS | ✓ | | Spalart-Allmaras one-equation turbulence model | S175 |
| Oberhagemann et al. (2009, 2010, 2015) | CFD-FEM | Comet | ANSYS | ✓ | | Not reported | An LNG carrier, and 18000 TEU container ship |
| Ma and Mahfuz (2012) | CFD-FEM | CFX | ANSYS | | ✓ | Not reported | multi-hull ship |
| Ley et al. (2013) and Ley and el Moctar (2014) | CFD-FEM | StarCCM+ | ANSYS | ✓ | | Laminar | Ferry and Ultra Large Container Vessel |
| Dhavalikar et al. (2015) | CFD-FEM | StarCCM+ | ANSYS | ✓ | | SST $k$-$\omega$ | Ferry |
| Takami et al. (2018) | CFD-FEM | StarCCM+ | LS-DYNA | ✓ | | SST $K$-$\omega$ | 6,600TEU Container ship |
| Paik et al. (2009) | CFD-FEM | CFDShip-IOWA version 4/ABAQUS | CFDShip-IOWA version 4/ ABAQUS | ✓ | ✓ | DES | S175 |
| Robert et al. (2015) | CFD-theoretical beam | ICARE | N/A | | ✓ | $K$-ω Wilcox model | Barge |
| Lakshmynarayanana et al. (2015) and Lakshmynarayanana and Temarel (2019) | CFD-FEM | StarCCM+ | ABAQUS | | ✓ | SST $k$-$\omega$ | Barge and S175 |
| Benhamou et al. (2018) | CFD-FEM | OpenFOAM | Not Reported (FEM) | | ✓ | Not Reported | 4400TEU Containership |
| McVicar et al. (2018) | CFD-FEM | Star-CCM+ | ABAQU | ✓ | ✓ | Menter Shear Stress Transport (SST) | wave-piercing catamaran |
| Lakshmynarayanana and Hirdaris (2020) | CFD-FEM | StarCCM+ | ABAQUS | ✓ | ✓ | SST $k$-$\omega$ | S175 |
| Sun et al. (2021) | CFD-FEM | StarCCM+ | ABAQUS | | ✓ | $k$-$\varepsilon$ | 6750-TEU |
| Pal et al. (2022) | CFD-FEM | StarCCM+ | LSDyna | ✓ | | SST $k$-$\omega$ | 6600TEU containership |
| Liao et al. (2024) | CFD-FEM | StarCCM+ | ABAQUS | | ✓ | the standard $k-\varepsilon$ model | Trimaran |
| Jiao et al. (2021a, b) | CFD-FEM | StarCCM+ | ABAQUS | | ✓ | Realizable $k$-$\varepsilon$ | S175 |
| Wei et al. (2022, 2023) | CFD-DMB | OpenFOAM | N/A | | ✓ | Blended $k$-$\omega$/$k$-$\varepsilon$ | S175 |
| Ma et al. (2024) | CFD-FEM | STAR-CCM+ | ABAQUS | | ✓ | Realizable $k$-$\varepsilon$ | 21000 TEU container ship |
| Xie et al. (2024) | CFD-FEM | ICFD (LSDyna) | LSDyna | | ✓ | Variational multiscale approach | Barge and KVLCC2 ship |
| Xie et al. (2025) | CFD-FEM | STAR-CCM+ | LSDyna | | ✓ | SST $k$-$\omega$ | Not a specifically classed |
| Chen et al. (2024a, 2025), Jiao et al. (2025b), Chang et al. (2025) | CFD-FEM | STAR-CCM+ | ABAQUS | | ✓ | Realizable $k$-$\varepsilon$ two-layer turbulence model | S175 and 21000 TEU |

**Table 25**
A summary of CFD studies that are performed to solve flexible motions of objects interacting with water waves.

| Authors | Method | CFD Solver | CSD Solver | Coupling | | Turbulence model | Problem |
|---|---|---|---|---|---|---|---|
| | | | | One way | Two-way | | |
| Huang et al. (2019) | FVM-FVM | solids4foam | solids4foam | | ✓ | Laminar | Wave-ice interaction |
| Huang and Li (2022) | FVM-FVM | solids4foam | solids4foam | | ✓ | Laminar | Wave interactions with submerged breakwater |
| Tavakoli et al. (2022) | FVM-FVM | solids4foam | solids4foam | | ✓ | Laminar | Wave interaction with viscoelastic ice |
| Brown et al. (2022) | FVM-FVM | solids4foam | solids4foam | | ✓ | Laminar | Wave interaction with a thin plate |
| Zhang et al. (2022) | FVM-FVM | solids4foam | solids4foam | | ✓ | Laminar | Wave interaction with breakwater |
| He et al. (2022) | FVM-DEM | StarCCM+ | StarCCM+ | | ✓ | Laminar | Wave-ice interactions with consideration of ice breaking |
| Hu et al. (2023) | FVM-FVM | solids4foam | solids4foam | | ✓ | Laminar | Wave interaction with a vertical wall |
| Hu and Li (2023) | FVM-FVM | solids4foam | solids4foam | | ✓ | stabilised turbulence model | Wave impact on a vertical wall |
| Gu et al. (2023) | FVM-FEM | StarCCM+ | ABAQUS | | ✓ | Not reported | Wave interaction with floating structures |
| Sun et al. (2023, 2024a) | FVM-FEM | OpenFOAM | CalculiX | | ✓ | Not reported | Wave interaction with vertical plates |
| Wang et al. (2022b, 2024a), Wei et al. (2024a) | FVM-FEM (nonlinear) | NEWTANK | In-house code | | ✓ | Not reported | Wave interactions with slender vertical bodies |
| Behnen et al. (2022, 2025) | FEM-FEM | ICFD | LS-Dyna | | ✓ | Laminar | Wave-ice interactions |
| Zhang et al. (2025a) | FVM-FEM | StarCCM+ | ABAQUS | | ✓ | SST $k$-$\omega$ | Wave interactions with VLFS |

also employed to derive analytical models for predicting wave attenuation. This was first done by Mei and Liu (1987), who idealised mud using the Bingham model and water using the shallow-water equations. In another study, Soltanpour and Samsami (2011) integrated both viscoelastic and plastic properties to formulate the dispersion relation for the wave-mud system.

While viscoelastic models were widely adopted by scholars throughout the 1990s and 2000s, two recent elastic-based models have been developed in 2011 and 2020. One such model was introduced by Mohapatra and Sahoo (2011), who formulated wave motion over an elastic bed extending infinitely in length. Later, Rashidi-Juybari et al. (2020) developed another hydroelastic model. In their model, the motion of the elastic bed was formulated using a modified Euler–Bernoulli beam theory, with the inclusion of a damping term that generates a damping force proportional to vertical velocity. A summary of models giving the dispersion relationship is outlined in Table 22.

#### 5.6.2. Phase-resolving models

The phase-resolving models have also been used for solving wave-mud interactions under inviscid fluid assumptions. Dispersion relationships developed analytically, may be used in such models to well couple mud motion and fluid motion, or dispersion of waves may be developed via solving the problem (e.g. GN modelling approach).

Four different groups of phase-resolving wave-mud interaction models under the inviscid fluid assumption can found in the literature. A detailed summary of these models with the relevant references is presented in Table 23. The first set of models are developed on the basis of TRIADS modelling approach. In these models, nonlinear mild-slope waves are assumed to propagate in the fluid domain, and the evolution of energy for each wave component is formulated by incorporating a dissipation rate, along with triad interactions (sum and difference interactions between wave modes propagating in the water). Mud-induced dissipative terms can be included in the governing equations, but researchers have primarily favoured the formulation by Ng (2000). The study by Kaihatu et al. (2007) exemplifies this research direction. Further developments in this modelling framework are presented in Kaihatu and Tahvildari (2012), Safak et al. (2017), and Tahvildari and Sharifineyestani (2019). It is worth noting that these studies have consistently modelled the mud layer using Ng (2000), but there remains room to explore other dispersion relationships for the wave-mud system, depending on the rheological properties of the mud. In all TRIADS models, mud is treated as a viscous layer that dampens fluid motions, and its elastic deformation is not modelled.

Another group of nonlinear wave-mud interaction models found in the literature are based on nonlinear shallow water wave propagation. The governing fluid equations are solved in the time domain, where nonlinearity is fully retained within the modelling. Jiang and LeBlond (1993) used this approach to solve the problem. The mud layer was treated as Bingham plastic fluid. Under this formulation of Bingham plastic idealisation, no flow emerges unless the shear stress exceeds the critical yield stress. Once the yield stress is exceeded, the mud behaves as a viscoplastic fluid. And if the shear stress drops below the threshold, the mud stops moving and again behaves like a solid. The fluid motion in the mud was governed by the Navier–Stokes equations, modified to incorporate Bingham plastic rheology.

The third type of model developed for phase-resolving wave-mud interaction under inviscid fluid assumptions in the literature is based on Boussinesq-type wave equations, incorporating weak dispersion and nonlinearity. The Garnier et al. (2013) model developed a model, the sketch of which is shown in Fig. 45, using a Boussinesq-type mode. Nonlinearity in the model was captured using perturbative expansions, and the problem was solved in the frequency domain for different harmonics. This allows tracking the amplitude evolution of both the free surface and water-mud interface along the nearshore zone. The authors showed that mud-induced dissipation significantly dampens the 2nd, 3rd, and 4th harmonics of the wave, particularly in elastic-dominated muds. This is because resonance effects, which enhance energy absorption at specific frequencies, can dominate when the muddy layer behaves more like an elastic layer. Another example of Boussinesq-type model developed to solve a weakly nonlinear wave-mud interaction problem is the work of Xia (2014).

The fourth group of models developed for wave–mud interaction is based on the GN equations. This approach has been presented in the literature by Kostikov et al. (2024), who modelled wave propagation over a viscoelastic layer treated using a KV model. Nonlinearity is incorporated in the model directly within the GN formulations. The model does not capture all nonlinear phenomena, such as wave breaking, which are typically captured through CFD modelling, as will be discussed in Sub-section 5.6.

## 6. CFD model

This section presents a review of CFD models used to solve the problems covered in this research. The review, however, is limited to mesh-based models used or developed for solving FFSI problems under the viscous liquid assumption, as meshless ones would need a separate review paper. As will be explained in sub-section 6.1, flexible wave–structure interaction and global ship hydroelasticity are covered together in a single sub-section, rather than being looked at in two different sub-sections.

### 6.1. Flexible wave-structure interactions and global ship hydroelasticity

CFD modelling of the flexible wave-structure interactions and global

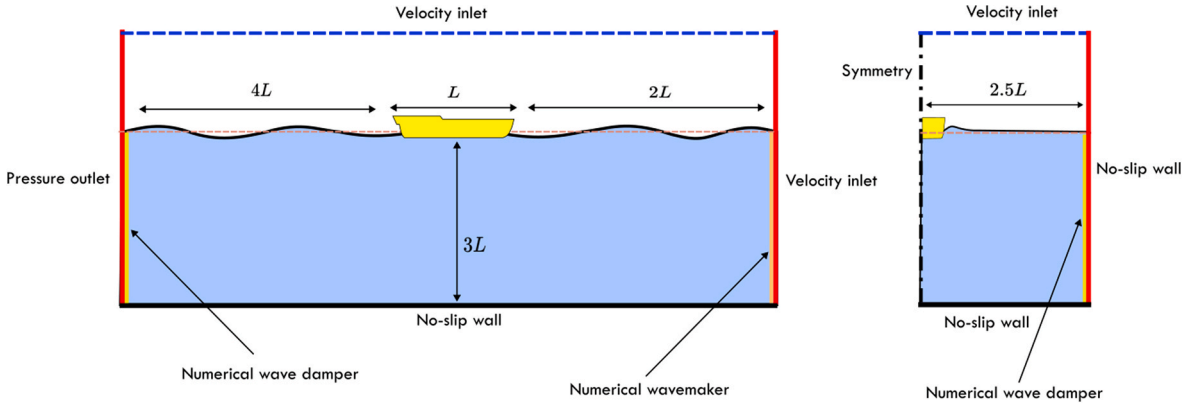


**Fig. 46.** CFD domain used for solving the fluid flow around a flexible ship. The dimensions are set to be equal to those set by Lakshmynarayanana and Hirdaris (2020). Here, $L$ denotes the length between perpendiculars.

ship hydroelasticity are very similar to each other. This is because models developed for solving the related FFSI problem use any CFD code (mostly Comet, OpenFOAM, STARTCCM+, ICFD) that solve three-dimensional fluid flow around a ship or a flexible marine structure and solve the dynamic response of a ship/structure using any preferred structural idealisation, depending on the need. Unlike, the potential flow-based models introduced in sub-sections 5.1 and 5.2, the CFD-based models are not restricted in modelling nonlinearities and solve the problem for a fully nonlinear condition, as explained in Section 3. Hence, they are capable of considering both wave nonlinearities and body nonlinearities. The lists of CFD-based studies for modelling global ship hydroelasticity and wave–structure interactions are presented in Tables 24 and 25, respectively.

To solve interactions between any flexible structure/ship and water waves using CFD, fluid motions and flexible bodies may be coupled or decoupled depending on the topology of the structure, wave nonlinearity and relative length of the water waves with respect to the length of the structure. This need has been studied by some researchers who compared one-way and two-way modelling results against each other and those of experiments and will be explained more detail in the remaining of this sub-section. In general, a CFD tank is created with wave generation at one end and wave absorption at the other ends (e.g. Lakshmynarayanana and Hirdaris, 2020). The ship or flexible marine structure is placed within this tank. Assuming symmetric conditions (i.e., following seas or head seas), the ship is typically positioned at a distance $D_1$ from the inlet boundary, defined as a velocity inlet, and at a distance $D_2$ from the outlet boundary, defined as a pressure outlet (see Fig. 46). Lakshmynarayanana and Hirdaris (2020), using Star-CCM+, designed a CFD tank with $D_1 = 2L$ and $D_2 = 4L$ when modelling ship hydroelasticity, where $L$ is the ship length. More recently, Karola et al. (2024), who modelled wave-induced ship motions at full scale using OpenFOAM-v202206, designed a tank by setting $D_1 = 2\lambda$ and $D_2 = 3\lambda$, where $\lambda$ is the wavelength. Readers interested in a CFD domain modelling a flexible ship in a non-symmetric condition are referred to Chen

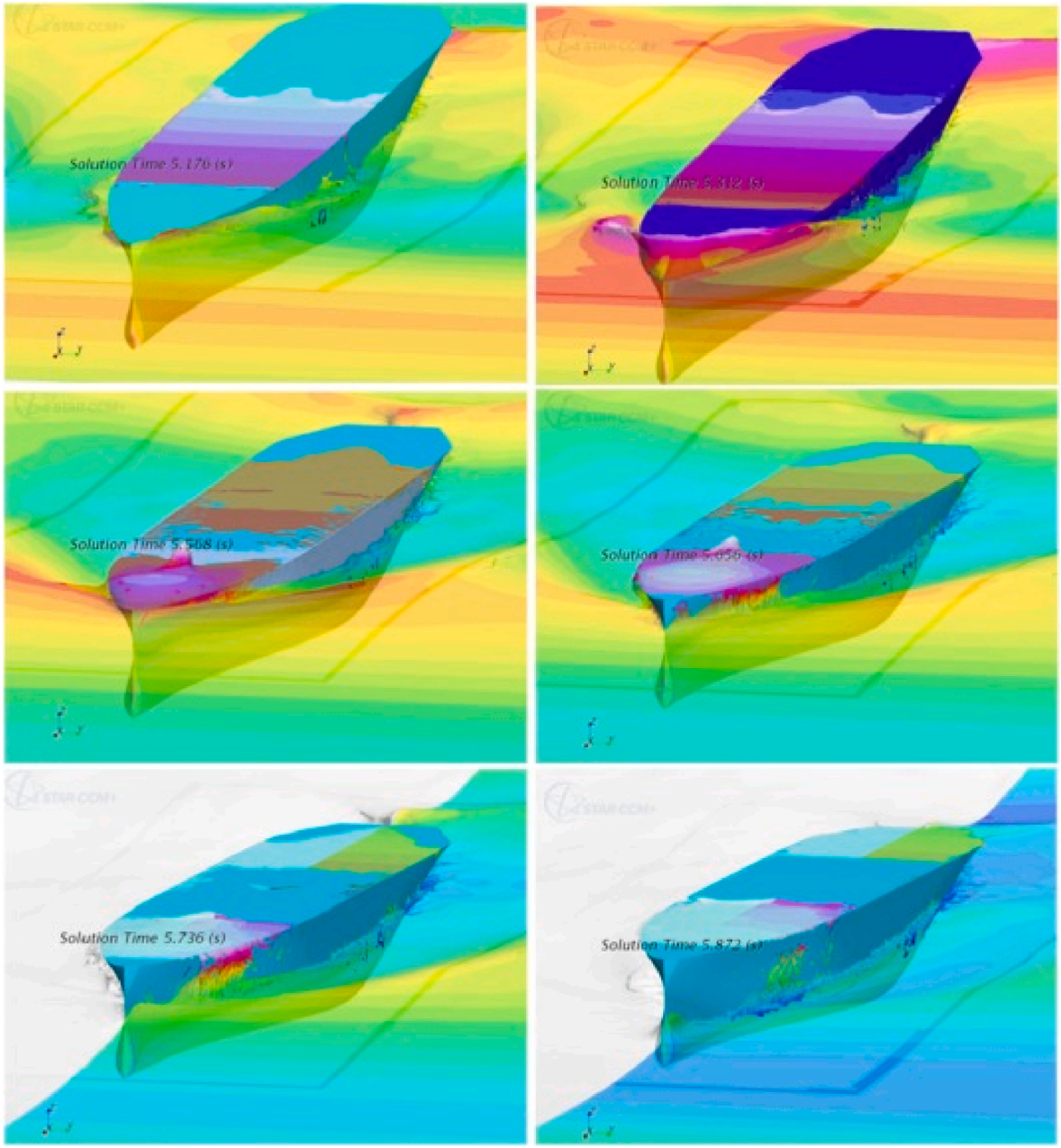


**Fig. 47.** An elastic ship exposed to water waves, modelled using CFD runs by Lakshmynarayanana and Hirdaris (2020). © Elsevier.

et al. (2024a).

#### 6.1.1. One-way models for global ship hydroelasticity

The very early studies aimed at modelling the hydroelastic motions of ships and structures exposed to waves using CFD codes began in the mid-2000s, notably by el Moctar et al. (2006). In this study, el-Moctar et al. (2006) employed a RANS-based CFD code to solve the fluid motion around a flexible ship subjected to water waves. The hydrodynamic pressures obtained from the CFD model were then applied to the solid interface of the ship structure to compute its elastic response using an FEM solver. While the rigid body motions of the ship were coupled with the fluid motion, the flexible motions and fluid dynamics were not.

Subsequent research followed a similar one-way coupling approach, and they mostly focused on hydroelasticity modelling of ships/barges advancing/floating on wavy water surfaces (e.g. Wilson et al., 2008; Lee et al., 2009; Oberhagemann et al., 2009, 2010, 2015; Ley et al., 2013, 2014; Dhavalikar et al., 2015).

The one-way coupling approach of the models developed to address ship hydroelasticity may have potential limitations: one is the effect of elastic motion of the ship on wave field which is not captured as elastic responses are not fed back to the fluid domain, and the other is the effect of water on elastic modes of the ship (i.e. wet modes), as a dry hull of the ship may be modelled in a FEM code (or any other Computational Solid Dynamic solver, CSD). Researchers have overcome this challenge using two distinct methods. The first involves modelling the water as an external medium interacting with the elastic structure within the CSD solver (e.g. Wilson et al., 2008), while the second utilises the Lewis form approach to calculate the added mass (e.g. Oberhagemann et al., 2009). The former approach has been seen to be more popular.

One set of one-way coupling simulations was conducted by Takami et al. (2018). The authors compared their CFD-FEM results with those of weakly nonlinear 2D and 3D models, noting that the vertical bending moments predicted by all models were comparable, though the viscous-based simulations demonstrated a higher level of accuracy in predicting the rigid body response of the ship. The authors observed that the natural frequency of the CFD-FEM model differed from experimental results, which they attributed to the limitations of the one-way coupling approach.

#### 6.1.2. Emergence of two-way models for global ship hydroelasticity

The shift towards two-way coupling of the flexible fluid-structure interactions between water waves and structures/ships using CFD approaches occurred shortly after the introduction of the early one-way models. This development took place in 2009 with the study by Paik et al. (2009). They coupled CFDShip-Iowa version 4.0 with ABAQUS to solve the dynamic responses of S175 container ship in water waves. The

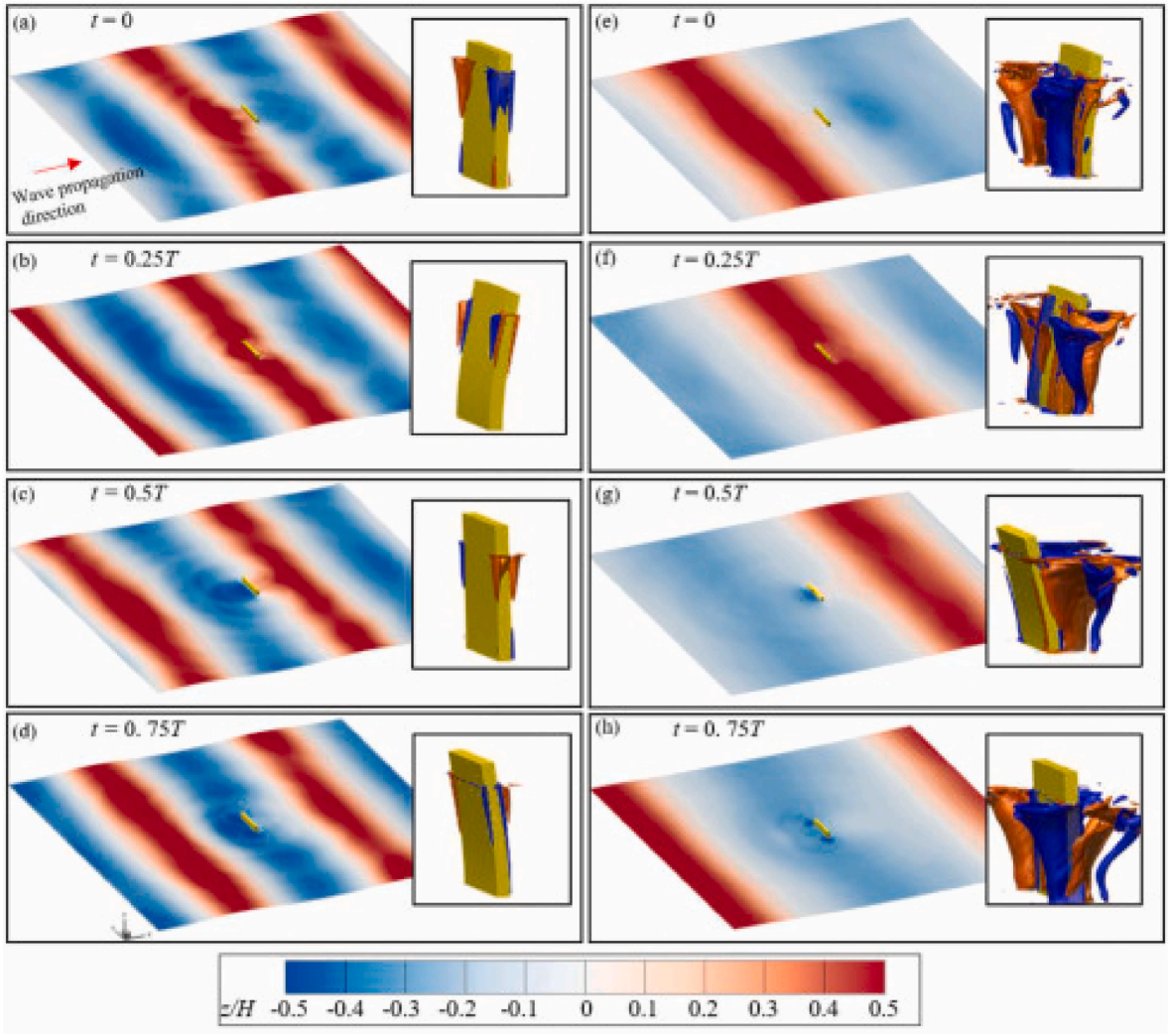


**Fig. 48.** An elastic wall exposed to regular head waves with two different wavelengths, 5*D* and 10*D*, where *D* is the wall depth. The water surface is represented by *z* and normalised by *H*, the wave height. The close-up views show iso-surfaces of vorticity formed around the flexible structure, with red indicating positive vorticity values. These snapshots are taken from Wang et al. (2024a). © Elsevier.

model employed a LSM to track the air-water interface.

Following the two-way flexible FSI model developed by Paik et al. (2009), Robert et al. (2015), and Lakshmynarayanana et al. (2015), Lakshmynarayanana and Temarel (2019, 2020) introduced a new generation of fully coupled FFSI models for ship global hydroelasticity. However, the model developed by Robert et al. (2015) idealised ship structural motions using a theoretical beam model, whereas Lakshmynarayanana and Temarel (2019, 2020) used FEM modelling. Other models can be found in Jiao et al. (2021a, b), Xie et al. (2024, 2025), and Ma et al. (2024). Two recent CFD-FEM models that differ significantly from previous works by solving the dynamic responses of ships in oblique waves (whereas all other models focused on symmetric responses) are presented in the scholarly works of Chen et al. (2024a) and Jiao et al. (2025a).

With the gradual development of two-way coupling models for global ship hydroelasticity, researchers began to compare predictions of one-way simulations with two-way simulations. However, the first comparison between these two coupling approaches was initiated in the study by Paik et al. (2009). The computational time for a two-way coupled simulation to be run for 10 s of physical time can be as much as twelve times that of a one-way coupled model (Takami and Iijima, 2020). These studies primarily focused on ship hydroelasticity, with researchers not showing much interest in flexible wave-structure interactions. Some other studies were performed by McVicar et al. (2018) and Lakshmynarayanana and Hirdaris (2020). McVicar et al. (2018) showed that a one-way coupling model, with updated added mass produced vertical bending moments that were very similar to those predicted by the two-way coupling approach, and that two-way coupling is not necessary if the nonlinear time variation of added mass is adequately incorporated into the structural modelling of the ship. In the study carried out by Lakshmynarayanana and Hirdaris (2020), it was found that the one-way coupling approach significantly under-predicted the 2-node wave load component compared to the two-way approach. The authors concluded that the effects of structural flexibility might become more pronounced at higher frequencies, where the one-way coupling approach tends to under-predict wave loads. Snapshots of CFD simulations of Lakshmynarayanana and Hirdaris (2020) are illustrated in Fig. 47.

There have been some recent advancements in two-way modelling of global ship hydroelasticity using the two-phase solver of OpenFOAM by Benhamou et al. (2018) and Wei et al. (2022, 2023). Interestingly, Wei et al. (2022) developed a novel coupling between OpenFOAM and a structural solver that employs a DMB approach to idealise the ship structure. This approach is particularly significant, as it represents the first attempt to couple CFD a DMB approach for the hydroelastic modelling of ships and structures exposed to water waves.

#### 6.1.3. *Emergence of models addressing wave interaction with flexible marine structures*

While much of the focus in viscous-based modelling of flexible structures and ships exposed to water waves has traditionally been on ships, flexible structures (e.g. breakwater and ice sheet) began to receive increased attention starting with the CFD-based study by Huang et al. (2019). The authors further developed *solids4Foam* code (Cardiff et al., 2025), a fluid-solid interaction library within OpenFOAM, to simulate flexible wave-structure interactions. Both the fluid and the flexible motions of the solid were discretised using FVM, significantly improving simulation efficiency by eliminating the need to transfer data between separate fluid and solid solvers, as all computations occur within a single. This study, along with the developed code, inspired a series of subsequent research efforts and marked a significant shift towards CFD modelling of flexible wave-structure interactions, including those carried out by Huang and Li (2022), Hu et al. (2023), Hu and Li (2023), Tavakoli et al. (2022), Zhang et al. (2022), Luo and Huang (2024), and Brown et al. (2022).

In parallel with studies using solids4Foam to simulate the hydroelastic responses of marine structures interacting with water waves, other CFD-based investigations have emerged since 2022. Examples can be found in Gu et al. (2023), Sun et al. (2023, 2024a), Zhang et al. (2025a), who coupled CFD models with FEM; Wang et al. (2022b, 2024a), Wei et al. (2024b), who coupled a CFD model (namely NEWTANK, sourced from Liu and Lin, 2008) with a nonlinear FEM model to simulate the dynamic responses of vertical slender bodies and nonlinear motions; and Wei et al. (2024b), who coupled CFD models with DMB using a quasi-static mooring module to model dynamic responses of a moored flexible floating structure. In addition, examples of using ICFD

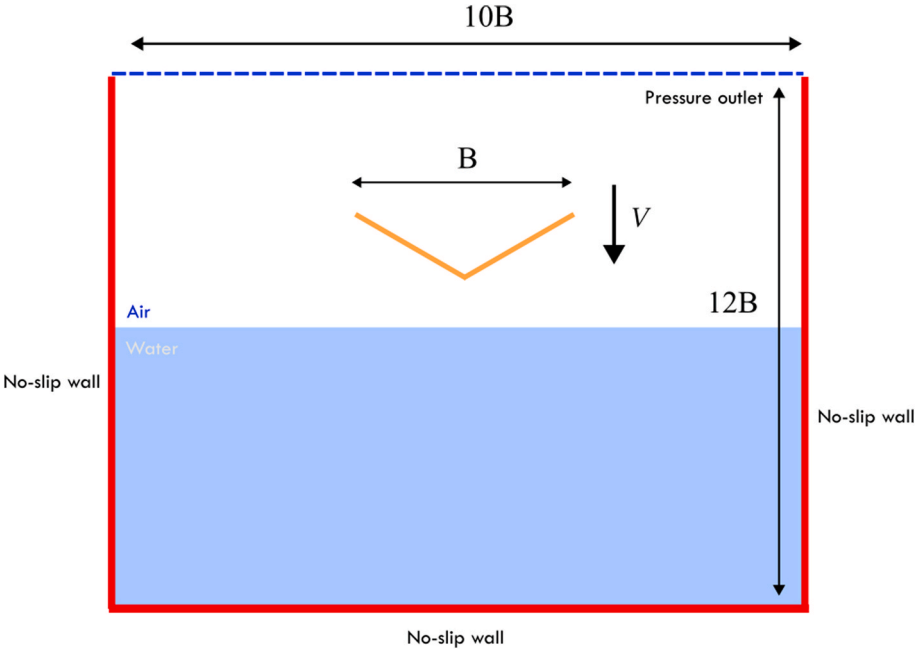


**Fig. 49.** An example of a CFD domain designed for a water entry problem. The dimensions are set to be equal to those of Hosseinzadeh and Tabri (2021b). Here *B* is the beam of the wedge.

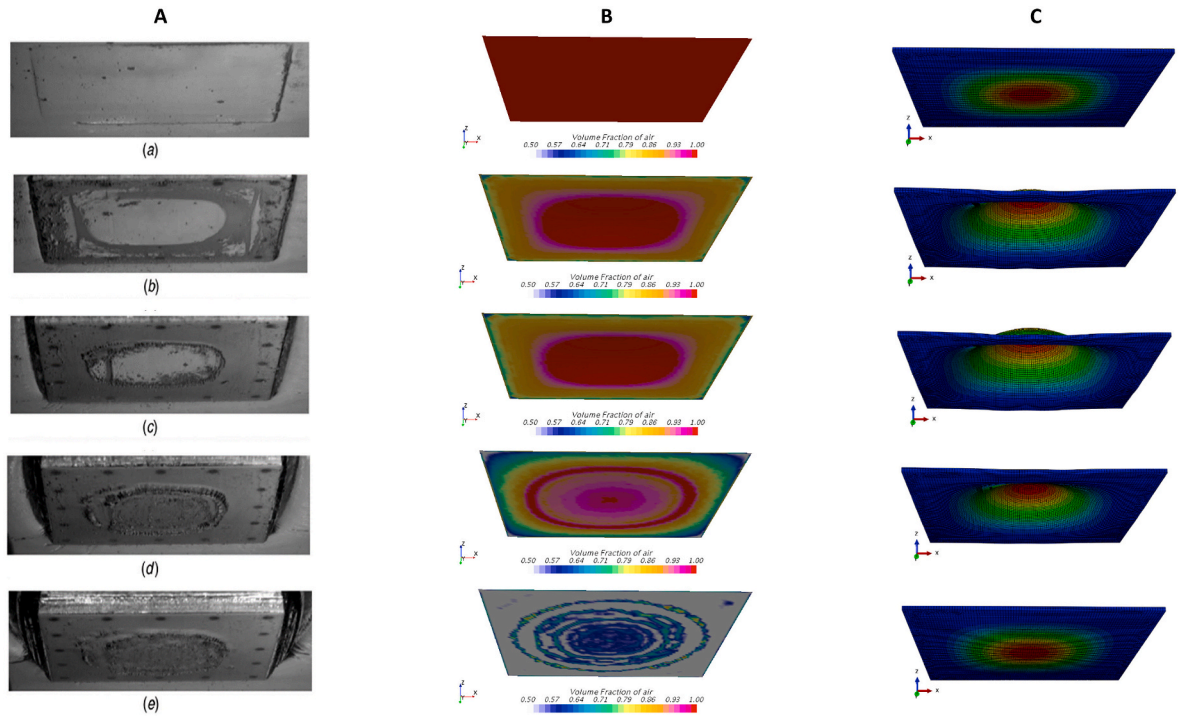


**Fig. 50.** Snapshots from simulations of flat plate water entry run by Yan et al. (2022). The left panels display experimental photographs capturing the water entry process and air entrapment formation. The middle panels illustrate the evolution of air entrapment during the FFSI simulations. The right panels show the resulting structural deformation of the plate. © Elsevier.

(LS-Dyna) for wave-ice interaction modelling can be found in two papers published by Behnen et al. (2022, 2025). Snapshots of simulations run by NEWTANK code is shown in Fig. 48.

Recent efforts in the realm of CFD-based modelling of flexible wave-structure interactions have introduced the innovative use of CFD-DEM coupling to study interactions between water waves and flexible structures/ships. He et al. (2022) pioneered the use of CFD-DEM for this problem, which has traditionally been employed in ocean engineering to model pack ice and its interactions with ships or offshore structures (e.g. Huang et al., 2020), by adapting it to simulate the flexible motions of ice covers exposed to water waves. In their study, part of a numerical tank was fully covered with ice particles, and the motion of these particles under wave-induced forces in the water medium was numerically modelled. This one-way coupling approach allowed the authors to incorporate ice break-up into their simulations, representing a significant advancement in flexible wave-ice interaction modelling.

#### 6.1.4. *Future research directions*

While significant progress has been made in modelling flexible FSI problems, including global ship hydroelasticity and floating structures/seawalls, and various codes have been developed, there remain areas for further development. A clear gap at the present stage lies in the limited understanding of the differences between one-way and two-way coupling approaches for simulating global ship hydroelasticity under oblique wave and beam sea conditions. Another notable research gap lies in the comparison of one-way and two-way coupling approaches for flexible wave-structure interactions. As a final note, IBM-based models have not yet been developed for modelling flexible wave–structure interactions and global ship hydroelasticity. This is reasonable when it comes to ships, as modelling a hull girder using IBM would be very challenging. However, for floating structures, such as box-shaped bodies or thin sea ice, the challenge appears to be less severe. Therefore, there is still room for the development of IBM-based models for flexible wave–structure interactions.

### 6.2. *Flexible slamming*

The slamming problem has been a subject of numerous CFD-based studies in ocean engineering since the 2000s. Various CFD codes have been developed to simulate the water entry of different 2D and 3D bodies, each tailored for specific applications. Early studies, particularly in the early 2000s, primarily addressed the water entry of rigid bodies (e.g. Fairlie-Clarke and Tveitnes, 2008). Over time, however, CFD-based simulations began to be applied to flexible water entry problems.

This line of research closely followed earlier inviscid-flow-based studies aimed at developing models for flexible slamming in the 2000s

**Table 26**
A summary of CFD simulations conducted to model flexible bottom slamming.

| Authors | Method | CFD solver | CSD solver | Turbulence model | Is compressibility considered? | 3D or 2D |
|---|---|---|---|---|---|---|
| Xie et al. (2018) | FVM-FEM | FLUENT | ANSYS | Laminar | No | 3D stiffened plate |
| Xie et al. (2019) | FVM-FEM | FLUENT | ANSYS | Laminar | Yes | 3D stiffened plate |
| Yamada et al. (2020), | FEM-FEM | ICFD | LS-DYNA | Laminar | No | 3D stiffened plate |
| Truong et al. (2021) | FVM-FEM | ICFD | LS-DYNA | Laminar | No | 3D stiffened plate |
| Truong et al. (2021) | FEM-FEM | StarCCM+ | ABAQUS | $k$-$\varepsilon$ turbulence model | Yes | 3D stiffened plate |
| Truong et al. (2021) | FEM-FEM | CFX | ANSYS | Laminar | No | 3D stiffened plate |
| Yan et al. (2021, 2022) | FVM-FEM | StarCCM+ | ABAQUS | Laminar | Yes | 3D plate |
| Tavakoli et al. (2023c) | FVM-FVM | solids4foam | solids4foam | Laminar | No | 2D plate |
| Jiao et al. (2024) | FVM-FEM | StarCCM+ | ABAQUS | $k$-$\varepsilon$ turbulence model | Yes | 3D stiffened plate |

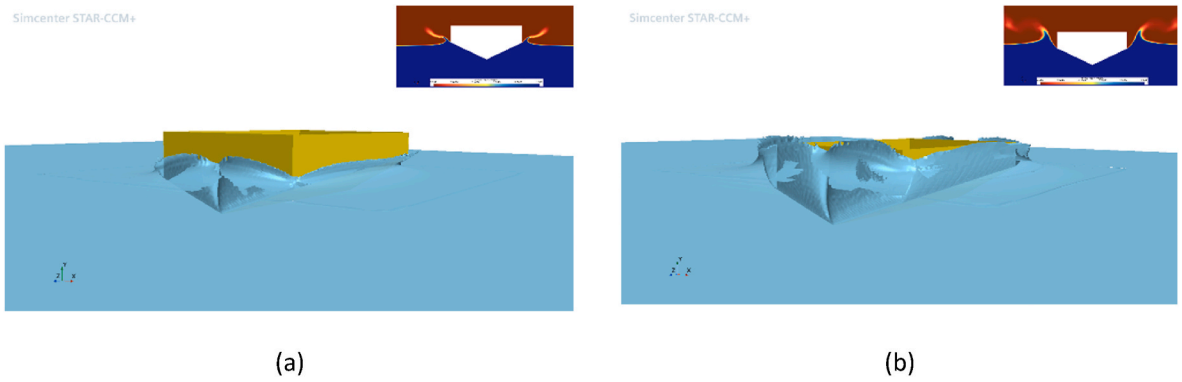


**Fig. 51.** CFD–FEM simulations of the FFSI water entry of a 3D wedge were performed by Hosseinzadeh (2023). Snapshots (a) and (b) illustrate two different stages of the water entry process. The 2D views of the air–water phase around the midship section of the 3D wedge are shown in the upper-right corner of each snapshot.

(e.g. Bereznitski, 2001; Stenius et al., 2007). Similar to other problems discussed in this section, CFD-based studies in this area emerged as a natural progression, building upon the foundational theoretical models developed under the non-viscous flow assumption to create more robust viscous-based models. To model the problem using CFD, a CFD water entry lab needs to be designed. The body is either assumed to move towards the water with a constant speed, or in contrast water is assumed to flow towards the solid body, which is initially dry. If a free fall water entry is modelled, however, the flow is not set to move towards the body, and body under the force of gravity is placed above the water surface and falls in it. Hence, a dynamic mesh motion may also be required, for managing of which an overset mesh is mostly favoured. In the literature, one can see that the width of the tank is mostly set to be in-between 5B to 10B, where B is beam of the object. A shorter width may cause blockage and increase hydrodynamic pressure. An example of a CFD tank used for modelling the water entry problem is shown in Fig. 49.

### 6.2.1. *First generation of models*

The first significant modelling of flexible water entry using CFD approaches was conducted in the early 2010s by Maki et al. (2011). They coupled OpenFOAM with a structural analysis code to predict the dynamic response of an elastic wedge using mode superposition, with the modes calculated via a commercial FEM code. Although their approach employed a one-way coupling method, it is widely regarded as a foundational study that spurred further research over the following decade. Building on this work, Piro and Maki (2013) later upgraded the model to a two-way coupling framework by introducing a linearised BC at the fluid-solid interface. Parallelly, Liao et al. (2013) developed a two-way coupling method to address the hydroelastic slamming problem of wedge-shaped bodies, and used IBM to track the fluid-solid interface. The fluid motions were solved using a FDM discretisation approach, while the structural motion equations were resolved through modal

**Table 28**
A summary of hybrid models developed for flexible slamming.

| Authors | CFD solver | CSD solver | Coupling | | Case Study |
|---|---|---|---|---|---|
| | | | One-way | Two-way | |
| Volpi et al. (2017) | CFDShip-Iowa | ANSYS | ✓ | ✓ | Planing boat |
| Diez et al. (2022) and Lee et al. (2024) | CFDShip-Iowa | ANSYS | ✓ | ✓ | Planing boat |
| Diez et al. (2022) and Lee et al. (2024) | StarCCM+ | NASTRAN | ✓ | ✓ | Planing boat |

**Table 27**
A summary of CFD simulations conducted to model flexible slamming scenarios, excluding bottom slamming.

| Authors | Method | CFD solver | CSD solver | Coupling | | Case Study | Simulation Conditions |
|---|---|---|---|---|---|---|---|
| | | | | One-way | Two-way | | |
| Maki et al. (2011) | FVM-FEM | OpenFOAM | ABAQUS | ✓ | | 2D Wedge-shape body | Constant speed water entry |
| Liao et al. (2013) | FDM-FEM (IBM approach) | In-house | In-house | | ✓ | 2D Wedge-shape body | Constant speed water entry |
| Piro and Maki (2013) | FVM-FEM | OpenFOAM | ABAQUS | | ✓ | 2D Wedge-shape body | Constant speed water entry |
| Izadi et al. (2018) | FVM-FEM | StarCCM+ | StarCCM+ | | ✓ | 2D Wedge-shape body | Constant speed oblique/asymmetric water entry |
| Javanmardi and Ghadimi (2019) | FVM-FEM | CFX | ANSYS | ✓ | | 2D section of Semi-Piercing propeller | Constant speed water entry (multi-phase fluid dynamics) |
| Hosseinzadeh and Tabri (2021b) | FVM-FEM | StarCCM+ | StarCCM+ | | ✓ | 2D Wedge-shape body | Free wall water entry |
| Mesa et al. (2022) | FVM-FEM | OpenFOAM | ABAQUS | ✓ | ✓ | 3D inclined plate | Ditching |
| Yan et al. (2023) | FVM-FEM | StarCCM+ | ABAQUS | | ✓ | Flat plat and 2D Wedge water entry | Constant speed water entry |
| Tavakoli et al. (2023b) | FVM-FVM | solids4foam | solids4foam | | ✓ | 2D Wedge water entry | Constant speed water entry |
| Tavakoli and Hirdaris (2023) | FVM-FVM | solids4foam | solids4foam | | ✓ | 2D Wedge water entry | Constant speed oblique water entry |
| Hosseinzadeh et al. (2023b) | FVM-FEM | StarCCM+ | ABAQUS | | ✓ | 3D non-prismatic wedge-shaped body | Free fall water entry |
| Chen et al. (2023b) | FVM-FEM | StarCCM+ | ABAQUS | | ✓ | 3D wedge | Water entry in rough water |
| Sun et al. (2024b) | FVM-FEM | OpenFOAM | CalculiX | | ✓ | Curved wedges | Constant speed water entry |
| Yang et al. (2024) | FVM-FEM | StarCCM+ | ABAQUS | | ✓ | Sphere | Hyperelastic water entry |

superposition using FEM. They reported that their model could not successfully capture the higher-order vibrations of the structure before chine wetting, which was seen to be monitored by BEM-FEM approach.

#### 6.2.2. Flat plate models: bottom slamming

There has been a surge in modelling the flexible hydroelastic behaviour of flat objects using CFD since 2018. It started with the work of Xie et al. (2018). They developed a strongly two-way coupled model that employed the FVM and FEM to discretise the fluid and solid motion equations, respectively. However, their study assumed the fluid to be incompressible, which could be a limitation. At that time, CFD codes capable of predicting impact loads on rigid bodies while accounting for fluid compressibility had already been developed (e.g. Ma et al., 2016). Addressing this limitation, Xie et al. (2019) advanced their earlier model by introducing a CFD-FEM framework that could simulate the hydroelastic response of a flexible body entering water while considering fluid compressibility.

Other studies were conducted by Yamada et al. (2020), Truong et al. (2021), and Yan et al. (2021, 2022), who coupled different CFD–CSD models to solve flexible flat plate problems. Among these models, the work of Truong et al. (2021) is introduced in more details. The authors presented a benchmarking analysis of the dynamic responses and impact loads of a stiffened plate during slamming events. This study utilised LS-DYNA ALE, LS-DYNA ICFD, ANSYS CFX, and StarCCM+/ABAQUS codes, with the latter three solving the fluid problem under viscous flow assumptions. For the StarCCM+/ABAQUS runs, the fluid was modelled as compressible, a turbulent flow regime was considered, and a $k$-$\varepsilon$ turbulence model was employed. All simulations adopted a two-way coupling approach, enabling detailed analysis of their performance in modelling the flexible FSI of a plate entering water. Snapshots of the simulations by Yan et al. (2022) are shown in Fig. 50.

In a different study, Tavakoli et al. (2023c) simulated the dynamic responses of elastic plates entering water using an FVM–FVM coupling approach implemented in solids4Foam. The authors demonstrated how complicated CFD models can be formulated into a model that predicts the hydroelastic response of a plate entering water. This study, however, is limited to incompressible fluid cases. Future research needs to further develop the code to address such limitations. A detailed list of CFD studies modelled flexible bottom slamming is presented in Table 26.

#### 6.2.3. Wedge shaped bodies and non-flat bodies

Within the body of research on slamming of non-flat structures, running parallel to the research on flexible bottom slamming since 2018. These investigations have mostly followed the one-way or two-way FVM–FEM coupling approach developed by Maki et al. (2011) and Piro and Maki (2013), with researchers generally favouring the two-way approach. Studies were mostly focused on the 2D problems. Notable two-way FVM–FEM studies were conducted by Izadi et al. (2018), Hosseinzadeh et al. (2020), Hosseinzadeh and Tabri (2021b), Yan et al. (2023) and Sun et al. (2024b) on the slamming of wedge-shaped bodies. The model developed by Izadi et al. (2018) effectively simulated the oblique-asymmetric slamming of flexible wedges, broadening its applicability to anti-symmetric whipping scenarios.

A very different FVM–FEM-based study is presented in Javanmardi and Ghadimi (2019). The authors investigated the dynamic responses of a very thin wedge resembling a 2D section of the blade of a surface-piercing propeller. Unlike other studies discussed in this subsection, they addressed a three-phase flow involving liquid water, vapour, and air to account for the expected cavitation during the water entry of such a thin object.

The FVM–FVM modelling approach has also been used to model the flexible slamming of wedge-shaped bodies. This was initially done by Tavakoli et al. (2023b), who numerically modelled the dynamic responses of various elastic wedges entering water at a constant speed. Building on this work, Tavakoli and Hirdaris (2023) further extended the model to simulate the dynamic responses of wedges entering water at an oblique speed. They demonstrated how the deflection patterns were affected by the asymmetry introduced by oblique entry conditions.

Three-dimensional modelling of flexible slamming (other than bottom slamming) has also emerged since the 2020s. The 3D flexible ditching of an inclined plate was first modelled by Mesa et al. (2022), who numerically replicated the ditching experiments of Iafrati (2016). But more importantly, the first 3D study on the flexible slamming of wedge-shaped bodies falling into water was conducted by Hosseinzadeh et al. (2023b), who used the same coupling of StarCCM+ and ABAQUS, with snapshots shown in Fig. 51. They simulated the slamming behaviour of a 3D non-prismatic wedge-shaped body falling into water and compared their numerical results with those obtained using LS-DYNA for inviscid fluid simulations. Their results showed that higher-order responses arose in the solutions predicted by the numerical model developed under inviscid fluid assumptions, aligning with earlier observations by Liao et al. (2013).

In another study, Chen et al. (2023b) developed a model to simulate the dynamic responses of elastic 3D wedges entering rough water. They generated water waves on one side of a numerical tank and considered two different sets of rigid modes: in one case, only the primary rigid mode was activated, while in the other, three rigid modes were activated. Finally, in another 3D modelling effort, Yang et al. (2024) numerically simulated the dynamic responses of a hyperelastic flexible ball entering water. Similar to most works covered in this subsection,

**Table 29**
A summary of CFD studies performed to model flexible marine propellers.

| Study | CFD code | CSD code | one-way | Two-way | Turbulence model | Propeller modelled |
|---|---|---|---|---|---|---|
| Mulcahy et al. (2010) | CFD-ACE+ | SYSPLY | | ✓ | An RNG $k$-$\varepsilon$ *turbulence* | Composite propellers |
| He et al. (2012) | CFX | ANSYS | | ✓ | SST $k$-$\omega$ | Composite propellers |
| Kolekar and Banerjee (2013) | CFX | ANSYS | ✓ | | SST $k$-$\omega$ | Turbine blade |
| Hong et al. (2011) | CFX | ANSYS | | | Not reported | Composite propellers |
| Han et al. (2015) | StarCCM+ | ABAQUS | | ✓ | SST $k$-$\omega$ | Composite propellers |
| Das and Kapuria (2016), | ANSYS ICEM CFD 12.0 | ANSYS | | ✓ | The standard $k$-$\varepsilon$ model | Composite propellers |
| Hong et al. (2017) | CFX | ANSYS | | ✓ | SST $k$-$\varepsilon$ | Composite propellers |
| Lee et al. (2017) | Star-CCM+ | ABAQUS | | ✓ | SST $k$-$\omega$ | Composite propellers |
| Zhang and Lu (2018) | Fluent | ANSYS | ✓ | ✓ | SST $k$-$\omega$ | Composite propellers |
| Javanmardi and Ghadimi (2018) | CFX | ANSYS | ✓ | | SST $k$-$\omega$ | SPP |
| Maljaars et al. (2018) | ReFRESCO | MSC Marc/Mentat | | ✓ | SST $k$-$\omega$ | Composite propellers |
| Vijayanandh et al. (2020) | Fluent | ANSYS | | ✓ | Not reported | Flexible propellers |
| Zhang et al. (2020) | ICEM | ANSYS | | ✓ | SST $k$-$\omega$ | Composite propellers |
| Masoomi and Mosavi (2021) | OpenFOAM | Abaqus | ✓ | | Two equation $k$-$\varepsilon$ | Flexible propellers |
| Kim et al. (2022) | STAR-CCM+ | Abaqus | | ✓ | realizable $k$-$\omega$ | Composite propellers |
| Zhang et al. (2023b) | CFX | ANSYS | | ✓ | SST $k$-$\omega$ | Composite propellers |
| Kiss-Nagy et al. (2024) | Fluent | ANSYS | ✓ | | SST $k$-$\omega$ | Flexible propellers |
| Rama Krishna et al. (2022) | ICEM | ANSYS | ✓ | ✓ | LES | Flexible propellers |
| Bushehri et al. (2025) | StarCCM+ | StarCCM+ | | ✓ | The $k$-$\varepsilon$ turbulence method | SPP |

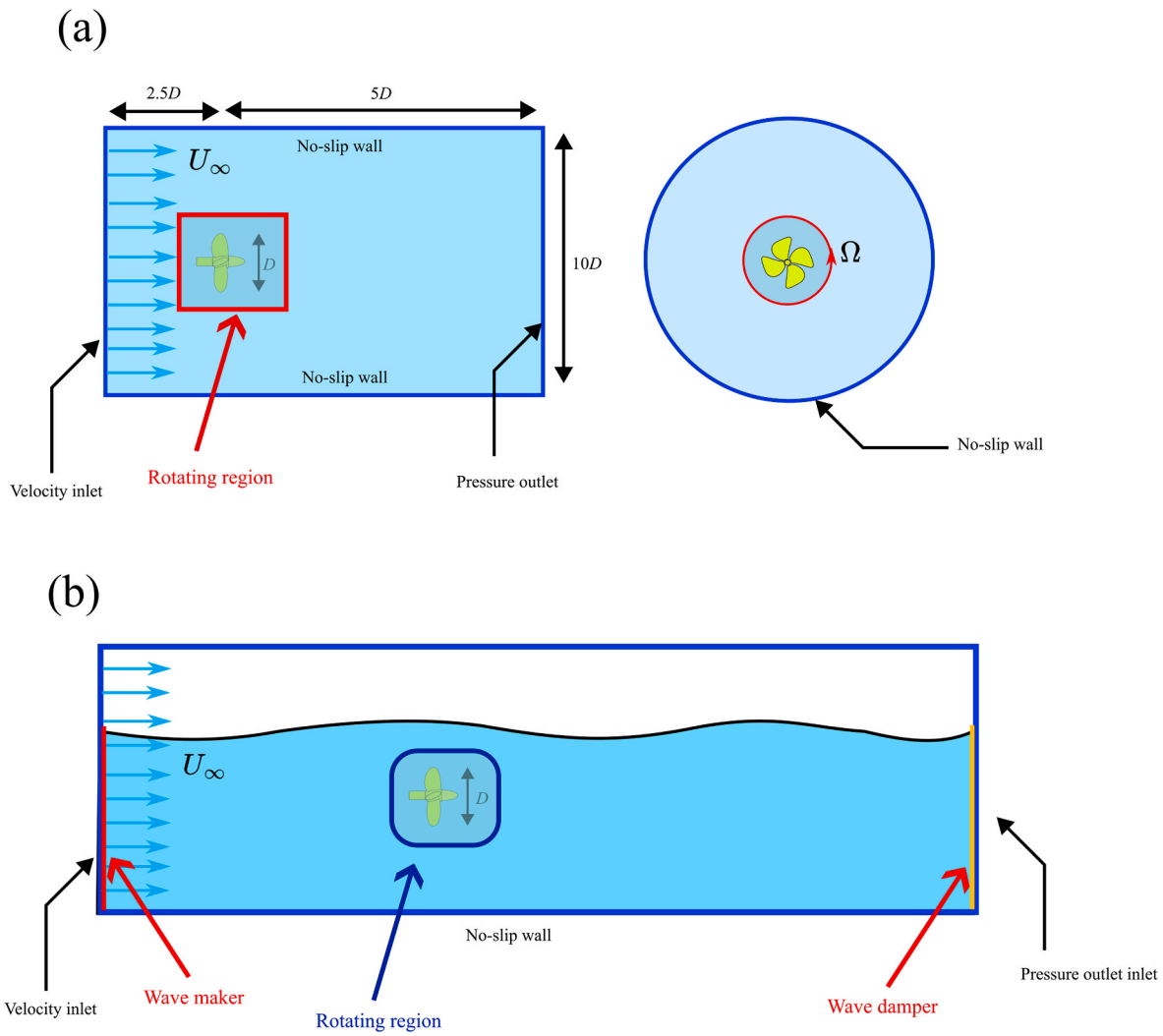


**Fig. 52.** Two examples of computational domains that can be used for modelling fluid motion around marine propellers. The upper panel (a) illustrates a fully submerged propeller rotating at an angular velocity $\Omega$, based on the setup proposed by Posa et al. (2022). The lower panel (b) shows a propeller operating in the presence of water waves. The tank is filled with water and equipped with a wave maker at one end and a wave absorber at the other, inspired by the work of Zhang et al. (2021c). This configuration can also be used for tests without waves or with varying immersion depths, particularly relevant when the propeller approaches the free surface, such as SPPs. In both configurations, the propeller is placed within a rotating region of the computational domain.

they used a coupling of StarCCM+ and ABAQUS to solve problem. A detailed summary of studies conducted to model flexible slamming scenarios, excluding bottom slamming, is presented in Table 27.

#### 6.2.4. Ship-scale hybrid models

A distinct line of research on flexible water entry differs from conventional studies emerged in the late 2010s, summarised in Table 28. In these studies, the flexible slamming problem is modelled by integrating a CFD model that solves the rigid body motions of a high-speed ship or boat in waves with a code that locally simulates the slamming of the portion of the hull re-entering the water. This line of study was initiated by Volpi et al. (2017) and subsequently advanced by Diez et al. (2022) and Lee et al. (2024). In the former study, CFDShip-Iowa V4.5 was coupled with ANSYS, while the later studies employed various combinations of CFD and FEM codes, including CFDShip-Iowa V4.5/ANSYS, STAR-CCM+/STAR-CCM+, and STAR-CCM+/NASTRAN. Diez et al. (2022) focused on regular wave conditions, whereas Lee et al. (2024) extended the approach to simulate the problem under irregular wave conditions, broadening the applicability of this modelling framework. These models offer highly realistic simulations of the problem and can be classified as bridging the studies covering whipping and those covering local flexible slamming phenomena. However, the computational time required is significantly higher than that of models developed for simulating conventional water entry problems.

#### 6.2.5. Re-emergence of non-body fitted models

As discussed earlier in Section 3, body-fitted methods are generally preferred for FFSI problems involving ships, marine structures, and propellers, as they can accurately model complex geometries and provide better stress predictions within the solid body compared to non-body-fitted methods. Yet, recent progress has been made in applying the IBM to such problems, notably in a series of studies by Di et al. (2021, 2024). In the earlier work, Di et al. (2021) employed IBM to simulate the water entry of rigid bodies and notably coupled the model with a DEM solver to simulate the water entry of multiple bodies. The free surface flow was captured using a level-set method. In the later study, Di et al. (2024) extended this approach by coupling the IBM model with a FEM solver, thereby establishing an FFSI framework for flexible body water entry problems.

#### 6.2.6. Future research directions

In sum, CFD-based codes developed for simulating the dynamic

responses of flexible objects entering water have demonstrated high accuracy. However, there are still some unresolved challenges. Still a deeper understanding of when and where one-way or two-way coupling is required. One other area requiring further investigation is the role of three-dimensional effects in water entry dynamics under asymmetric flow patterned caused by the oblique speed. An intriguing research gap lies in developing simplified equations for bending moments and shear forces using CFD-based models that can be integrated into global ship hydroelasticity models, particularly those based on 2D strip theory. Another area not yet addressed by CFD-based models is the water entry of flexible objects that do not have a wedge or flat shape. As discussed, the only studies investigating the dynamic responses of objects with non-standard topologies are those by Javanmardi and Ghadimi (2019) and Yang et al. (2024), which are far from sufficient. Last but not least, a significant research gap in the field of water entry involves understanding fluid motions in aerated liquids or at the water-air interface during the water entry of flexible bodies. While CFD models for rigid bodies in aerated liquids have been developed, equivalent models for elastic bodies remain unexplored, underscoring an important direction for future studies. Aerated liquid conditions can arise in different contexts, such as wave breaking or the operation of an air lubrication system installed on the bottom of a ship.

### 6.3. Flexible marine propellers

CFD modelling of flexible marine propellers may enable the capture of fluid dynamic phenomena that cannot be resolved using inviscid-based flow modelling. Compared to inviscid-based flow simulations, modelling the viscous flow around a flexible propeller demands significantly more computational time due to various complexities, such as viscosity, turbulence, and mesh deformation. To simulate this problem, a CFD-based cavitation tunnel or tank setup must be created, in which the propeller performance is modelled and coupled with a computational solid mechanics' code. The propeller is typically assumed to have no longitudinal rigid motion; instead, the incoming flow is modelled as moving toward the propeller, similar to standard ship resistance or propulsion tests. A summary of CFD studies on flexible marine propellers is presented in Table 29.

The rotational motion of propeller can be imposed in one of two ways: (1) by rotating the entire computational domain, or (2) by defining a rotating subdomain in which the propeller is placed. The first approach is feasible when the propeller is fully submerged (Fig. 52a), and when free surface, gravity, and wave effects are not considered (e.g. Helal et al., 2018). In this case, the propeller is placed inside a cylindrical CFD domain, and the entire domain is rotated at the same angular velocity as the propeller. Alternatively, the propeller can be placed in a CFD tunnel fully filled with water with a rotational zone (as shown in Fig. 52a), or a CFD tank partially filled with water, with an air–water interface, where the two-phase flow is driven from one side to the other (as shown in Fig. 52b). The latter configuration is particularly useful for simulating SPPs or evaluating the influence of surface waves on propeller performance (e.g. Javanmardi and Ghadimi, 2018).

The problem can be solved for uniform and non-uniform flow, in the former of which simulations would be run until the results converge (an equilibrium is established, e.g. Maljaars et al., 2018). But when it comes to solving FFSI for a propeller in a non-uniform flow, a non-uniform flow pattern is mostly prescribed at the inflow boundary condition, and then the unsteady pressure and velocity fields are solved via the fluid solver at each time step and transferred to the fluid–solid interface. This may be done through decoupling of the fluid and solid solvers, or via loose or tight coupling. Simulations are run for a sufficient physical time over which harmonic analysis can be performed (e.g. He et al., 2012).

#### 6.3.1. Early two-way CFD–FEM studies (2010–2012)

The earliest CFD-based simulations of flexible propellers did not emerge until 2010. The first notable study was conducted by Mulcahy et al. (2010). This was a two-way coupling modelling and unlike what has seen in CFD-based modelling of the flexible ships exposed to water waves, and flexible water entry studies (covered in previous sub-sections), the earliest state-of-art CFD-based model was not done based on a one-way based approach. In their study, Mulcahy et al. (2010) introduced a numerical framework designed to optimise the performance of marine composite propellers operating under off-design conditions caused by non-uniform flow environments. The fluid flow problem was solved using the CFD-ACE + code. This research was followed by another study conducted by He et al. (2012). The authors

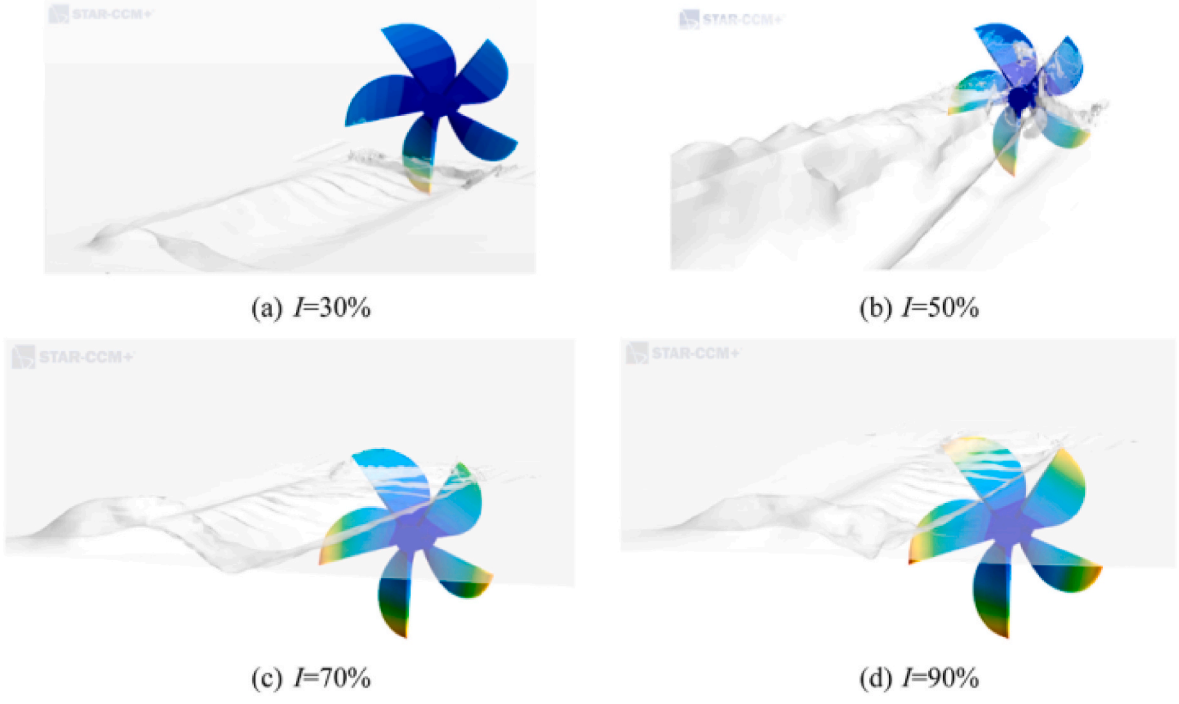


**Fig. 53.** Deformations of blades of a SPP propeller in different immersion. These resulted are presented in Bushehri et al. (2025). © Elsevier.

modelled the flexible motions of a composite propeller exposed to non-uniform flow.

They employed the SST k–ω turbulence model and solved the fluid dynamics and solid dynamics problems using ANSYS CFX and ANSYS, respectively. Similar to Mulcahy et al. (2010), a two-way coupling approach was utilised. The FEM model, constructed within ANSYS, employed layered solid elements with a symmetric stacking sequence to idealise the propeller structure.

#### 6.3.2. *Expansion of two-way coupling studies*

Since 2012, several other models have been developed to solve the FFSI of marine propellers. One example is the scholarly work of Hong et al. (2017), in which the authors adopted a similar modelling approach (similar to He et al., 2012) to study the hydro-structural responses of the 438x series of skewed propellers, comparing the performance of composite propellers to that of metal propellers. Other two-way CFD-based studies investigating the performance and dynamic responses of composite propellers can be found in the works of Han et al. (2015), Das and Kapuria (2016), Kim et al. (2022), Zhang et al. (2020), Zhang et al. (2023b) and Li et al. (2024).

#### 6.3.3. *One-way vs two-way coupling approaches*

While two-way coupling dominates the literature on CFD-based modelling of flexible propellers, one-way coupling approaches are also present (e.g. Kolekar and Banerjee, 2013; Vijayanandh et al., 2020; Masoomi and Mosavi, 2021). An example is the study by Kolekar and Banerjee (2013), who numerically modelled steel turbines operating in uniform currents using a one-way coupling method. Their research demonstrated the applicability of this approach for the engineering-based optimisation of such devices. Another example is the study by Kiss-Nagy et al. (2024).

Although comparisons between CFD-based one-way and two-way coupling approaches are more commonly covered in the context of global ship hydroelasticity and flexible water entry, as discussed in previous sub-sections, such studies are less prevalent in the realm of flexible propellers. A notable contribution in this area was made by Rama Krishna et al. (2022), who numerically modelled the performance, dynamic response, and sound pressure levels of the DTMB 4119 flexible propeller using both one-way and two-way coupling methods. The fluid dynamics problem was solved using the ICEM CFD code, while structural responses were solved via ANSYS. It was found that the two-way coupling predicted larger blade deflections and resulting stresses compared to the one-way coupling, although the differences were small enough to be justifiably neglected if the final deflection of the propeller blade was the primary concern. However, in the early stages of the simulation, the two-way coupling method predicted significantly larger deflections. The authors concluded that, while one-way coupling can be sufficient for certain applications, the two-way coupling approach should be favoured when analysing the performance of flexible composite propellers under off-design conditions, as it provides greater

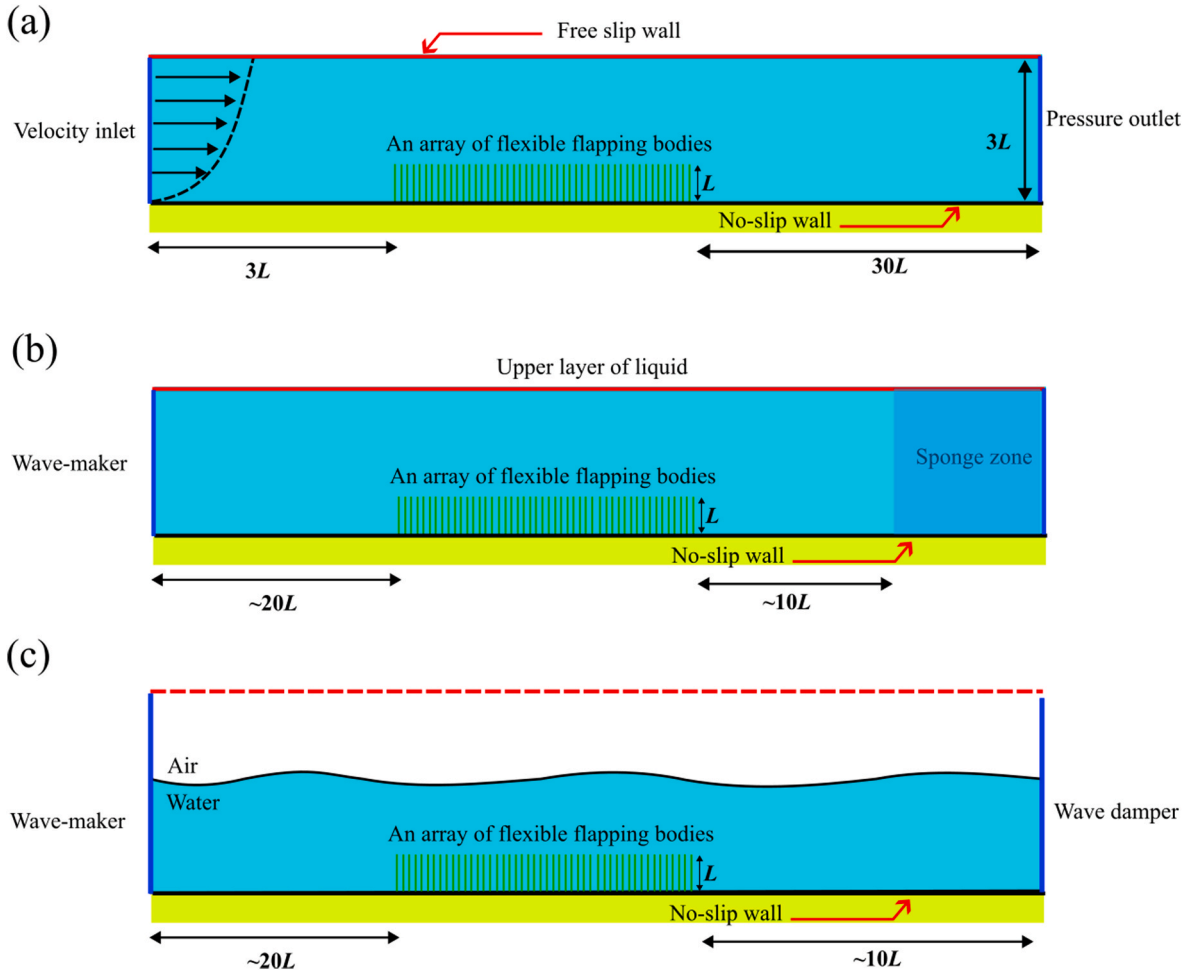


**Fig. 54.** Three examples of CFD domains used to simulate fluid flow around flexible marine vegetation. Panel (a) shows submerged vegetation exposed to a steady current, with flow prescribed at the inlet boundary. The setup and dimensions are inspired by the work of O'Connor and Revell (2019). Panels (b) and (c) illustrate domains designed to model flexible marine vegetation under wave conditions. Panel (b) corresponds to a non-hydrostatic model, while panel (c) represents a hydrostatic model. Both wave-related setups are inspired by the work of Chen et al. (2019c).

**Table 30**
A summary of CFD studies conducted to model the dynamic responses of marine vegetation.

| Reference | Flow | Fluid model | Free surface modelled? |
|---|---|---|---|
| Velasco et al. (2008) | Current | Steady Navier-Stokes (4 zones) | No |
| Dijkstra and Uittenbogaard (2010) | Current | 1DV RANS ($k$-$\varepsilon$) | No |
| Li and Xie (2011) | Current | VLES | No |
| Mattis et al. (2015) | Current | LES | No |
| Xu et al. (2022) | Current | LES | No |
| O'Connor and Revell (2019) | Current | Lattice Boltzmann | No |
| Maza et al. (2013) | Wave | Hydrostatic RANS ($k$-$\varepsilon$) | Yes |
| Chen et al. (2017) | Wave | Hydrostatic RANS ($k$-$\varepsilon$) | Yes |
| Chen and Zou (2019) | Wave | RANS ($k$-$\varepsilon$) | Yes |
| Chen et al. (2019c) | Wave | RANS ($k$-$\varepsilon$) | Yes |
| Mattis et al. (2018) | Wave | LES (LSM used for free surface modelling) | Yes |

fidelity in capturing hydroelastic interactions.

### 6.3.4. CFD vs inviscid modelling

The question of whether CFD-based modelling is necessary, given the considerably shorter computational time required for inviscid-based simulations, has also been addressed in the literature by Maljaars et al. (2018). The authors conducted a study to evaluate the performance of two modelling approaches, namely, a BEM–FEM code and a CFD–FEM code, in predicting the dynamic responses of composite propellers. It was found that the BEM–FEM approach could reasonably predict the bending responses of composite propellers, despite its limitations in capturing viscous effects and eddy generation. The BEM-FEM method struggled to accurately capture the twisting of the propeller blade. At low advance ratios, this limitation was hypothesised to stem from strong leading-edge vortex separation, while at high advance ratios, it was attributed to dominant viscous effects that were not well captured by the BEM model. The greatest agreement between the twisting predictions of the two methods was observed at intermediate advance ratios. The.

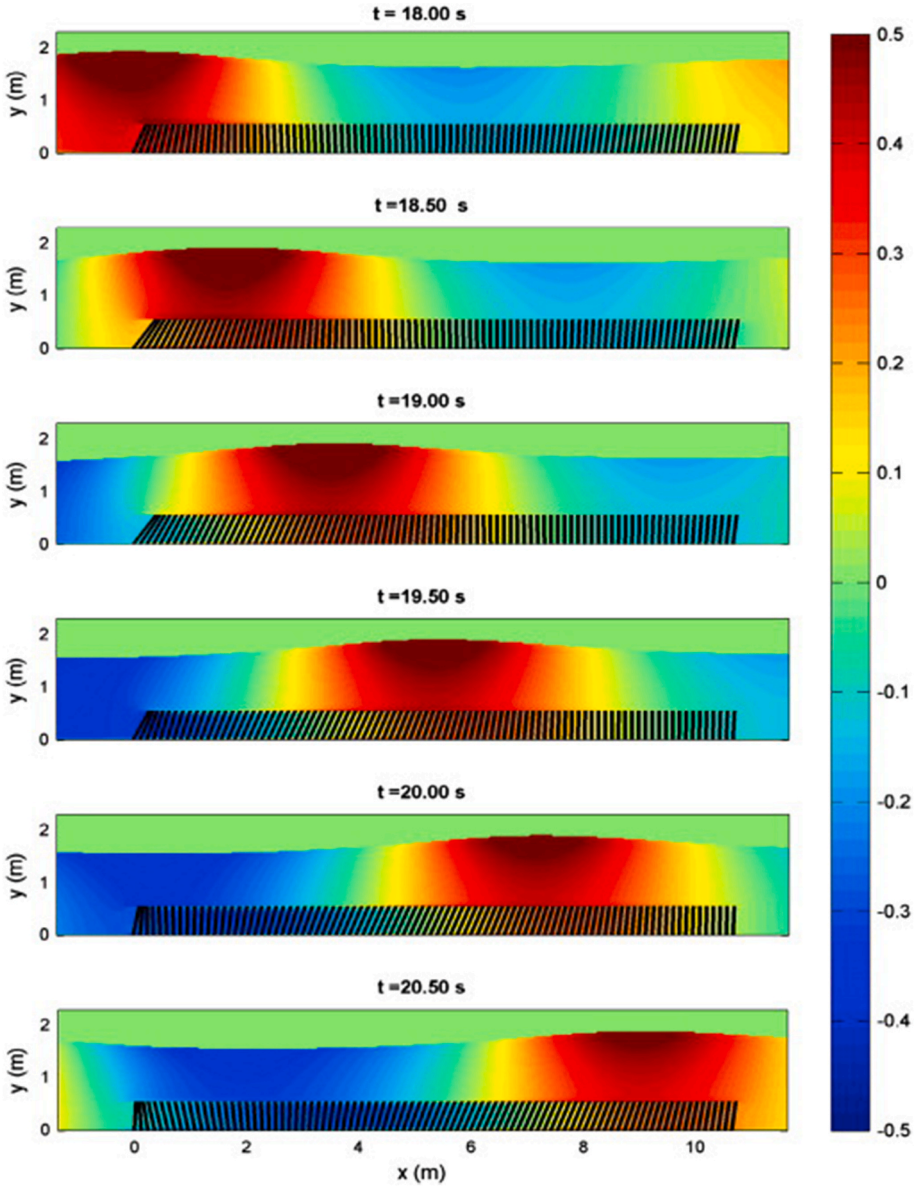


**Fig. 55.** Snapshots showing the velocity field (horizontal component) and instantaneous dynamic response of marine vegetation exposed to water waves found by running the CFD model developed by Maza et al. (2013). This snapshot is taken from Maza et al. (2013). © Elsevier.

#### 6.3.5. Modelling flexible surface-piercing propellers

Notable efforts have also been made in modelling Surface-Piercing Propellers (SPPs), a significantly more complex problem due to the need to account for free surface effects and cavitation. These factors introduce multiphase flow modelling.

The first significant attempt in this area was conducted by Javanmardi and Ghadimi (2018), who numerically simulated the dynamic responses of an SPP using a one-way coupling approach. Their study reported the hydrodynamic performance of the propeller but did not directly validate the flexible FSI model, owing to the lack of experimental data on vibratory responses of SPPs. The authors observed that, for the partially ventilated propeller, the normalised stress on each blade peaked when the blade was positioned at a 45-degree angle relative to the calm waterline. In contrast, for the fully ventilated propeller, the peak stress was seen to emerge when the blade was vertically aligned with the waterline.

Following the work of Javanmardi and Ghadimi (2018), Bushehri et al. (2025) conducted both one-way and two-way coupling simulations to model the dynamic responses of SPPs (Fig. 53). The authors performed simulations under open-water conditions and observed that the predictions of propeller performance and blade dynamic responses from one-way and two-way coupling approaches did not show significant deviations. They concluded that a one-way coupling approach is sufficient for simulating hydroelastic responses of SPPs under open water conditions, hypothesising that the relatively small vibratory responses of the blade, compared to its diameter, result in minimal influences on the surrounding fluid flow. However, the study of Bushehri et al. (2025) focused on a propeller with high stiffness. For more flexible blades, where the natural frequency is lower, the potential for resonance may increases.

#### 6.3.6. Future research directions

Overall, the research on CFD-based modelling of flexible propellers has shown significant promise, with authors developing robust tools for both one-way and two-way coupling approaches to predict the performance and dynamic responses of composite propellers in the absence of free-surface effects, as well as SPPs operating in the presence of highly nonlinear free-surface effects. Despite these advancements, there remains considerable room for future research. One potential avenue is the development of hybrid models to significantly reduce computational time. For instance, the fluid flow around the propeller could be solved using a viscous assumption, while the fluid in the remaining domain can be modelled via an inviscid-fluid solver. Additionally, while several studies have compared different models for predicting the dynamic responses and performance of marine propellers a holistic benchmarking study is still missing. Beyond that, there has not been much research on performance of flexible marine propellers in waves, though such modelling has been done for rigid propellers. This leaves us with some more future research opportunities in modelling of such problem (e.g. Zhao et al., 2017).

### 6.4. Flexible marine vegetation

When it comes to CFD modelling of flexible marine vegetation, it is typically modelled under the action of marine currents or waves. The modelling approach for submerged marine vegetation exposed to marine currents may share similarities with that of air flow interactions with canopies (e.g. Ikeda et al., 2001). However, when it comes to water wave interactions with marine vegetation, similarities in setting up the model between land and marine environments would not be present. The FFSI models developed for flexible marine vegetation are mostly based on non-body-fitted methods (e.g., the IBM approach), as the

**Table 31**
A summary of CFD studies conducted to model the wave-mud interactions.

| Study | Dimensionality and Solver | Free-surface capture | Mud rheology/ bed model | Water–mud interface treatment | Turbulence/ flow resolution | Sediment transport modelled? | Integration of FFSI solvers | Key strengths |
|---|---|---|---|---|---|---|---|---|
| Zhao et al. (2006) | 1DV RANS (implicit waves) | None (linear wave kinematics prescribed) | KV-type visco-elastic solid | Not tracked | Calibrated eddy-viscosity coefficients | | Partitioned (fluid over prescribed moving wall) | Handles background currents; first visco-elastic mud in CFD |
| Hsu et al. (2009) | 1DV RANS | None | Bingham-like fluid mud | Not tracked | High-resolution $k$–$\varepsilon$ | ✓ (erosion flux) | Partitioned (wave velocities prescribed) | Captures vertical structure and erosion over soft bed |
| Torres-Freyermuth and Hsu (2010) | 2DV RANS (COBRAS) | VOF | Non-Newtonian fluid mud (no rigid bed) | Implicit (single-phase) | $k$–$\varepsilon$ (depth-integrated SGS) | ✓ (mobile fluid mud) | Monolithic | Predicts wave damping + mud transport in high-conc. fluid layer |
| Niu and Yu (2010) | 2DV RANS | VOF | Single-layer viscous/visco-plastic mud | Explicit VOF interface | $k$–$\omega$ SST | | Monolithic | First explicit interface + nonlinear (5th-order Stokes) waves |
| Hsu et al. (2013) | 2DV RANS | VOF | Homog. fully fluidised mud (static in time) | Implicit | $k$–$\varepsilon$ | | Monolithic | Accurate damping rates; velocity profiles through mud |
| Hejazi et al. (2013) | 2DV ALE-RANS | ALE free-surface | Newtonian viscous mud | Mesh follows mud deformation | Buoyant $k$–$\varepsilon$ | | Mixed (fluid mesh moves with mud) | Simultaneous surface and bed deformation; good damping and dispersion |
| Niu and Yu (2014) | 2DV RANS | VOF | Two-layer: (i) Newtonian viscous, (ii) visco-elastic/ plastic | Explicit (dual interfaces) | $k$–$\omega$ SST | | Monolithic | Captures complex rheology; strong nonlinear waves |
| Deng et al. (2017) | 2DV DNS | LSM | Newtonian viscous mud | Implicit | DNS (all scales resolved) | | Monolithic | Fully resolves turbulence; benchmark for low-Re cases |

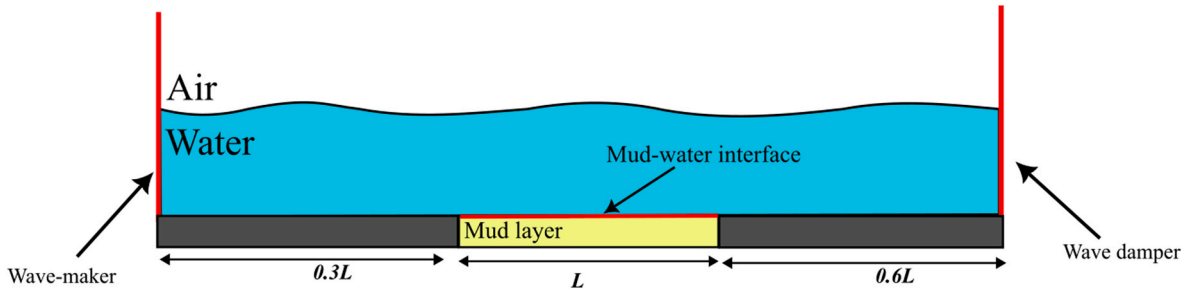


**Fig. 56.** An example of a CFD domain designed for modelling wave–mud interactions. The dimensions are not to scale. Dimensions are just set to be equal to those of flume experiments presented in Niu and Yu (2014).

flexible motions of the marine vegetation are expected to be relatively large.

Different models, such as RANS, LES, and the one-dimensional vertical (1DV) k–ε turbulence model have been employed by various research teams to model the FFSI of flexible marine vegetation. Specifically, the 1DV *k–ε* turbulence model is preferred when depth-averaged turbulence needs to be considered. When modelling the interactions between flexible marine vegetation and marine currents (Fig. 54a), the free surface does not need to be tracked, unlike in cases where interactions between waves and marine vegetation are modelled (Fig. 54b and c).

Two different sets of research directions within CFD-modelling of the flexible marine vegetation is covered in this section. The first ones are related to non-oscillatory flow interactions with marine vegetation and the second one covers the temporal evolution of studies aimed at modelling wave-driven flows with marine vegetation. A summary of CFD studies conducted to model the dynamic responses of marine vegetation is outlined in Table 30.

#### 6.4.1. *Non-oscillatory flow and submerged marine vegetation*

The research conducted by Velasco et al. (2008) is introduced first, as it is one of the earlier studies and was developed under reasonable simplifications appropriate for that time. The authors aimed to model the flexible motions of a submerged plant stem subjected to a hydrodynamic flow stream. The fluid motion was governed by steady momentum balance equations, while the solid motion of the plant stem was idealised using a cantilever beam model. The fluid domain was discretised in the vertical direction, and a finite difference method (FDM) was used to solve the governing equations. Later, Dijkstra and Uittenbogaard (2010) developed another FFSI model for flexible marine vegetation exposed to marine currents. A one-dimensional vertical (1DV) k–ε turbulence model was used for the fluid equations, and the plant was divided into a finite number of highly flexible segments. The authors noted that a very flexible plant stem tends to follow the flow direction, and for this reason, momentum and inertia forces, along with drag, need to be considered in the modelling.

Another notable study on the numerical modelling of viscous marine currents interacting with flexible vegetation was conducted by Li and Xie (2011). The plant stem was formulated using a nonlinear beam equation, which was then decomposed and solved using a quasi-linearised central finite difference scheme, as detailed in Al-Saddar and Al-Rawi (2006). Mattis et al. (2015) also introduced another LES-based model, in which the motion of the solid was idealised using a beam model, with the plant assumed to exhibit 3D bending. Another FFSI study on the mutual interactions between marine vegetation, also based on the LES approach for fluid modelling, was conducted by Xu et al. (2022). In addition, a coupled Lattice Boltzmann–FEM approach is found in the literature, conducted by O'Connor and Revell (2019). Similar to other models, an IBM approach was used to couple the fluid and solid motions.

#### 6.4.2. *Wave-driven flow and marine vegetation*

The surge of CFD-based approaches for modelling of marine vegetation interacting with water waves emerged in 2010s. The work by Maza et al. (2013) can be labelled as one of the pioneering ones. The authors developed a Hydrostatic RANS solver and used a *k–ε* equation to model turbulence motion. The plant motion was solved under a linear deformation hypothesis, and their effects on the fluid motion was introduced to the fluid domain by adding the related terms to the turbulence equations. Snapshots of the simulations run by Maza et al. (2013) are shown in Fig. 55. A similar study was later conducted by Z. Chen et al. (2017).

Another RANS-based modelling study was later carried out by Chen and Zou (2019). Similar to previous studies conducted in earlier years, an IBM approach was used to couple fluid and solid motions, though the solid motion was modelled within a Lagrangian framework. In a parallel study, Chen et al. (2019c) conducted an interesting set of simulations on wave-vegetation interactions, employing a single-phase flow model and two RANS-based models that captured the water surface using the VOF method. Wave generation in the RANS-based models was implemented using IHFOAM in one case and waves2Foam in the other. However, despite the development of different fluid models, the authors did not account for flexible motion. This omission leaves room for future research to extend these models to incorporate the flexibility of marine vegetation.

A level-set-based approach for solving this problem can also be found in the literature, as demonstrated by Mattis et al. (2018). The authors idealised the fluid motion using the level-set method and the LES approach, and, similar to previous studies in this subsection, an IBM approach was used to couple the fluid and solid problems.

### 6.5. *Wave–mud interaction*

The multiphysical problem of wave–mud interactions has been increasingly investigated using CFD approaches, with a summary of relevant studies presented in Table 31. These models often capture free surface deformations using techniques like VOF, level-set or ALE techniques, along with appropriate wave generation schemes (e.g. Niu and Yu, 2010). The VOF and Level Set methods, along with their differences and limitations, were introduced in Sub-section 3.1.4. on Consequently, these setups resemble those used in wave–structure or wave–vegetation interaction problems, all of which were covered in the previous subsections of this section. A typical CFD domain used to model such wave-mud interaction, inspired by Niu and Yu (2010, 2014), is shown in Fig. 56.

The mud layer is typically treated as a viscous layer or non-Newtonian material (as discussed in subsection 5.6). While wave–mud interaction is fundamentally a flexible fluid–structure problem, CFD treatments often simplify it to a viscous flow over a soft bed. One of the earliest studies, Zhao et al. (2006), employed a viscoelastic solid model (KV-type) for the mud. The model prescribed wave motion using linear theory without capturing free surface deformation, and relied on

**Table 32**
Future outlook of FFSI modelling in ocean engineering.

| Problem | General comment on understanding | Limitations and improvement needs in inviscid models | CFD modelling gaps and opportunities | Benchmarking gaps | Integration into engineering and nature-based protection | Design codes and classification rules | Ocean wave modelling |
|---|---|---|---|---|---|---|---|
| Wave–Structure Interaction | Enable efficient wave–floe interaction models (thousands of floes) in MIZs and deepen understanding of related nonlinear hydrodynamics. | Improved modelling of hydroelastic effects, including deformation, mode coupling, and added-mass variation, through improved wave–structure coupling for accurate prediction of stress and energy exchange. | Lack of understanding of one-way versus two-way modelling. | Very limited and last time was done in 2000s. | Consideration of FFSI in design of marine structure is very limited to academia, and the environmental impact needs to be considered. | Hydroelasticity is often overlooked in breakwater design codes and in rules presenting loads on marine structures. | Better parametrisation of the wave-decay in different ice fields (e.g. grease ice) is required. |
| Ship hydroelasticity | Limited understanding of asymmetric flexible ship responses, and global loads in oblique waves, and extreme conditions. | Development of highly nonlinear yet computationally efficient 3D models. | Nonlinear FEM is not considered. | Not all recent models are considered in the latest benchmarking. | Not yet integrated into holistic ship design models | Classification rules typically assume a rigid body when calculating VBM, HBM, and TM. | N/A |
| Flexible slamming | Lack of awareness regarding dynamic analyses of different slamming problems, and integration of hybrid global–local flexible ship models. | Advanced Wagner-type models that capture fluid nonlinearity and flow separation, especially under asymmetric or oblique impacts, are still lacking. | Lack of understanding of one-way versus two-way modelling and need to develop aerated flexible slamming. | Only bottom slamming of stiffened plates is tested with some limited models. | Flexible slamming is not yet considered in holistic ship design models. | Flexible slamming is scarcely addressed in current design rules. | N/A |
| Flexible marine propellers | Realistic conditions, including flexible propeller operating in waves and during ship manoeuvre are still missing. | Improved modelling of hydroelastic effects like deformation, mode coupling, and added-mass changes Better wave–structure coupling to predict deformation, stress, and energy transfer | More efficient models solving flexible marine propellers, especially in self-propulsion tests are recommended to be done. | No benchmarking studies exist beyond basic validation cases. | Research is largely academic and has yet to be translated into engineering practice. | Propeller design rules provide stress calculation procedures but neglect flexibility in evaluating bending and torsional moments. | N/A |
| Marine Vegetation | There is a lack of experimental validation and comprehensive hydrodynamic coefficients, limiting the practical application of rational models for flexible marine vegetation under large deformations and oscillatory flows | More advanced model for large deformations is recommended to be developed. | CFD models are limited, with their uncertainties largely unexplored. | No benchmarking studies exist beyond basic validation cases. | Nature-based coastal protection using marine vegetation is mostly limited to research studies; future studies should incorporate climate change projections to support practical application. | N/A | A more accurate formulation that can be easily implement in wave models is required. |
| Wave–mud interactions | Limited understanding of time-dependent rheology (e.g. thixotropy) and nonlinear viscoelasticity under wave forcing. | Inviscid models cannot capture dissipation due to fluid–mud coupling or the feedback of bed deformation on wave motion | CFD models rarely represent mud as a viscoelastic or poro-viscoelastic solid | No benchmarking studies exist beyond basic validation cases. | Often treated as passive layers; not yet integrated into fully coupled wave–seabed–structure models | No engineering guidelines for flexible or fluidised mud layers exists; navigability and seabed response not incorporated into coastal/port design codes | Easier and more accurate formulation/ parametrisation that can be easily implement in wave models is required. |

calibrated turbulence parameters. The authors suggested that the model could be extended to simulate irregular wave propagation over a muddy seabed. However, two key limitations can be identified in this model: (I) the reliance on parameter tuning to achieve acceptable accuracy, and (II) the absence of free surface deformation in the modelling. Its strength was in handling background currents, though it lacked predictive capability for free surface effects.

Hsu et al. (2009) developed a high-resolution 1DV model to solve turbulent wave-induced motion above a muddy layer. The primary focus of this research was on sediment transport over a Bingham-like mud layer, again without modelling surface deformation. The wave velocity profile was prescribed, and the model excelled at estimating erosion flux.

Later, more advanced RANS-based two-dimensional models emerged. These models can track free surface deformation, simulate turbulent flow, and potentially estimate sediment transport. Torres--Freyermuth and Hsu (2010) used a CFD code named COBRAS to simulate waves over a high-concentration flocculated mud layer without a defined wave–mud interface. The mud layer was modelled as a non-Newtonian fluid. The model could predict both wave damping and sediment dynamics, but it was limited to mobile fluid mud above the gelling concentration, but not a consolidated muddy seabed. The authors suggested further development of the model to incorporate highly concentrated and consolidated mud layers.

Hsu et al. (2013) improved this by using a VOF method for free surface deformation tracking and modelling the mud as homogeneous, fully fluidised, and temporally static. The mud–water interface was not explicitly tracked. Nevertheless, the model provided predictions of velocity profiles within the mud layer and successfully calculated the mud-induced wave damping rate. The results from the numerical and linear models were found to be in good agreement, although the nonlinear numerical model showed relatively a better level of accuracy.

Niu and Yu (2010, 2014) explicitly tracked the water–mud interface using VOF in a RANS framework. Niu and Yu (2010) modelled a single-layer muddy bed. In contrast, their 2014 model used a two-layer approach: a Newtonian viscous upper layer and a viscoelastic–plastic lower layer. These models effectively represented complex mud rheology and nonlinear wave fields (e.g., fifth-order Stokes waves), but lacked sediment transport prediction capabilities. The authors acknowledged this shortcoming and suggested it as a direction for future work, an extension that, to date, has not been implemented.

Hejazi et al. (2013) introduced an ALE-based RANS model that captured both free surface and mud deformation. Turbulent fluid motion was simulated using a two-equation buoyant $k$–$\varepsilon$ turbulence model. The mud layer was treated as a Newtonian fluid, and wave damping and wave dispersion were accurately predicted, although erosion and fluidization processes were not considered. A more recent development was made by Deng et al. (2017), who used DNS with a LSM to simulate wave propagation over a viscous mud layer. All relevant turbulent scales were resolved, making the modelling suitable for relatively low Reynolds numbers. One of the main limitations of the DNS approach, when compared to other CFD methods, is its high computational cost.

Despite this progress, current CFD-based studies on wave–mud interactions remain limited, but they have undergone a gradual evolution over time. Early approaches were predominantly 1DV models that neglected free surface deformation. These have since advanced to 2DV frameworks capable of tracking surface deformation, and more recently, DNS methods have been employed to resolve turbulent flow motion above the mud layer, although notably, no LES or VLES models have yet been applied in this context.

While KV-type viscoelastic mud modelling has been introduced (e.g. Zhao et al., 2006), most CFD-based studies treat mud as a non-Newtonian or viscoplastic material (Bingham-like), neglecting elastic behaviour and resonant responses, which are crucial in some damping scenarios. This represents a clear gap and a promising direction for future research. Moreover, none of the models have defined the mud displacement (vertical or even lateral) as a field variable in the governing equations. This stands in contrast to typical practices in wave–structure interaction modelling and flexible slamming simulations using CFD, where displacement fields are explicitly solved. It also differs from several inviscid-based wave–mud interaction models (see subsection 5.6), where vertical deformation is clearly introduced in the problem. This distinction likely stems from the FFSI framework used in CFD modelling of wave–mud systems, where the interface dynamics emerge through momentum exchange and are tracked using VOF or ALE approaches. While effective for capturing fluid-fluid or fluid-solid interface evolution, this formulation does not account for elastic restoring forces or structurally governed interface motion.

Interestingly, in contrast to many FFSI problems in ocean engineering which are typically modelled using a partitioned approach, several wave–mud interaction studies adopt a monolithic modelling strategy, such as those by Deng et al. (2017) and Niu and Yu (2010), where interface motion is embedded in the fluid dynamics. Nevertheless, partitioned methods, such as that used by Zhao et al. (2006), are also present in the literature.

Future research may benefit from incorporating mud displacement fields governed by elastic or viscoelastic structural equations. Such a formulation unifies fluid-dominant and structure-dominant paradigms and better capture the physics of wave–mud interaction problem involving resonance and strong coupling effects.

## 7. Future directions in FFSI modelling in Ocean engineering

Following the state-of-the-art review presented in Sections 3 to 6, a solid understanding of the modelling landscape and existing gaps in FFSI problems covered in the present review paper have been established. These diverse problems and modelling approaches can now be concertedly brought under a single umbrella to frame the future outlook for research in FFSI modelling across the range of cases considered, which is outlined in Table 32. This outlook is drawn from the previous discussions, insights from previous review papers, the identified needs for I) benchmarking studies, II) the integration of FFSI into design and classification rules, and the III) incorporation of FFSI into broader ocean modelling frameworks.

### 7.1. Research outlooks from foundational reviews and gaps ahead

Upon reviewing the development in FFSI modelling of the considered problem, the current state of research can be broadly compared with future outlooks as seen through the lens of foundational review and technical papers by Faltinsen (2000), Chen et al. (2006b), Hirdaris and Temarel (2009), Kapsenberg (2011), and Young et al. (2016), Squire (2020), Robillard et al. (2023). These papers primarily outlined the limitations of the models available at the time and anticipated key research directions.

The need to develop nonlinear FFSI models for ship hydroelasticity and wave–structure interactions was highlighted by Chen et al. (2006b) and Hirdaris and Temarel (2009) in 2000s, an outlook that has largely materialised, as evidenced by the development of numerous weakly nonlinear panel models, strip theories, and CFD models over the past decade. In specific, a notable surge in CFD-based approaches occurred during the 2010s, as anticipated by Hirdaris and Temarel (2009), although nonlinearity in the FEM modelling of the ship structure remains largely unaddressed.

While nonlinear and advanced three-dimensional models for wave–structure interactions and global ship hydroelasticity have advanced over time, Squire (2020) noted that modelling wave propagation in marginal ice zones (MIZs) containing thousands of non-circular ice floes remains computationally high with existing wave-structure models. A potential direction for future research is therefore the development of more efficient numerical methods or reduced-order models capable of accurately capturing the physics more efficiently.

The need to consider local effects on slam loads, including air entrapment and flexible deformation, was raised by Kapsenberg (2011), and has since been addressed in several FFSI slamming models. However, the choice between dynamic and static modelling approaches remains unresolved and warrants further fundamental investigation. Faltinsen (2000), on the other hand, highlighted a critical issue concerning the actual impact velocity at the precise moment of slamming, which arises from the fully nonlinear behaviour of fluid motion around the body during impact. Some progress has been made in this area by Volpi et al. (2017), Diez et al. (2022), and Lee et al. (2024), although these studies have focused on high-speed planing hulls rather than ships and other types of marine vehicles. Therefore, future research should continue to pursue this line of investigation.

Progress in the numerical and experimental modelling of flexible propellers is limited to idealised conditions as observed in the previous sections, with many models neglecting realistic operating scenarios, a limitation identified by Young et al. (2016) as a potential future research direction. Addressing this gap should be considered one of the most important priorities for future research.

Finally, Robillard et al. (2023) noted that current wave–mud interaction models are overly simplified and are formulated based on time-independent rheological relationships. The asymmetric nature of thixotropy needs to be taken into account. Research has not yet addressed these aspects, although it has only been two years since Robillard et al. (2023) raised this concern.

### 7.2. Current state and gaps in benchmarking

Benchmarking analyses in FFSI modelling of various problems in the maritime environment are critically important (Storhaug et al., 2022) and are mostly commonly conducted in the context of wave–structure interactions (Riggs et al., 2006), global ship hydroelasticity (Parunov et al., 2024), and flexible slamming (Truong et al., 2021). Most benchmarking studies have focused on global ship hydroelasticity, from the early efforts of Watanabe and Guedes Soares (1999) to the most recent work by Parunov et al. (2024). However, even in these studies, not all available models have been included.

A similar concern applies to the benchmarking of flexible slamming problems, where current efforts are mostly confined to bottom slamming of stiffened plates and rely on only two computational codes (Truong et al., 2021). No benchmarking analyses have been conducted for flexible marine propellers, despite the recommendation by Young et al. (2016), and benchmarking efforts in marine vegetation modelling and wave–mud interactions are virtually absent, and studies are limited to validation of models.

### 7.3. Translating FFSI research into engineering applications and nature-based design

The integration of hydroelastic models into ocean engineering design was emphasised by Hirdaris and Temarel (2009), who called for the incorporation of ship hydroelasticity models into the ship design process. This need remains pressing, particularly in light of recent advances in holistic ship optimisation tools (e.g., Papanikolaou, 2010; Kondratenko et al., 2023), which often still overlook hydroelastic effects.

In contrast, greater progress has been made in marine propeller research, where FFSI codes have been more successfully integrated into propulsion system design (e.g., He et al., 2012). However, even in this area, the research remains largely confined to academia and has yet to see widespread adoption in industry.

Flexible wave–structure interaction models could be valuable for the design of marine structures, coastal protection system and wave energy converters, including configurations involving arrays of flexible energy devices. However, this research too remains mostly academic, and the environmental impacts of such systems also warrant careful consideration.

In addition, marine vegetation can naturally protect coastal areas (Van Slobbe et al., 2013; de Vriend et al., 2015); however, research in this area is immature and largely confined to academic investigations (e.g. Unguendoli et al., 2023). Further studies are therefore needed with the aim of developing naturally protected coastlines using marine vegetation (e.g. Marino et al., 2025), which also requires an understanding of future climate conditions (Seddon et al., 2020).

Finally, wave-mud interaction can be potentially used in the design of offshore structure. Yet, the flexible mud is treated as a passive layer and not integrated into fully coupled wave–seabed–structure models. That should be a future research direction.

### 7.4. The need for hydroelastic considerations in design standards

In practice-oriented research and design, it is very important to integrate hydroelasticity into classification rules, and this is relevant to ship structural design. While current rules include some limited hydroelastic considerations (e.g. in Det Norske Veritas, 2017), such as design pressures on bottom sections exposed to slamming these are far from sufficient. The primary concerns lie in the calculation of VMB, HBM, and TM in ship design rules. Properly accounting for these hydroelastic effects would enable more accurate predictions of minimum plate thicknesses by considering the flexible response of the structure. However, in existing classification rules (e.g., BV Rules, Part B; see Bureau Veritas, 2025; Det Norske Veritas, 2017), the equations used to define sea loads are still based on the assumption of a rigid hull. Therefore, it is strongly recommended that future efforts address this important practical gap.

A similar limitation exists in classification rules for marine propellers. Although strength design procedures are provided (e.g., Bureau Veritas, 2023), they typically consider only static effects, with no detailed guidance on accounting for dynamic effects or hydroelasticity in calculating the bending moments acting on the blades.

The same comment also applies to marine structures, including offshore wind turbines, breakwaters, VLFs, and TLPs, which dominantly consider loads from a rigid, yet flexibility of structure can be important (e.g. in Jonkman et al., 2020; Li, 2022; Ran et al., 2023). Related rules are recommended to revisit their local and global load equations by consideration of hydroelasticity for the cases required. Rules still do not consider possible-wave mud interactions.

### 7.5. Limitations of current FFSI models in ocean modelling

Ocean wave climate modelling requires physical models or empirical equations that can be directly applied to wave models. This is particularly relevant to wave–ice interactions, wave–vegetation interactions, and wave–mud interactions. Existing models are often highly idealised and may fail to capture the underlying physical processes accurately. As noted by Squire (2020), current wave–ice interaction models still fall short in predicting the observed wave energy decay in real ice fields. Therefore, future research in these areas should aim to deliver more realistic predictions of wave energy attenuation, which may be achieved not only through improved model development but also through refined parameterisation approaches.

### 7.6. Next steps in CFD-CSD modelling of marine vegetation and wave-mud interactions

It has been noted that, the progress in FFSI modelling of marine vegetation and wave–mud interactions have been relatively slow, particularly in the context of CFD modelling, compared to other problems covered in this review. Notable advancements have been made in inviscid flow and theoretical modelling approaches, but CFD-based models remain limited. A valuable next step in advancing CFD-based modelling of both marine vegetation and wave–mud interactions would be to conduct fundamental studies focused on setting up robust

CFD–CSD frameworks.

### 7.7. Emerging role of Artificial Intelligence in FFSI modelling

Beyond the limitations discussed, the recent and rapid introduction of Artificial Intelligence (AI) into various ocean engineering problems (e.g. Zhang et al., 2024, 2025b) presents new opportunities for application in FFSI modelling. AI techniques can be employed for time-domain prediction of dynamic responses, solving governing equations using Physics-Informed Neural Networks (PINNs) or Physics-Guided Neural Networks (PGNNs), surrogate modelling, and accelerating numerical simulations of FFSI through data-driven approaches (see a review on accelerating CFD codes using Machine Learning in Caron et al., 2024). Although their application in this area is currently limited, the potential is significant, and it will be exciting to observe how these methods evolve and expand within the field over the next decade.

Two examples of the potential use of AI in FFSI modelling within the marine environment are briefly outlined here. The first is the application of AI to predict the time history of transient dynamic responses of ships or flexible marine structures subjected to wave loading using various AI-based time-series prediction methods (see an example of using AI for short-term prediction of loads acting on a trimaran in Tang et al., 2025). The second example is the use of AI to directly solve FFSI problems across space and time. For instance, PINNs can be trained to model flexible wave–structure interactions (see examples of wave modelling with PINNs in Chen et al., 2024b; Zhan et al., 2025), with their performance benchmarked against CFD and inviscid-based models. Many other applications are possible, which require inspiration from recent AI-based studies and up-to-date knowledge of AI tools, as well as an understanding of how they can be integrated with FFSI data, models, and governing equations to provide intelligent hydrodynamic tools for engineers and researchers.

## 8. Concluding remarks

This paper reviewed state-of-the-art FFSI models across six key maritime application areas: flexible wave–structure interactions, ship hydroelasticity, flexible slamming, flexible marine propellers, marine vegetation interactions, and wave–mud interactions. The review illustrated how advanced FFSI models are becoming indispensable tools for ocean engineers involved in ship and marine structure design, developing innovative coastal protection solutions (both nature-based and engineered), and predicting oceanic climate impacts.

Through a systematic analysis of model developments within each problem class, the review identified fundamental similarities and differences in modelling approaches, fluid and structural idealisations, coupling strategies between solvers, and methods for integrating complex physical processes in FFSI analyses.

Significant advancements have occurred over the past two decades, reflecting a clear transition from purely analytical or simplified mathematical models toward sophisticated numerical methods capable of capturing complex real-world phenomena. This progression represents substantial progress in accurately simulating challenging maritime scenarios.

To continue this advancement, several key challenges and directions have been identified for future research:

- Developing computationally efficient yet high-fidelity numerical models;
- Establishing standardised benchmarks for rigorous validation and verification;
- Bridging the gap between advanced research models and practical engineering applications;
- Enhancing simulation accuracy to realistically represent complex maritime environments.

Progress in these areas will require deeper interdisciplinary collaboration among ocean engineers, computational scientists, industry stakeholders, and policymakers. Ultimately, such collaboration will ensure that FFSI models continue to evolve into robust tools, improving the reliability, safety, and resilience of maritime infrastructure and environmental solutions in an era of rapid oceanic and climatic change.

## CRediT authorship contribution statement

**Sasan Tavakoli:** Writing – review & editing, Writing – original draft, Visualization, Formal analysis, Conceptualization. **Mansi Singh:** Writing – review & editing, Writing – original draft, Visualization, Conceptualization. **Saeed Hosseinzadeh:** Writing – review & editing, Writing – original draft, Visualization, Conceptualization. **Zhengyu Hu:** Writing – review & editing, Writing – original draft, Visualization, Conceptualization. **Yaniln Shao:** Writing – review & editing, Writing – original draft, Conceptualization. **Shan Wang:** Writing – review & editing, Writing – original draft, Conceptualization. **Luofeng Huang:** Writing – review & editing, Writing – original draft, Conceptualization. **Apostolos Grammatikopoulos:** Writing – review & editing, Writing – original draft, Conceptualization. **Yuzhu Pearl Li:** Writing – review & editing, Writing – original draft, Conceptualization. **Danial Khojasteh:** Writing – review & editing, Writing – original draft, Conceptualization. **Jin Liu:** Writing – review & editing, Writing – original draft, Conceptualization. **Azam Dolatshah:** Writing – review & editing, Writing – original draft, Conceptualization. **Hui Cheng:** Writing – review & editing, Writing – original draft, Conceptualization. **Spyros Hirdaris:** Writing – review & editing, Writing – original draft, Supervision.

## Declaration of competing interest

The authors declare the following financial interests/personal relationships which may be considered as potential competing interests: Luofeng Huang is a Deputy Editor of Ocean Engineering. Spyros Hirdaris and Shan Wang are Guest Editors of the VSI of Ocean Engineering, Hydroelasticity of Marine Structures: From Ships to Offshore Renewables. Sasan Tavakoli, Shan Wang, Spyros Hirdaris, and Yanlin Shao are Editorial Board Members of Ocean Engineering. The authors declare that there are no other known competing financial interests or personal relationships that could have appeared to influence the work reported in this paper.

## References

Aarsnes, J.V., 1994. An experimental investigation of the effect of structural elasticity on slamming loads and structural response. Techn. Rep. MARINTEK A/S.
Abrahams, I.D., 2002. On the application of the Wiener–Hopf technique to problems in dynamic elasticity. Wave Motion 36 (4), 311–333.
Abrahamsen, B.C., Grytten, F., Hellan, Ø., Søreide, T.H., Faltinsen, O.M., 2023. Hydroelastic response of concrete shells during impact on calm water. J. Fluid Struct. 116, 103804.
Abrate, S., 2011. Hull slamming. Appl. Mech. Rev. 64 (6), 060803.
Abroug, I., Abcha, N., Jarno, A., Marin, F., 2020. Laboratory study of non-linear wave–wave interactions of extreme focused waves in the nearshore zone. Nat. Hazards Earth Syst. Sci. 20 (12), 3279–3291. https://doi.org/10.5194/nhess-20-3279-2020.
Afshar, R., Alavyoon, N., Ahlgren, A., Gamstedt, E.K., 2021. Full scale finite element modelling and analysis of the 17th-century warship Vasa: a methodological approach and preliminary results. Eng. Struct. 231, 111765.
Agarwal, S., Colomés, O., Metrikine, A.V., 2024. Dynamic analysis of viscoelastic floating membranes using monolithic Finite Element method. J. Fluid Struct. 129, 104167. https://doi.org/10.1016/j.fluidstructs.2024.104167.
Aksu, Ş., 1993. Steady State and Transient Responses of Flexible Ship Structures Travelling in Irregular Seaways. University of Southampton. Doctoral dissertation.
Al-Ani, M., Belmont, M., 2021. On fully describing the probability distribution of quiescent periods from sea spectral density. IEEE J. Ocean. Eng. 46 (1), 143–155.
Al-Saddar, S., Al-Rawi, R.A.O., 2006. Finite difference scheme for large-deflection analysis of non-prismatic cantilever beams subjected to different types of continuous and discontinuous loadings. Arch. Appl. Mech. 75, 459–473.
Alam, M.R., Liu, Y., Yue, D.K., 2009. Bragg resonance of waves in a two-layer fluid propagating over bottom ripples. Part I. Perturbation analysis. J. Fluid Mech. 624, 191–224.

Aleebrahim, M.A., Jamali, M., 2023. Laboratory study of instability-driven mixing of fluid mud under surface wave motion. Phys. Fluids 35 (8).
Allen, T., Battley, M., 2015. Quantification of hydroelasticity in water impacts of flexible composite hull panels. Ocean Eng. 100, 117–125.
Almashan, N., Dalrymple, R.A., 2015. Damping of waves propagating over a muddy bottom in deep water: experiment and theory. Coast. Eng. 105, 36–46.
American Bureau of Shipping, 2021. Guidance Notes on Nonlinear Finite Element Analysis of Marine and Offshore Structures. ABS.
Andersen, I.M.V., Jensen, J.J., 2014. Measurements in a container ship of wave-induced hull girder stresses in excess of design values. Mar. Struct. 37, 54–85. https://doi.org/10.1016/j.marstruc.2014.02.006.
Baarholm, G.S., Jensen, J.J., 2004. Influence of whipping on long-term vertical bending moment. J. Ship Res. 48, 261–272.
Babanin, A.V., 2006. On a wave-induced turbulence and a wave-mixed upper ocean layer. Geophys. Res. Lett. 33 (20), L20605. https://doi.org/10.1029/2006GL027308.
Babanin, A.V., Haus, B.K., 2009. On the existence of water turbulence induced by nonbreaking surface waves. J. Phys. Oceanogr. 39 (10), 2675–2679. https://doi.org/10.1175/2009JPO4202.1.
Bakti, F.P., Jin, C., Kim, M.-H., 2021. Practical approach of linear hydro-elasticity effect on vessel with forward speed in the frequency domain. J. Fluid Struct. 101, 103204. https://doi.org/10.1016/j.jfluidstructs.2020.103204.
Balmforth, N.J., Craster, R.V., 1999. Ocean waves and ice sheets. J. Fluid Mech. 395, 89–124.
Barjasteh, M., Zeraatgar, H., Javaherian, M.J., 2016. An experimental study on water entry of asymmetric wedges. Appl. Ocean Res. 58, 292–304.
Behnen, J., von Bock und Polach, R.U.F., Klein, M., Ehlers, S., 2022. Hydrodynamic and mechanic response of a floating flexible ice floe in regular waves with the ICFD method. In: Proceedings of the ASME 2022 41st International Conference on Ocean, Offshore and Arctic Engineering, 6. OMAE.
Behnen, J., Demir, O., Francis, O.P., Gedikli, E.D., 2025. Nonlinear dynamics of wave-induced overwash and attenuation in floating flexible plates. Ocean Eng. 325, 120719.
Belik, O., Bishop, R.E.D., Price, W.D., 1980. On the Slamming Response of Ships to Regular Head Waves, 122. Transactions of the Royal Institution of Naval Architects, pp. 325–337.
Benhamou, A., Seng, S., Monroy, C., de Lauzon, J., Malenica, Š., 2018. Hydroelastic simulations in OpenFOAM®: a case study on a 4400TEU containership. In: Proceedings of the 8th International Conference on Hydroelasticity in Marine Technology (Seoul, Korea, September 9–13, 2018).
Benjamin, A.C., Freitas, S.M.S., Jacob, B.P., Ebecken, N.F.F., 1999. Geometric and material nonlinear analysis of offshore framed structures. Presented at the Ninth International Offshore and Polar Engineering Conference. Brest, France, May 30 – June 4, 1999. Paper Number: ISOPE-I-99-389.
Bennetts, L.G., Williams, T.D., 2015. Water wave transmission by an array of floating discs. Proc. R. Soc. A 471 (2184), 20140698.
Bennetts, L.G., Biggs, N.R.T., Porter, D., 2007. A multi-mode approximation to wave scattering by ice sheets of varying thickness. J. Fluid Mech. 579, 413–443.
Bennetts, L.G., Alberello, A., Meylan, M.H., Cavaliere, C., Babanin, A.V., Toffoli, A., 2015. An idealised experimental model of ocean surface wave transmission by an ice floe. Ocean Model. 96, 85–92. https://doi.org/10.1016/j.ocemod.2015.07.007.
Bennetts, L.G., Williams, T.D., Porter, R., 2024. A thin-plate approximation for ocean wave interactions with an ice shelf. J. Fluid Mech. 984, A48.
Bereznitski, A., 2001. Slamming: the role of hydroelasticity. Int. Shipbuild. Prog. 48 (4), 333–351.
Bi, C., Wu, M.S., Law, A.W.-K., 2022. Surface wave interaction with a vertical viscoelastic barrier. Appl. Ocean Res. 120, 103073.
Bingham, A.E., Hampshire, J.K., Miao, S.H., 2001. Motions and loads of a trimaran traveling in waves. Proc. 6th International Conference on Fast Sea Transportations, pp. 167–176.
Birk, L., 2019. Fundamentals of Ship Hydrodynamics, Potential Flow. Wiley, pp. 177–190. https://doi.org/10.1002/9781119191575.ch.
Bishop, R.E.D., Price, W.G., 1974. On modal analysis of ship strength. Proc. Roy. Soc. Lond. 341, 121–134.
Bishop, R.E.D., Price, W.G., 1976a. On modal analysis of ship strength. Proc. R. Soc. London, A 349 (1657), 157–167.
Bishop, R.E.D., Price, W.G., 1976b. On the transverse strength of ships with large deck openings. Proc. R. Soc. London, A 349 (169), 169–182.
Bishop, R.E.D., Price, W.G., 1979. Hydroelasticity of Ships. Cambridge University Press, Cambridge.
Bishop, R.E.D., Taylor, R.E., 1973. On wave-induced stress in a ship executing symmetric motions. Phil. Trans. Roy. Soc. Lond. Math. Phys. Sci. 275 (1247), 1–32.
Bishop, R.E.D., Price, W.G., Tam, P.K.Y., 1977. A unified dynamic analysis of ship response to waves. RINA Transact. 119, 363–390.
Bishop, R.E.D., Price, W.G., Tam, P.K.Y., 1978. On the Dynamics of Slamming, 120. Transactions of the Royal Institution of Naval Architects, pp. 259–280.
Bishop, R.E.D., Price, W.G., Temarel, P., 1980. Antisymmetric Vibration of Ship Hulls, 122. Transactions of the Royal Institution of Naval Architects, pp. 197–208.
Bishop, R.E.D., Price, W.G., Wu, Y., 1986. A general linear hydroelasticity theory of floating structures moving in a seaway. Phil. Trans. Roy. Soc. Lond. Math. Phys. Sci. 316, 375–426.
Blake, W.K., Maga, L.J., 1975. On the flow-excited vibrations of cantilever struts in water. I. Flow-induced damping and vibration. J. Acoust. Soc. Am. 57, 610–625.
Blasques, J.P., Berggreen, C., Andersen, P., 2010. Hydro-elastic analysis and optimization of a composite marine propeller. Mar. Struct. 23 (1), 22–38.
Borsje, B.W., van Wesenbeeck, B.K., Dekker, F., Paalvast, P., Bouma, T.J., van Katwijk, M.M., de Vries, M.B., 2011. How ecological engineering can serve in coastal protection. Ecol. Eng. 37 (2), 113–122. https://doi.org/10.1016/j.ecoleng.2010.11.027.
Brown, S.A., Xie, N., Hann, M.R., Greaves, D.M., 2022. Investigation of wave-driven hydroelastic interactions using numerical and physical modelling approaches. Appl. Ocean Res. 129, 103363.
Brunet, Y., 2020. Turbulent flow in plant canopies: historical perspective and overview. Boundary-Layer Meteorol. 177 (2–3), 315–364.
Bureau Veritas, 2023. Propeller in Composite Materials (NI663 – March 2023). Bureau Veritas Marine & Offshore.
Bureau Veritas, 2025. Rules for the Classification of Steel Ships – Part B: Hull and Stability (NR467, January 2025 Edition). Bureau Veritas Marine & Offshore.
Bureš, L., Sato, Y., Pautz, A., 2021. Piecewise linear interface-capturing volume-of-fluid method in axisymmetric cylindrical coordinates. J. Comput. Phys. 436, 110291.
Bushehri, M.P., Haghighi, M.R.G., Malekzadeh, P., Bahmyari, E., 2025. Fluid-structure interaction analysis of an elastic surface-piercing propellers. J. Fluid Struct. 132, 104228. https://doi.org/10.1016/j.jfluidstructs.2025.104228.
Calclough, W., Russell, J., 1972. Development of a composite propeller blade with a carbon fibre reinforced plastics spar. Aeronaut. J. 76 (733), 53–57.
Cardiff, P., Demirdžić, I., 2021. Thirty years of the finite volume method for solid mechanics. Arch. Comput. Methods Eng. 28, 3721–3780. https://doi.org/10.1007/s11831-020-09523-0.
Cardiff, P., Batistić, I., Tukovic, Ž., 2025. solids4foam: a toolbox for performing solid mechanics and fluid-solid interaction simulations in OpenFOAM. J. Open Source Softw. 10 (108), 7407. https://doi.org/10.21105/joss.07407.
Caron, C., Lauret, P., Bastide, A., 2024. Machine Learning to speed up Computational Fluid Dynamics engineering simulations for built environments: a review. Build. Environ., 112229
Chabchoub, A., Hoffmann, N.P., Akhmediev, N., 2011. Rogue wave observation in a water wave tank. Phys. Rev. Lett. 106 (20), 204502. https://doi.org/10.1103/PhysRevLett.106.204502.
Chakraborty, R., Mondal, A., Gayen, R., 2016. Interaction of surface water waves with a vertical elastic plate: a hypersingular integral equation approach. Z. Angew. Math. Phys. 1–18.
Chang, L., Piao, S., Leng, X., He, Z., Zhu, Z., 2020. Inverted pendulum model for turn-planning for biped robot. Phys. Commun. 42, 101168. https://doi.org/10.1016/j.phycom.2020.101168.
Chang, X., Chen, Z., Jiao, J., Ma, B., 2025. Experimental and numerical investigation on springing and whipping responses of a 21000TEU containership. Ocean Eng. 338, 121979. https://doi.org/10.1016/j.oceaneng.2025.121979.
Chatzimarkou, E., Michailides, C., Onoufriou, T., 2022. Performance of a coupled level-set and volume-of-fluid method combined with free surface turbulence damping boundary condition for simulating wave breaking in OpenFOAM. Ocean Eng. 265, 112572. https://doi.org/10.1016/j.oceaneng.2022.112572.
Chen, Z., 2017. A nonlinear hydroelastic method considering wave memory effect for ship load responses in irregular waves. J. Cent. S. Univ. 24, 2058–2070. https://doi.org/10.1007/s11771-017-3615-5.
Chen, H.-C., Chen, C.-R., 2023. CFD simulation of a container ship in random waves using a coupled level-set and volume of fluid method. J. Hydrodyn. 35 (2), 222–231. https://doi.org/10.1007/s42241-023-0019-x.
Chen, W., Li, Y.P., 2025. Simulation of a wall-mounted stem in uniform flow. J. Fluid Mech. 1013, A17.
Chen, H., Zou, Q.P., 2019. Eulerian–Lagrangian flow-vegetation interaction model using immersed boundary method and OpenFOAM. Adv. Water Resour. 126, 176–192.
Chen, B., Neely, S., Michael, T., Gowing, S., Szwerc, R., Buchler, D., Schult, R., 2006a. Design, fabrication and testing of pitch-adapting (flexible) composite propellers. The SNAME Propellers/Shafting Symposium'06. Sept, Williamsburg, VA, pp. 12–13.
Chen, X.-j., Wu, Y.-s., Cui, W.-c., Jensen, J.J., 2006b. Review of hydroelasticity theories for global response of marine structures. Ocean Eng. 33, 439–457.
Chen, H., Zou, Q., Liu, Z., 2017. A coupled RANS-VOF and finite element model for wave interaction with highly flexible vegetation. Coast. Eng. Proceed. 35 (waves), 25.
Chen, Z., Jiao, J., Li, H., 2017. Time-domain numerical and segmented ship model experimental analyses of hydroelastic responses of a large container ship in oblique regular waves. Appl. Ocean Res. 67, 78–93.
Chen, Z., Gui, H., Dong, P., Yu, C., 2019a. Numerical and experimental analysis of hydroelastic responses of a high-speed trimaran in oblique irregular waves. Int. J. Nav. Archit. Ocean Eng. 11 (1), 409–421.
Chen, C., Sun, T., Wei, Y., Wang, C., 2019b. Computational analysis of compressibility effects on cavity dynamics in high-speed water-entry. Int. J. Nav. Archit. Ocean Eng. 11 (1), 495–509.
Chen, H., Liu, X., Zou, Q.P., 2019c. Wave-driven flow induced by suspended and submerged canopies. Adv. Water Resour. 123, 160–172.
Chen, D., Feng, X., Hou, C., Chen, J.F., 2022a. A coupled frequency and time domain approach for hydroelastic analysis of very large floating structures under focused wave groups. Ocean Eng. 255, 111393.
Chen, H., Tong, X., Chen, Y., He, J., 2022b. Theoretical and experimental studies on the hydrodynamic damping of elastic rotating propeller blades. Int. J. Nav. Archit. Ocean Eng. 14, 100446.
Chen, Y., Zhang, X., Liu, L., Tian, X., Li, X., Cheng, Z., 2023a. A discrete-module-finite-element hydroelasticity method in analyzing dynamic response of floating flexible structures. J. Fluid Struct. 117, 103825.
Chen, Z., Jiao, J., Wang, S., Soares, C.G., 2023b. CFD-FEM simulation of water entry of a wedged grillage structure into Stokes waves. Ocean Eng. 275, 114159.
Chen, Z., Jiao, J., Chang, X., Ma, B., 2024a. Numerical and experimental study of asymmetrical wave loads and hydroelastic responses of ship in oblique regular

waves. Appl. Ocean Res. 153, 104254. https://doi.org/10.1016/j.apor.2024.104254.
Chen, L., Li, B., Luo, C., et al., 2024b. WaveNets: physics-informed neural networks for full-field recovery of rotational flow beneath large-amplitude periodic water waves. Eng. Comput. 40, 2819–2839. https://doi.org/10.1007/s00366-024-01944-w.
Chen, Z., Jiao, J., Xu, W., Jiang, C., Chen, S., 2025. Numerical simulation of ship hydroelastic responses in short-crested irregular waves. Mar. Struct. 103, 103858. https://doi.org/10.1016/j.marstruc.2025.103858.
Cheng, S., Tsarau, A., Evers, K.-U., Shen, H., 2019. Floe size effect on gravity wave propagation through ice covers. J. Geophys. Res.: Oceans 123 (12), 9205–9221. https://doi.org/10.1029/2018JC014094.
Cho, I.H., 2021. Liquid sloshing in a swaying/rolling rectangular tank with a flexible porous elastic baffle. Mar. Struct. 75, 102865.
Cho, I.H., Kim, M.H., 2000. Interactions of horizontal porous flexible membrane with waves. J. Waterw. Port, Coast. Ocean Eng. 126 (5), 245–253.
Chuang, S.L., 1970. Investigation of Impact of Rigid and Elastic Bodies with Water. Naval Ship Research and Development Center (NSRDC), Washington, D. C. Report Number-3248.
Chuang, S.L., 1973. Slamming tests of three-dimensional models in calm water and waves. David Taylor Model Basin (DTMB). Report Number-4095 (USA).
Chung, H., Fox, C., 2002. Calculation of wave-ice interaction using the Wiener-Hopf technique. New Zealand J. Math 31 (1), 1–18.
Chwang, A.T., Chan, A.T., 1998. Interaction between porous media and wave motion. Annu. Rev. Fluid Mech. 30, 53–84. https://doi.org/10.1146/annurev.fluid.30.1.53.
Ciampolini, M., Balduzzi, F., Romani, L., Bellucci, L., Bianchini, A., Ferrara, G., 2022. Development of an improved and versatile 2D+t modelling methodology for planing crafts. Ocean Eng. 265, 112615. https://doi.org/10.1016/j.oceaneng.2022.112615.
Collins, C.O., Rogers, W.E., Lund, B., 2017. An investigation into the dispersion of ocean surface waves in sea ice. Ocean Dyn. 67 (2), 263–280.
Collins, I., Hossain, M., Dettmer, W., Masters, I., 2021. Flexible membrane structures for wave energy harvesting: a review of the developments, materials and computational modelling approaches. Renew. Sustain. Energy Rev. 151, 111478. https://doi.org/10.1016/j.rser.2021.111478.
Colomés, O., Verdugo, F., Akkerman, I., 2022. A monolithic finite element formulation for the hydroelastic analysis of very large floating structures. Int. J. Numer. Methods Eng. https://doi.org/10.1002/nme.7140.
Couston, L.A., Jalali, M.A., Alam, M.R., 2017. Shore protection by oblique seabed bars. J. Fluid Mech. 815, 481–510.
Crary, A.P., Cotell, R.D., Oliver, J., 1952. Geophysical studies in the Beaufort sea. EOS, Transact. Am. Geophys. Union 33 (2), 211–216.
Cui, L., Chen, Z., Feng, Y., Li, G., Liu, J., 2021a. An improved VOF method with anti-ventilation techniques for the hydrodynamic assessment of planing hulls – Part 1: theory. Ocean Eng. 237, 109687. https://doi.org/10.1016/j.oceaneng.2021.109687.
Cui, L., Chen, Z., Feng, Y., Li, G., Liu, J., 2021b. An improved VOF method with anti-ventilation techniques for the hydrodynamic assessment of planing hulls–Part 2: applications. Ocean Eng. 237, 109505. https://doi.org/10.1016/j.oceaneng.2021.109505.
Cummins, W.E., 1962. The impulse response function and ship motions. Schiśtechnik 9, 101–109.
Cunbao, Z., Jiazhong, Z., Wenhu, H., 2007. Vibration reduction of floating elastic plates in water waves. Mar. Struct. 20 (1–2), 71–99.
Da Silva, A.T., Peregrine, D.H., 1990. Nonlinear perturbations on a free surface induced by a submerged body: a boundary integral approach. Eng. Anal. Bound. Elem. 7 (4), 214–222. https://doi.org/10.1016/0955-7997(90)90038-V.
Dalrymple, R.A., Liu, P.L.F., 1978. Waves over soft muds: a two-layer fluid model. J. Phys. Oceanogr. 8 (6), 1121–1131.
Dalrymple, R.A., Kirby, J.T., Hwang, P.A., 1984. Wave diffraction due to areas of energy dissipation. J. Waterw. Port, Coast. Ocean Eng. 110, 67–79.
Darcy, H.P.G., 1856. Les fontaines publiques de la ville de Dijon. Dalmont, Paris.
Das, S., Cheung, K.F., 2012a. Scattered waves and motions of marine vessels advancing in a seaway. Wave Motion 49 (1), 181–197.
Das, S., Cheung, K.F., 2012b. Hydroelasticity of marine vessels advancing in a seaway. J. Fluid Struct. 34, 271–290.
Das, H.N., Kapuria, S., 2016. On the use of bend–twist coupling in full-scale composite marine propellers for improving hydrodynamic performance. J. Fluid Struct. 61, 132–153. https://doi.org/10.1016/j.jfluidstructs.2015.11.008.
Datta, R., Guedes Soares, C., 2020. Analysis of the hydroelastic effect on a container vessel using coupled BEM–FEM method in the time domain. Ships Offshore Struct. 15 (4), 393–402.
Datta, N., Siddiqui, M.A., 2013. Dynamic response of axially loaded plates with intermediate fixities to transient hydrodynamic impact loads. In: International Conference on Offshore Mechanics and Arctic Engineering, 55430. American Society of Mechanical Engineers. V009T12A019.
Datta, N., Siddiqui, M.A., 2016. Hydroelastic analysis of axially loaded Timoshenko beams with intermediate end fixities under hydrodynamic slamming loads. Ocean Eng. 127, 124–134.
Datta, R., Rodrigues, J.M., Guedes Soares, C., 2011. Study of the motions of fishing vessels by a time domain panel method. Ocean Eng. 38 (5–6), 782–792. https://doi.org/10.1016/j.oceaneng.2010.12.020.
Datta, R., Fonseca, N., Soares, C.G., 2013. Analysis of the forward speed effects on the radiation forces on a fast ferry. Ocean Eng. 60, 136–148.
Dawson, T.H., 1978. Wave propagation over a deformable sea floor. Ocean Eng. 5 (4), 227–234.
De Langre, E., 2008. Effects of wind on plants. Annu. Rev. Fluid Mech. 40 (1), 141–168.
de Vriend, H.J., van Koningsveld, M., Aarninkhof, S.G., de Vries, M.B., Baptist, M.J., 2015. Sustainable hydraulic engineering through building with nature. J. Hydro-Environ. Res. 9 (2), 159–171. https://doi.org/10.1016/j.jher.2014.06.004.
De Wit, P.J., Kranenburg, C., 1996. On the effects of a liquefied mud bed on wave and flow characteristics. J. Hydraul. Res. 1996 (1). https://doi.org/10.1080/00221689609498761.
Dean, W.R., 1945. On the reflection of surface waves by a flat plate floating vertically. Math. Proc. Camb. Phil. Soc. 41, 231–238.
Dean, C.H., 1966. The attenuation of ocean waves near the open ocean/pack ice boundary. Paper Presented at the Symposium on Antarctic Oceanography, Scientific Committee on Antarctic Research, Santiago, Chile, September 13–16, 1966.
Dean, R.G., Dalrymple, R.A., 1991. Water Wave Mechanics for Engineers and Scientists, 2. World Scientific, Englewood Cliffs. Prentice-Hall, New Jersey.
Delefortrie, G., Vantorre, M., Eloot, K., Verwilligen, J., Lataire, E., 2010. Squat prediction in muddy navigation areas. Ocean Eng. 37 (16), 1464–1476. https://doi.org/10.1016/j.oceaneng.2010.08.003.
Deng, B., Hsu, T.-J., Chou, Y.-J., 2017. Numerical study on the dissipation of water waves over a viscous fluid-mud layer. J. Fluid Mech. 829, 230–255.
Dessi, D., Mariani, R., 2008. Analysis and prediction of slamming-induced loads of a high-speed monohull in regular waves. J. Ship Res. 52 (1), 71–86.
Det Norske Veritas, 2013. DNV-RP-C208: Determination of Structural Capacity by Non-linear FE Analysis Methods. Det Norske Veritas.
Det Norske Veritas, 2017. Environmental Conditions and Environmental Loads. DNVGL-RP-C205, August 2017 Edition.
Dhavalikar, S., Awasare, S., Joga, R., Kar, A.R., 2015. Whipping response analysis by one-way fluid-structure interaction—a case study. Ocean Eng. 103, 10–20.
Di, Y., Zhao, L., Mao, J., Eldad, A., 2021. A resolved CFD-DEM-IBM algorithm for water entry problems. Ocean Eng. 240, 110014.
Di, Y., Zhao, L., Mao, J., 2024. A hybrid FEM–IBM–level set algorithm for water entry of deformable body. Ocean Eng. 306, 118007. https://doi.org/10.1016/j.oceaneng.2023.118007.
Diez, M., Lee, E.J., Harrison, E.L., Powers, A.M., Snyder, L.A., Jiang, M.J., Bay, R.J., Lewsi, R.R., Kubina, E.R., Mucha, P., Stern, F., 2022. Experimental and computational fluid-structure interaction analysis and optimization of deep-V planing-hull grillage panels subject to slamming loads – Part I: regular waves. Mar. Struct. 85. https://doi.org/10.1016/j.marstruc.2022.103256. Article 103256.
Dijkstra, J.T., Uittenbogaard, R.E., 2010. Modeling the interaction between flow and highly flexible aquatic vegetation. Water Resour. Res. 46, W12547.
Ding, G., Jiang, N., Gao, X., Wang, F., Wu, X., 2022. Deformation monitoring of propeller underwater operation based on fiber optic grating sensing network. Ocean Eng. 264, 112308.
Dobrovol'skaya, Z.N., 1969. On some problems of similarity flow of fluids with a free surface. J. Fluid Mech. 36, 805–829.
Dolatshah, A., Bennetts, L.G., Meylan, M.H., Monty, J.P., Toffoli, A., 2019a. An experimental model of wind-induced rafting of pancake ice floating on waves. In: Proceedings of the 34th International Workshop on Water Waves and Floating Bodies, pp. 7–10.
Dolatshah, A., Bennetts, L.G., Meylan, M.H., Monty, J.P., Toffoli, A., 2019b. An experimental model of wind-induced rafting of pancake ice floating on waves. In: Proceedings of the 34th International Workshop on Water Waves and Floating Bodies, pp. 7–10. Newcastle, Australia.
Donea, J., Huerta, A., Ponthot, J.-Ph, Rodriguez-Ferran, A., 2004. Arbitrary Lagrangian–eulerian methods. In: Fundamentals, 1. John Wiley & Sons, Ltd. ISBN: 0-470-84699-2.
Dong, C., Sun, S., Song, H., Wang, Q., 2019. Numerical and experimental study on the impact between a free falling wedge and water. Int. J. Nav. Archit. Ocean Eng. 11 (1), 233–243.
Drummen, I., Storhaug, G., Moan, T., 2008. Experimental and numerical investigation of fatigue damage due to wave-induced vibrations in a containership in head seas. J. Mar. Sci. Technol. 13 (4), 428–445. https://doi.org/10.1007/s00773-008-0006-5.
Duan, L., Zhu, L., Chen, M., Pedersen, P.T., 2020. Experimental study on the propagation characteristics of the slamming pressures. Ocean Eng. 217, 107868.
Duan, W.Y., Wang, H.X., Chen, J.K., et al., 2022. TEBEM for springing responses of a container ship with sailing speed and nonlinear effects in time domain. Eng. Anal. Bound. Elem. 140, 406–420.
Ducoin, A., Barber, R.B., Wildy, S.J., Codrington, J.D., Baker, A., 2023. Experimental evaluation of the use of embedded fiber Bragg gratings to measure steady and unsteady flow-induced marine propeller blade deformation. Ocean Eng. 281, 114889.
Dudley, J.M., Genty, G., Mussot, A., Chabchoub, A., Dias, F., 2019. Rogue waves and analogies in optics and oceanography. Nature Rev. Phys. 1 (9), 675–689. https://doi.org/10.1038/s42254-019-0100-0.
Eastridge, J.R., Taravella, B.M., 2017. An experimental study in the hydroelastic response of an aluminum wedge in drop tests. In: SNAME American Towing Tank Conference. SNAME. D011S002R004.
Ebrahimi, M., Azimi, A.H., 2025a. Energy losses due to entry of disks into water and viscous fluid mixtures. Int. J. Heat Fluid Flow 109, 109943. https://doi.org/10.1016/j.ijheatfluidflow.2025.109943.
Ebrahimi, M., Azimi, A.H., 2025b. Cavity dynamics by the entry of annular disks into non-Newtonian ambient. Ocean Eng. 321, 120379. https://doi.org/10.1016/j.oceaneng.2025.120379.
El Aouad, S., Larcher, A., Hachem, E., 2022. Anisotropic adaptive body-fitted meshes for CFD. Comput. Methods Appl. Mech. Eng. 400, 115562. https://doi.org/10.1016/j.cma.2022.115562.

el Moctar, O., Schellin, T.E., Priebe, T., 2006. CFD and FE methods to predict wave loads and ship structural response. Paper Presented at the 26th Symposium on Naval Hydrodynamics, Rome, Italy.
Elgar, S., Raubenheimer, B., 2008. Wave dissipation by muddy seafloors. Geophys. Res. Lett. 35 (7).
Elishakoff, I., 2020. Handbook on Timoshenko-Ehrenfest Beam and Uflyand-Mindlin Plate Theories. World Scientific, Singapore. ISBN 978-981-3236-51-6.
Evans, D.V., Davies, T.V., 1968. Wave-ice Interaction, Report No. 1313. Davidson Lab, Stevens Inst. of Tech., Hoboken, NJ.
Ewing, M., Crary, A.P., Thorne Jr., A.M., 1934. Propagation of elastic waves in ice. Part I. J. Appl. Phys. 5 (6), 165–168.
Fairlie-Clarke, A.C., Tveitnes, T., 2008. Momentum and gravity effects during the constant velocity water entry of wedge-shaped sections. Ocean Eng. 35 (7), 706–716. https://doi.org/10.1016/j.oceaneng.2008.01.014.
Faltinsen, O.M., 1997. The effect of hydroelasticity on ship slamming. Philos. Trans. R. Soc. London, Ser. A 355, 1–17.
Faltinsen, O.M., 1999. Water entry of a wedge by hydroelastic orthotropic plate theory. J. Ship Res. 43, 180–193.
Faltinsen, O.M., 2000. Hydroelastic slamming. J. Mar. Sci. Technol. 5, 49–65.
Faltinsen, O., Zhao, R., 1991a. Numerical prediction of ship motions at high forward speed. Phil. Trans. Roy. Soc. Lond. Math. Phys. Sci. 334, 241–257.
Faltinsen, O., Zhao, R., 1991b. Flow predictions around high-speed ships in waves. Proceedings of the Mathematical Approaches in Hydrodynamics. Society for Industrial and Applied Mathematics, Philadelphia, PA, USA, pp. 265–288.
Feng, S., Zhang, G., el Moctar, O., Sun, Z., Zhang, Z., 2021a. A semi-analytical method to simulate hydroelastic slamming of 2D structural sections by coupling Wagner theory with the finite element method. Ocean Eng. 240, 109998.
Feng, S., Zhang, G., Wan, D., Jiang, S., Sun, Z., Zong, Z., 2021b. On the treatment of hydroelastic slamming by coupling boundary element method and modal superposition method. Appl. Ocean Res. 112, 102595.
Feng, S., Zhang, G., Jiang, C., Jiang, S., el Moctar, O., Ma, Y., 2024. Investigation of fluid added mass matrix during hydroelastic slamming of wedges. Phys. Fluids 36 (1), 2024 Jan 1.
Ferro, P., Landel, P., Landrodie, C., Guillot, S., Pescheux, M., 2025. Enhanced Level-Set Method for free surface flow applications. Int. J. Multiphas. Flow 185, 105126.
Flügge, W., 1975. Viscoelasticity in three dimensions. Viscoelasticity 159–187.
Forristall, G.Z., Reece, A.M., 1985. Measurements of wave attenuation due to a soft bottom: the SWAMP experiment. J. Geophys. Res.: Oceans 90 (C2), 3367–3380.
Fox, C., Squire, V.A., 1994. On the oblique reflexion and transmission of ocean waves from shore fast sea ice. Philos. Trans. R. Soc. London, Ser. A: Phys. Eng. Sci. 347 (1682), 185–218. https://doi.org/10.1098/rsta.1994.0039.
French, M.J., 1979. Water Wave Energy Conversion Device Using Flexible Membranes (U.S. Patent No. 6075824). U.S. Department of Energy, Office of Scientific and Technical Information, OSTI ID, 6075824. Retrieved from.
Fu, S., Zhang, S., Cui, W., 2022. Hydroelasticity theory. In: Cui, W., Fu, S., Hu, Z. (Eds.), Encyclopedia of Ocean Engineering. Springer, Singapore, p. 341. https://doi.org/10.1007/978-981-10-6946-8_341.
Fukasawa, T., Yamamoto, Y., Fujino, M., Motora, S., 1981. Motion and Longitudinal Strength of a Ship in Head Sea and the Effects of Nonlinearities (4th Report) Experiment. Journal of the Society of Naval Architects of Japan, p. 150.
Gade, H.G., 1958. Effects of a Nonrigid, Impermeable Bottom on Plane Surface Waves in Shallow Water.
Gao, J., Zhu, W., Jin, Y., Gong, P., 2025. Steady-state nonlinear dynamics of a flexible beam with large deformation under oscillatory flow. J. Fluid Struct. 136, 104327. https://doi.org/10.1016/j.jfluidstructs.2025.104327.
Garnier, E.-I., Huang, Z., Mei, C., 2013. Nonlinear long waves over a muddy beach. J. Fluid Mech. 718, 371–397. https://doi.org/10.1017/jfm.2012.617.
Ge, J., Chen, C., Wang, Z., Ke, K., Yi, J., Ding, P., 2020. Dynamic response of the fluid mud to a tropical storm. J. Geophys. Res.: Oceans 125 (3), e2019JC015419. https://doi.org/10.1029/2019JC015419.
Gerritsma, J., Beukelman, W., 1967. Analysis of the Modified Strip Theory for the Calculation of Ship Motions and Wave Bending Moments. Nederlands Ship Research Centre. Technical Report No. 96S.
Geyer, W.R., Hill, P.S., Kineke, G.C., 2004. The transport, transformation and dispersal of sediment by buoyant coastal flows. Cont. Shelf Res. 24 (7), 927–949. https://doi.org/10.1016/j.csr.2004.02.006.
Ghassemi, H., Saryazdi, M.G., Ghassabzadeh, M., 2012. Influence of the skew angle on the hydroelastic behaviour of a composite marine propeller. Proc. IME M J. Eng. Marit. Environ. 226 (4), 346–359.
Gotoh, H., Khayyer, A., 2018. On the state-of-the-art of particle methods for coastal and ocean engineering. Coast. Eng. J. 60 (1), 79–103. https://doi.org/10.1080/21664250.2018.1436243.
Graebel, W.P., 2007. Advanced Fluid Mechanics. Academic Press.
Grammatikopoulos, A., 2023. A review of physical flexible ship models used for hydroelastic experiments. Mar. Struct. 90. https://doi.org/10.1016/j.marstruc.2023.103436.
Grammatikopoulos, A., Banks, J., Temarel, P., 2020. Prediction of the vibratory properties of ship models with realistic structural configurations produced using additive manufacturing. Mar. Struct. 73.
Grammatikopoulos, A., Banks, J., Temarel, P., 2021. The design and commissioning of a fully elastic model of a uniform container ship. Mar. Struct. 78.
Grasso, N., Hallmann, R., Scholcz, T., Zondervan, G., Maljaars, P., Schouten, R., 2019. 'Measurements of the hydro-elastic behaviour of flexible composite propellers in nonuniform flow at model and full scale'. Sixth International Symposium on Marine Propulsors smp'19. Rome, Italy. May.
Green, A.E., Laws, N., Naghdi, P.M., 1974. On the theory of water waves. Proceed. Royal Soc. London. A. Mathemat. Phys. Sci. 338 (1612), 43–55.
Green, A.E., Naghdi, P.M., 1976. Directed fluid sheets. Proceed. Royal Soc. London. A. Mathemat. Phys. Sci. 347, 447–473. https://doi.org/10.1098/rspa.1976.0023.
Greenhill, A.G., 1886. Wave motion in hydrodynamics. Am. J. Math. 9 (1), 62–96. https://doi.org/10.2307/2369499.
Gu, M.X., Wu, Y.S., Xia, J.Z., 1989. Time domain analysis of non-linear hydroelastic response of ships. Proceedings of the 4th International Symposium on Practical Design of Ships and Other Floating Structures (PRADS). Varna, Bulgaria.
Gu, N., Liang, D., Zhou, X., Ren, H., 2023. A CFD-FEA method for hydroelastic analysis of floating structures. J. Mar. Sci. Eng. 11 (4), 737.
Haase, H., Soproni, J.P., Abdel-Maksoud, M., 2015. Numerical analysis of a planing boat in head waves using a 2D+t method. Ship Technol. Res. 62 (3), 131–139. https://doi.org/10.1080/09377255.2015.1073824.
Haddara, M.R., Guedes Soares, C., 1999. Wind loads on marine structures. Mar. Struct. 12 (3), 199–209. https://doi.org/10.1016/S0951-8339(99)00023-4.
Halliday, J.R., Dorrell, D.G., Wood, A.R., 2011. An application of the Fast Fourier Transform to the short-term prediction of sea wave behaviour. Renew. Energy 36 (6), 1685–1692.
Han, S., Lee, H., Song, M.C., Chang, B.J., 2015. Investigation of hydro-elastic performance of marine propellers using fluid-structure interaction analysis. In: ASME International Mechanical Engineering Congress and Exposition, 57465. American Society of Mechanical Engineers. https://doi.org/10.1115/IMECE2015-51089. V07AT09A038.
Han, J., Li, Y., Zhao, X., Liu, T., Gu, Y., He, S., Li, P., Sun, R., 2025. Numerical study of regular wave dynamics for optimizing coral reef restoration. Ocean Eng. 315, 119768.
Hara, Y., Yamatogi, T., Murayama, H., Uzawa, K., Kageyama, K., 2011. Performance evaluation of composite marine propeller for a fishing boat by fluid-structure interaction analysis. In: 18th International Conference on Composite Materials. Jeju Island, Korea, p. 6.
Harris, H.G., Sabnis, G., 1999. In: Structural Modelling and Experimental Techniques, second ed. CRC Press.
Hartmann, M.C.N., Onorato, M., De Vita, F., Clauss, G., Ehlers, S., von Bock und Polach, F., Schmitz, L., Hoffmann, N., Klein, M., 2022. Hydroelastic potential flow solver suited for nonlinear wave dynamics in ice-covered waters. Ocean Eng. 259, 111756. https://doi.org/10.1016/j.oceaneng.2022.111756.
Hasan, M.S., Hoskoti, L., Deepu, P., Sucheendran, M.M., 2023. Nonlinear oscillations of a flexible fiber under gravity waves. Eur. Phys. J.: Spec. Top. 232 (4), 867–876. https://doi.org/10.1140/epjs/s11734-022-00683-w.
Hassan, M.U., Meylan, M.H., Peter, M.A., 2009. Water-wave scattering by submerged elastic plates. Q. J. Mech. Appl. Math. 62 (3), 321–344.
Hassoon, O.H., Tarfaoui, M., Alaoui, A.E.M., 2017. An experimental investigation on dynamic response of composite panels subjected to hydroelastic impact loading at constant velocities. Eng. Struct. 153, 180–190.
Hayter, E., Mehta, A.J., 1982. Modeling of estuarial fine sediment transport for tracking pollutant movement. Coastal and Oceanographic Engineering Department. University of Florida.
He, X.D., Hong, Y., Wang, R.G., 2012. Hydroelastic optimisation of a composite marine propeller in a non-uniform wake. Ocean Eng. 39, 14–23. https://doi.org/10.1016/j.oceaneng.2011.10.007.
He, K., Ni, B., Xu, X., Wei, H., Xue, Y., 2022. Numerical simulation on the breakup of an ice sheet induced by regular incident waves. Appl. Ocean Res. 120, 103024. https://doi.org/10.1016/j.apor.2021.103024.
He, Y., Wang, J., He, J., Li, Y., Feng, X., Chabchoub, A., 2025. Lifetime characterisation of extreme wave localisations in crossing seas. J. Fluid Mech. 1008, A3. https://doi.org/10.1017/jfm.2025.155.
Heins, A.E., 1948. Water waves over a channel of finite depth with a dock. Am. J. Math. 70 (4), 730–748.
Hejazi, M.I., Soltanpour, M., Sami, S., 2013. Numerical modeling of wave-mud interaction using projection method. Ocean Eng. 70, 1–13.
Helal, M.M., Ahmed, T.M., Banawan, A.A., Kotb, M.A., 2018. Numerical prediction of sheet cavitation on marine propellers using CFD simulation with transition-sensitive turbulence model. Alex. Eng. J. 57 (4), 3805–3815.
Heller, S.R., Abramson, H.N., 1959. Hydroelasticity: a new naval science. J. Am. Soc. Naval Eng. 71 (2), 205–209.
Henry, P.-Y., Myrhaug, D., 2013. Wave-induced drag force on vegetation under shoaling random waves. Coast. Eng. 78, 13–20. https://doi.org/10.1016/j.coastaleng.2013.03.004.
Heo, K., Kashiwagi, M., 2019. A numerical study of second-order springing of an elastic body using higher-order boundary element method (HOBEM). Appl. Ocean Res. 93, 101903.
Hermundstad, O.A., 1995. Theoretical and Experimental Hydroelastic Analysis of High Speed Vessels. NTNU, Trondheim, Norway. PhD Thesis.
Hermundstad, O., Aarsnes, J., Moan, T., 1994. Hydroelastic response analysis of high-speed monohull. In: F, et al. (Eds.), Hydroelasticity in Marine Technology, NTNU, Norway, pp. 245–259. Balkema, Rotterdam. Proceedings of the 1st International Conference.
Hermundstad, O.A., Aarsnes, J.V., Moan, T., 1999. Linear hydroelastic analysis of high-speed catamarans and monohulls. J. Ship Res. 43 (1), 48–63.
Hirdaris, S.E., Temarel, P., 2009. Hydroelasticity of ships: recent advances and future trends. Proc. IME M J. Eng. Marit. Environ. 223 (3), 305–330.
Hirdaris, S.E., Price, W.G., Temarel, P., 2003. Two- and three-dimensional hydroelastic analysis of a bulker in waves. Mar. Struct. 16, 627–658.
Hirdaris, S.E., White, N.J., Angoshtari, N., Johnson, M.C., Lee, Y., Bakkers, N., 2010. Wave loads and flexible fluid-structure interactions: current developments and

future directions. Ships Offshore Struct. 5 (4), 307–325. https://doi.org/10.1080/17445301003626263.
Hirdaris, S.E., Bai, W., Dessi, D., Ergin, A., Gu, X., Hermundstad, O.A., Huijsmans, R., Iijima, K., Nielsen, U.D., Parunov, J., Fonseca, N., 2014. Loads for use in the design of ships and offshore structures. Ocean Eng. 78, 131–174.
Hirdaris, S., Parunov, J., Qui, W., Iijima, K., Wang, X., Wang, S., Brizzolara, S., Guedes Soares, C., 2023. Review of the uncertainties associated with hull girder hydroelastic response and wave load predictions. Mar. Struct. 89, 103383.
Hirt, C.W., Nichols, B.D., 1981. Volume of fluid (VOF) method for the dynamics of free boundaries. J. Comput. Phys. 39 (1), 201–225.
Hong, Y., He, X.D., Gao, X., 2011. Dynamic responses of composite marine propeller in spatially wake. Polym. Polym. Compos. 19, 523–529.
Hong, Y., Wilson, P.A., He, X.D., Wang, R.G., 2017. Numerical analysis and performance comparison of the same series of composite propellers. Ocean Eng. 144, 211–223.
Hong, Y., Heo, K., Kashiwagi, M., 2021. Hydroelastic analysis of a ship with forward speed using orthogonal polynomials as mode functions of Timoshenko beam. Appl. Ocean Res. 112, 102696. https://doi.org/10.1016/j.apor.2021.102696.
Hosseini, A., Tavakoli, S., Dashtimanesh, A., Mikkola, T., Hirdaris, S., 2024. Drift test analysis of a conventional planing hull utilising CFD and 2D+t models. Ocean Eng. 308, 118226. https://doi.org/10.1016/j.oceaneng.2024.118226.
Hosseinzadeh, S., 2023. Fluid-structure Interaction Analysis of Impact-Induced Loads and Hydroelastic Responses of Ship Structures. Tallinn University of Technology. Doctoral dissertation.
Hosseinzadeh, S., Tabri, K., 2021a. Free-fall water entry of a variable deadrise angle aluminium wedge: an experimental study. In: Developments in the Analysis and Design of Marine Structures. CRC Press, pp. 29–37.
Hosseinzadeh, S., Tabri, K., 2021b. Hydroelastic effects of slamming impact loads during free-fall water entry. Ships Offshore Struct. 16 (Suppl. 1), 68–84.
Hosseinzadeh, S., Tabri, K., 2024. Experimental study on the dynamic response of a 3-D wedge under asymmetric impact. J. Hydrodyn. 1–12.
Hosseinzadeh, S., Izadi, M., Tabri, K., 2020. Free fall water entry of a two-dimensional asymmetric wedge in oblique slamming: a numerical study. In: International Conference on Offshore Mechanics and Arctic Engineering, 84409. American Society of Mechanical Engineers. V008T08A013.
Hosseinzadeh, S., Tabri, K., Hirdaris, S., Sahk, T., 2023a. Slamming loads and responses on a non-prismatic stiffened aluminium wedge: Part I. Experimental study. Ocean Eng. 279, 114510.
Hosseinzadeh, S., Tabri, K., Topa, A., Hirdaris, S., 2023b. Slamming loads and responses on a non-prismatic stiffened aluminium wedge: Part II. Numerical simulations. Ocean Eng. 279, 114309. https://doi.org/10.1016/j.oceaneng.2023.114309.
Houtani, H., Komoriyama, Y., Matsui, S., Oka, M., Sawada, H., Tanaka, Y., Tanizawa, K., 2018. Designing a hydro-structural model ship to experimentally measure its vertical-bending and torsional vibrations. In: 8th International Conference. on Hydroelasticity in Marine Technology, Seoul, Korea.
Howison, S.D., Ochendon, J.R., Wilson, S.K., 1991. Incompressible water-entry problems at small deadrise angles. J. Fluid Mech. 222, 215–230.
Hsu, T.-J., Ozdemir, C.E., Traykovski, P.A., 2009. High-resolution numerical modeling of wave-supported gravity-driven mudflows. J. Geophys. Res.: Oceans 114 (C5).
Hsu, W.Y., Hwung, H.H., Hsu, T.J., Torres-Freyermuth, A., Yang, R.Y., 2013. An experimental and numerical investigation on wave-mud interactions. J. Geophys. Res.: Oceans 118 (3), 1126–1141.
Hu, Z., Li, Y., 2023. Two-dimensional simulations of large-scale violent breaking wave impacts on a flexible wall. Coast. Eng. 185, 104370. https://doi.org/10.1016/j.coastaleng.2023.104370.
Hu, Z., Li, Y.P., 2025. Breaking wave impacts on an elastic plate. J. Fluid Mech. 1015, A54.
Hu, J.J., Wu, Y.S., Tian, C., Wang, X.L., Zhang, F., 2012. Hydroelastic analysis and model tests on the structural responses and fatigue behaviours of an ultra-large ore carrier in waves. Proc. IME M J. Eng. Marit. Environ. 226 (2), 135–155.
Hu, Z., Huang, L., Li, Y., 2023. Fully-coupled hydroelastic modeling of a deformable wall in waves. Coast. Eng. 179, 104245. https://doi.org/10.1016/j.coastaleng.2022.104245.
Huang, L., Li, Y., 2022. Design of the submerged horizontal plate breakwater using a fully coupled hydroelastic approach. Comput. Aided Civ. Infrastruct. Eng. 37 (7), 826–843.
Huang, Z.H., Huhe, A., Zhang, Y., 1992. An Experimental Study of the Properties of Fluid Mud in Xishu, Lianyungang. Institute of Mechanics, Chinese Academy of Sciences (in Chinese). Technical Report IMCAS STR-92019.
Huang, L., Ren, K., Li, M., Tuković, Ž., Cardiff, P., Thomas, G., 2019. Fluid-structure interaction of a large ice sheet in waves. Ocean Eng. 182, 102–111. https://doi.org/10.1016/j.oceaneng.2019.04.024.
Huang, L., Tuhkuri, J., Igrec, B., Li, M., Stagonas, D., Toffoli, A., Cardiff, P., Thomas, G., 2020. Ship resistance when operating in floating ice floes: a combined CFD&DEM approach. Mar. Struct. 74, 102817. https://doi.org/10.1016/j.marstruc.2020.102817.
Huang, L., Lu, W., Yang, J., Dong, Q., 2022a. Experimental study on surface waves around a novel model of ice floe. Cold Reg. Sci. Technol. 193, 103380. https://doi.org/10.1016/j.coldregions.2021.103380.
Huang, L., Li, Y., Benites-Munoz, D., Windt, C.W., Feichtner, A., Tavakoli, S., et al., 2022b. A review on the modelling of wave-structure interactions based on OpenFOAM. OpenFOAM® J. 2, 116–142.
Huang, J., Lowe, R.J., Ghisalberti, M., Hansen, J.E., 2024. Wave transformation across impermeable and porous artificial reefs. Coast. Eng. 189, 104488. https://doi.org/10.1016/j.coastaleng.2023.104488.
Huera-Huarte, F.J., Jeon, D., Gharib, M., 2011. Experimental investigation of water slamming loads on panels. Ocean Eng. 38 (11–12), 1347–1355.
Humamoto, T., Fujita, K., 2002. Wet-mode superposition for evaluating the hydroelastic response of floating structures with arbitrary shape. In: ISOPE International Ocean and Polar Engineering Conference. ISOPE. ISOPE-I.
Iafrati, A., 2016. Experimental investigation of the water entry of a rectangular plate at high horizontal velocity. J. Fluid Mech. 799, 637–672.
Iafrati, A., Grizzi, S., Siemann, M.H., Benítez Montañés, L., 2015. High-speed ditching of a flat plate: experimental data and uncertainty assessment. J. Fluid Struct. 55, 501–525. https://doi.org/10.1016/j.jfluidstructs.2015.03.019.
Iafrati, A., Grizzi, S., Olivieri, F., 2021. Experimental investigation of fluid–structure interaction phenomena during aircraft ditching. AIAA J. 59 (5), 1561–1574.
Iijima, K., Yao, T., Moan, T., 2008. Structural response of a ship in severe seas considering global hydroelastic vibrations. Mar. Struct. 21, 420–445.
Ikeda, S., Yamada, T., Toda, Y., 2001. Numerical study on turbulent flow and honami in and above flexible plant canopy. Int. J. Heat Fluid Flow 22 (3), 252–258.
Ilyas, M., Meylan, M.H., Lamichhane, B., Bennetts, L.G., 2018. Time-domain and modal response of ice shelves to wave forcing using the finite element method. J. Fluid Struct. 80, 113–131.
Im, H.-I., Vladimir, N., Malenica, Š., Cho, D.-S., 2017. Hydroelastic response of 19,000 TEU class ultra large container ship with novel mobile deckhouse for maximizing cargo capacity. Int. J. Nav. Archit. Ocean Eng. 9 (3), 339–349.
Inglis, C.E., 1929. Natural Frequencies and Modes of Vibration in Beams of Non-uniform Mass and Section, 72. Transactions of the Royal Institution of Naval Architects, pp. 145–166.
ISSC, 1973. Proceedings of the 5th International Ship Structures Congress. Hamburg.
Izadi, M., Ghadimi, P., Fadavi, M., others, 2018. Hydroelastic analysis of water impact of flexible asymmetric wedge with an oblique speed. Meccanica 53 (12), 2585–2617.
Jain, M., Mehta, A.J., 2009. Role of basic rheological models in determination of wave attenuation over muddy seabeds. Cont. Shelf Res. 29 (3), 642–651.
Jalalisendi, M., Porfiri, M., 2018. Water entry of compliant slender bodies: theory and experiments. Int. J. Mech. Sci. 149, 514–529.
Jang, C.D., Jung, J.J., Korobkin, A.A., 2007. An approach to estimating the hull girder response of a ship due to springing. J. Mar. Sci. Technol. 12, 95–101. https://doi.org/10.1007/s00773-007-0242-0.
Jaramillo, S., Sheremet, A., Allison, M.A., Reed, A.H., Holland, K.T., 2009. Wave-mud interactions over the muddy Atchafalaya subaqueous clinoform, Louisiana, United States: wave-supported sediment transport. J. Geophys. Res.: Oceans 114 (C4). https://doi.org/10.1029/2008JC004821.
Jaswon, M.A., Symm, G.T., 1977. Integral Equation Methods in Potential Theory and Elastostatics.
Javanmardi, N., Ghadimi, P., 2018. Hydroelastic analysis of a semi-submerged propeller using simultaneous solution of Reynolds-averaged Navier–Stokes equations and linear elasticity equations. Proc. IME M J. Eng. Marit. Environ. 232 (2), 199–211.
Javanmardi, N., Ghadimi, P., 2019. Hydroelastic analysis of surface piercing hydrofoil during initial water entry phase. Scientia Iranica B: Mech. Eng. 26 (1), 295–310.
Javanmardi, N., Ghadimi, P., Tavakoli, S., 2018. Probing into the effects of cavitation on hydrodynamic characteristics of surface piercing propellers through numerical modeling of oblique water entry of a thin wedge. Brodogradnja/Shipbuild. 69 (2), 1–18. https://doi.org/10.21278/brod69109.
Javdani, S., Fabian, M., Carlton, J.S., Sun, T., Grattan, K.T.V., 2016. Underwater free-vibration analysis of full-scale marine propeller using a fiber Bragg grating-based sensor system,". In: IEEE Sensors Journal, 16, pp. 946–953 no. 4, Feb.15, 2016.
Jeng, D.-S., Lin, Y.-S., 2000. Poroelastic analysis of the wave–seabed interaction problem. Comput. Geotech. 26 (1), 43–64. https://doi.org/10.1016/S0266-352X(99)00032-4.
Jenkins, N., Maute, K., 2016. An immersed boundary approach for shape and topology optimization of stationary fluid–structure interaction problems. Struct. Multidiscip. Optim. 53, 131–150. https://doi.org/10.1007/s00158-015-1342-4.
Jensen, J., 1991. Fatigue analysis of ship hulls under non-Gaussian wave loads. Mar. Struct. 4, 279–294. I.S.S.C. 1970 Proc. Fourth Int. Ship Struct. Congr. Tokyo.
Jensen, J., Pedersen, P.T., 1979. Wave-induced Bending Moments in Ships: A Quadratic Theory, 121. Transactions of the Royal Institution of Naval Architects, pp. 151–165.
Jensen, J., Pedersen, P.T., 1981. Bending moments and shear forces in ships sailing in irregular waves. J. Ship Res. 24, 243–251.
Jiang, L., LeBlond, P.H., 1993. Numerical modeling of an underwater Bingham plastic mudslide and the waves which it generates. J. Geophys. Res.: Oceans 98 (C6), 10303–10317.
Jiang, L., Kioka, W., Ishida, A., 1990. Viscous damping of cnoidal waves over fluid-mud seabed. J. Waterw. Port, Coast. Ocean Eng. 116 (4), 470–491.
Jiang, Z., Kujala, P., Hirdaris, S., Li, F., Mikkola, T., Suominen, M., 2024. The influence of waves and hydrodynamic interaction on energy-based evaluation of ice loads during a glancing impact in sea states. Ocean Eng. 310, 118719.
Jiao, J., Huang, S., Wang, S., Guedes Soares, C., 2021a. A CFD–FEA two-way coupling method for predicting ship wave loads and hydroelastic responses. Appl. Ocean Res. 117, 102919. https://doi.org/10.1016/j.apor.2021.102919.
Jiao, J., Huang, S., Guedes Soares, C., 2021b. Viscous fluid–flexible structure interaction analysis on ship springing and whipping responses in regular waves. J. Fluid Struct. 106, 103354.
Jiao, J., Chen, Z., Xu, S., 2024. CFD-FEM simulation of water entry of aluminium flat stiffened plate structure considering the effects of hydroelasticity. Brodogradnja 75 (1). Article 75108.
Jiao, J., Chen, Z., He, L., Jiang, C., Geng, Y., 2025a. Numerical study on hydroelastic responses and bending-torsion coupled loads of a ship in oblique regular waves. Ocean Eng. 315, 119904.
Jiao, J., Chen, Z., Chen, S., Jiang, C., Si, H., 2025b. Ship hydroelasticity responses in long-crested irregular waves by CFD-FEM simulation in comparison with segmented model experiment. Ocean Eng. 326, 120886. https://doi.org/10.1016/j.oceaneng.2025.120886.

Joe, B.-J., Choi, Y.-S., Jang, W.-S., Hong, S.-Y., Song, J.-H., Kwon, H.-W., 2021. Fatigue predictions for flexible marine propellers using FSI analysis considering Euler force in the rotating frame. Mar. Struct. 75, 102887.
Jonkman, J., Branlard, E., Hall, M., Hayman, G., Platt, A., Robertson, A., 2020. Implementation of Substructure Flexibility and Member-Level Load Capabilities for Floating Offshore Wind Turbines in OpenFAST (No. NREL/TP-5000-76822). National Renewable Energy Lab.(NREL), Golden, CO (United States).
Judge, C.Q., Ibrahim, A.M., 2025. Experimental investigation of motions and global hull girder bending moment of a semi-displacement vessel. Ocean Eng. 320, 120295. https://doi.org/10.1016/j.oceaneng.2025.120295.
Judge, C., Troesch, A.W., Perlin, M., 2004. Initial water impact of a wedge at vertical and oblique angles. J. Eng. Math. 48, 279–303. https://doi.org/10.1023/B:ENGI.0000018362.41573.57.
Jung, S., 2025. Water entry and exit in nature: review. Interface Focus 15 (2), 20240055. https://doi.org/10.1098/rsfs.2024.0055.
Kafshgarkolaei, H.J., Lotfollahi-Yaghin, M.A., Mojtahedi, A., 2019. A modified orthonormal polynomial series expansion tailored to thin beams undergoing slamming loads. Ocean Eng. 182, 38–47.
Kaihatu, J.M., Tahvildari, N., 2012. The combined effect of wave–current interaction and mud-induced damping on nonlinear wave evolution. Ocean Model. 41, 22–34.
Kaihatu, J.M., Sheremet, A., Holland, K.T., 2007. A model for wave propagation of nonlinear surface waves over viscous mud. Coast. Eng. 54 (10), 752–764.
Kaligatla, R.B., Koley, S., Sahoo, T., 2015. Trapping of surface gravity waves by a vertical flexible porous plate near a wall. Z. Angew. Math. Phys. 66, 2677–2702.
Kalliontzis, D., 2022. Fluid–structure interaction with ALE formulation and skeleton-based structural models. J. Fluid Struct. 110, 103513. https://doi.org/10.1016/j.jfluidstructs.2022.103513.
Kalyanaraman, B., Meylan, M.H., Bennetts, L.G., Lamichhane, B.P., 2020. A coupled fluid-elasticity model for the wave forcing of an ice-shelf. J. Fluid Struct. 97, 103074. https://doi.org/10.1016/j.jfluidstructs.2020.103074.
Kanoria, M., Mandal, B.N., Chakrabarti, A., 1999. The Wiener-Hopf solution of a class of mixed boundary value problems arising in surface water wave phenomena. Wave Motion 29 (3), 267–292.
Kapsenberg, G.K., 2011. Slamming of ships: where are we now? Philos. Trans. R. Soc. A Math. Phys. Eng. Sci. 369 (1947), 2892–2919.
Kara, F., 2011. Time domain prediction of added-resistance of ships. J. Ship Res. 55 (3), 163–184.
Kara, F., 2015. Time domain prediction of hydroelasticity of floating bodies. Appl. Ocean Res. 51, 1–13.
Kara, F., 2022. Application of time-domain methods for marine hydrodynamic and hydroelasticity analyses of floating systems. Ships Offshore Struct. 17 (7), 1628–1645. https://doi.org/10.1080/17445302.2021.1937798.
Karola, A., Tavakoli, S., Mikkola, T., Matusiak, J., Hirdaris, S., 2024. The influence of wave modelling on the motions of floating bodies. Ocean Eng. 306, 118067.
Kashiwagi, M., 1998. A B-spline Galerkin scheme for calculating the hydroelastic response of a very large floating structure in waves. J. Mar. Sci. Technol. 3 (1), 37–49.
Kashiwagi, M., Mizokami, S., Yasukawa, H., Fukushima, Y., 2000. Prediction of wave pressure and loads on actual ships by the enhanced unified theory. In: Proceedings of the 23rd Symposium on Naval Hydrodynamics, Val de Reuil.
Kawakita, C., 2019. An experimental study on hydrodynamic performance of flexible composite model propellers. Sixth International Symposium on Marine Propulsors Smp'19. Rome, Italy, May 2019.
Keijdener, C., Hendrikse, H., Metrikine, A., 2018. The effect of hydrodynamics on the bending failure of level ice. Cold Reg. Sci. Technol. 153, 106–119. https://doi.org/10.1016/j.coldregions.2018.04.019.
Keller, J.B., 1998. Gravity waves on ice-covered water. J. Geophys. Res.: Oceans 103 (C4), 7663–7669. https://doi.org/10.1029/97JC02966.
Kerwin, J., Lee, C.-S., 1978. Prediction of Steady and Unsteady Marine Propeller Performance by Numerical Lifting-Surface Theory, 86. Transactions of the Society of Naval Architects and Marine Engineers, pp. 218–253.
Keser, A., Verdult, M., Seyffert, H., Grammatikopoulos, A., 2023. The design, production, verification, and calibration of an elastic model of a catamaran for hydroelastic experiments. 13th Symposium on High-Speed Marine Vehicles (HSMV 2023), pp. 139–148. https://doi.org/10.3233/PMST230019.
Khabakhpasheva, T.I., Korobkin, A.A., 2002. Hydroelastic behaviour of compound floating plate in waves. J. Eng. Math. 44, 21–40.
Khabakhpasheva, T.I., Korobkin, A.A., 2013. Elastic wedge impact onto a liquid surface: Wagner's solution and approximate models. J. Fluid Struct. 36, 32–49.
Khabakhpasheva, T.I., Korobkin, A.A., Malenica, S., 2024. Water entry of an elastic conical shell. J. Fluid Mech. 980, A34. https://doi.org/10.1017/jfm.2024.17.
Khayyer, A., Gotoh, H., Falahaty, H., Shimizu, Y., 2018. An enhanced ISPH–SPH coupled method for simulation of incompressible fluid–elastic structure interactions. Comput. Phys. Commun. 232, 139–164. https://doi.org/10.1016/j.cpc.2018.06.016.
Kim, J.W., Bai, K.J., 1999. A finite element method for two-dimensional water-wave problems. Int. J. Numer. Methods Fluid. 30 (1), 105–122.
Kim, J.-H., Kim, Y., 2014. Numerical analysis on springing and whipping using fully-coupled FSI models. Ocean Eng. 91, 28–50.
Kim, Y., Kim, J.-H., 2016. Benchmark study on motions and loads of a 6750-TEU containership. Ocean Eng. 119, 262–273.
Kim, M.H., Koo, W.C., Hong, S.Y., 2000. Wave interactions with 2D structures on/inside porous seabed by a two-domain boundary element method. Appl. Ocean Res. 22 (5), 255–266.
Kim, J.W., Bai, K.J., Ertekin, R.C., Webster, W.C., 2003. A strongly-nonlinear model for water waves in water of variable depth—the irrotational Green-Naghdi model. J. Offshore Mech. Arctic Eng. 125 (1), 25–32.
Kim, Y., Kim, K.H., Kim, Y., 2009a. Analysis of hydroelasticity of floating ship-like structure in time domain using a fully coupled hybrid BEM-FEM. J. Ship Res. 53 (1), 31–47.
Kim, Y., Kim, K.H., Kim, Y., 2009b. Springing analysis of seagoing vessel using fully coupled BEM-FEM in the time domain. Ocean Eng. 36, 785–796.
Kim, Y., Kim, Y., Kang, B.C., Kim, K.H., 2010. Study on global ship hydroelasticity by using a fully coupled BEM-FEM in time domain. Proceedings of the 28th Symposium on Naval Hydrodynamics, Pasadena, USA.
Kim, K.-H., Bang, J.-S., Kim, J.-H., Kim, Y., Kim, S.-J., Kim, Y., 2013. Fully coupled BEM-FEM analysis for ship hydroelasticity in waves. Mar. Struct. 33, 71–99.
Kim, J.-H., Kim, Y., Korobkin, A., 2014. Comparison of fully coupled hydroelastic computation and segmented model test results for slamming and whipping loads. Int. J. Nav. Archit. Ocean Eng. 6 (4), 1064–1081.
Kim, J.H., Ahn, B.K., Ruy, W.S., Kim, G.D., Lee, C.S., 2019. Fluid-structure interaction analysis of flexible composite propellers. In: Okada, T., Suzuki, K., Kawamura, Y. (Eds.), Practical Design of Ships and Other Floating Structures. PRADS 2019, Lecture Notes in Civil Engineering, 63. Springer, Singapore.
Kim, S.J., Körgersaar, M., Ahmadi, N., Taimuri, G., Kujala, P., Hirdaris, S., 2021. The influence of fluid-structure interaction modelling on the dynamic response of ships subject to collision and grounding. Mar. Struct. 75, 102875. https://doi.org/10.1016/j.marstruc.2020.102875.
Kim, J.-H., Lee, H., Kim, S.-H., Choi, H.-Y., Hah, Z.-H., Seol, H.-S., 2022. Performance prediction of composite marine propeller in non-cavitating and cavitating flow. Appl. Sci. 12 (10), 5170. https://doi.org/10.3390/app12105170.
Kim, D., Tezdogan, T., Incecik, A., 2022a. A high-fidelity CFD-based model for the prediction of ship manoeuvrability in currents. Ocean Eng. 256, 111492. https://doi.org/10.1016/j.oceaneng.2022.111492.
Kirezci, C., Babanin, A.V., Chalikov, D.V., 2021. Modelling rogue waves in 1D wave trains with the JONSWAP spectrum, by means of the High Order Spectral Method and a fully nonlinear numerical model. Ocean Eng. 231, 108715. https://doi.org/10.1016/j.oceaneng.2021.108715.
Kiss-Nagy, K., Simongáti, G., Ficzére, P., 2024. Investigation of 3D printed underwater thruster propellers using CFD and structural simulations. Period. Polytech. - Mech. Eng. 68 (1), 70–77. https://doi.org/10.3311/PPme.23795.
Kobayashi, N., Raichle, A.W., Asano, T., 1993. Wave attenuation by vegetation. J. Waterw. Port, Coast. Ocean Eng. 119 (1), 30–48. https://doi.org/10.1061/ASCE.0733-950X.1993.119:1.30.
Koch, E.W., Barbier, E.B., Silliman, B.R., Reed, D.J., Perillo, G.M.E., Hacker, S.D., Granek, E.F., Primavera, J.H., Muthiga, N., Polasky, S., Halpern, B.S., Kennedy, C.J., Kappel, C.V., Wolanski, E., 2009. Non-linearity in ecosystem services: temporal and spatial variability in coastal protection. Front. Ecol. Environ. 7 (1), 29–37. https://doi.org/10.1890/080126.
Kohout, A.L., Meylan, M.H., 2009. Wave scattering by multiple floating elastic plates with spring or hinged boundary conditions. Mar. Struct. 22 (4), 712–729.
Kohout, A.L., Meylan, M.H., Plew, D.R., 2011. Wave attenuation in a marginal ice zone due to the bottom roughness of ice floes. Ann. Glaciol. 52 (57), 118–122. https://doi.org/10.3189/172756411795931510.
Kolekar, N., Banerjee, A., 2013. A coupled hydro-structural design optimization for hydrokinetic turbines. J. Renew. Sustain. Energy 5 (5), 053146.
Koley, S., Kaligatla, R.B., Sahoo, T., 2015. Oblique wave scattering by a vertical flexible porous plate. Stud. Appl. Math. 135 (1), 1–34.
Kondratenko, A.A., Kujala, P., Hirdaris, S.E., 2023. Holistic and sustainable design optimization of Arctic ships. Ocean Eng. 275, 114095.
Korkmaz, F.C., Güzel, B., 2017. Water entry of cylinders and spheres under hydrophobic effects; Case for advancing deadrise angles. Ocean Eng. 129, 240–252.
Korobkin, A.A., 2004. Analytical models of water impact. Eur. J. Appl. Math. 15, 821–838.
Korobkin, A.A., Khabakhpasheva, T., 2022. Three-dimensional hydroelastic impact onto a floating circular plate. In: Dessi, D., Iafrati, A. (Eds.), Proc. Of 9th Int. Conf. on Hydroetasticity in Marine Tech., pp. 79–88. Rome, Italy.
Korobkin, A., Gueret, R., Malenica, Š., 2006. Hydroelastic coupling of beam finite element model with Wagner theory of water impact. J. Fluid Struct. 22 (4), 493–504.
Korobkin, A.A., Khabakhpasheva, T.I., Shishmarev, K.A., 2023. Eigen modes and added-mass matrices of hydroelastic vibrations of complex structures. J. Fluid Mech. 970, A14.
Kostikov, V., Hayatdavoodi, M., Ertekin, R.C., 2021. Hydroelastic interaction of nonlinear waves with floating sheets. Theor. Comput. Fluid Dynam. 35 (4), 515–537.
Kostikov, V.K., Hayatdavoodi, M., Ertekin, R.C., 2022. Drift of elastic floating ice sheets by waves and current: multiple sheets. Phys. Fluids 34 (5), 057113. https://doi.org/10.1063/5.0091538.
Kostikov, V., Hayatdavoodi, M., Ertekin, R.C., 2024. Nonlinear waves propagating over a deformable seafloor. Phys. Fluids 36 (9). https://doi.org/10.1063/5.0227362.
Kristiansen, T., Faltinsen, O.M., 2012. Modelling of current loads on aquaculture net cages. J. Fluid Struct. 34, 218–235.
Kristiansen, T., Faltinsen, O.M., 2015. Experimental and numerical study of an aquaculture net cage with floater in waves and current. J. Fluid Struct. 54, 1–26.
Kumar, A., Lal Krishna, G., Anantha Subramanian, V., 2019. Design and analysis of a carbon composite propeller for podded propulsion. In: Proceedings of the Fourth International Conference in Ocean Engineering (ICOE2018), 1. Springer, Singapore, pp. 203–215. https://doi.org/10.1007/978-981-13-3119-0_13.
Kundu, S., Gayen, R., Datta, R., 2018. Scattering of water waves by an inclined elastic plate in deep water. Ocean Eng. 167, 221–228.

Kuznetsov, N.G., Maz'ia, V.G., Vainberg, B., 2002. Linear Water Waves: a Mathematical Approach. Cambridge University Press.
Kvalsvold, J., Faltinsen, O.M., 1993. Hydroelastic modelling of slamming against the wetdeck of a catamaran. In: Pro Second Int Conf Fast Sea Transportation, Fast', 93, pp. 681–697. Japan.
Kvalsvold, J., Faltinsen, O.M., 1994. Slamming Loads on Wetdecks of Multihull Vessels. Pro Second Int Conf Hydroelasticity in Marine Technology, Trondheim, Norway, pp. 205–220.
Kvalsvold, J., Faltinsen, O.M., 1995. Hydroelastic modelling of wetdeck slamming on multihull vessels. J. Ship Res. 39, 225–239.
Lafaurie, B., Nardone, C., Scardovelli, R., Zaleski, S., Zanetti, G., 1994. Modelling merging and fragmentation in multiphase flows with SURFER. J. Comput. Phys. 113 (1), 134–147. https://doi.org/10.1006/jcph.1994.1123.
Lakshmynarayanana, P.A.K., Hirdaris, S., 2020. Comparison of nonlinear one- and two-way FFSI methods for the prediction of the symmetric response of a containership in waves. Ocean Eng. 203, 107179. https://doi.org/10.1016/j.oceaneng.2020.107179.
Lakshmynarayanana, P.A., Temarel, P., 2019. Application of CFD and FEA coupling to predict dynamic behaviour of a flexible barge in regular head waves. Mar. Struct. 65, 308–325.
Lakshmynarayanana, P.A., Temarel, P., 2020. Application of a two-way partitioned method for predicting the wave-induced loads of a flexible containership. Appl. Ocean Res. 96, 102052. https://doi.org/10.1016/j.apor.2020.102052.
Lakshmynarayanana, P.A., Temarel, P., Chen, Z., 2015. Coupled fluid-structure interaction to model three-dimensional dynamic behaviour of ship in waves. Proceedings of the 7th International Conference on Hydroelasticity in Marine Technology, Split, Croatia, September 16–19, 2015.
Lamas-Pardo, M., Iglesias, G., Carral, L., 2015. A review of Very Large Floating Structures (VLFS) for coastal and offshore uses. Ocean Eng. 109, 677–690.
Lamb, H., 1932. Hydrodynamics. Cambridge University Press, Cambridge, UK.
Lavroff, J., Davis, M.R., Holloway, D.S., Thomas, G.A., 2013. Wave slamming loads on wave-piercer catamarans operating at high speed determined by hydro-elastic segmented model experiments. Mar. Struct. 33, 120–142. https://doi.org/10.1016/j.marstruc.2013.05.001.
Lawrie, J.B., Abrahams, I.D., 2007. A brief historical perspective of the Wiener–Hopf technique. J. Eng. Math. 59, 351–358.
Leclercq, T., de Langre, E., 2018. Reconfiguration of elastic blades in oscillatory flow. J. Fluid Mech. 838, 606–630.
Lee, H., 2015. Water wave generation with source function in the level set finite element framework. J. Mech. Sci. Technol. 29 (9), 3699–3706. https://doi.org/10.1007/s12206-015-0815-5.
Lee, C.H., Newman, J.N., 2006. WAMIT User Manual. WAMIT, Inc.
Lee, D., Maki, K., Wilson, R., Troesch, A.W., Vlahopoulos, N., 2009. Dynamic response of a marine vessel due to wave-induced slamming. Vibro-Impact Dynam. Ocean Syst. Relat. Probl. 161–172.
Lee, H., Song, M.-C., Suh, J.-C., Chang, B.-J., 2014. Hydro-elastic analysis of marine propellers based on a BEM-FEM coupled FSI algorithm. Int. J. Nav. Archit. Ocean Eng. 6 (3), 562–577.
Lee, H., Song, M.C., Han, S., et al., 2017. Hydro-elastic aspects of a composite marine propeller in accordance with ply lamination methods. J. Mar. Sci. Technol. 22, 479–493.
Lee, I.J., Kim, E.S., Kwon, S.H., 2020. A 3D direct coupling method for steady ship hydroelastic analysis. J. Fluid Struct. 94, 102891.
Lee, S.I., Boo, S.H., Kim, B.I., 2021. Application of fatigue damage evaluation considering linear hydroelastic effects of very large container ships using 1D and 3D structural models. Appl. Sci. 11 (7), 3001.
Lee, E.J., Diez, M., Harrison, E.L., Jiang, M., Snyder, L.A., Powers, A.M., Bay, R.J., Serani, A., Nadal, M.L., Kubina, E.R., Stern, F., 2024. Experimental and computational fluid-structure interaction analysis and optimization of Deep-V planing-hull grillage panels subject to slamming loads – Part II: irregular waves. Ocean Eng. https://doi.org/10.1016/j.oceaneng.2023.116346. Article 116346.
Lei, J., Fan, D., Angera, A., Liu, Y., Nepf, H., 2021. Drag force and reconfiguration of cultivated Saccharina latissima in current. Aquacult. Eng. 94, 102169.
Leroch, S., Varga, M., Eder, S.J., Vernes, A., Rodriguez Ripoll, M., Ganzenmüller, G., 2016. Smooth particle hydrodynamics simulation of damage induced by a spherical indenter scratching a viscoplastic material. Int. J. Solid Struct. 81, 188–202. https://doi.org/10.1016/j.ijsolstr.2015.11.025.
Leroyer, A., Wackers, J., Queutey, P., Guilmineau, E., 2011. Numerical strategies to speed up CFD computations with free surface—application to the dynamic equilibrium of hulls. Ocean Eng. 38 (17–18), 2070–2076.
Lewis, S.G., Hudson, D.A., Turnock, S.R., Taunton, D.J., 2010. Impact of a free-falling wedge with water: synchronized visualization, pressure and acceleration measurements. Fluid Dyn. Res. 42 (3), 035509.
Ley, J., el Moctar, O., 2014. An enhanced 1-way coupling method to predict elastic global hull girder loads. Proceed. ASME 2014 33rd Int. Conf. Ocean, Offshore Arctic Eng. (OMAE) 10. V04BT02A023.
Ley, J., Oberhagemann, J., Amian, C., Langer, M., Shigunov, V., Rathje, H., Schellin, T.E., 2013. Green water loads on a cruise ship. Proceedings of the ASME 2013 32nd International Conference on Ocean, Offshore and Arctic Engineering (OMAE), p. 10. V007T08A005.
Li, L., 2022. Full-coupled analysis of offshore floating wind turbine supported by very large floating structure with consideration of hydroelasticity. Renew. Energy 189, 790–799. https://doi.org/10.1016/j.renene.2022.03.063.
Li, C.W., Xie, J.F., 2011. Numerical modeling of free surface flow over submerged and highly flexible vegetation. Adv. Water Resour. 34 (4), 468–477.
Li, L., Fu, S., Xu, Y., Wang, J., Yang, J., 2013. Dynamic responses of floating fish cage in waves and current. Ocean Eng. 72, 297–303.
Li, J., Rao, Z., Su, J., Qu, Y., Hua, H., 2018. A numerical method for predicting the hydroelastic response of marine propellers. Appl. Ocean Res. 74, 188–204.
Li, Y., Ong, M.C., Tang, T., 2020a. A numerical toolbox for wave-induced seabed response analysis around marine structures in the openfoam® framework. Ocean Eng. 195, 106678.
Li, H., Gedikli, E.D., Lubbad, R., Nord, T.S., 2020b. Laboratory study of wave-induced ice-ice collisions using robust principal component analysis and sensor fusion. Cold Reg. Sci. Technol. 172, 103010. https://doi.org/10.1016/j.coldregions.2020.103010.
Li, J., Qu, Y., Zhang, Z., et al., 2020c. Parametric analysis on hydroelastic behaviors of hydrofoils and propellers using a strongly coupled finite element/panel method. J. Mar. Sci. Technol. 25, 148–161.
Li, J., Qu, Y., Chen, Y., Hua, H., 2021. Numerical analysis on dynamic behaviors of coupled propeller-shafting system of underwater vehicles. Appl. Ocean Res. 110, 102613.
Li, P., Xie, H., Liu, F., Liu, X., Li, H., 2022a. Experimental study on the water entry of a 3D bow-flared model with various inclination angles. Ocean Eng. 259, 111834. https://doi.org/10.1016/j.oceaneng.2022.111834.
Li, J., Qu, Y., Chen, Y., Hua, H., Wu, J., 2022b. BEM-FEM coupling for the hydroelastic analysis of propeller-shafting systems in non-uniform flows. Ocean Eng. 247, 110424.
Li, J., Qu, Y., Zhang, Z., Xie, D., Hua, H., Wu, J., 2023. Fluid-structure interaction analysis of the propeller-shafting system in a non-uniform wake. Ocean Eng. 289 (Part 1), 116189.
Li, M., Hong, Y., Si, B., Ding, Y., Tang, Z., Wang, R., He, X., 2024. Numerical and experimental study of the cavitation performance of a composite propeller. Phys. Fluids 36 (10), 103303. https://doi.org/10.1063/5.0228410.
Liao, K., Hu, C., Duan, W., 2013. Two-dimensional numerical simulation of an elastic wedge water entry by a coupled FDM-FEM method. J. Mar. Sci. Appl. 2 (2), 163–169.
Liao, X.Y., Xia, J.S., Chen, Z.Y., Tang, Q., Zhao, N., Zhao, W.D., Gui, H.B., 2024. Application of CFD and FEA coupling to predict structural dynamic responses of a trimaran in uni- and bi-directional waves. China Ocean Eng. 38 (1), 81–92.
Lighthill, M.J., 1971. Large-amplitude elongated-body theory of fish locomotion. Proc. Roy. Soc. Lond. B Biol. Sci. 179, 125–138.
Lin, H., Lin, J., 1996. Nonlinear hydroelastic behavior of propellers using a finite element method and lifting surface theory. J. Mar. Sci. Technol. 1 (2), 114–124.
Lin, Q., Lu, D.Q., 2013. Hydroelastic interaction between obliquely incident waves and a semi-infinite elastic plate on a two-layer fluid. Appl. Ocean Res. 43, 71–79.
Lin, C.C., Lee, Y.J., Hung, C.-S., 2009. Optimization and experiment of composite marine propellers. Compos. Struct. 89 (2), 206–215.
Lin, J., Naceur, H., Laksimi, A., Coutellier, D., 2014. On the implementation of a nonlinear shell-based SPH method for thin multilayered structures. Compos. Struct. 108, 905–914. https://doi.org/10.1016/j.compstruct.2013.10.008.
Linton, C.M., McIver, P., 2001. Handbook of Mathematical Techniques for Wave/structure Interactions. Chapman and Hall/CRC Press, Boca Raton, Florida.
Linton, C.M., McIver, M., 2002. The existence of Rayleigh–Bloch surface waves. J. Fluid Mech. 470, 85–90.
Liu, P.L.F., Chan, I.C., 2007. On long-wave propagation over a fluid-mud seabed. J. Fluid Mech. 579, 467–480.
Liu, P.L.F., Chan, I.C., 2007a. A note on the effects of a thin visco-elastic mud layer on small amplitude water-wave propagation. Coast. Eng. 54 (3), 233–247.
Liu, D., Lin, P., 2008. A numerical study of three-dimensional liquid sloshing in tanks. J. Comput. Phys. 227 (8), 3921–3939. https://doi.org/10.1016/j.jcp.2007.12.009.
Liu, X., Sakai, S., 2002. Time domain analysis on the dynamic response of a flexible floating structure to waves. J. Eng. Mech. 128 (1), 48–56.
Liu, Y., Yue, D.K., 1998. On generalized Bragg scattering of surface waves by bottom ripples. J. Fluid Mech. 356, 297–326.
Liu, W., Song, X., Pei, Z., Li, Y., 2017. Experiment study of hydroelasto-buckling ship model in a single wave. Ocean Eng. 142, 102–114. https://doi.org/10.1016/j.oceaneng.2017.06.044.
Liu, S., Gatin, I., Obhrai, C., Ong, M.C., Jasak, H., 2019. CFD simulations of violent breaking wave impacts on a vertical wall using a two-phase compressible solver. Coastal Engineering 154, 103564. https://doi.org/10.1016/j.coastaleng.2019.103564.
Liu, Q., Rogers, W.E., Babanin, A., Li, J., Guan, C., 2020. Spectral modeling of ice-induced wave decay. Journal of Physical Oceanography 50 (6), 1583–1604.
Liu, W., Luo, W., Yang, M., Xia, T., Huang, Y., Wang, S., Leng, J., Li, Y., 2022a. Development of a fully coupled numerical hydroelasto-plastic approach for offshore structure. Ocean Engineering 258, 111713.
Liu, X., Liu, F., Ren, H., Chen, X., Xie, H., 2022b. Experimental investigation on the slamming loads of a truncated 3D stern model entering into water. Ocean Engineering 252, 110873.
Liu, X., Lu, Y., Yu, H., Ma, L., Li, X., Li, W., et al., 2022c. In-situ observation of storm-induced wave-supported fluid mud occurrence in the subaqueous yellow river delta. Journal of Geophysical Research: Oceans 127 (7), e2021JC018190.
Liu, W., Luo, W., Yang, M., Xia, T., Huang, Y., Wang, S., Leng, J., Li, Y., 2022d. Development of a fully coupled numerical hydroelasto-plastic approach for offshore structure. Ocean Engineering 258, 111713. https://doi.org/10.1016/j.oceaneng.2022.111713.
Logvinovich, G.V., 1973. Hydrodynamics of Flows with Free Boundaries. Naukova Dumka, Kyiv, Ukraine.
Loukogeorgaki, E., Michailides, C., Angelides, D.C., 2012. Hydroelastic analysis of a flexible mat-shaped floating breakwater under oblique wave action. J. Fluids Struct. 31, 103–124.
Lu, C.H., He, Y.S., Wu, G.X., 2000. Coupled analysis of nonlinear interaction between fluid and structure during impact. Journal of fluids and structures 14 (1), 127–146.

Lu, L., Ren, H., Li, H., Zou, J., Chen, S., Liu, R., 2023. Numerical method for whipping response of ultra large container ships under asymmetric slamming in regular waves. Ocean Engineering 287 (Part 2), 115830. https://doi.org/10.1016/j.oceaneng.2023.115830.
Lu, Y., Liu, W., Zou, Q., Zhang, Y., Qu, H., Song, X., 2024. Hydroelasto-plastic experiment and numerical investigation on a three-cabin ship model in waves. Applied Ocean Research 145, 103901. https://doi.org/10.1016/j.apor.2024.103901.
Luhar, M., Nepf, H.M., 2011. Flow-induced reconfiguration of buoyant and flexible aquatic vegetation. Limnology and Oceanography 56 (6), 2003–2017. https://doi.org/10.4319/lo.2011.56.6.2003.
Luhar, M., Nepf, H., 2016. Wave-induced dynamics of flexible blades. Journal of Fluids and Structures 61, 20–41.
Luke, J.C., 1967. A variational principle for a fluid with a free surface. Journal of Fluid Mechanics 27 (2), 395–397.
Luo, C., Huang, L., 2024. Energy efficiency analysis of a deformable wave energy converter using fully coupled dynamic simulations. Oceans 5 (2), 227–243.
Luo, H., Wang, H., Guedes Soares, C., 2012. Numerical and experimental study of hydrodynamic impact and elastic response of one free-drop wedge with stiffened panels. Ocean Engineering 40, 1–14.
Luo, P., Zhang, J., Cao, Y., Song, S., 2024. Simulation of wave scattering over a floating platform in the ocean with a coupled CFD-IBM model. Theoretical and Applied Mechanics Letters 14 (3), 100516. https://doi.org/10.1016/j.taml.2024.100516.
Lv, J., Grenestedt, J.L., 2013. Some analytical results for the initial phase of bottom slamming. Marine structures 34, 88–104.
Lv, J., Grenestedt, J.L., 2015. Analytical study of the responses of bottom panels to slamming loads. Ocean Engineering 94, 116–125.
Ma, S., Mahfuz, H., 2012. Finite element simulation of composite ship structures with fluid structure interaction. Ocean Engineering 52, 52–59. https://doi.org/10.1016/j.oceaneng.2012.06.009.
Ma, Z.H., Causon, D.M., Qian, L., Mingham, C.G., Mai, T., Greaves, D., Raby, A., 2016. Pure and aerated water entry of a flat plate. Physics of Fluids 28 (1), 016104. https://doi.org/10.1063/1.4939767.
Ma, B., Chang, X., Chen, Z., Jiao, J., 2024. Hydroelasticity of a 21000TEU containership under freak waves by fluid-flexible structure interaction simulations. Ocean Engineering 314, 119748. https://doi.org/10.1016/j.oceaneng.2024.119748.
Maa, J.P.Y., Mehta, A.J., 1990. Soft mud response to water waves. Journal of Waterway, Port, Coastal, and Ocean Engineering 116 (5), 634–650.
Macpherson, H., 1980. The attenuation of water waves over a non-rigid bed. Journal of Fluid Mechanics 97 (4), 721–742.
Mai, T., Mai, C., Raby, A., Greaves, D.M., 2020. Hydroelasticity effects on water-structure impacts. Experiments in Fluids 61, 1–19.
Maki, K.J., Lee, D., Troesch, A.W., Vlahopoulos, N., 2011. Hydroelastic impact of a wedge-shaped body. Ocean Engineering 38 (4), 621–629.
Malenica, Š., Molin, B., Remy, F., Senjanović, I., 2003. Hydroelastic response of a barge to impulsive and non-impulsive wave load. In: Hydroelasticity in Marine Technology, pp. 107–115. Oxford, UK.
Malenica, S., Stumpf, E., Sireta, F.-X., Chen, X.-B., 2008. Consistent hydro-structure interface for evaluation of global structural responses in linear seakeeping. Proceedings of the ASME 2008 27th International Conference on Offshore Mechanics and Arctic Engineering (OMAE2008-57077), pp. 61–68. Estoril, Portugal, June 15–20, 2008.
Maljaars, P.J., Dekker, J.A., 2014. Hydro-elastic analysis of flexible marine propellers. 2nd International Conference on Maritime Technology and Engineering (MARTECH). Taylor & Francis (CRC Press), Lisbon, Portugal, pp. 705–715. https://doi.org/10.1201/b17494-94.
Maljaars, P.J., Kaminski, M.L., Den Besten, J.H., 2017. Finite element modelling and model updating of small scale composite propellers. Composite structures 176, 154–163. https://doi.org/10.1016/j.compstruct.2017.04.023.
Maljaars, P., Bronswijk, L., Windt, J., Grasso, N., Kaminski, M., 2018. Experimental validation of fluid–structure interaction computations of flexible composite propellers in open water conditions using BEM-FEM and RANS-FEM methods. Journal of Marine Science and Engineering 6 (2), 51. https://doi.org/10.3390/jmse6020051.
Maljaars, P.J., Grasso, N., Den Besten, J.H., Kaminski, M.L., 2020. BEM–FEM coupling for the analysis of flexible propellers in non-uniform flows and validation with full-scale measurements. Journal of Fluids and Structures 95, 102946.
Mallard, W.W., Dalrymple, R.A., 1977. Water Waves Propagating over a Deformable Bottom. Offshore Technology Conference.
Mandal, B.N., Chakrabarti, A., 2000. Water Wave Scattering by Barriers. WIT Press, Southampton.
Mao, Y., Young, Y.L., 2016. Influence of skew on the added mass and damping characteristics of marine propellers. Ocean Engineering 121, 437–452.
Marchenko, A., Haase, A., Jensen, A., Lishman, B., Rabault, J., Evers, K.-U., Shortt, M., Thiel, T., 2021. Laboratory investigations of the bending rheology of floating saline ice and physical mechanisms of wave damping in the HSVA Hamburg Ship Model Basin Ice Tank. Water 13 (8), 1080. https://doi.org/10.3390/w13081080.
Marino, M., Nasca, S., Alkharoubi, A.I.K., Cavallaro, L., Foti, E., Musumeci, R.E., 2025. Efficacy of Nature-based Solutions for coastal protection under a changing climate: a modelling approach. Coastal Engineering 198, 104700. https://doi.org/10.1016/j.coastaleng.2025.104700.
Marjoribanks, T.I., Hardy, R.J., 2014. High-resolution numerical modelling of flow–vegetation interactions. Journal of Hydraulic Research 52 (6), 775–793. https://doi.org/10.1080/00221686.2014.948502.
Markov, A., Stolle, J., Henteleff, R., Nistor, I., Van, D.P., Murphy, E., Cornett, A., 2023. Deformation of Spartina patens and Spartina alterniflora stems under irregular wave action. Coastal Engineering Journal 00 (00), 1–22. https://doi.org/10.1080/21664250.2023.2195030.
Maron, A., Kapsenberg, G., 2014. Design of a ship model for hydroelastic experiments in waves. Journal of Naval Architecture and Ocean Engineering 6 (4), 1130–1147. https://doi.org/10.2478/IJNAOE-2013-235.
Martin, S., Kauffman, P., 1981. A field and laboratory study of wave damping by grease ice. Journal of Glaciology 27 (96), 283–313.
Masoomi, M., Mosavi, A., 2021. The one-way FSI method based on RANS-FEM for the open water test of a marine propeller at the different loading conditions. Journal of Marine Science and Engineering 9 (4), 351. https://doi.org/10.3390/jmse9040351.
Mathew, J., Mytheenkhan, B., Kurian, N.P., 1995. Mudbanks of the southwest coast of India. I: wave characteristics. Journal of Coastal Research 11 (1), 168–178.
Mattis, S.A., Dawson, C.N., Kees, C.E., Farthing, M.W., 2015. An immersed structure approach for fluid-vegetation interaction. Advances in Water Resources 80, 1–16.
Mattis, S.A., Kees, C.E., Wei, M.V., Dimakopoulos, A., Dawson, C.N., 2018. Computational model for wave attenuation by flexible vegetation. Journal of Waterway, Port, Coastal, and Ocean Engineering 145 (1). https://doi.org/10.1061/(ASCE)WW.1943-5460.0000487.
Maza, M., Lara, J.L., Losada, I.J., 2013. A coupled model of submerged vegetation under oscillatory flow using Navier–Stokes equations. Coastal Engineering 80, 16–34. https://doi.org/10.1016/j.coastaleng.2013.04.009.
McVicar, J., Lavroff, J., Davis, M.R., Thomas, G., 2018. Fluid–structure interaction simulation of slam-induced bending in large high-speed wave-piercing catamarans. Journal of Fluids and Structures 82, 35–58.
Mehta, A.J., 1989. On estuarine cohesive sediment suspension behavior. Journal of Geophysical Research: Oceans 94 (C10), 14303–14314. https://doi.org/10.1029/JC094iC10p14303.
Mei, C.C., Liu, K.-F., 1987. A Bingham-plastic model for a muddy seabed under long waves. Journal of Geophysical Research: Oceans 92 (C13), 14581–14594.
Mei, C.C., Tuck, E.O., 1980. Forward scattering by long thin bodies. SIAM Journal on Applied Mathematics 39 (1), 178–191.
Mei, C.C., Stiassnie, M., Yue, D.K.P., 2005. Theory and applications of ocean surface waves. Advanced Series on Ocean Engineering 1136. World Scientific.
Mei, C.C., Krotov, M., Huang, Z., Huhe, A., 2010. Short and long waves over a muddy seabed. Journal of Fluid Mechanics 643, 33–58.
Meirelles, S., Vinzon, S.B., 2016. Field observation of wave damping by fluid mud. Marine Geology 376, 194–201. https://doi.org/10.1016/j.margeo.2016.
Mesa, J.D., Maki, K.J., Graham, M.T., 2022. Numerical analysis of the impact of an inclined plate with water at high horizontal velocity. Journal of Fluids and Structures 114, 103684. https://doi.org/10.1016/j.jfluidstructs.2022.103684.
Meyerhoff, W.K., 1965a. Die Berechnung hydroelastischer Stöße. Schiffstechnik 12 (60), 18–30.
Meyerhoff, W.K., 1965b. Die Berechnung hydroelastischer Stöße. Schiffstechnik 12 (61), 49–64.
Meylan, M., 1993. The Behaviour of Sea Ice in Ocean Waves. University of Otago. Ph.D. thesis).
Meylan, M.H., 1995. A flexible vertical sheet in waves. Int. J. Offshore Polar Eng. 5 (2), 105–110.
Meylan, M.H., 2021. Time-dependent motion of a floating circular elastic plate. Fluids 6 (1), 29.
Meylan, M.H., Squire, V.A., 1995. The response of a thick flexible raft to ocean waves. International Journal of Offshore and Polar Engineering 5 (3), 198–203.
Meylan, M.H., Squire, V.A., 1996. Response of a circular ice floe to ocean waves. J. Geophys. Res. 101, 8869–8884.
Meylan, M.H., Bennetts, L.G., Cavaliere, C., Alberello, A., Toffoli, A., 2015a. Experimental and theoretical models of wave-induced flexure of a sea ice floe. Physics of Fluids 27 (4), 041704. https://doi.org/10.1063/1.4919107.
Meylan, M.H., Yiew, L.J., Bennetts, L.G., French, B.J., Thomas, G.A., 2015b. Surge motion of an ice floe in waves: comparison of a theoretical and an experimental model. Annals of Glaciology 56 (69), 155–159. https://doi.org/10.3189/2015AoG69A646.
Meziane, B., Alaoui, A.E.M., Nême, A., Leble, B., Bellanger, D., 2022. Experimental investigation of the influence of the panel stiffness on the behaviour of a wedge under slamming. Journal of Fluids and Structures 114, 103702.
Michele, S., Renzi, E., 2019. A second-order theory for an array of curved wave energy converters in open sea. J. Fluids Struct 88, 315–330.
Michele, S., Sammarco, P., d'Errico, M., 2018. Weakly nonlinear theory for oscillating wave surge converters in a channel. J. Fluid Mech. 834, 55–91.
Michele, S., Buriani, F., Renzi, E., van Rooij, M., Jayawardhana, B., Vakis, A., 2020. Wave energy extraction by flexible floaters. Energies 13, 6167.
Michele, S., Zheng, S., Greaves, D.M., 2022. Wave energy extraction from a floating flexible circular plate. Ocean Eng 245, 110275.
Michele, S., Zheng, S., Renzi, E., Borthwick, A.G.L., Greaves, D.M., 2024. Hydroelastic theory for offshore floating plates of variable flexural rigidity. Journal of Fluids and Structures 125, 104060.
Miles, J.W., 1977. On Hamilton's principle for surface waves. Journal of Fluid Mechanics 83 (1), 153–158.
Mindlin, R.D., 1951. Influence of rotary inertia and shear on flexural motions of isotropic, elastic plates. Journal of Applied Mechanics 18 (1), 31–38.
Mittal, R., Iaccarino, G., 2005. Immersed boundary methods. Annual Review of Fluid Mechanics 37 (1), 239–261. https://doi.org/10.1146/annurev.fluid.37.061903.175743.
Mizokami, S., Yasukawa, H., Kuroiwa, T., et al., 2001. Wave loads on a container ship in rough seas. Journal of the Society of Naval Architects of Japan 189, 181–192 (in Japanese).

Moe, H., Fredheim, A., Hopperstad, O.S., 2010. Structural analysis of aquaculture net cages in current. Journal of Fluids and Structures 26 (3), 503–516. https://doi.org/10.1016/j.jfluidstructs.2010.01.007.
Mohapatra, S.C., Sahoo, T., 2011. Surface gravity wave interaction with elastic bottom. Applied Ocean Research 33 (1), 31–40.
Montiel, F.F., 2012. Numerical and Experimental Analysis of Water Wave Scattering by Floating Elastic Plates. University of Otago. Doctoral dissertation.
Montiel, F., Bonnefoy, F., Ferrant, P., Bennetts, L.G., Squire, V.A., Marsault, P., 2013a. Hydroelastic response of floating elastic discs to regular waves. Part 1. Wave basin experiments. Journal of Fluid Mechanics 723, 604–628.
Montiel, F., Bennetts, L.G., Squire, V.A., Bonnefoy, F., Ferrant, P., 2013b. Hydroelastic response of floating elastic discs to regular waves. Part 2. Modal analysis. Journal of Fluid Mechanics 723, 629–652. https://doi.org/10.1017/jfm.2013.124.
Morabito, M.G., 2015. Prediction of planing hull side forces in yaw using slender body oblique impact theory. Ocean Engineering 101, 47–57. https://doi.org/10.1016/j.oceaneng.2015.04.017.
Mosig, J.E., Montiel, F., Squire, V.A., 2015. Comparison of viscoelastic-type models for ocean wave attenuation in ice-covered seas. Journal of Geophysical Research: Oceans 120 (9).
Motley, M., Young, Y.L., 2012. Scaling of the transient hydroelastic response and failure mechanisms of self-adaptive composite marine propellers. International Journal of Rotating Machinery 2012. https://doi.org/10.1155/2012/632856.
Motley, M.R., Liu, Z., Young, Y.L., 2009. Utilizing fluid–structure interactions to improve energy efficiency of composite marine propellers in spatially varying wake. Composite Structures 90 (3), 304–313.
Mulcahy, N.L., Prusty, B.G., Gardiner, C.P., 2010. Hydroelastic tailoring of flexible composite propellers. Ships and Offshore Structures 5 (4), 359–370.
Muzaferija, S., 1998. Computation of free surface flows using interface-tracking and interface-capturing methods. Nonlinear water-wave interaction. Computational Mechanics. Southampton.
Nandi, K., Sarkar, B., Hossain, S., De, S., 2024. Wave interaction with multiple thin flexible porous barriers in water of uniform finite depth. Ocean Engineering 309 (Part 2), 118475. https://doi.org/10.1016/j.oceaneng.2024.118475.
Nelli, F., Bennetts, L.G., Skene, D.M., Monty, J.P., Lee, J.H., Meylan, M.H., Toffoli, A., 2017. Reflection and transmission of regular water waves by a thin, floating plate. Wave Motion 70, 209–221. https://doi.org/10.1016/j.wavemoti.2016.09.003.
Newman, J.N., 1964. A slender-body theory for ship oscillations in waves. Journal of Fluid Mechanics 18 (4), 409–417. https://doi.org/10.1017/S0022112064000305.
Newman, J.N., 1977. Marine Hydrodynamics. MIT Press.
Newman, J.N., 1994. Wave effects on deformable bodies. Appl. Ocean Res. 16, 47–59.
Newyear, K., Martin, S., 1997. A comparison of theory and laboratory measurements of wave propagation and attenuation in grease ice. Journal of Geophysical Research: Oceans 102 (C11), 25091–25099.
Ng, C.-O., 2000. Water waves over a muddy bed: a two-layer Stokes' boundary layer model. Coastal Engineering 40 (3), 221–242.
Ng, C.-O., Mei, C.C., 1994. Roll waves on a shallow layer of mud modelled as a power-law fluid. Journal of Fluid Mechanics 263, 151–184.
Ni, X., Cheng, X., Lu, Y., Wu, B., Wang, Q., Zhang, K., Yu, J., 2020. Evaluation of hydroelastic responses of a 180k DWT large bulk carrier. Ocean Engineering 199, 106948.
Niazmand Bilandi, R., Dashtimanesh, A., Tavakoli, S., 2020. Hydrodynamic study of heeled double-stepped planing hulls using CFD and 2D+T method. Ocean Engineering 196, 106813. https://doi.org/10.1016/j.oceaneng.2019.106813.
Niazmand Bilandi, R., Tavakoli, S., Dashtimanesh, A., 2021. Seakeeping of double-stepped planing hulls. Ocean Engineering 236, 109475. https://doi.org/10.1016/j.oceaneng.2021.109475.
Niedzwecki, J.M., Huston, J.R., 1992. Wave interaction with tension leg platforms. Ocean Engineering 19 (1), 21–37.
Niu, X., Yu, X., 2010. A numerical model for wave propagation over muddy slope. Journal of Hydraulic Research 48 (Suppl. 1), 20–26.
Niu, X., Yu, X., 2014. Numerical study on wave propagation over a fluid-mud layer with different bottom conditions. Coastal Engineering 91, 164–177.
Noble, B., 1959. Methods Based on the Wiener–Hopf Technique for the Solution of Partial Differential Equations. Pergamon Press, New York, NY.
Oberhagemann, J., Holtmann, M., Ould, el Moctar, Schellin, T.E., Kim, D., 2009. Stern slamming of a LNG carrier. Journal of Offshore Mechanics and Arctic Engineering 131 (3), 031103.
Oberhagemann, J., Ould, el Moctar, Holtmann, M., Schellin, T., Bertram, V., Kim, D.W., 2010. Hydro-elastic simulation of stern slamming and whipping. The International Journal of Ocean and Climate Systems 1 (3–4), 179–188.
Oberhagemann, J., Shigunov, V., Radon, M., Mumm, H., Won, S.-I., 2015. Hydrodynamic load analysis and ultimate strength check of an 18000 TEU containership. Journal of Offshore Mechanics and Arctic Engineering 137 (4), 041701. https://doi.org/10.1115/1.4031312.
Ochi, M.K., Motter, L.E., 1973. Prediction of Slamming Characteristics and Hull Response for Ship Design, 81. Transactions of the Society of Naval Architects and Marine Engineers.
Olsson, E., Kreiss, G., 2005. A conservative level set method for two phase flow. Journal of computational physics 210 (1), 225–246.
Onorato, M., Residori, S., Bortolozzo, U., Montina, A., Arecchi, F.T., 2013. Rogue waves and their generating mechanisms in different physical contexts. Physics Reports 528 (2), 47–89. https://doi.org/10.1016/j.physrep.2013.03.001.
Osher, S., Sethian, J.A., 1988. Fronts propagating with curvature-dependent speed: algorithms based on Hamilton-Jacobi formulations. Journal of computational physics 79 (1), 12–49.
O'Connor, J., Revell, A., 2019. Dynamic interactions of multiple wall-mounted flexible flaps. Journal of Fluid Mechanics 870, 189–216. https://doi.org/10.1017/jfm.2019.266.
Paik, K.-J., Carrica, P.M., Lee, D., Maki, K., 2009. Strongly coupled fluid–structure interaction method for structural loads on surface ships. Ocean Engineering 36 (17–18), 1346–1357.
Paik, B., Kim, G., Kim, K., Seol, H., Hyan, B., Lee, S., Jung, Y., 2013. Investigation on the performance characteristics of the flexible propellers. Ocean Eng 73, 139–148.
Pal, S.K., Datta, R., Sunny, M.R., 2018. Fully coupled time domain solution for hydroelastic analysis of a floating body. Ocean Engineering 153, 173–184.
Pal, S.K., Ono, T., Takami, T., Tatsumi, A., Iijima, K., 2022. Effect of springing and whipping on exceedance probability of vertical bending moment of a ship. Ocean Engineering 266, 112600. https://doi.org/10.1016/j.oceaneng.2022.112600.
Pan, J., Zhang, W.Z., Sun, Z.M., Qu, X., Xu, M.C., 2024. Experimental study on the dynamical response of elastic trimaran model under slamming load. Journal of Marine Science and Technology 29 (1), 20–35.
Panciroli, R., Porfiri, M., 2014. Hydroelastic impact of piezoelectric structures. International Journal of Impact Engineering 66, 18–27.
Panciroli, R., Porfiri, M., 2015. Analysis of hydroelastic slamming through particle image velocimetry. J. Sound Vib. 347, 63–78.
Panciroli, R., Abrate, S., Minak, G., Zucchelli, A., 2012. Hydroelasticity in water-entry problems: comparison between experimental and SPH results. Composite Structures 94 (2), 532–539.
Panciroli, R., Shams, A., Porfiri, M.J.O.E., 2015. Experiments on the water entry of curved wedges: high speed imaging and particle image velocimetry. Ocean Engineering 94, 213–222.
Papanikolaou, A., 2010. Holistic ship design optimization. Computer-Aided Design 42 (11), 1028–1044. https://doi.org/10.1016/j.cad.2009.07.002.
Paprota, M., 2023. A Fourier Galerkin method for ship waves. Ocean Engineering 271, 113796.
Părău, E., Dias, F., 2002. Nonlinear effects in the response of a floating ice plate to a moving load. Journal of Fluid Mechanics 460, 281–305. https://doi.org/10.1017/S0022112002008236.
Park, J.H., Temarel, P., 2007. The influence of nonlinearities on wave-induced motions and loads predicted by two-dimensional hydroelasticity analysis. In: Proceedings of the 10th International Symposium on PRADS, 1, pp. 27–34. Houston, Texas.
Park, D.-M., Kim, J.-H., Kim, Y., 2017. Numerical study of mean drift force on stationary flexible barge. Journal of Fluids and Structures 74, 445–468.
Park, D.-M., Kim, J.-H., Kim, Y., 2019. Numerical study of added resistance of flexible ship. Journal of Fluids and Structures 85, 199–219.
Park, S., Wang, Z., Stern, F., Husser, N., Brizzolara, S., Morabito, M., Lee, E., 2022. Single- and two-phase CFD V&V for high-speed stepped planing hulls. Ocean Engineering 261, 112047. https://doi.org/10.1016/j.oceaneng.2022.112047.
Parker, W.R., Kirby, R., 1982. Time dependent properties of cohesive sediment relevant to sedimentation management—European experience. In: Kennedy, V.S. (Ed.), Estuarine Comparisons. Academic Press, pp. 573–589.
Parra, S.M., Sree, D.K.K., Wang, D., Rogers, E., Lee, J.H., Collins III, C.O., Law, A.W.-K., Babanin, A.V., 2020. Experimental study on surface wave modifications by different ice covers. Cold Regions Science and Technology 174, 103042. https://doi.org/10.1016/j.coldregions.2020.103042.
Parunov, J., Badalotti, T., Feng, Q., Gu, X., Iijima, K., Ma, N., Qiu, W., Wang, S., Wang, X., Yang, P., Yoshida, Y., Zhang, Z., Guedes Soares, C., 2024. Benchmark on the prediction of whipping response of a warship model in regular waves. Marine Structures 94, 103549.
Passerotti, G., Bennetts, L.G., von Bock und Polach, F., Alberello, A., Puolakka, O., Dolatshah, A., Monbaliu, J., Toffoli, A., 2022. Interactions between irregular wave fields and sea ice: a physical model for wave attenuation and ice breakup in an ice tank. Journal of Physical Oceanography 52 (7), 1431–1446.
Peddamallu, P., Rajendran, S., Saripilli, J., Zhou, X., 2024. Coupling a time-domain code with a RANS solver for slamming analysis. Ships and Offshore Structures 1–14. Published online.
Pedersen, P.T., 1985. Nonlinear structural response. Report of Committee II.2. 9th International Ship Structures Congress, Santa Margherita.
Pena, B., Huang, L., 2021. A review on the turbulence modelling strategy for ship hydrodynamic simulations. Ocean Engineering 241, 110082. https://doi.org/10.1016/j.oceaneng.2021.110082.
Peseux, B., Gornet, L., Donguy, B., 2005. Hydrodynamic impact: numerical and experimental investigations. J. Fluid Struct. 21, 277–303.
Peskin, C.S., 2002. The immersed boundary method. Acta Numerica 11, 479–517. https://doi.org/10.1017/S0962492902000077.
Piedra Cueva, I., 1993. On the response of a muddy bottom to surface water waves. Journal of Hydraulic Research 31 (5), 681–696.
Piro, D.J., Maki, K.J., 2013. Hydroelastic analysis of bodies that enter and exit water. Journal of Fluids and Structures 37, 134–150.
Polly, G., Mérigaud, A., Thiria, B., Godoy-Diana, R., 2025. Experiments on water-wave interactions with a horizontal submerged elastic plate. Journal of Fluid Mechanics 1007, R4. https://doi.org/10.1017/jfm.2025.90.
Porter, R., Evans, D.V., 2007. Diffraction of flexural waves by finite straight cracks in an elastic sheet over water. Journal of fluids and structures 23 (2), 309–327.
Porter, D., Porter, R., 2004. Approximations to wave scattering by an ice sheet of variable thickness over undulating bed topography. Journal of Fluid Mechanics 509, 145–179.
Posa, A., Broglia, R., Felli, M., Cianferra, M., Armenio, V., 2022. Hydroacoustic analysis of a marine propeller using large-eddy simulation and acoustic analogy. Journal of Fluid Mechanics 947, A46. https://doi.org/10.1017/jfm.2022.692.

Prüter, I., Spröer, F., Keimer, K., Lojek, O., Windt, C., Schürenkamp, D., Bihs, H., Nistor, I., Goseberg, N., 2025. A comprehensive numerical study on the current-induced fluid–structure interaction of flexible submerged vegetation. Journal of Fluids and Structures 133, 104232. https://doi.org/10.1016/j.jfluidstructs.2024.104232.

Pu, J., Lu, D.Q., 2023. Suppression of the hydroelastic responses of a composite very large floating structure by a submerged elastic ring. Applied Ocean Research 141, 103780.

Quartel, S., Kroon, A., Augustinus, P.G.E.F., van Santen, P., Tri, N.H., 2007. Wave attenuation in coastal mangroves in the red river delta, Vietnam. Journal of Asian Earth Sciences 29 (4), 576–584. https://doi.org/10.1016/j.jseaes.2006.05.008.

Rabault, J., Sutherland, G., Jensen, A., Christensen, K.H., Marchenko, A., 2019. Experiments on wave propagation in grease ice: combined wave gauges and PIV measurements. Journal of Fluid Mechanics 864, 876–898. https://doi.org/10.1017/jfm.2019.16.

Rajendran, S., Fonseca, N., Guedes Soares, C., 2011. Time domain comparison with experiments for ship motions and structural loads on a container ship in abnormal waves. In: Proceedings of the 30th International Conference on Offshore Mechanics and Arctic Engineering (OMAE2011), pp. 919–927.

Rajendran, S., Fonseca, N., Guedes Soares, C., 2012. In: Guedes Soares, C., Garbatov, Y., Sutulo, S., Santos, T.A. (Eds.), Experiment and Time Domain Method Comparison for the Responses of a Container Ship Induced by the Three Sisters Abnormal Waves. Taylor & Francis, UK, pp. 223–230.

Rajendran, S., Fonseca, N., Guedes Soares, C., 2015. Effect of surge motion on the vertical responses of ships in waves. Ocean Engineering 96, 125–138.

Rajendran, S., Fonseca, N., Guedes Soares, C., 2016. A numerical investigation of the flexible vertical response of an ultra large containership in high seas compared with experiments. Ocean Engineering 122, 293–310. https://doi.org/10.1016/j.oceaneng.2016.05.038.

Rama Krishna, V., Sanaka, S.P., Pardhasaradhi, N., Raghava Rao, B., 2022. Hydro-elastic computational analysis of a marine propeller using two-way fluid structure interaction. Journal of Ocean Engineering and Science 7 (3), 280–291. https://doi.org/10.1016/j.joes.2021.07.003.

Ran, X., Leroy, V., Bachynski-Polić, E.E., 2023. Hydroelastic response of a flexible spar floating wind turbine: numerical modelling and validation. Ocean Engineering 286 (Part 2), 115635. https://doi.org/10.1016/j.oceaneng.2023.115635.

Ranta, J., Polojärvi, A., Tuhkuri, J., 2018. Ice loads on inclined marine structures: virtual experiments on ice failure process evolution. Marine Structures 57, 72–86. https://doi.org/10.1016/j.marstruc.2017.09.003.

Rashidi-Juybari, S., Fathi, A., Afrasiab, H., 2020. Hydroelastic analysis of surface gravity wave interacting with elastic plate resting on a linear viscoelastic foundation. Marine Systems & Ocean Technology 15, 286–298. https://doi.org/10.1007/s40868-020-00085-1.

Reddy, J.N., 2007. In: Theory and Analysis of Elastic Plates and Shells, second ed. CRC Press, Taylor & Francis.

Reinhard, M., Korobkin, A.A., Cooker, M.J., 2013. Water entry of a flat elastic plate at high horizontal speed. Journal of Fluid Mechanics 724, 123–153.

Reissner, E., 1945. The effect of transverse shear deformation on the bending of elastic plates. Journal of Applied Mechanics 12, 69–77.

Ren, H., Zhang, K., Li, H., 2018. Research of springing and whipping influence on ultra-large containerships' fatigue analysis. Journal of Shanghai Jiaotong University (Science) 23 (4), 429–437. https://doi.org/10.1007/s12204-018-1956-3.

Ren, Z., Javaherian, M.J., Gilbert, C.M., 2021. Kinematic and inertial hydroelastic effects caused by vertical slamming of a flexible V-shaped wedge. Journal of Fluids and Structures 103, 103257.

Ren, Z., Javaherian, M.J., Gilbert, C.M., 2023. A verification and validation study on a loosely two-way coupled hydroelastic model of wedge water entry. Journal of Ship Research 67 (3), 197–212.

Rienecker, M.M., Fenton, J.D., 1981. A Fourier approximation method for steady water waves. Journal of fluid mechanics 104, 119–137.

Riesner, M., el Moctar, O., 2021a. Assessment of wave-induced higher-order resonant vibrations of ships at forward speed. Journal of Fluids and Structures 101, 103262.

Riesner, M., el Moctar, O., 2021b. A numerical method to compute global resonant vibrations of ships at forward speed in oblique waves. Applied Ocean Research 108, 102520. https://doi.org/10.1016/j.apor.2020.102520.

Riesner, M., Ley, J., el Moctar, O., 2018. An efficient approach to predict wave-induced global hydroelastic ship response. In: Proceedings of the 8th International Conference. on Hydroelasticity in Marine Technology, Seoul, Korea.

Riggs, H.R., Suzuki, H., Yasuzawa, Y., Kim, J.W., Ertekin, R.C., 2006. Hydroelastic Response of the ISSC VLFS Benchmark. Hydroelasticity in Marine Technology, Wuxi, China.

Riggs, H.R., Niimi, K.M., Huang, L.L., 2007. Two benchmark problems for three-dimensional, linear hydroelasticity. Journal of Offshore Mechanics and Arctic Engineering 129 (3), 149–157.

Riyansyah, M., Wang, C.M., Choo, Y.S., 2010. Connection design for two-floating beam system for minimum hydroelastic response. Mar. Struct. 23, 67–87.

Robert, M., Monroy, C., Reliquet, G., Drouet, A., Ducoin, A., Guillerm, P.-E., Ferrant, P., 2015. Hydroelastic response of a flexible barge investigated with a viscous flow solver. In: Proceedings of the 7th International Conference on Hydroelasticity in Marine Technology, Split, Croatia.

Robillard, D.J., Mehta, A.J., Safak, I., 2023. Comments on wave-induced behavior of a coastal mud. Coastal Engineering 186, 104400.

Robin, G. de Q., 1963. Wave propagation through fields of pack ice. Philosophical Transactions of the Royal Society of London. Series A 255 (1057), 313–339.

Rogers, W.E., Holland, K.T., 2009. A study of dissipation of wind-waves by mud at Cassino beach, Brazil: prediction and inversion. Continental Shelf Research 29 (3), 676–690.

Rokvam, S.Ø., Vedvik, N.P., Mark, L., Rømcke, E., Ølnes, J.S., Savio, L., Echermeyer, A., 2021. Experimental verification of the elastic response in a numeric model of a composite propeller blade with bend twist deformation. Polymers 13 (21), 3766. https://doi.org/10.3390/polym13213766.

Russo, S., Jalalisendi, M., Falcucci, G., Porfiri, M., 2018. Experimental characterization of oblique and asymmetric water entry. Experimental Thermal and Fluid Science 92, 141–161.

Safak, I., Sheremet, A., Davis, J., Kaihatu, J.M., 2017. Nonlinear wave dynamics in the presence of mud-induced dissipation on Atchafalaya shelf, Louisiana, USA. Coastal Engineering 130, 52–64.

Sahoo, T., 2012. Mathematical Techniques for Wave Interaction with Flexible Structures. CRC Press.

Sahoo, T., Yip, T.L., Chwang, A.T., 2001. Scattering of surface waves by a semi-infinite floating elastic plate. Physics of Fluids 13 (11), 3215–3222.

Sakai, S., Hanai, K., 2002. Empirical formula of dispersion relation of waves in sea ice. In: Ice in the Environment: Proceedings of the 16th IAHR International Symposium on Ice, pp. 327–335.

Sakakiyama, T., Byker, E.W., 1989. Mass transport velocity in mud layer due to progressive waves. Journal of Waterway, Port, Coastal, and Ocean Engineering 115 (5), 614–633.

Salvesen, N., Tuck, E.O., Faltinsen, O., 1970. Ship motions and sea loads. Trans. Soc. nav. Archit. mar. Engrs 78, 250–287.

Sarrate, J., Huerta, A., Donea, J., 2001. Arbitrary Lagrangian-eulerian formulation for fluid-rigid body interaction. Computer Methods in Applied Mechanics and Engineering 190 (24–25), 3171–3188. https://doi.org/10.1016/S0045-7825(00)00315-4.

Savio, L., 2015. 'Measurements of the deflection of a flexible propeller blade by means of stereo imaging'. Fourth International Symposium on Marine Propulsors, Smp'15 Austin, Texas, USA. June 2015.

Savio, L., Koushan, K., 2019. Open water characteristics of three model scale flexible propellers. VIII International Conference on Computational Methods in Marine Engineering, MARINE 2019.

Savio, L., Sileo, L., Kyrre Ås, S., 2020. 'A comparison of physical and numerical modeling of homogenous isotropic propeller blades'. Journal of Marine Science and Engineering 8 (1), 21. https://doi.org/10.3390/jmse8010021.

Savio, L., Jenssen, Y., Henry, P.Y., Franzosi, G., 2024. Experimental investigation on the flow and deformation fields of an elastic propeller. Eighth International Symposium on Marine Propulsors, Smp'24. Berlin, Germany, March 2024.

Schlachter, G., 1989. Hull girder loads in a seaway including non-linear effects. Schiffs Technik 36, 169–180.

Seaver, M., Trickey, S.T., Nichols, J.M., 2006. Strain measurements from FBGs embedded in rotating composite propeller blades. In: Optical Fiber Sensors. Optica Publishing Group, p. ThD2.

Seddon, N., Chausson, A., Berry, P., Girardin, C.A., Smith, A., Turner, B., 2020. Understanding the value and limits of nature-based solutions to climate change and other global challenges. Philosophical Transactions of the Royal Society B: Biological Sciences 375 (1794), 20190120. https://doi.org/10.1098/rstb.2019.0120.

Sengupta, D., Datta, R., Sen, D., 2016. A simplified approach for computation of nonlinear ship loads and motions using a 3D time-domain panel method. Ocean Engineering 117, 99–113. https://doi.org/10.1016/j.oceaneng.2016.03.015.

Sengupta, D., Pal, S.K., Datta, R., 2017. Hydroelasticity of a 3D floating body using a semi-analytic approach in the time domain. Journal of Fluids and Structures 71, 96–115.

Sengupta, D., Show, T.K., Hirdaris, S., Datta, R., 2023. A semi-analytic method for the analysis of the symmetric hydroelastic response of a container ship under slamming and green water loads. Proceedings of the Institution of Mechanical Engineers, Part M: Journal of Engineering for the Maritime Environment 237 (4), 831–845. https://doi.org/10.1177/14750902231165808.

Senjanović, I., Grubišić, R., 1991. Coupled horizontal and torsional vibration of a ship hull with large hatch openings. Computers & Structures 41 (2), 213–226.

Senjanović, I., Malenica, Š., Tomašević, S., 2008. Investigation of ship hydroelasticity. Ocean Engineering 35 (5–6), 523–535.

Senjanović, I., Malenica, Š., Tomašević, S., 2009a. Hydroelasticity of large container ships. Marine Structures 22 (2), 287–314.

Senjanović, I., Tomašević, S., Vladimir, N., 2009b. An advanced theory of thin-walled girders with application to ship vibrations. Marine Structures 22 (3), 387–437.

Seo, B., Shin, H., 2020. Experimental study of slamming effects on wedge and cylindrical surfaces. Applied Sciences 10 (4), 1503.

Shakeel, A., Kirichek, A., Chassagne, C., 2020. Rheological analysis of mud from port of hamburg, Germany. Journal of Soils and Sediments 20 (6), 2553–2562.

Shams, A., Porfiri, M., 2015. Treatment of hydroelastic impact of flexible wedges. Journal of Fluids and Structures 57, 229–246.

Shams, A., Zhao, S., Porfiri, M., 2017. Hydroelastic slamming of flexible wedges: modeling and experiments from water entry to exit. Physics of Fluids 29 (3).

Shao, Y.-L., Faltinsen, O.M., 2012. A numerical study of the second-order wave excitation of ship springing in infinite water depth. Proceedings of the Institution of Mechanical Engineers, Part M: Journal of Engineering for the Maritime Environment 226 (2), 103–119.

Shaw, D.C., 1985. Perturbational results for diffraction of water-waves by nearly-vertical barriers. IMA journal of applied mathematics 34 (1), 99–117.

Sheremet, A., Stone, G.W., 2003. Observations of nearshore wave dissipation over muddy sea beds. Journal of Geophysical Research: Oceans 108 (C11).

Sheremet, A., Jaramillo, S., Su, S.-F., Allison, M.A., Holland, K.T., 2011. Wave-mud interaction over the muddy Atchafalaya subaqueous clinoform, Louisiana, United States: wave processes. Journal of Geophysical Research: Oceans 116 (C6). https://doi.org/10.1029/2010JC006644.
Shi, Y., Mei, C., 1996. A finite element time domain modal formulation for large amplitude free vibrations of beams and plates. Journal of sound and vibration 193 (2), 453–464.
Shin, K.-H., Jo, J.-W., Hirdaris, S.E., Jeong, S.-G., Park, J.B., Lin, F., Wang, Z., White, N., 2015. Two- and three-dimensional springing analysis of a 16,000 TEU container ship in regular waves. Ships and Offshore Structures 10 (5), 498–509.
Shiraishi, K., Sawada, Y., Arakawa, D., 2023. Deformed shape estimation for flexible composite marine propellers by image registration. Journal of Marine Science and Technology 28 (1), 221–233. https://doi.org/10.1007/s00773-022-00918-1.
Show, T.K., Hirdaris, S., Datta, R., 2022. A fully coupled time-domain BEM-FEM method for the prediction of symmetric hydroelastic responses of ships with forward speed. Shock and Vibration 2022.
Singh, M., Gayen, R., 2023a. Mathematical study on the potential flow past a vertical submerged flexible plate of non-uniform thickness. Journal of Fluids and Structures 116, 103795.
Singh, M., Gayen, R., 2023b. Performance of two vertically submerged piezoelectric plate wave energy converters in presence of a non-flat flexible barrier. Renewable Energy 212, 382–393.
Singh, M., Gayen, R., Kundu, S., 2022. Linear water wave propagation in the presence of an inclined flexible plate with variable porosity. Archive of Applied Mechanics 92 (9), 2593–2615.
Singh, M., Meylan, M., Gayen, R., 2023. Time-domain motion of a floating or obliquely submerged non-uniform elastic plate. Phys. Fluids 35, 047117.
Skene, D.M., Bennetts, L.G., Meylan, M.H., Toffoli, A., 2015. Modelling water wave overwash of a thin floating plate. Journal of Fluid Mechanics 777, 1–13. https://doi.org/10.1017/jfm.2015.378.
Skjørdal, S., Faltinsen, O., 1980. A linear theory of springing. Journal of Ship Research 24 (2), 74–84.
Smith, C.S., 1966. Measurement of service stresses in warships. Conference on Stresses in Service. Inst. of Civil Engineers, London, pp. 1–8.
Söding, H., 1982. Leckstabilität in Seegang. Report 429 of the Institut für Schiffbau. Hamburg.
Söding, H., 2009. Computation of springing transfer functions. Proceedings of the Institution of Mechanical Engineers, Part M: Journal of Engineering for the Maritime Environment 223 (3), 291–304.
Soltanahmadi, A., 1992. Determination of flexible riser natural frequencies using Fourier analysis. Marine structures 5 (2–3), 193–203.
Soltanpour, M., Samsami, F., 2011. A comparative study on the rheology and wave dissipation of kaolinite and natural Hendijan coast mud, the Persian Gulf. Ocean Dynamics 61 (2), 295–309.
Soltanpour, M., Samsami, F., Shibayama, T., Yamao, S., 2014. Study of irregular wave-current-mud interaction. In: Proceedings of ICCE, 1. ASCE, p. 27, 34.
Soltanpour, M., Shamsnia, S.H., Shibayama, T., Nakamura, R., 2018. A study on mud particle velocities and mass transport in wave-current-mud interaction. Applied Ocean Research 78, 267–280.
Spinosa, E., Iafrati, A., 2021. Experimental investigation of the fluid-structure interaction during the water impact of thin aluminium plates at high horizontal speed. International Journal of Impact Engineering 147, 103673.
Squire, V.A., 1984. A theoretical, laboratory, and field study of ice-coupled waves. Journal of Geophysical Research 89 (C5), 8069–8079.
Squire, V.A., 2007. Of ocean waves and sea-ice revisited. Cold Regions Science and Technology 49 (2), 110–133.
Squire, V.A., 2020. Ocean wave interactions with sea ice: a reappraisal. Annual Review of Fluid Mechanics 52, 37–60. https://doi.org/10.1146/annurev-fluid-010719-060301.
Squire, V.A., Allan, A., 1977. Propagation of flexural gravity waves in sea ice. In: Symposium on Sea Ice Processes and Models, Proceedings, 2. University of Washington, Seattle, USA [pages if known]).
Squire, V.A., Dugan, J.P., Wadhams, P., Rottier, P.J., Liu, A.K., 1995. Of ocean waves and sea ice. Oceanographic Literature Review 8 (42), 620.
Sree, D.K.K., Law, A.W.-K., Shen, H.H., 2017. An experimental study on the interactions between surface waves and floating viscoelastic covers. Wave Motion 70, 195–208. https://doi.org/10.1016/j.wavemoti.2016.08.003.
Sree, D.K.K., Law, A.W.-K., Shen, H.H., 2018. An experimental study on gravity waves through a floating viscoelastic cover. Cold Regions Science and Technology 155, 289–299. https://doi.org/10.1016/j.coldregions.2018.08.003.
Sree, D.K.K., Law, A.W.-K., Shen, H.H., 2020. An experimental study of gravity waves through segmented floating viscoelastic covers. Applied Ocean Research 101, 102233. https://doi.org/10.1016/j.apor.2020.102233.
Stavovy, A.B., Chuang, S.L., 1976. Analytical determination of slamming pressures for high-speed vehicles in waves. Journal of Ship Research 20 (4).
Stenius, I., Rosn, A., Kuttenkeuler, J., 2007. Explicit FE-modelling of hydroelasticity in panel-water impacts. International Shipbuilding Progress 54 (2/3), 111–127.
Stenius, I., Rosn, A., Kuttenkeuler, J., 2011. Hydroelastic interaction in panel-water impacts of high-speed craft. Ocean Engineering 38, 371–381.
Stenius, I., Rosén, A., Battley, M., Allen, T., 2013. Experimental hydroelastic characterization of slamming loaded marine panels. Ocean Engineering 74, 1–15.
Storhaug, G., Vidic-Perunovic, J., Rüdinger, F., others, 2003. Springing/whipping response of a large ocean going vessel—a comparison between numerical simulations and full scale measurements. In: Proceedings of Hydroelasticity in Marine Technology, pp. 117–129. Oxford, UK.
Storhaug, G., Paiva, A., Dessi, D., Zhang, G., Drummen, I., Moro, L., Holtmann, M., Shyu, R.-J., Wang, S., Dhavalikar, S., Wang, S., Sævik, S., Wu, W., Huh, Y.-C., Yamada, Y., 2022. Committee II.2: dynamic response. In: Proceedings of the 21st International Ship and Offshore Structures Congress, 1. https://doi.org/10.5957/ISSC-2022-COMMITTEE-II-2. Vancouver, Canada.
Su, W., Cesnik, C.E.S., 2011. Strain-based geometrically nonlinear beam formulation for modeling very flexible aircraft. International Journal of Solids and Structures 48 (16–17), 2349–2360. https://doi.org/10.1016/j.ijsolstr.2011.04.012.
Sun, H., 2007. A Boundary Element Method Applied to Strongly Nonlinear Wave-Body Interaction Problems.
Sun, H., Faltinsen, O.M., 2011. Dynamic motions of planing vessels in head seas. Journal of Marine Science and Technology 16 (2), 168–180. https://doi.org/10.1007/s00773-011-0123-4.
Sun, H., Wang, D.Y., 2018. Experimental and numerical analysis of hydrodynamic impact on stiffened side of three-dimensional elastic stiffened plates. Advances in Mechanical Engineering 10 (4), 1687814018767705.
Sun, Z., Liu, G.J., Zou, L., Zheng, H., Djidjeli, K., 2021a. Investigation of non-linear ship hydroelasticity by CFD-FEM coupling method. Journal of Marine Science and Engineering 9, 511. https://doi.org/10.3390/jmse9050511.
Sun, Z., Korobkin, A., Sui, X.P., Zhi, Z., 2021b. A semi-analytical model of hydroelastic slamming. Journal of Fluids and Structures 101, 103200.
Sun, W.Y., Nakamura, T., Cho, Y.-H., Mizutani, N., 2023. Numerical investigation of solitary wave attenuation by a vertical plate-type flexible breakwater using an FVM–FEM coupled model. Part 1: linear elastic isotropic material. Ocean Engineering 285, 115368. https://doi.org/10.1016/j.oceaneng.2023.115368.
Sun, W., Nakamura, T., Cho, Y., Mizutani, N., 2024a. Numerical investigation of solitary wave attenuation by a vertical plate-type flexible breakwater constructed using hyperelastic Neo-Hookean material. Journal of Marine Science and Engineering 12 (6), 1004. https://doi.org/10.3390/jmse12061004.
Sun, S.-L., Sun, J.-Y., Wang, S., Li, Y.-H., Ren, H.-L., 2024b. Fluid–structure interaction analysis of curved wedges entering into water. Physics of Fluids 36 (10), 102121. https://doi.org/10.1063/5.0157608.
Sussman, M., Puckett, E.G., 2000. A coupled level set and volume-of-fluid method for computing 3D and axisymmetric incompressible two-phase flows. J. Comput. Phys. 162, 301–337. https://doi.org/10.1006/jcph.2000.6537.
Sutherland, G., Halsne, T., Rabault, J., Jensen, A., 2017. The attenuation of monochromatic surface waves due to the presence of an inextensible cover. Wave Motion 68, 88–96.
Swidan, A., Thomas, G., Ranmuthugala, D., Amin, W., Penesis, I., Allen, T., Battley, M., 2016. Experimental drop test investigation into wetdeck slamming loads on a generic catamaran hullform. Ocean Engineering 117, 143–153.
Sy, S., Murea, C.M., 2008. A stable time advancing scheme for solving fluid–structure interaction problem at small structural displacements. Computer Methods in Applied Mechanics and Engineering 198 (2), 210–222. https://doi.org/10.1016/j.cma.2008.07.010.
Tahvildari, N., Sharifineyestani, E., 2019. A numerical study on nonlinear surface wave evolution over viscoelastic mud. Coastal Engineering 154, 103557.
Taira, K., Colonius, T., 2007. The immersed boundary method: a projection approach. Journal of Computational Physics 225 (2), 2118–2137. https://doi.org/10.1016/j.jcp.2007.03.005.
Takami, T., Iijima, K., 2020. Numerical investigation into combined global and local hydroelastic response in a large container ship based on two-way coupled CFD and FEA. Journal of Marine Science and Technology 25 (3), 346–362.
Takami, T., Matsui, S., Oka, M., Iijima, K., 2018. A numerical simulation method for predicting global and local hydroelastic response of a ship based on CFD and FEA coupling. Marine Structures 59, 368–386.
Taketani, T., Kimura, K., Ando, S., Yamamoto, K., 2013. Study on performance of a ship propeller using a composite material. In: Third International Symposium on Marine Propulsors. Launceston. Tasmania, Australia.
Tang, Y., Sun, S.L., Abbasnia, A., Soares, C.G., Ren, H.L., 2023. A fully nonlinear BEM-beam coupled solver for fluid–structure interactions of flexible ships in waves. Journal of Fluids and Structures 121, 103922.
Tang, H., Zhu, R., Wan, Q., Ren, D., 2025. Short-term prediction of trimaran load based on data driven technology. Brodogradnja 76 (1). Article 76101.
Tao, Z., 1996. Theoretical and Experimental Investigations of Large Amplitude Ship Motions and Loads in Regular Head Seas. Department of Naval Architecture & Ocean Engineering, University of Glasgow. Doctoral thesis.
Tao, Z., Incecik, A., 2000. Nonlinear ship motion and global bending moment predictions in regular head seas. International Shipbuilding Progress 47 (452), 353–378.
Tassin, A., Korobkin, A.A., Cooker, M.J., 2014. On analytical models of vertical water entry of a symmetric body with separation and cavity initiation. Appl. Ocean Res. 48, 33–41.
Tavakoli, S., Babanin, A.V., 2021. Wave energy attenuation by drifting and non-drifting floating rigid plates. Ocean Engineering 226, 108717. https://doi.org/10.1016/j.oceaneng.2021.108717.
Tavakoli, S., Babanin, A.V., 2023. A collection of wet beam models for wave-ice interaction. Cryosphere 17 (2), 939–958. https://doi.org/10.5194/tc-17-939-2023.
Tavakoli, S., Dashtimanesh, A., 2019. A six-DOF theoretical model for steady turning maneuver of a planing hull. Ocean Engineering 189, 106328. https://doi.org/10.1016/j.oceaneng.2019.106328.
Tavakoli, S., Hirdaris, S., 2023. The hydroelastic slamming in oblique seas. In: 42nd Proceedings of the International Conference on Offshore Mechanics and Arctic Engineering, 86878. American Society of Mechanical Engineers. V005T06A017.
Tavakoli, S., Niazmand Bilandi, R., Mancini, S., De Luca, F., Dashtimanesh, A., 2020. Dynamic of a planing hull in regular waves: comparison of experimental, numerical

and mathematical methods. Ocean Engineering 217, 107959. https://doi.org/10.1016/j.oceaneng.2020.107959.
Tavakoli, S., Huang, L., Azhari, F., Babanin, A.V., 2022. Viscoelastic wave–ice interactions: a computational fluid–solid dynamic approach. Journal of Marine Science and Engineering 10 (9), 1220.
Tavakoli, S., Khojasteh, D., Haghani, M., Hirdaris, S., 2023a. A review on the progress and research directions of ocean engineering. Ocean Engineering 272, 113617.
Tavakoli, S., Babanin, A.V., Hirdaris, S., 2023b. Hydroelastic analysis of hard chine sections entering water—observations for use in preliminary design stage. Journal of Offshore Mechanics and Arctic Engineering 145 (5), 051901.
Tavakoli, S., Mikkola, T., Hirdaris, S., 2023c. A fluid–solid momentum exchange method for the prediction of hydroelastic responses of flexible water entry problems. Journal of Fluid Mechanics 965, A19.
Tavakoli, S., Zhang, M., Kondratenko, A.A., Hirdaris, S., 2024a. A review on the hydrodynamics of planing hulls. Ocean Engineering 303, 117046. https://doi.org/10.1016/j.oceaneng.2024.117046.
Tavakoli, S., Kirezci, C., Lee, J., Sgarioto, D., Skvortsov, A.T., Babanin, A.V., 2024b. A simple method for calculating the probability of quiescent periods in random seas for maritime search and rescue operations. Ocean Engineering 304, 117838. https://doi.org/10.1016/j.oceaneng.2024.117838.
Tavakoli, S., Lee, J., Sgarioto, D., Skvortsov, A.T., Babanin, A.V., 2025. Field-based study and parametrisation of quiescent periods in ocean waves. Ocean Engineering 320, 120301. https://doi.org/10.1016/j.oceaneng.2025.120301.
Teixeira-Duarte, F., Clemente, D., Giannini, G., Rosa-Santos, P., Taveira-Pinto, F., 2022. Review on layout optimization strategies of offshore parks for wave energy converters. Renewable and Sustainable Energy Reviews 163, 112513.
Teng, B., Cheng, L., Liu, S.X., Li, F.J., 2001. Modified eigenfunction expansion methods for interaction of water waves with a semi-infinite elastic plate. Applied Ocean Research 23 (6), 357–368.
Thorne, R.C., 1953. Multipole expansions in the theory of surface waves. In: Mathematical Proceedings of the Cambridge Philosophical Society, 49. Cambridge University Press, pp. 707–716, 4.
Tian, C., Wu, Y.S., 2006. The non-linear hydroelastic responses of a ship travelling in waves. In: Proc. 4th Int. Conf. Hydroelasticity in Marine Technology, pp. 13–24.
Tian, F.-B., Dai, H., Luo, H., Doyle, J.F., Rousseau, B., 2014. Fluid–structure interaction involving large deformations: 3D simulations and applications to biological systems. Journal of Computational Physics 258, 451–469. https://doi.org/10.1016/j.jcp.2013.10.008.
Tian, J., Zhang, Z., Ni, Z., Hua, H., 2017. Flow-induced vibration analysis of elastic propellers in a cyclic inflow: an experimental and numerical study. Applied Ocean Research 65, 47–59.
Timoshenko, S., 1953. History of Strength of Materials. McGraw-Hill, New York.
Tkacheva, L.A., 2001. Surface wave diffraction on a floating elastic plate. Fluid Dynamics 36 (5), 776–789.
Tkacheva, L.A., 2003. Plane problem of surface wave diffraction on a floating elastic plate. Fluid Dynamics 38 (3), 465–481.
Tödter, S., El Moctar, O., Neugebauer, J., Schellin, T.E., 2020. Experimentally measured hydroelastic effects on impact-induced loads during flat water entry and related uncertainties. Journal of Offshore Mechanics and Arctic Engineering 142 (1), 011604.
Toffoli, A., Bennetts, L.G., Meylan, M.H., Cavaliere, C., Alberello, A., Elsnab, J., Monty, J. P., 2015. Sea ice floes dissipate the energy of steep ocean waves. Geophysical Research Letters 42 (20), 8547–8554. https://doi.org/10.1002/2015GL065937.
Toffoli, A., Pitt, J.P.A., Alberello, A., Bennetts, L.G., 2022. Modelling attenuation of irregular wave fields by artificial ice floes in the laboratory. Philosophical Transactions of the Royal Society A 380 (2235), 20210255.
Toki, N., Hatakenaka, K., Takahashi, T., et al., 1983. Experimental and theoretical approach to the estimation of non-linear vertical wave loads. Journal of the Society of Naval Architects of Japan 154, 141–150.
Torres-Freyermuth, A., Hsu, T.-J., 2010. On the dynamics of wave-mud interaction: a numerical study. Journal of Geophysical Research: Oceans 115 (C7).
Traykovski, P., Trowbridge, J., Kineke, G., 2015. Mechanisms of surface wave energy dissipation over a high-concentration sediment suspension. Journal of Geophysical Research: Oceans 120 (3), 1638–1681.
Truong, D.D., Jang, B.-S., Janson, C.-E., Ringsberg, J.W., Yamada, Y., Takamoto, K., Kawamura, Y., Ju, H.-B., 2021. Benchmark study on slamming response of flat-stiffened plates considering fluid-structure interaction. Marine Structures 79, 103040. https://doi.org/10.1016/j.marstruc.2021.103040.
Tschisgale, S., Fröhlich, J., 2020. An immersed boundary method for the fluid–structure interaction of slender flexible structures in viscous fluid. Journal of Computational Physics 423, 109806.
Tseng, Y., Ferziger, J.H., 2003. A ghost-cell immersed boundary method for flow in complex geometry. Journal of Computational Physics 192 (2), 593–623. https://doi.org/10.1016/S0021-9991(03)00504-9.
Tveitnes, T., Fairlie-Clarke, A.C., Varyani, K., 2008. An experimental investigation into the constant velocity water entry of wedge-shaped sections. Ocean Engineering 35 (14–15), 1463–1478.
Ubbink, O., Issa, R.I., 1999. A method for capturing sharp fluid interfaces on arbitrary meshes. J. Comput. Phys. 153, 26–50.
Ucar, M., Hmedi, M., Uzunoglu, E., Oguz, E., 2025. Effect of panel method codes in estimating the time-domain responses of floating wind turbines. Brodogradnja 76 (2). Article 76203.
Unguendoli, S., Biolchi, L.G., Aguzzi, M., Pillai, U.P.A., Alessandri, J., Valentini, A., 2023. A modeling application of integrated nature based solutions (NBS) for coastal erosion and flooding mitigation in the Emilia–Romagna coastline (northeast Italy). Science of the Total Environment 867, 161357. https://doi.org/10.1016/j.scitotenv.2023.161357.
Ursell, F., 1947. The effect of a fixed vertical barrier on surface waves in deep water. Mathematical Proceedings of the Cambridge Philosophical Society 43 (3), 374–382.
Van Nuffel, D., 2014. Experimental Study of the Slamming Induced Pressures, Forces and Deformations of Quasi-Rigid and Deformable Bodies during Vertical Water Entry (Doctoral Dissertation. Ghent University.
Van Nuffel, D., Vepa, K.S., De Baere, I., Degrieck, J., De Rouck, J., Van Paepegem, W., 2013. Study on the parameters influencing the accuracy and reproducibility of dynamic pressure measurements at the surface of a rigid body during water impact. Experimental mechanics 53, 131–144.
Van Slobbe, E., de Vriend, H.J., Aarninkhof, S., Lulofs, K., de Vries, M., Dircke, P., 2013. Building with nature: in search of resilient storm surge protection strategies. Natural Hazards 66 (3), 1461–1480. https://doi.org/10.1007/s11069-013-0612-3.
Vasin, A.D., 1993. Hydroelastic interaction of a wedge-shaped construction entering a liquid. Fluid Dynamics 28 (3), 387–392. https://doi.org/10.1007/BF01062136.
Velasco, D., Bateman, A., Medina, V., 2008. A new integrated, hydro-mechanical model applied to flexible vegetation in riverbeds. Journal of Hydraulic Research 46 (5), 579–597.
Vettori, D., Nikora, V., 2017. Morphological and mechanical properties of blades of Saccharina latissimi. Estuarine, Coastal and Shelf Science 196, 1–9.
Vettori, D., Nikora, V., 2021. Flow-seaweed interactions of Saccharina latissima at a blade scale: turbulence, drag force, and blade dynamics, 81, 61.
Vidic-Perunovic, J., Juncher Jensen, J., 2005. Non-linear springing excitation due to a bidirectional wave field. Marine Structures 18 (4), 332–358.
Vijayanandh, R., Venkatesan, K., Kumar, M.S., Kumar, G.R., Jagadeeshwaran, P., Kumar, R.R., 2020. Comparative fatigue life estimations of Marine Propeller by using FSI. In: Journal of Physics: Conference Series, 1473. IOP Publishing, 012018. https://doi.org/10.1088/1742-6596/1473/1/012018, 1.
Vijith, P.P., Rajendran, S., 2023. Hydroelastic effects on the vertical bending moment of a container ship in head and oblique seas. Ocean Engineering 285, 115385.
Vincent, L., Xiao, T., Diorio, Y., Jung, S., Kanso, E., 2018. Dynamics of water entry. Journal of Fluid Mechanics 846, 508–535. https://doi.org/10.1017/jfm.2018.273.
Vlasov, V.Z., 1961. Thin-walled Elastic Beams. Israel Program for Scientific Translations, Jerusalem.
Voermans, J.J., Rabault, J., Filchuk, K., Ryzhov, I., Heil, P., Marchenko, A., Collins III, C. O., Dabboor, M., Sutherland, G., Babanin, A.V., 2020. Experimental evidence for a universal threshold characterizing wave-induced sea ice break-up. The Cryosphere 14 (11), 4265–4278. https://doi.org/10.5194/tc-14-4265-2020.
Volpi, S., Diez, M., Sadat-Hosseini, H.S., Kim, D.H., Stern, F., Thodal, R.S., Grenestedt, J. L., 2017. Composite bottom panel slamming of a fast planing hull via tightly coupled fluid-structure interaction simulations and sea trials. Ocean Engineering 143, 240–258. https://doi.org/10.1016/j.oceaneng.2017.06.001.
von Kármán, T.H., 1929. The Impact on Seaplane Floats during Landing (No. NACA-TN-321).
Wadhams, P., 1972. Measurement of wave attenuation in pack ice by inverted echo sounding. In: Karlsson, T. (Ed.), Sea Ice. Proceedings of an International Conference. Reykjavik, Iceland, May 10–13, 1971. National Research Council, Reykjavík, Iceland, pp. 255–260.
Wadhams, P., 1975. Airborne laser profiling of swell in an open ice field. Journal of Geophysical Research 80, 4520–4528.
Wadhams, P., 1978. Wave decay in the marginal ice zone measured from a submarine. Deep Sea Research 25, 23–40.
Wadhams, P., 1979. Field experiments on wave-ice interaction in the Labrador and east Greenland currents, 1978. Polar Record 19 (121), 373–376.
Wadhams, P., Squire, V.A., Goodman, D.J., Cowan, A.M., Moore, S.C., 1988. The attenuation rates of ocean waves in the marginal ice zone. Journal of Geophysical Research 93 (C6), 6799–6818.
Wagner, H., 1932. Über Stoß-Gleitvorgänge an der Oberfläche von Flüssigkeiten. ZAMM 12.
Wang, S., Guedes Soares, C., 2011. Numerical prediction of slamming loads on a rigid wedge subjected to water entry using an explicit finite element method. In: Guedes Soares and Garbatov. CRC Press, pp. 41–50. MARSTRUCT 2011.
Wang, S., Guedes Soares, C., 2013a. Slam induced loads on bow-flared sections with various roll angles. Ocean Engineering 67, 45–57. https://doi.org/10.1016/j.oceaneng.2013.04.009.
Wang, S., Guedes Soares, C., 2013b. Numerical study on hydroelastic water entry of a wedge. In: Proceedings of the 16th International Maritime Association of the Mediterranean (IMAM 2014). CRC Press, pp. 199–206.
Wang, S., Guedes Soares, C., 2014a. Numerical prediction of slamming loads during water entry of bow-flared sections. International Journal of Maritime Engineering 156 (A4), 303–316. https://doi.org/10.3940/rina.ijme.2014.a4.304.
Wang, S., Guedes Soares, C., 2014b. Numerical study on the water impact of 3D bodies by an explicit finite element method. Ocean Engineering 78, 73–88. https://doi.org/10.1016/j.oceaneng.2013.12.008.
Wang, S., Guedes Soares, C., 2016a. Experimental and numerical study of the slamming load on the bow of a chemical tanker in irregular waves. Ocean Engineering 111, 369–383. https://doi.org/10.1016/j.oceaneng.2015.11.045.
Wang, S., Guedes Soares, C., 2016b. Stern slamming of a chemical tanker in irregular head waves. Ocean Engineering 122, 322–332. https://doi.org/10.1016/j.oceaneng.2016.05.013.
Wang, S., Guedes Soares, C., 2017. Review of ship slamming loads and responses. Journal of Marine Science and Application 16, 427–445. https://doi.org/10.1007/s11804-017-1437-3.

Wang, S., Guedes Soares, C., 2018. Simplified approach to dynamic responses of elastic wedges impacting with water. ocean engineering 150, 81–93. https://doi.org/10.1016/j.oceaneng.2017.12.043.
Wang, S., Guedes Soares, C., 2025. Statistical characterization on slamming and green water impact onto a chemical tanker in extreme sea conditions. Marine Structures 103, 103818. https://doi.org/10.1016/j.marstruc.2025.103818.
Wang, H., Hu, Z., 2023. Modeling wave attenuation by vegetation with accompanying currents in SWAN. Acta Oceanologica Sinica 42, 63–76. https://doi.org/10.1007/s13131-023-2199-1.
Wang, R., Shen, H.H., 2010. Experimental study on surface wave propagating through a grease-pancake ice mixture. Cold Regions Science and Technology 61 (2–3), 90–96. https://doi.org/10.1016/j.coldregions.2010.01.011.
Wang, D., Wu, Y., 1998. Three-dimensional hydroelastic analysis in time domain with application to an elastic ship model. Journal of Hydrodynamics, Series B 10 (4), 54–61.
Wang, C., Wu, G., 2011. A brief summary of finite element method applications to nonlinear wave-structure interactions. Journal of Marine Science and Application 10, 127–138.
Wang, Z., Xia, J., 1992. Differential method for the non-linear hydroelastic analysis of ships. In: Theories and Applications of Computational Mechanics. Science Press, China (in Chinese).
Wang, Z., Yang, J., Koo, B., Stern, F., 2009. A coupled level set and volume-of-fluid method for sharp interface simulation of plunging breaking waves. International Journal of Multiphase Flow 35 (3), 227–246. https://doi.org/10.1016/j.ijmultiphaseflow.2008.11.004.
Wang, S., Karmakar, D., Guedes Soares, C., 2016. Hydroelastic impact of a horizontal floating plate with forward speed. Journal of Fluids and Structures 60, 97–113. https://doi.org/10.1016/j.jfluidstructs.2015.11.005.
Wang, A., Kim, H.T., Wong, K.P., Yu, M., Kiger, K.T., Duncan, J.H., 2019. Spray formation and structural deformation during the oblique impact of a flexible plate on a quiescent water surface. Journal of Ship Research 63 (3), 154–164.
Wang, C., Wang, G., Huang, B., 2020a. Characteristics and dynamics of compressible cavitating flows with special emphasis on compressibility effects. International Journal of Multiphase Flow 130, 103357. https://doi.org/10.1016/j.ijmultiphaseflow.2020.103357.
Wang, Y., Wu, W., Soares, C.G., 2020b. Experimental and numerical study of the hydroelastic response of a river-sea-going container ship. Journal of Marine Science and Engineering 8 (12), 978. https://doi.org/10.3390/jmse8120978.
Wang, S., Islam, H., Guedes Soares, C., 2021. Uncertainty due to discretization on the ALE algorithm for predicting water slamming loads. Marine Structures 80, 103086. https://doi.org/10.1016/j.marstruc.2021.103086.
Wang, S., Rolland, Y., Guedes Soares, C., 2022. Analytical and numerical analysis of slamming induced vibrations on composite plates. Ocean Eng 258, 111643.
Wang, C., Ren, B., Lin, P., 2022a. A coupled flow and beam model for fluid–slender body interaction. Journal of Fluids and Structures 115, 103781.
Wang, H., Duan, W., Chen, J., Ma, S., 2022b. A numerical method to compute flexible vertical responses of containerships in regular waves. Ocean Engineering 266, 112828. https://doi.org/10.1016/j.oceaneng.2022.112828.
Wang, S., Rolland, Y., Guedes Soares, C., 2022c. Analytical and numerical analysis of slamming induced vibrations on composite plates. Ocean Engineering 258, 111643.
Wang, C., Wei, Y., Chen, W., Huang, L., 2024a. Hydroelastic modelling of a deformable wave energy converter including power take-off. Marine Structures 98, 103678.
Wang, C., Wei, Y., Chen, W., Huang, L., 2024b. Interactive effects of deformable wave energy converters operating in close proximity. Energy 308, 132905.
Watanabe, I., Guedes Soares, C., 1999. Comparative study on the time-domain analysis of non-linear ship motions and loads. Marine Structures 12 (2), 153–170. https://doi.org/10.1016/S0951-8339(98)00038-8.
Wei, Y., Incecik, A., Tezdogan, T., 2022. A fully coupled CFD-DMB approach on the ship hydroelasticity of a containership in extreme wave conditions. Journal of Marine Science and Engineering 10 (11), 1778.
Wei, Y., Incecik, A., Tezdogan, T., 2023. A hydroelasticity analysis of a damaged ship based on a two-way coupled CFD-DMB method. Ocean Engineering 274, 114075.
Wei, Y., Wang, C., Chen, W., Huang, L., 2024a. Array analysis on a seawall type of deformable wave energy converters. Renewable Energy 225, 120344.
Wei, Y., Yu, S., Jin, P., Huang, L., Elsherbiny, K., Tezdogan, T., 2024b. Coupled analysis between catenary mooring and VLFS with structural hydroelasticity in waves. Marine Structures 93, 103516. https://doi.org/10.1016/j.marstruc.2023.103516.
Wei, Z., Shao, Y., Kristiansen, T., Kristiansen, D., 2024c. A fully explicit wave-vegetation interaction model and its application in waves over a floating seaweed farm. The 39th International Workshop on Water Waves and Floating Bodies, 14-17 April 2024, St Andrews, Scotland.
Wei, Z., Shao, Y., Kristiansen, T., Kristiansen, D., 2024d. An efficient numerical solver for highly compliant slender structures in waves: application to marine vegetation. Journal of Fluids and Structures 129, 104170. https://doi.org/10.1016/j.jfluidstructs.2024.104170.
Wei, Y., Zhang, J., Liu, K., Pan, J., Zhang, L., Chen, W., Zhang, Q., 2025a. Numerical study of the influence of hydrofoil hydrodynamic performance considering near-free surface. Brodogradnja 76 (1). Article 76108.
Wei, Z., Weiss, M., Kristiansen, T., Kristiansen, D., Shao, Y., 2025b. Wave attenuation by cultivated seaweeds: a linearized analytical model. Coastal Engineering 195, 104642. https://doi.org/10.1016/j.coastaleng.2023.104642.
Wells, J.T., Coleman, J.M., 1981. Physical processes and fine-grained sediment dynamics, coast of Surinam, South America. Journal of Sedimentary Research 51 (4), 1053–1068.
Wenyang, D., 2012. Taylor expansion boundary element method for floating body hydrodynamics. In: Proceedings of the 27th International Workshop on Water Waves and Floating Bodies. Copenhagen, Denmark.
Weymouth, G.D., Yue, D.K.P., 2010. Conservative volume-of-fluid method for free-surface simulations on cartesian-grids. Journal of Computational Physics 229 (8), 2853–2865.
Whitham, G.B., 1967. Variational methods and applications to water waves. Proceedings of the Royal Society of London. Series A. Mathematical and Physical Sciences 299 (1456), 6–25.
Williams, S.J., Jeng, D.-S., 2007. The effects of a porous-elastic seabed on interfacial wave propagation. Ocean Engineering 34 (13), 1818–1831. https://doi.org/10.1016/j.oceaneng.2006.11.001.
Williams, T.D., Meylan, M.H., 2012. The Wiener–Hopf and residue calculus solutions for a submerged semi-infinite elastic plate. Journal of Engineering Mathematics 75, 81–106.
Williams, T.D., Bennetts, L.G., Squire, V.A., Dumont, D., Bertino, L., 2013. Wave–ice interactions in the marginal ice zone. Part 1: theoretical foundations. Ocean Modelling 71, 81–91.
Wilson, R., Lei, J., Karman Jr, S., Whitfield, D.L., et al., 2008. Simulation of large amplitude ship motions for prediction of fluid-structure interaction. Paper Presented at the 27th ONR Symposium on Naval Hydrodynamics, Rome, Italy.
Winterwerp, J.C., de Boer, G.J., Greeuw, G., van Maren, D.S., 2012. Mud-induced wave damping and wave-induced liquefaction. Coastal Engineering 64, 102–112.
Wu, Y., 1984. Hydroelasticity of Floating Bodies. University of Brunel. Doctoral dissertation.
Wu, Y.-S., Cui, W.-C., 2009. Advances in the three-dimensional hydroelasticity of ships. Proceedings of the Institution of Mechanical Engineers, Part M: Journal of Engineering for the Maritime Environment 223 (3), 331–348. https://doi.org/10.1243/14750902JEME159.
Wu, M.K., Moan, T., 2005. Efficient calculation of wave-induced ship responses considering structural dynamic effects. Applied Ocean Research 27 (2), 81–96.
Wu, Y., Xia, J.Z., Du, S.X., 1991. Two Engineering Approaches to Hydroelastic Analysis of Slender Ships. China Ship Scientific Research Center (CSSRC). Technical Report No. 91004, English version.
Wu, M.K., Hermundstad, O., Moan, T., 1993. Hydroelastic analysis of ship hulls at high forward speed. In: Proceedings of FAST, pp. 699–711. Yokohama, Japan.
Wu, Y.S., Maeda, H., Kinoshita, T., 1997. The second order hydrodynamic actions on a flexible body. Journal of the Institution of Industrial Scientists 49 (4), 8–19.
Wu, X., Zhang, X., Tian, X., Li, X., Lu, W., 2020. A review on fluid dynamics of flapping foils. Ocean Engineering 195, 106712. https://doi.org/10.1016/j.oceaneng.2019.106712.
Wu, Q., Wang, K., Kong, D., Zhang, J., Liu, T., 2023. Numerical simulation of subsonic and transonic water entry with compressibility effect considered. Ocean Engineering 281, 114984. https://doi.org/10.1016/j.oceaneng.2023.114984.
Xia, Y.-Z., 2014. The attenuation of shallow-water waves over seabed mud of a stratified viscoelastic model. Coastal Engineering Journal 56 (4), 1450021. https://doi.org/10.1142/S0578563414500211.
Xia, J., Gu, M., Wu, Y., 1987. Linear and Nonlinear Wave-Induced Responses of Traveling Elastic Ships. Ship Behavior Research (4). (in Chinese).
Xia, J.Z., Wang, Z.H., Jensen, J.J., 1998. Non-linear wave loads and ship responses by a time-domain strip theory. Marine Structures 11 (3), 101–123.
Xie, H., Ren, H., Qu, S., Tang, H., 2018. Numerical and experimental study on hydroelasticity in water-entry problem of a composite ship-hull structure. Composite Structures 201, 942–957. https://doi.org/10.1016/j.compstruct.2018.06.045.
Xie, H., Ren, H., Li, H., Tao, K., 2019. Quantitative analysis of hydroelastic characters for one segment of hull structure entering into water. Ocean Engineering 173, 469–490. https://doi.org/10.1016/j.oceaneng.2018.12.051.
Xie, B., He, G., Zhao, C., Jing, P., Pal, S.K., Iijima, K., Jin, R., Chen, B., Ghassemi, H., 2024. Experimental and numerical investigation on the hydroelastic response of barge and KVLCC2 ship. Ocean Engineering 307, 118081.
Xie, H., Peng, H., Liu, F., Liu, X., Ren, H., 2024a. Hydroelastic analysis of an elastic thin-walled structure obliquely impacting a calm water surface. Thin-Walled Structures 197, 111638.
Xie, B., Pal, S.K., Iijima, K., Tatsumi, A., Badalotti, T., 2025. Investigation of higher-order springing of a ship in regular waves by experimental analysis and two-way CFD-FEA coupled method. Marine Structures 99, 103712. https://doi.org/10.1016/j.marstruc.2024.103712.
Xu, B., Guyenne, P., 2022. Assessment of a porous viscoelastic model for wave attenuation in ice-covered seas. Applied Ocean Research 122, 103122. https://doi.org/10.1016/j.apor.2022.103122.
Xu, G.D., Duan, W.Y., Wu, G.X., 2008. Numerical simulation of oblique water entry of an asymmetrical wedge. Ocean Engineering 35 (16), 1597–1603. https://doi.org/10.1016/j.oceaneng.2008.08.002.
Xu, D., Liu, J., Wu, Y., Ji, C., 2022. Numerical investigation of the dynamics of flexible vegetations in turbulent open-channel flows. Journal of Hydrodynamics 34 (4), 681–699. https://doi.org/10.1007/s42241-022-0057-96-5.
Xue, S., Xu, G., Xie, W., Xu, L., Jiang, Z., 2023. Characteristics of freak wave and its interaction with marine structures: a review. Ocean Engineering 287, 115764. https://doi.org/10.1016/j.oceaneng.2023.115764.
Yago, K., Endo, H., 1996. On the hydroelastic response of box-shaped floating structure with shallow draft. Journal of the Society of Naval Architects of Japan 1996 (180), 341–352.
Yamada, Y., Takamoto, K., Nakanishi, T., Chong, M., Komoriyama, Y., 2020. Numerical study on the slamming impact of stiffened flat panel using ICFD method: effect of structural rigidity on the slamming impact. In: International Conference on Offshore

Mechanics and Arctic Engineering, 84331. American Society of Mechanical Engineers. V02BT02A006.
Yamamoto, Y., Fujino, M., Fukasawa, T., 1978. Motion and longitudinal strength of a ship in head sea and the effects of non-linearities. Journal of the Society of Naval Architects of Japan 1978 (143), 179–187.
Yan, D., Hosseinzadeh, S., Lakshmynarayanana, A., Mikkola, T., Hirdaris, S., 2021. Comparative study on numerical hydroelastic analysis of impact-induced loads. In: Of the 23rd Numerical Towing Tank Symposium, p. 6.
Yan, D., Mikkola, T., Lakshmynarayanan, A., Tödter, S., Schellin, T.E., Neugebauer, J., Ould el Moctar, B., Hirdaris, S., 2022. A study into the FSI modelling of flat plate water entry and related uncertainties. Marine Structures 86, 103296.
Yan, D., Mikkola, T., Kujala, P., Hirdaris, S., 2023. Hydroelastic analysis of slamming induced impact on stiff and flexible structures by two-way CFD-FEA coupling. Ships and Offshore Structures 18 (9), 1300–1312. https://doi.org/10.1080/17445302.2022.2116231.
Yang, P., Gu, X., 2015. Analysis on the hydroelastic responses and structural strength of VLFS module. J. Ship Mech. 19, 553–565.
Yang, W., Yu, G., 2018. Rheological response of natural soft coastal mud under oscillatory shear loadings. Journal of Waterway, Port, Coastal, and Ocean Engineering 144 (4), 05018005.
Yang, P., Gu, X.-k., Ding, J., 2018. 3D nonlinear hydroelastic response and load prediction of a large bulk carrier in time domain. Journal of Ship Mechanics 22 (12), 1495–1507.
Yang, P., Li, J., Gu, X., Wu, D., 2019. Application of the 3D time-domain Green's function for finite water depth in hydroelastic mechanics. Ocean Engineering 189, 106386.
Yang, P., Li, J., Wu, D., Zhang, W., 2020. Irregular frequency elimination of three-dimensional hydroelasticity in frequency domain. Ocean Engineering 196, 106817.
Yang, P., Feng, Q., Chen, H., Wen, L., 2021. Combined backbone application on numerical simulations and a model experiment of a 20,000 TEU container ship. Ocean Engineering 223, 108662. https://doi.org/10.1016/j.oceaneng.2021.108662.
Yang, L., Zhang, S., Kang, H., Wang, X., Ji, Z., Wang, Q., 2024. Impact responses of hyperelastic spheres on water and rigid surfaces. Ocean Engineering 299, 117203. https://doi.org/10.1016/j.oceaneng.2023.1172036-3.
Yettou, E.M., Desrochers, A., Champoux, Y., 2006. Experimental study on the water impact of a symmetrical wedge. Fluid Dynamics Research 38 (1), 47.
Yiew, L.J., Bennetts, L.G., Meylan, M.H., Thomas, G.A., French, B.J., 2017. Wave-induced collisions of thin floating disks. Physics of Fluids 29 (12), 127102. https://doi.org/10.1063/1.5003310.
Yiew, L.J., Parra, S.M., Wang, D., Sree, D.K.K., Babanin, A.V., Law, A.W.K., 2019. Wave attenuation and dispersion due to floating ice covers. Applied Ocean Research 87, 256–263.
Yin, K., Xu, S., Gong, S., Zhou, R., Wang, Y., 2021a. Effects of wave nonlinearity on submerged flexible vegetation dynamics and wave attenuation. Ocean Engineering 241, 110103. https://doi.org/10.1016/j.oceaneng.2021.110103.
Yin, K., Xu, S., Huang, W., Liu, S., Li, M., 2021b. Numerical investigation of wave attenuation by coupled flexible vegetation dynamic model and xbeach wave model. Ocean Engineering 235, 109357.
Yin, K., Xu, S., Gong, S., Chen, J., Wang, Y., Li, M., 2022. Modelingwave attenuation by submerged flexible vegetation with XBeach phase-averaged model. Ocean Engineering 257, 111646.
Yoo, D.-H., Jang, B.-S., Yim, K.-H., 2017. Nonlinear finite element analysis of failure modes and ultimate strength of flexible pipes. Marine Structures 54, 50–72. https://doi.org/10.1016/j.marstruc.2017.05.001.
Young, Y.L., 2007a. Time-dependent hydroelastic analysis of cavitating propulsors. Journal of Fluids and Structures 23 (2), 269–295.
Young, Y.L., 2007b. Time-dependent hydroelastic analysis of cavitating propellers. Journal of Fluids and Structures 23 (2), 269–295. https://doi.org/10.1016/j.jfluidstructs.2006.09.004.
Young, Y.L., 2008. Fluid–structure interaction analysis of flexible composite marine propellers. Journal of Fluids and Structures 24 (6), 799–818.
Young, Y.L., 2010. Dynamic hydroelastic scaling of self-adaptive composite marine rotors. Composite Structures 92 (1), 97–106.
Young, Y.L., Baker, J.W., Motley, M.R., 2010a. Reliability-based design and optimization of adaptive marine structures. Composite Structures 92 (2), 244–253.
Young, Y.L., Motley, M.R., Yeung, R.W., 2010b. Three-dimensional numerical modeling of the transient fluid-structural interaction response of tidal turbines. ASME Journal of Offshore Mechanics and Arctic Engineering 132 (1), 011101.
Young, Y.L., Motley, M.R., Barber, R., Chae, E.J., Garg, N., 2016. Adaptive composite marine propulsors and turbines: progress and challenges. Applied Mechanics Reviews 68, 060803.
Yu, Z., 2025. Water impact damage considering hydro-plastic interactions: extensive experimental and numerical validation, and structural design recommendations. Marine Structures 101, 103766.
Yu, J., Rogers, W.E., Wang, D.W., 2019a. A scaling for wave dispersion relationships in ice-covered waters. Journal of Geophysical Research: Oceans 124 (11), 8035–8051. https://doi.org/10.1029/2019JC015413.
Yu, P., Li, H., Ong, M.C., 2019b. Hydroelastic analysis on water entry of a constant-velocity wedge with stiffened panels. Marine Structures 63, 215–238.
Yurchenko, D., Alevras, P., 2013. Dynamics of the N-pendulum and its application to a wave energy converter concept. International Journal of Dynamics and Control 1, 290–299.
Zarnick, E.E., 1978. A Nonlinear Mathematical Model of Motions of a Planing Boat in Regular Waves. David W. Taylor Naval Ship Research and Development Center.
Zhai, Y., Klahn, M., Onorato, M., Fuhrman, D.R., 2025. Fully nonlinear simulations of rogue wave formation in finite-depth irregular waves. Journal of Fluid Mechanics 1017, A23. https://doi.org/10.1017/jfm.2025.10464.
Zhan, C., Zhang, T., Zhang, S., Yang, D., 2025. Solving complex flood wave propagation using split Coefficient-based Physical Informed Neural Network. Journal of Hydrology 654, 132835. https://doi.org/10.1016/j.jhydrol.2025.132835.
Zhang, X., Lu, D., 2018. An extension of a discrete-module-beam-bending-based hydroelasticity method for a flexible structure with complex geometric features. Ocean Engineering 163, 22–28. https://doi.org/10.1016/j.oceaneng.2018.05.050.
Zhang, X., Nepf, H., 2022. Reconfiguration of and drag on marsh plants in combined waves and current. Journal of Fluids and Structures 110, 103539.
Zhang, X., Nepf, H., 2024. Laboratory data linking the reconfiguration of and drag on individual plants to the velocity structure and wave dissipation over a meadow of salt marsh plants under waves with and without current. Earth Syst. Sci. Data 16, 1047–1062.
Zhang, M., Schreier, S., 2022. Review of wave interaction with continuous flexible floating structures. Ocean Engineering 264, 112404. https://doi.org/10.1016/j.oceaneng.2022.112404.
Zhang, L., Gerstenberger, A., Wang, X., Liu, W.K., 2004. Immersed finite element method. Computer Methods in Applied Mechanics and Engineering 193 (21–22), 2051–2067. https://doi.org/10.1016/j.cma.2003.12.044.
Zhang, X., Lu, D., Guo, F., Gao, Y., Sun, Y., 2018. The maximum wave energy conversion by two interconnected floaters: effects of structural flexibility. Applied Ocean Research 71, 34–47.
Zhang, X., Hong, Y., Liu, W., Yang, F., Wang, R., 2020. Improving the propulsion performance of composite propellers under off-design conditions. Applied Ocean Research 100, 102164. https://doi.org/10.1016/j.apor.2020.102164.
Zhang, D., Wang, W., Sun, H., Bernitsas, M.M., 2021a. Influence of turbulence intensity on vortex pattern for a rigid cylinder with turbulence stimulation in flow induced oscillations. Ocean Engineering 237, 109349. https://doi.org/10.1016/j.oceaneng.2021.109349.
Zhang, G., Feng, S., Zhang, Z., Chen, Y., Sun, Z., Zong, Z., 2021b. Investigation of hydroelasticity in water entry of flexible wedges with flow detachment. Ocean Engineering 222, 108580.
Zhang, W., Ma, N., Gu, X., Feng, P., 2021c. RANS simulation of open propeller dynamic loads in regular head waves considering coupled oblique-flow and free-surface effect. Ocean Engineering 234, 108741.
Zhang, M., Yu, H., Feng, G., et al., 2021d. Investigation on effects of springing and whipping on fatigue damages of ultra-large container ships in irregular seas. Journal of Marine Science and Technology 26, 432–458. https://doi.org/10.1007/s00773-020-00748-z.
Zhang, C.W., Zhuang, Q.Z., Li, J.X., others, 2022. Hydroelastic investigation on a pile breakwater integrated with a flexible tail for long-wave attenuation. China Ocean Engineering 36 (6–2), 667–681.
Zhang, H., Sun, B., Li, Z., Wang, F., 2023a. Wave attenuation and motion response of floating breakwater with sponge material. Ocean Engineering 277, 114325.
Zhang, D., Dong, L., Wu, Q., Zhang, J., Wang, G., 2023b. Global cavitation and hydrodynamic characteristics of a composite propeller in non-uniform wake. Journal of Hydrodynamics 35 (3), 498–515.
Zhang, M., Tsoulakos, N., Kujala, P., Hirdaris, S., 2024. A deep learning method for the prediction of ship fuel consumption in real operational conditions. Engineering Applications of Artificial Intelligence 130, 107425.
Zhang, G., Li, Q., Jiang, C., el Moctar, O., Sun, Z., 2025a. Constraint effects on the hydroelasticity of very large floating structures. Ocean Engineering 331, 121304. https://doi.org/10.1016/j.oceaneng.2025.121304.
Zhang, M., Wang, H., Conti, F., Manderbacka, T., Remes, H., Hirdaris, S., 2025b. A hybrid deep learning method for the real-time prediction of collision damage consequences in operational conditions. Engineering Applications of Artificial Intelligence 145, 110158.
Zhao, R., Faltinsen, O.M., 1993. Water entry of two-dimensional bodies. Journal of Fluid Mechanics 246, 593–612.
Zhao, R., Faltinsen, O.M., Aarsnes, J.V., 1996. Water entry of arbitrary two-dimensional sections with and without flow separation. Proceedings of the 21st Symposium on Naval Hydrodynamics, pp. 408–423.
Zhao, Z.D., Lian, J.J., Zhang, J.S., 2006. Interactions among waves, current, and mud: numerical and laboratory studies. Advances in Water Resources 29 (11), 1731–1744, 6-6.
Zhao, C., Hu, C., Wei, Y., Zhang, J., Huang, W., 2008. Diffraction of surface waves by floating elastic plates. Journal of fluids and structures 24 (2), 231–249.
Zhao, X., Shen, H.H., Cheng, S., 2015a. Modeling ocean wave propagation under sea ice covers. Acta Mechanica Sinica 31 (1), 1–15.
Zhao, C., Hao, X., Liang, R., Lu, J., 2015b. Influence of hinged conditions on the hydroelastic response of compound floating structures. Ocean Engineering 101, 12–24.
Zhao, Q., Guo, C., Su, Y., Liu, T., Meng, X., 2017. Study on unsteady hydrodynamic performance of propeller in waves. Journal of Hydrodynamics 16 (6–4), 305–312.
Zhao, W., Leira, B.J., Feng, G., Gao, C., Cui, T., 2021. A reliability approach to fatigue crack propagation analysis of ship structures in polar regions. Marine Structures 80, 103075. https://doi.org/10.1016/j.marstruc.2021.103075.
Zhao, K., Yang, S.-F., Yuan, P.-Y., Shi, F.-L., Ming, F.-R., 2025. Numerical investigation of aerated water entry by multiphase Riemann SPH method. Ocean Engineering 333, 121244. https://doi.org/10.1016/j.oceaneng.2025.121244.
Zhou, B., Amini-Afshar, M., Bingham, H.B., Shao, Y., Malenica, Š., Andersen, M.H., 2024a. Solving for hydroelastic ship response using a high-order finite difference method on overlapping grids at zero speed. Marine Structures 95, 103602. https://doi.org/10.1016/j.marstruc.2024.103602.
Zhou, B., Amini-Afshar, M., Bingham, H.B., Shao, Y., Henshaw, W.D., 2024b. Solving for hydroelastic ship response using Timoshenko beam modes at forward speed. Ocean Engineering 300, 117267. https://doi.org/10.1016/j.oceaneng.2024.117267.

Zhu, S., Moan, T., 2014. Investigation into the nonlinear hydroelastic response of an 8600-TEU containership model advancing in regular waves. Ships and Offshore Structures 9 (5), 531–549.
Zhu, L., Huguenard, K., Fredriksson, D.W., 2019. Dynamic analysis of longline aquaculture systems with a coupled 3D numerical model. Int. Ocean Polar Eng. Conf. ISOPE pp. ISOPE-I.
Zhu, L., Zou, Q.P., Huguenard, K., Fredriksson, D.W., 2020a. Mechanisms for the asymmetric motion of submerged aquatic vegetation in waves: a consistent-mass cable model. Journal of Geophysical Research: Oceans 125.
Zhu, L., Duan, L., Chen, M., Yu, T.X., Pedersen, P.T., 2020b. Equivalent design pressure for ship plates subjected to moving slamming impact loads. Marine Structures 71, 102741.
Zhu, L., Huguenard, K., Fredriksson, D.W., Lei, J., 2022. Wave attenuation by flexible vegetation (and suspended kelp) with blade motion: analytical solutions. Advances in Water Resources 162, 104148. https://doi.org/10.1016/j.advwatres.2022.104148.
Zondervan, G., Grasso, N., Lafeber, W., 2017. Hydrodynamic design and model testing techniques for composite ship propellers. In: Fifth International Symposium on Marine Propulsion. Finland, Espoo.
Zou, D., Zhang, J., Ta, N., Rao, Z., 2017. The hydroelastic analysis of marine propellers with consideration of the effect of the shaft. Ocean Engineering 131, 95–106.
Zou, D., Zhang, J., Ta, N., Rao, Z., 2019a. Study on the axial exciting force characteristics of marine propellers considering the effect of the shaft and blade elasticity. Applied Ocean Research 89, 141–153.
Zou, D., Jiao, C., Ta, N., Rao, Z., 2019b. Theoretical study on the axial excitation force transmission characteristics of marine propellers. Ocean Engineering 189, 106364.
Zou, D., Zhang, J., Liu, G., Ta, N., Rao, Z., 2020. Study on characteristics of propeller exciting force induced by axial vibration of propulsion shafting: theoretical analysis. Ocean Engineering 202, 106942.
Zou, D., Xu, J., Zhang, J., Lv, F., Ta, N., Rao, Z., 2021. The hydroelastic analysis of marine propellers considering the effect of the shaft: theory and experiment. Ocean Engineering 221, 108547.
Zou, J., Li, H., Sun, Z., Han, B., Wang, Z., 2024. Experimental analysis of bow flare slamming and whipping responses in a ship at different sailing speeds. Ocean Engineering 305, 117896. https://doi.org/10.1016/j.oceaneng.2024.117896.